# Dynamic Stability of Laminated Composite Stiffened Shell Panels with Cutouts Subjected to Non-Uniform In-Plane Harmonic Edge Loading



**Shuvendu Narayan Patel**

# Dynamic Stability of Laminated Composite Stiffened Shell Panels with Cutouts Subjected to Non-Uniform In-Plane Harmonic Edge Loading

*A Thesis submitted to*
*Indian Institute of Technology, Kharagpur*
*for the award of the degree of*

**Doctor of Philosophy**
**in**
**Engineering**

by

**Shuvendu Narayan Patel**

**Department of Aerospace Engineering**
**Indian Institute of Technology**
**Kharagpur-721302, West Bengal, India**

**September 2006**

**Dedicated**

To my

Loving cousin Late **Prashant Patel,**

Parents, Family Members and Teachers.

**Indian Institute of Technology,**
**Kharagpur-721302, (WB), India.**

**Department of Aerospace Engineering.**

# *Certificate*

This is to certify that the thesis entitled '***Dynamic stability of laminated composite stiffened shell panels with cutouts subjected to non-uniform in-plane harmonic edge loading***' being submitted to the Indian Institute of Technology, Kharagpur by ***Shuvendu Narayan Patel*** for the award of the degree of **Doctor of Philosophy** in engineering is a record of bonafide research work carried out by him under our supervision and guidance, and ***Mr. Patel*** fulfills the requirements of the regulations of the degree. The results embodied in this thesis have not been submitted to any other University or Institute for the award of any degree or diploma.

**P.K. Datta**

Professor,
Department of Aerospace Engineering,
Indian Institute of Technology,
Kharagpur-721 302, India.

**A.H. Sheikh**

Associate Professor,
Department of Ocean Engineering
and Naval Architecture,
Indian Institute of Technology,
Kharagpur-721 302, India.

# Acknowledgements

It is a great opportunity to express my profound gratitude with deep indebtedness to my honourable PhD supervisors **Prof. Prosun Kumar Datta**, Professor, Department of Aerospace Engineering and **Prof. Abdul Hamid Sheikh**, Associate Professor, Department of Ocean Engineering and Naval Architecture, I.I.T. Kharagpur for their excellent guidance, constant inspiration, motivation, encouragement and support throughout the research work. I adore Prof. Datta and Prof. Sheikh for their good qualities and working with them was really a joy. The memory of the moment I have passed with them will be carried out throughout my life.

I express my sincere gratitude to the previous Heads, Department of Aerospace Engineering **Prof. A.K. Ghosh** and **Prof. G. Bandyopadhyay**, and present head **Prof. P.K. Datta**, who extended the entire academic, computational and other related facilities of the department for the smooth progress of the work.

I am very much obliged to the Doctoral Scrutiny Committee (DSC) members, late **Prof. P.K. Sinha**, **Prof. M.K. Laha**, Department of Aerospace Engineering and **Prof. R. Karmakar**, Department of Mechanical Engineering for their valuable suggestions, discussions and timely and critical evaluation of the work.

With all humbleness, I owe a lot to **Prof. S. Parthan** (retired)**, Prof. N. Singh, Prof. M. Sinha, Prof. A. Ghosh, Prof. S.C. Pradhan, Prof. B.N. Singh, Prof. T.V. Rao, Prof. K.P. Sinhamahapatra** and **Prof. D. K. Maiti** of the department for their moral support.

I acknowledge the help received in various manners from all the faculties and staff members of the department of Aerospace Engineering whose excellent co-operation made me stay here homely, pleasantly and enjoyably. Thanks are due to **Mr. Bera** for extending his kind help in all needed computer related jobs.

I am thankful to my seniors **Dr. S. K. Sahu** (NIT Rourkela), **Dr. Ravi Kumar L.** (BMSCE Bangalore) and **Dr. A. K. L. Srivastava** (NIT Jamsedpur) for their timely suggestions and help.

I owe a lot to **Prof. S. Ghosh** department of Metallurgical and Materials Engineering, who gave me many useful tips for the solution of some problems during my research period at IIT Kharagpur.

I am thankful to my friend **Radha** of my village and friends **Suresh, Phalguni, Khan** and **Ramji** of B.C.Roy hall whose co-operation and guidance regarding the value of human life helped me a lot to short-out many problems during the period of my research work. I am also thankful to my other friends **Ashok, Raju, Debdas, Dilip** and all other, who helped me in many cases at IIT Kharagpur.

My friends and co-scholars **Ratnakar, Dr. Zahanjir Hussain, Kundu, Latifa, Rajesh, Shantanu, Dr. Asutosh, Shintu, Dipak, Ajay, Haraprasad, Pabitra, Prashant, Satis, Dalai, Subrat and Padmanav** made me stay in the Institute in a memorable and happy environment.

I extend sincere gratitude to all my family members, respected parents and relatives for their encouragement and co-operation shown during this period. I am especially grateful to my little sisters **Jhili** and **Mili** for their love, which has helped me in many ways during my research work. I am very much thankful to my wife **Niyati** who has tolerated all the sufferings during the last year of my work and looked for this day patiently. She has helped me a lot in managing all necessary issues of the research work without which it would be very difficult to submit the thesis in time.

It is a long journey to come to this point in my life. I am very fortunate to get the help of persons like **Pratap Dada**, **Sharma Sir**, **Samir, Sudhir Dadu** and many others, during this journey. **Sharma Sir's** help in preparing for Orissa JEE is beyond my capacity to express in words. I am sincerely indebted to all of them and grateful to Lord.

Finally, I express my love to the supreme personality of Godhead **Lord Jagannath (Krishna)** who gave me some opportunities to prepare Prasadam for Him during my staying period at IIT Kharagpur.

**Indian Institute of Technology** **Shuvendu Narayan Patel**

**Kharagpur**

# About the Author

**Shuvendu Narayan Patel** received his primary and secondary education in his village Kuntara, Sambalpur District, Orissa. He completed his higher secondary (+2 Science) from Kuchinda College Kuchinda. He finished his B.E. degree in Civil Engineering from University College of Engineering, Burla (Orissa) in 1997. Then he got his M.E. degree in Civil Engineering from Regional Engineering College (Present N.I.T) Rourkela, in the specialization of Structural Engineering in the year 2002. He joined the doctoral program in 2002 as an Institute Research Scholar, in the department of Aerospace Engineering, Indian Institute of Technology, Kharagpur.

The author's research interest lies in finite element method for structural engineering applications, computational mechanics, composite structures, analysis and design of composite stiffened and un-stiffened structures.

# List of Publications

The following technical papers are prepared out of this present study.

## Journals Published/Communicated:

1. **S.N. Patel, P.K. Datta and A.H. Sheikh** (2006), “Dynamic instability analysis of laminated composite stiffened shell panels subjected to in-plane harmonic edge loading”, *Structural Engineering and Mechanics*, **22**(4), 483-510.
2. **S.N. Patel, P.K. Datta and A.H. Sheikh** (2006), “Buckling and dynamic instability analysis of stiffened shell panels”, *Thin Walled Structures*, **44**(3), 321-333.
3. **S.N. Patel, P.K. Datta and A.H. Sheikh**, “Dynamic instability analysis of stiffened shell panels subjected to partial edge loading along the edges”, *International Journal of Mechanical Sciences*. (Under Revision)
4. **S.N. Patel, P.K. Datta and A.H. Sheikh,** “Parametric instability analysis of laminated composite stiffened plate subjected to non-uniform in-plane harmonic edge loading”, *Journal of Structural Engineering, ASCE*. (Communicated)
5. **S.N. Patel, P.K. Datta and A.H. Sheikh,** “Vibration and parametric instability analysis of laminate composite stiffened shell panels subjected to non-uniform in-plane harmonic edge loading”, *Computers and Structures*. (Communicated)
6. **S.N. Patel, P.K. Datta and A.H. Sheikh,** “On stability of laminated composite stiffened plates with square cutout”, *Composite Structures*. (Communicated)
7. **S.N. Patel, P.K. Datta and A.H. Sheikh,** “Dynamic stability analysis of stiffened shell panels with cutouts”, *Journal of Applied Mechanics, ASME*. (Communicated)
8. **S.N. Patel, P.K. Datta and A.H. Sheikh,** “Effect of non-uniform in-plane pulsating edge loading on dynamic stability of stiffened shell panels with cutouts”, *Journal of Sound and Vibration*. (Communicated)

## Conferences Proceedings:

1. **S.N. Patel, P.K. Datta and A.H. Sheikh**, "Vibration and buckling of composite curved panels using a degenerated shell element", *National Conference on Emerging Trends in Structural Mechanics and Composites (ETSMC-2003)*, Nov 1-2, Dept of Civil Engineering, NIT Rourkela.
2. **S.N. Patel, P.K. Datta and A.H. Sheikh**, "Dynamic stability of composite stiffened plates", *Third International Conference on Theoretical, Applied, Computational and Experimental Mechanics (ICTACEM-2004)*, Dec 28-30, Dept. of Aerospace engg, IIT Kharagpur.
3. **S.N. Patel, P.K. Datta and A.H. Sheikh**, "Dynamic instability analysis of laminated composite stiffened cylindrical shell panels", *National Conference on Composite Component Construction (CCC-2005)*, Sept 12-13, Department of Mechanical Engineering, JNTU College of Engineering, Kakinada, A.P.
4. **S.N. Patel, P.K. Datta and A.H. Sheikh**, "Dynamic instability analysis of cross-ply laminated composite stiffened plate subjected to in-plane edge loading", *Structural Engineering Convention (SEC-2005)*, Dec 14-16, Dept of Civil Engineering, IISc Bangalore.
5. **S.N. Patel, P.K. Datta and A.H. Sheikh**, "Dynamic stability analysis of angle-ply composite stiffened plate", *50$^{th}$ Congress of the Indian Society of Theoretical and Applied Mechanics (ISTAM-2005), an International Meet*, Dec 14-17, Dept. of Mechanical Engineering, IIT Kharagpur.
6. **S.N. Patel, P.K. Datta and A.H. Sheikh**, "Dynamic instability analysis of composite stiffened plate with cutouts", *National Conference on Emerging Trends in Mechanical Engineering (ETIME-2006)*, Feb 10-11, Dept. of Mechanical Engineering, BMS College of Engineering, Bangalore.

# Contents

# Abstract

**T**he work presented in this dissertation describes the vibration, buckling and dynamic instability behaviour of stiffened shell panels (isotropic and laminated composite) with/without cutouts under uniform and various non-uniform in-plane edge loadings.

The eight-noded isoparametric degenerated shell element and a compatible three-noded curved beam element are used to model the shell panels and the stiffeners respectively. As the usual formulation of degenerated beam element is found to overestimate the torsional rigidity, an attempt has been made to reformulate it in an efficient manner. Moreover the new formulation for the beam element requires five degrees of freedom per node as that of shell element. In the present investigation the analysis for free vibration, buckling(static stability) and dynamic stability of the isotropic and laminated composite stiffened shell panels with and/or without cutout are implemented by a computer program written in Fortran-90. The elastic stiffness, mass and geometric stiffness matrices of the elements are derived with the help of suitable interpolation functions (shape functions) within the element and integrating various expressions over the element volume by Gauss quadrature numerical technique. As the stress field is non-uniform, due to arbitrary nature of applied in-plane load, boundary conditions, stiffeners, and cutout in the structure, pre-buckling stress analysis is carried out using finite element method to determine the stresses. These stresses at the Gauss points are used to formulate the geometric stiffness matrix. The elastic stiffness, mass and geometric stiffness matrices are computed for all the shell elements and stiffener elements of the entire structure. The elemental matrices are assembled together to form the corresponding global matrices. The skyline storage algorithm is used to keep big size matrices in single array.

Qualitative results are presented to show the effects of geometry of shell panels, aspect ratio, lamination scheme, stiffening scheme, static and dynamic load factors, non-uniform loading type, load band width, ply stacking scheme in the stiffener and boundary condition on the stability boundary. The effects of cutout on vibration, buckling and

instability regions are also presented. All the parameters are seen to have significant effects on the stability behaviour of the isotropic and laminated composite stiffened shell panels.

Thesis organization: The entire thesis is organized into **Six** chapters.

**Chapter-1** includes the general introduction and importance of the present studies. The general method of solving static and dynamic stability of stiffened composite/isotropic shell panels with and without cutout has been briefly addressed in this chapter.

The review of related literature conforming to the scope of the study has been presented in **Chapter-2**. The various work done previously relating to stiffened plate and shells are briefly described in this chapter. The objective and scope of the present investigations are also presented here.

**Chapter-3** presents the finite element formulation, the governing equations and the method of solution of the problem under consideration. The analysis is focused mainly on the determination of the primary instability region, which is important in practical use.

The brief descriptions of the problems taken for the analysis are presented in **Chapter-4**. The description about the geometry of the stiffened panels, loading type, boundary conditions and material properties are also included in this chapter.

The detailed results and discussion on vibration, static stability (buckling) and dynamic stability characteristics of the isotropic and laminated composite stiffened shell panels with and without cutout subjected to uniform and non-uniform in-plane loading along the edges are presented in **Chapter-5**. The results are compared with the experimental and analytical values wherever possible and the discrepancies, if any, have been discussed. A good number of new problems are solved and the results are discussed to study the effects

of various parameters on buckling, vibration and dynamic stability characteristics of isotropic and laminated composite stiffened shell panels with and without cutouts.

The important conclusions drawn from the theoretical findings in the present investigation are listed in **Chapter-6**. The possible scope of extension of the present study has been appended to the concluding remarks. A list of references cited in the text is given after the end of this chapter. The details about the solution techniques and description of the computer program are enclosed in the **Appendix**.

**Key words:** Dynamic stability, vibration, buckling, finite element method, laminate composite stiffened shells, degenerated shell element, curved beam element, non-uniform in-pane loading and cutouts.

## List of Symbols

| | |
|---|---|
| $a$, $b$ | Base dimensions of the stiffened panel in $x$ and $y$ direction respectively |
| $ca$, $cb$ | Dimensions of the cutout in $x$ and $y$ direction respectively |
| $h$ | Thickness of the skin of the stiffened panel |
| $b_s$ | Width of the stiffeners |
| $d_s$ | Depth of stiffeners |
| $\xi$ - $\eta$ - $\zeta$ | Natural coordinate, ($\xi$ - $\eta$): curvilinear coordinates in the shell mid-surface and $\zeta$ : linear coordinate in the thickness direction |
| $x$-$y$-$z$ | Global Cartesian coordinates |
| $N_i$ | Shape function of the shell element |
| $\tilde{V}_{3i}$ | Vector connecting top and bottom points at node $i$, with length equal to the thickness $h_i$ of the shell element at node $i$ |
| $[J]$ | Jacobian matrix |
| $\bar{V}_{3i}$ | Normal vector at node $i$ |
| $\bar{V}_{1i}$, $\bar{V}_{2i}$ | Two orthogonal vectors perpendicular to $\bar{V}_{3i}$ |
| $\bar{v}_{1i}$, $\bar{v}_{2i}$, $\bar{v}_{3i}$ | Unit vectors along $\bar{V}_{1i}$, $\bar{V}_{2i}$ and $\bar{V}_{3i}$ directions respectively |
| $u_i$, $v_i$, $w_i$ | Translational displacements at node $i$ along $x$, $y$ and $z$ directions of the global Cartesian coordinates respectively |
| $\theta_{xi}$, $\theta_{yi}$ | Rotational displacements at node $i$ about $\bar{v}_{2i}$ and $\bar{v}_{1i}$ respectively |
| $\{\delta\}$ | Nodal displacement vector, shell element |
| $[N_D]$ | Matrix that relates the translational displacement ($u$, $v$ and $w$) at any point with the nodal displacement vector $\{\delta\}$ of the shell element |
| $x'$-$y'$-$z'$ | Local coordinate system, similar to that at the mid-surface corresponding to $\bar{V}_{1i}$, $\bar{V}_{2i}$ and $\bar{V}_{3i}$ . |
| $u'$, $v'$, $w'$ | Displacement component along $x'$, $y'$ and $z'$ respectively. |
| $[B]$ | Strain-displacement matrix of the shell element |

| | |
|---|---|
| $\{\varepsilon'\}$ | Strain vector in local coordinate ($x'$-$y'$-$z'$) system |
| $[Q]$ | Stress-strain (Constitutive) matrix of the shell element in the material axes (1- 2-3) system |
| $\theta$ | Angle of orientation of the material axes 1-2 with $x'$ - $y'$ plane |
| $\beta_s$ | Shear correction factor (5/6) |
| $[D']$ | Constitutive matrix of the shell element in local coordinates ($x'$-$y'$-$z'$) system |
| $[k_e]$ | Elastic stiffness matrix of the shell element |
| $[m_e]$ | The consistent mass matrix of the shell element |
| $\rho$ | Material density |
| $[k_g]$ | Geometric stiffness matrix of the shell element |
| $[\tau]$ | Initial stress matrix |
| $[B_G]$ | Strain-displacement matrix for calculation of geometric stiffness matrix of the shell element |
| $N_{si}$ | Shape function of the stiffener element |
| $[N_{Ds}]$ | Matrix that relates the translational displacement (*u*, *v* and *w*) at any point with the nodal displacement vector $\{\delta\}$ of the stiffener element |
| $\beta_t$ | Torsion correction factor |
| *e* | Eccentricity of the stiffener |
| *c* | Length of loading patch in (Type-I, Type-II and Type-III) loading and distance of concentrated load (Type-IV) form bottom edge |
| $\alpha$ | Static load factor |
| $\beta$ | Dynamic load factor |
| $\sigma$ | Applied stress in (Type-I, Type-II and Type-III) loading |
| *P* | Concentrated load, Type-IV |
| $[B_s]$ | Strain-displacement matrix of the stiffener element |

| | |
|---|---|
| $\left[D_s'\right]$ | Constitutive matrix of the stiffener element in local coordinates ($x'$-$y'$-$z'$) system |
| $\left[k_{es}\right]$ | Elastic stiffness matrix of the stiffener element |
| $\left[m_{es}\right]$ | The consistent mass matrix of the stiffener element |
| $\left[k_{gs}\right]$ | Geometric stiffness matrix of the stiffener element |
| $\left[B_{Gs}\right]$ | Strain-displacement matrix for calculation of geometric stiffness matrix of the stiffener element |
| $[K]$ | Global stiffness matrix |
| $[M]$ | Global mass matrix |
| $\left[K_G\right]$ | Global geometric stiffness matrix |

# List of Figures

# List of Tables

## Chapter-1

# Introduction

The uses of shell panels are common in many activities of aerospace, mechanical, civil and marine engineering structures. These structures experience in-plane forces in many situations. The presence of such loads significantly affects the free vibration characteristics of the structures. The buckling phenomenon may be considered as a particular case of free vibration problem with in-plane load, where as the load approaches towards its critical value of buckling, the frequency of vibration tends to zero. When the in-plane load becomes harmonic, it may lead to the condition of parametric resonance. It is found that certain combinations of the frequency of pulsating in-plane force and the natural frequencies of transverse vibration produce dynamic instability where the amplitude of the transverse vibration increases without bound. This phenomenon is entirely different from the usual resonance of forced vibration. In forced vibration when the frequency of the transverse forcing system matches with the natural frequency of the structure, resonance occurs. Thus the resonance phenomenon in forced vibration problem is relatively simple since the structure loses stability at constant frequencies of the transverse loads. On the other hand the instability in case of parametric resonance occurs over a range of frequencies of the in-plane force rather than a single value. Again parametric resonance of a structure may occur at load level much less than the static buckling load while the static instability of the structure sets in at the static buckling load values. Thus a structural component designed to withstand static buckling load may easily fail in an environment having periodic in-plane loading. So a designer ought to consider the parametric resonance aspect while dealing a structure subjected to dynamic loading atmosphere.

The use of composite material is steadily increasing in the present days due to its high strength/stiffness-to-weight ratio and these can be tailored through the variation of fiber orientation and stacking sequence to obtain an efficient design. In addition to that, the specific strength/stiffness of a panel can be enhanced by the use of a suitable stiffened structural form. These benefits have been exploited in the study of stiffened composite shell panel structure considered in the present investigation.

In lightweight metal construction such as aircraft, it has been observed that the in-plane loads are of considerable magnitude. These types of structures when stiffened can safely carry the loads even if the skin buckles. With more use of such structures buckling and dynamic instability analysis have gathered more importance. Moreover the in-plane loads are non-uniform in nature in many cases. Even if the applied stresses are uniform the stress distribution inside the panels becomes non-uniform due to the presence of stiffeners and different boundary conditions. The development of non-uniform patch loading can be understood from the discussion presented in the book by Bruhn [19]. Cases of practical interest arise when the in-plane stresses are caused by patch, triangular, point or any arbitrary forces acting along the boundary. Again the geometrical discontinuities like cutouts are inevitable in the aerospace, civil, mechanical and marine structures. In aerospace structures cutouts are commonly found as access ports for mechanical and electrical systems, or simply to reduce weight. Cutouts are sometimes provided for ventilation and to alter the resonant frequency of the structures. In addition, the designers often need to incorporate cutouts or openings to serve as doors and windows. In all these situations where the stress field is non-uniform, which may be either due to the non-uniform or discrete edge load, or due to the presence of different stiffening systems and boundary conditions, or due to the presence of discontinuities in the stiffened panels, the analysis for vibration, buckling and dynamic instability becomes quite complex. In such cases not only the stress field is non-uniform, the nature of the stresses may also be different in different regions. It is quite cumbersome and tedious to work out any closed form solutions to the aforesaid problems, though not impossible. Under these circumstances, one has to resort to some numerical techniques for the solution of these problems.

With the emergence of the digital computers, with their enormous computing speed and core memory capacity, the outlook of the structural analysts is being changed and helped in the evolution of various numerical methods such as the finite element, boundary element, finite strip, method of multiple scales. For treating arbitrary loading and boundary conditions, the finite element is known to be one of the suitable numerical methods because of its versatility. These numerical tools allow the researchers to model the structure in a more realistic manner with simpler mathematical forms.

The method of solution of dynamic stability class of problems discussed above involves first reducing the equations of motion to a system of Mathieu-Hill equations having periodic coefficients and the parametric resonance characteristics are studied from the solution of equations. Analytical solutions are available only for certain geometry, loading and boundary conditions. In general structural problem, the governing Mathieu-Hill equations lead to an infinite set of equations with unknown coefficients, which need to be truncated finite for finite degrees of freedom. The solution of dynamic stability of structures involves the determination of the eigenvalues corresponding to the instability regions by analytical methods or by numerical approach.

In order to model a shell panel without any significant approximation related to the representation of arbitrary shell geometry, structural deformation and other associated aspects, the isoparametric 3D degenerated shell element [1,160,119] having eight nodes is used. Though the concept of 3D degenerated shell element was initially proposed for isotropic shell [1] but it has been subsequently extended to the fiber reinforced laminated panels [106]. The present formulation differs from Panda and Natarajan [106] in the treatment of mapping in the thickness direction. Panda and Natarajan [106] have mapped the individual layers whereas the entire laminate is mapped in the present formulation. For the stiffeners, a compatible three-noded isoparametric curved beam element is used. The beam element is always placed along the edge of shell elements and this is intentionally not placed within the shell element in order to avoid the problem of stress jump within the shell element.

The basic concept underlying in the formulation of degenerated shell element [1] has been extended to derive beam/stiffener elements having any arbitrary curve geometry suitable for use in two or three-dimensional problems [35,13]. Again the formulation for isotropic beam [35,13] has been upgraded for laminated beam by Liao and Reddy [71] where the stiffener layers are stacked parallel to those of the shell (parallel stacking scheme). Unfortunately the 3D degenerated beam element based on the above formulation [35,13,71] has some problem in torsional mode since it overestimates torsonal rigidity [35]. The problem becomes more severe in case of stiffeners having narrow cross-section like blade stiffener, which is quite common in composite construction. Keeping this aspect in view, the stiffener element is reformulated where the above mentioned problem has been eliminated by using torsion correction factor. In order to achieve that the stiffener bending in the plane of the shell surface is neglected. This should not affect the solution accuracy since deformation of the stiffener in that plane will be very small due to high in-plane rigidity of the shell skin. Moreover, the new formulation has the advantage that it requires five degrees of freedom per node while it is six in case of existing formulations [35,13,71]. Actually the stiffener element will directly share the five nodal unknowns of the shell element. The beam element considered has a rectangular section where provision has been kept for parallel (Fig.1.1a) as well as perpendicular stacking schemes (Fig. 1.1b).

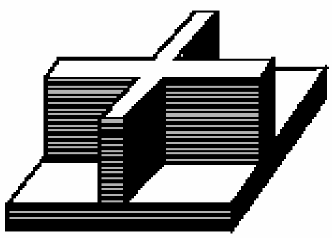

**Fig. 1.1a Parallel stacking schemes**

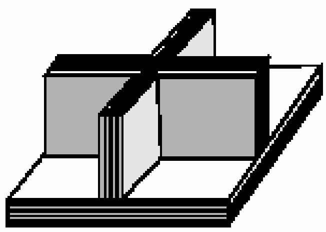

**Fig. 1.1b Perpendicular stacking schemes**

It is clear from the above discussion that the process of investigating the different aspects of dynamic stability of laminated composite and isotropic stiffened shell panel structure is on, and, hence, a study of the dynamic stability behaviour of such structures is a problem of current interest. The problem involves different complicated effects such as geometry, boundary conditions, anisotropy and structures with discontinuity and non-uniform in-plane stress distribution. The above-discussed aspects need attention and thus constitute a problem of current interest.

In the present investigation the analysis for vibration, buckling (static stability) and dynamic stability of the isotropic and laminated composite stiffened shell panels with and/or without cutout are implemented by a computer program written in Fortran-90. An attempt has been made to make the program as general as possible to carryout any type of analysis within the scope of the present investigation. The compiler used is Microsoft Developer Studio.

A thorough review of early works done in this field is an important requirement to arrive at the objective and scope of the present investigation. The detail review of literature along with discussions is presented below.

# Chapter-2
# Review of Literatures

## Introduction

The vast use of conventional metals, its alloys, and the ever-increasing demand of composite materials in plate and shell panel type of structure, have become the subject of research for many years. Though the investigation is mainly focused on dynamic stability of laminated composite and isotropic stiffened shell panels with/without cutouts, some relevant researches on vibration with and without in-plane load and buckling of un-stiffened/stiffened panels are also studied for the sake of its relevance. Some of the pertinent studies done recently are elaborately reviewed and critically discussed to identify the lacunae in the existing literature. The review part is mainly divided in two parts as literatures without cutout as **Part-I** and literatures with cutout as **Part-II**.

**Part-I (Without cutout)**

The studies are grouped in four sections as

***Vibration and buckling of un-stiffened plates and shells***
***Vibration and buckling of stiffened plates and shells***
***Dynamic stability of un-stiffened plates and shells***
***Dynamic stability of stiffened plates and shells***

In each section the considerations for various aspects of analysis are been taken care for both isotropic/composite materials and uniform/non-uniform loading cases.

***Vibration and buckling of un-stiffened plates and shells***

Due to their importance in structural mechanics, large numbers of references are available in the published literature dealing with vibration and static buckling behaviour of plates and shells subjected to uniform in-plane stresses.

The literature in vibration and buckling analysis of un-stiffened plates and shells are vast, hence the review is limited to most recent ones and relevant to the present investigation. Various methods used for vibration analysis such as Ritz technique, Levy's solution, finite difference method, finite element method, Galerkin method, differential quadrature method and method using boundary characteristics orthogonal polynomial (BCOP) has been reviewed extensively by Leissa [69,70] and Liew *et al.* [78] and Bhat *et al.* [15]. The pioneering works of Anderson *et al.* [6] and Leissa [68] for free vibration of rectangular plate are few of them.

The free vibration of thick rectangular plate is studied for 21 sets of different boundary conditions considering shear deformation by Liew *et al.* [75] using Rayleigh-Ritz method. The transverse vibration of thick rectangular plates subjected to in-plane loads, under 9 sets of boundary conditions is studied by Liew *et al.* [76] using Mindlin's first order shear deformation theory.

The buckling of plate subjected to localized edge loading is investigated for few cases by Khan and Walker [47]. The free vibration and buckling of rectangular plates are studied for oppositely directed concentrated force by Leissa and Ayoub [63]. Recently Deolasi and Datta [31] investigated the buckling and vibration of plates for non-uniform compressive and tensile loading.

A brief history of development of various shell theories is presented in the work of Qatu [116] and Liew *et al.* [77]. Vibration of singly curved shell is studied by Webster [157] and Petyt *et al.* [111]. Vibration of doubly curved shells is studied by Leissa and Kadi

[65]. The free vibration analysis of conoidal shells is investigated by Chakravorty *et al.* [21]. Vibration of simply supported cylindrical shell under uniform initial stresses has been studied by Armenakas [9] analytically using thin shell theory. The effect of non-uniform initial stresses is considered by Yang and Kim [158] using FEM based on Kirchhoff and Love assumption. The elastic stability of cylindrical shell under uniform axial compression has been studied over the years and recently by Sheinman and Simitses [132], Matsunga [82] and other researchers.

One can also find many published references regarding the vibration and buckling of composite plates and shells. Bert and Chen [14], Kabir [44] and many other researchers have investigated the free vibration characteristics of laminated plates using the Yang-Norris-Stavsky theory incorporating first shear deformation theory. The free vibration analysis of laminated plated are also studied by Tessler *et al.* [150] and Khdier and Reddy [49] using higher order shear deformation theory. Chakravorty *et al.* [22,23] have analyzed the free and forced vibration of laminated shell. Reddy [120] has developed an exact solution method for the bending analysis and vibration behaviour of moderately thick laminated shells. Chandrashekhara [24] has shown and analyzed the results of free vibration of doubly curved shells. Kumar *et al.* [53] have analyzed the tension buckling and dynamic stability behaviour of composite doubly curved panel subjected to partial edge loadings. Buckling and dynamic behaviour of laminated composite structures have been analyzed by Moita *et al.* [89]. They have presented the results of buckling of cylindrical shell with axial compression. Vibration and stability analysis of cross-ply and angle-ply laminated plates have been carried out using a global higher order plate theory by Matsunaga [83,84]. Recently free vibration analysis of completely free symmetric cross-ply rectangular plates is reported by Gorman and Ding [37]. The buckling of thick rectangular composite plates with partial edge load is investigated by Sundarresan *et al.* [149]. The buckling of uniaxially loaded cross-ply cylindrical shell is studied by Khdeir *et al.* [50] and Nosier and Reddy [104]. The buckling of doubly curved panels under uniform loading is studied by Librescu *et al.* [74], Carrera [20], Khdeir and Reddy [48], Sheinman and Reichman [131] and Kim [51].

***Vibration and buckling of stiffened plates and shells:***

A good deal of references is also available in the literature on stability and vibration of stiffened plates. The bending, stability and vibration of stiffened plates are well documented in the book by Troitsky [156]. Aksu [2] has presented a variational principle in conjunction with the finite difference method for the free vibration analysis of uni-directionally and crossed stiffened plates. Shastry and Rao [129] have analyzed the free vibration of stiffened plate. Mukherjee and Mukhopadhayay [92] have investigated the free vibration of eccentrically stiffened plates. The finite element analysis of eccentrically stiffened plates in free vibration is presented by Harik and Guo [39]. Sheikh and Mukhopadhayay [130] applied finite strip method to finite element methods and analyzed rectangular, skew and annular shape plate with concentric and eccentric stiffeners. The buckling of stiffened plates is investigated by many researchers with uniform loadings. Recently Srivastava *et al.* [143,144] have investigated the buckling and vibration behaviour of isotropic stiffened plates considering uniform and non-uniform loading using finite element method.

The vibration characteristics of stiffened cylindrical shell are analyzed by Stanley and Ganesan [148]. The free vibration of a thin cylindrical shell with discrete stiffeners is analyzed by Mead and Bardell [85,86] using wave propagation method. Recently Nayak and Bandyopadhyay [99,100] have reported the results for the free vibration of stiffened shallow shells and design aids of conoidal shells using finite element method. Samanta and Mukhopadhayay [127] have presented the free vibration analysis of stiffened shells using FEM. Vibration of initially stressed stiffened circular cylinders and panels is investigated by Patnaik and Sankaran [109]. Mustafa and Ali [95,96] have predicted the natural frequency of stiffened cylindrical shells and orthogonally stiffened curved panels using FEM.

With the advancement of the use of composite materials research is being carried regarding the vibration and buckling of composite plates and shells by many investigators. Recently the buckling behaviour of stiffened laminated plates is investigated by Guo *et al.* [38] using layer wise theory. Kumar and Mukhopadhyay [54] have developed a new finite element for buckling of laminated stiffened plates. Analysis for buckling and vibrations of composite stiffened shells and plates is made by Rikards *et al*. [121] using finite element method. Tripathy and Rao [155] have optimized the lay up of the stiffened composite cylindrical panels for maximum buckling load. The local buckling behaviour of discretely stiffened composite plates and cylindrical shells are investigated by Kassenge and Reddy [45]. Recently, Nayak and Bandyopadhyay [101] have reported the results for free vibration analysis of laminated stiffened shells using finite element method. In this analysis the stiffened shell element is obtained by combination of nine-noded doubly curved isoparametric thin shallow shell element with three-noded curved isoparametric beam element. Prusty and Satsangi [114] have given the results of transient dynamic analysis of laminated composite shell using finite element method.

***Dynamic stability of un-stiffened plates and shells:***

The first observation of parametric resonance is attributed to Faraday in 1831 and the first mathematical explanation of the phenomenon is given by Rayleigh in 1883. As per Bolotin [17] the first analysis of parametric resonance of a pinned perfect column is presented by Beliaev. The dynamic instability of plates under periodic in-plane force is first studied by Einaudi in the year 1936. An extensive bibliography of earlier works on these problems is given in review papers of Evan-Iwanowski [34], Ibrahim [43] and Simitses [134]. Hutt and Salam [42] first used the finite element method for the dynamic instability analysis of plates. Deolasi and Datta [31] and Sahu and Datta [126] studied the dynamic instability of plates and doubly curved panels with non-uniform edge loadings. Many references are also available in the literature regarding the dynamic instability of composite plates and shells with uniform loadings. The dynamic instability of composite laminates using a higher order theory is investigated by Chattopadhayay and Radu [26]. The dynamic instability analysis of a laminated composite circular cylindrical shell is presented by Ganapathi and Balamurugan [36]. The dynamic stability analysis of laminated cylindrical shells subjected to periodic axial loads is presented by Lam and Ng [56]. The dynamic instability of layered anisotropic circular cylindrical shells is investigated by Argento and Scott [7,8].

***Dynamic stability of stiffened plates and shells:***

The works on dynamic stability analysis of stiffened plates and shells are very few in the literature. Thomas and Abbas [151] have presented the vibration characteristics, buckling behaviour and dynamic stability of stiffened plates using finite element method. They have considered the effect of number of stiffeners and depth of stiffeners on frequencies of vibration, static buckling load and regions of dynamic instability. In this work they have presented the dynamic stability analysis of eccentrically stiffened plates for the first time. The parametric resonance of simply supported stiffened rectangular plates subjected to in-plane sinusoidal dynamic forces is investigated by Duffield and Willems [33]. They developed an analytical model for the stiffened plates with stiffeners, which are treated as discrete elements. They had shown that the location and size of the stiffeners have a significant effect on the boundaries of the parametric instability regions in comparison to the flat unstiffened plates. They had also performed experiments for the verification of the theoretical results for stiffened plates with a single centrally located stiffener transverse to the in-plane periodic force acting on two opposite edges. This is the only literature available regarding the experiments on dynamic instability of stiffened plates. Merrit and Willems [88] investigated the dynamic instability for skew stiffened isotropic plates. In this study the uniformly distributed load has been treated with simply supported boundary condition. The dynamic stability of radially stiffened annular plates with radial stiffener subjected to in-plane force is investigated by Mermertas and Belek [87]. In this study a sector and a beam finite element method is used. The instability regions are determined for a wide range of excitation frequency with different boundary conditions using Bolotin’s method. Inner and outer edges of the plates are subjected to equal in-plane forces. Recently, Srivastava *et al.* [141,142] have investigated the dynamic instability of isotropic stiffened plates with uniform and non-uniform edge loadings by finite element method. They have shown the effect of stiffener location, number of stiffeners, aspect ratio on the dynamic instability region of stiffened plates. Liao and Cheng [72,73] have given some results for dynamic instability of stiffened composite plates and shells with uniform in-plane forces using finite element method. They have studied only one example of stiffened shell panel having cylindrical geometry.

**Part-II (With cutout)**

Cutouts are inevitable in the aerospace, civil, mechanical and marine structures mainly for practical considerations. Thus the vibration and dynamic stability of structures with cutout are of great technical importance to understand the systems with in-plane compressive edge loadings. Despite the practical importance of the structural parts consisting of laminated composite stiffened shell panels, the number of technical papers and reports dealing with the subjects is limited due to the complexity involved in the analysis.

The discussions were made in the same sequence as that of Part-I in an unified manner. A finite element analysis of a clamped thin plate with different cutout sizes along with experiment was carried out by Monahan *et al.* [90]. Ritchie and Rhodes [122] have investigated theoretically and experimentally the behaviour of simply supported uniformly compressed rectangular plates with central holes, using a combination of Rayleigh-Ritz and finite element methods. The dynamic characteristics of rectangular plates with one and two cutouts using a finite difference formulation, based on variational principles were obtained by Aksu and Ali [3], along with experimental verification. There are other references [12,30,52,62,110,112,133] available in the literature on static stability and free vibration of plates with cutout, some of them deals with tension buckling cases. Recently Huang and Sakiyama [41], Lee *et al.* [59,60], Mundkar *et al.* [94] considered the effect of shear deformation to study the stability and vibration characteristics of plates having different shapes and sizes of cutouts. Kaushal and Bhat

[46] made a comparative study of vibration behaviour with cutout using finite element and Raleigh-Ritz methods. Ali and Atwal [5] reported the results of natural frequencies of simply supported rectangular plate with rectangular cutouts using Rayleigh-Ritz method. Paramasivam [107] used a finite difference approach in analyzing the effects of openings on fundamental frequencies of plates with simply supported and clamped boundary conditions. Sivasubramanian *et al.* [138] also studied free vibration of curved panels with cutouts. Avalosa and Laurab [10] performed a series of numerical experiments on vibrating simply supported rectangular plates with two rectangular holes with free edges. The buckling behavior of an elastoplastic cylindrical shell with a cutout under pure bending was investigated analytically and experimentally by Yeh *et al.* [159].

Lee and Lim [58] have presented the natural frequencies of isotropic and orthotropic plates with rectangular cutouts subjected to in-plane forces using Raleigh's method. Srivatsa and Murthy [139] have studied the critical buckling loads of laminated fiber reinforced plastic thin square panels with cutout using FEM, based on classical lamination theory. Lin and Kuo [80] also studied buckling of rectangular composite laminates with circular holes under in-plane static loading. Sivakumar *et al.* [136] have analyzed free vibration analysis of composite plates in the presence of cutouts undergoing large amplitude oscillations using FE approach. The buckling and post buckling of composite plates with cutouts are studied by Nemeth [102,103] elaborately and the results were compared with earlier works including experiment. Bailey and wood [11] studied stability of square CFRP panel with various cutout geometries by using ANSYS and experiment. Toda [154] investigated analytically and experimentally the effects of circular cutouts on resonant frequencies of thin cylindrical shells using Raleigh-Ritz approximations. Rossi [123] has dealt with the transverse vibrations of thin orthotropic rectangular plates with rectangular cutouts with fixed boundary conditions. The buckling behavior of compression loaded quasi-isotropic curved panels with a circular cutout is studied by Hilburger *et al.* [40] by nonlinear finite element method. Rajamani and Prabhakaran [117,118] have investigated the dynamic response of thin square, simply supported and clamped laminates with circular or square cutouts using finite element method. The results for free vibration of composite rectangular plates with rectangular cutout have been reported by Lee *et al.* [57] using Raleigh's method. The effects of cutouts on the natural frequencies of curved panels have been treated sparsely in the literature.

In regard to stiffened shell panels: Sivasubramanian *et al.* [137] have also reported the results for free vibration of longitudinally stiffened curved panels with cutouts by finite element method. Alagusundaramoorthy *et al.* [4] had carried out the experimental investigations for collapse on eighteen stiffened steel plates having initial imperfections under uniaxial compression with simply supported boundary conditions on both loading and unloading edges. Lam and Hung [55] applied the orthogonal polynomial and partitioning method to study the vibration of plates with stiffened opening. They have reported the results for natural frequency of fully clamped plates with stiffened opening. Paramshivam and Sridhar Rao [108] have given the results for free vibration of square plate with stiffened square openings. Recently, Srivastava *et al.* [146] have studied the effect of square cutouts on transverse vibration of stiffened plates with the in-plane uniform edge loading at plate boundary by finite element method.

The study of dynamic stability behaviour of stiffened/unstiffened shell panels with openings is relatively new. The earlier works available are very few. Datta [30] investigated experimentally the dynamic instability of tensioned sheet with central opening. A comprehensive review and analysis of the buckling, vibration and parametric instability problems of plates with different types of cutouts were made by Prabhakara and Datta [112]. Recently, Sahu and Datta [124,125] have investigated the effect of dynamic instability characteristics on doubly curved panels considering with square with global compression effect. Srivastava *et al.* [145,147] have studied the effect of square cutouts and stiffening scheme on dynamic instability of isotropic stiffened plates with the in-plane uniform and non-uniform edge loading at plate boundary using finite element method.

## Aim and scope of the present research work

A review of literature on the problems concerning the vibration, static and dynamic stability of structural elements reveals a considerable interest shown by the researchers in the past and present on various classes of free vibration, static and dynamic stability problems. However, many areas of practical importance of the subject remain unexplored or inadequately represented. In the case of isotropic/composite stiffened shell panels the literature available is mainly concerned with free vibration analysis. To the best of the author's knowledge the static stability analysis of isotropic/composite doubly curved stiffened shell panels with uniform/non-uniform edge loadings are not available in the literature. In regard to dynamic stability analysis, the few earlier works are mainly on isotropic stiffened plates. The author could not find any available work on the dynamic instability analysis of doubly curved stiffened shell panels with uniform/non-uniform edge loadings. The study of dynamic stability of laminated composite stiffened shell panels with cutout subjected to uniform and/or non-uniform in-plane loading at the boundary is new and can be studied extensively. The vast use of stiffened shell-type structures in many engineering activities compelled the author to have extensive study on static and dynamic instability analysis of isotropic and laminated composite stiffened shell panels with/without cutout subjected to uniform and non-uniform in-plane loading along the edges.

The aim of the present investigation is to study the buckling, vibration and dynamic stability behaviour of laminated composite and isotropic stiffened shell panels with and without cutout subjected to uniform and non-uniform loads, including partial and concentrated edge loadings, using finite element method. The effects of various parameters like number of stiffeners, lamination scheme, orientation of stiffeners, staking scheme in stiffeners, geometry of panels, eccentricity of stiffeners, size of stiffeners, loading type, width of the patch loading, position of the concentrated load, cutout size and boundary conditions are considered on the dynamic stability analysis of the stiffened shell panels. The stiffened shell panel problems identified for the present investigations are,

**1. Stiffened shell panels without cutout under uniform loading**

**(Part-I) Laminated composite stiffened shell panels**

- Vibration
- Buckling
- Dynamic stability

**(Part-II) Isotropic stiffened shell panels**

- Buckling
- Dynamic stability

**2. Laminated composite stiffened shell panels without cutout under non-uniform loading**

- Loading Type-I – Localized edge loading from one end of two opposite side.
- Loading Type-II – Localized edge loading from the center of two opposite side.
- Loading Type-III – Localized edge loading from both ends of two opposite side.
- Loading Type-IV – Concentrated edge loading of two opposite side.

Each part is studied in three sections as Buckling, Vibration and Dynamic stability.

**3. Laminated composite stiffened shell panels with square cutout under uniform/non-uniform loading**

- Loading Type-I – Localized edge loading from one end of two opposite side.
- Loading Type-II – Localized edge loading from the center of two opposite side.
- Loading Type-III – Localized edge loading from both ends of two opposite side.
- Loading Type-IV – Concentrated edge loading of two opposite side.

In this case also each part is studied in three sections as Buckling, Vibration and Dynamic stability. The details of loading type and geometry of the panels are shown in Chapter-4.

There is a vast scope of the present research work. The effect of tensile loading, follower force, geometric and material non-linearity, combination resonance, different sizes of cutout (circular, elliptical) etc. can considered for the dynamic stability analysis of laminated composite stiffened shell panels as the scope for future research.

## Chapter-3

# Mathematical Formulation

### 3.1 The Basic Problem

**T**his chapter presents the mathematical formulation for vibration, static and dynamic instability analysis of laminated composite stiffened shell panels of various geometry with/without cutout. The basic problem is a laminated doubly curved shell panel having laminated stiffener subjected to various non-uniform in-plane harmonic edge loadings. The flat, cylindrical, spherical and hyperbolic hyperboloid panels are obtained from the doubly curved shell panel as special cases by taking suitable radii of curvatures. The boundary conditions are incorporated in the most general way to cater the need of curved boundary and laminated composite cases.

### 3.2 Proposed Analysis

The governing equations for the dynamic instability of laminated composite doubly curved stiffened shell panels subjected to in-plane harmonic edge loading are developed. The presence of non-uniform external in-plane loads, boundary conditions, stiffeners and cutouts in the panel induce a non-uniform stress field in the structures. This necessitates the determination of the stress field as a prerequisite to the solution of the problems like vibration, buckling and dynamic stability behaviour of laminated composite stiffened shell panels. As the thickness of the structure is relatively smaller, the determination of stress field reduces to the solution of a plane stress problem in the panel skin and stiffeners (where the thickness and breath are small compared to length). The stiffened shell panels are modeled and the governing equations are solved by finite element method.

### 3.3 Finite Element Formulation

It has been mentioned in the previous section that the laminated composite stiffened shell panel structure is modeled by finite element technique. In order to have a better representation, the shell skin and stiffeners are mode led as discrete/separate elements. The formulation of these elements is presented below.

#### 3.3.1 Assumptions of the Analysis

The following assumptions are made in the present analysis,

1. The material in the stiffened shell panel skin and stiffeners obey Hooke's law.
2. The bending deformations follows Mindlin's hypothesis; the normal to the panel middle surface before bending remains straight, but not necessarily normal to the middle surface after bending.
3. The transverse normal stresses are neglected.
4. The thickness of the shell panel skin and stiffeners remain constant during deformation.

#### 3.3.2 Shell Element

The formulation of the shell element is based on the basic concept of Ahmed *et al.* [1], where the three-dimensional solid element used to model the shell is degenerated with the help of certain extractions obtained from the consideration that one of the dimension across the shell thickness is sufficiently small compared to other dimensions. The element has a quadrilateral shape having eight nodes as shown in Fig. 3.1 where the external top and bottom surfaces of the element are curved with linear variation across the shell thickness. Thus the geometry of an element can be described by the coordinates of a set of points taken at the top and bottom surfaces where the line joining a pair of points ($i_{top}$ and $i_{bottom}$) is along the thickness direction. The detail for the representation of element geometry is given below. The detail derivation of this element for isotropic case is available in the literature [1,159, 119].

**Geometry of the element**

The element geometry can be nicely represented by the natural coordinate system ($\xi$-$\eta$-$\zeta$) where the curvilinear coordinates ($\xi$-$\eta$) are in the shell mid-surface while $\zeta$ is linear coordinate in the thickness direction. According to the isoparametric formulation, these

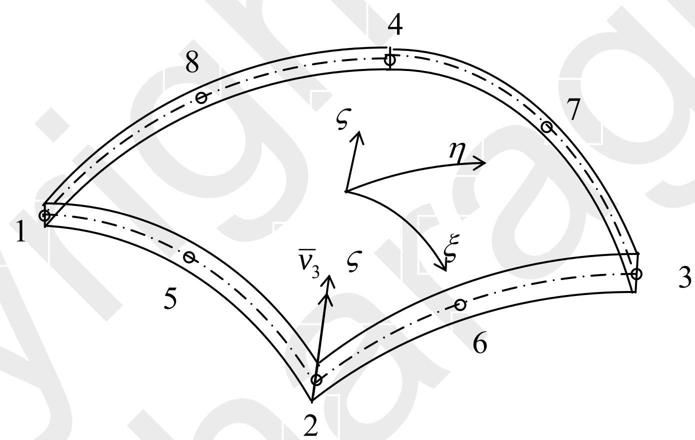


**Fig.3.1a Eight-noded quadrilateral degenerated shell element in curvilinear co-ordinates.**

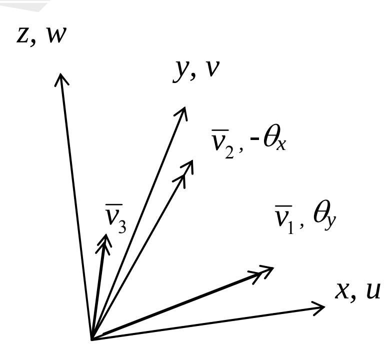


**Fig.3.1b Global Cartesian co-ordinate (*x, y* and *z*) and nodal vector system at any node *i*.**

coordinates ($\xi$, $\eta$ and $\zeta$) will vary from -1 to +1 on the respective faces of the element. With these, the relationship between the global Cartesian coordinates (*x*, *y* and *z*) of any point of the shell element with the curvilinear coordinates may be expressed as

$$\begin{Bmatrix} x \\ y \\ z \end{Bmatrix} = \sum N_i \frac{1+\zeta}{2} \begin{Bmatrix} x_i \\ y_i \\ z_i \end{Bmatrix}_{top} + \sum N_i \frac{1-\zeta}{2} \begin{Bmatrix} x_i \\ y_i \\ z_i \end{Bmatrix}_{bottom} \tag{1}$$

where $N_i$ are the quadratic serendipity shape functions in $(\xi, \eta)$ plane of the two-dimensional element. For 8-noded element, they are given in Table 3.1.

**Table 3.1 Shape functions for quadratic element (8 – noded element)**

| Locations of nodes | Expressions |
|---|---|
| Corner nodes | $N_i = \frac{1}{4}(1+\xi_0)(1+\eta_0)(\xi_0+\eta_0-1)$ |
| Midside nodes | At $\xi_i = 0$ $N_i = \frac{1}{2}(1-\xi^2)(1+\eta_0)$<br>At $\eta_i = 0$ $N_i = \frac{1}{2}(1+\xi_0)(1-\eta^2)$ |

$$\xi_0 = \xi\,\xi_i \;\&\; \eta_0 = \eta\,\eta_i$$

Eqn. (1) may be rewritten in terms of mid-surface nodal coordinates with the help of the nodal vector ($\tilde{V}_{3i}$ ,a vector connecting top and bottom points at node *i*, with length equal to the thickness $h_i$ of the shell element ) along the thickness direction as

$$\begin{Bmatrix} x \\ y \\ z \end{Bmatrix} = \sum N_i \begin{Bmatrix} x_i \\ y_i \\ z_i \end{Bmatrix} + \sum N_i \frac{\zeta}{2} \begin{Bmatrix} \tilde{V}_{3xi} \\ \tilde{V}_{3yi} \\ \tilde{V}_{3zi} \end{Bmatrix} \tag{2}$$

where

$$\{X_i\} = \begin{Bmatrix} x_i \\ y_i \\ z_i \end{Bmatrix} = \frac{1}{2}\begin{Bmatrix} x_i \\ y_i \\ z_i \end{Bmatrix}_{top} + \frac{1}{2}\begin{Bmatrix} x_i \\ y_i \\ z_i \end{Bmatrix}_{bottom} \tag{3}$$

$$\tilde{V}_{3i} = \begin{Bmatrix} \tilde{V}_{3xi} \\ \tilde{V}_{3yi} \\ \tilde{V}_{3zi} \end{Bmatrix} = \begin{Bmatrix} x_i \\ y_i \\ z_i \end{Bmatrix}_{top} - \begin{Bmatrix} x_i \\ y_i \\ z_i \end{Bmatrix}_{bottom} \tag{4}$$

The general expression for the Jacobian matrix may be expressed as

$$[J] = \begin{bmatrix} \frac{\partial x}{\partial \xi} & \frac{\partial y}{\partial \xi} & \frac{\partial z}{\partial \xi} \\ \frac{\partial x}{\partial \eta} & \frac{\partial y}{\partial \eta} & \frac{\partial z}{\partial \eta} \\ \frac{\partial x}{\partial \zeta} & \frac{\partial y}{\partial \zeta} & \frac{\partial z}{\partial \zeta} \end{bmatrix} \tag{5}$$

With the help of eqn. (2), eqn. (5) can be written as

$$[J] = \begin{bmatrix} \sum \frac{\partial N_i}{\partial \xi}\left(x_i + \frac{\zeta}{2}\tilde{V}_{3xi}\right) & \sum \frac{\partial N_i}{\partial \xi}\left(y_i + \frac{\zeta}{2}\tilde{V}_{3yi}\right) & \sum \frac{\partial N_i}{\partial \xi}\left(z_i + \frac{\zeta}{2}\tilde{V}_{3zi}\right) \\ \sum \frac{\partial N_i}{\partial \eta}\left(x_i + \frac{\zeta}{2}\tilde{V}_{3xi}\right) & \sum \frac{\partial N_i}{\partial \eta}\left(y_i + \frac{\zeta}{2}\tilde{V}_{3yi}\right) & \sum \frac{\partial N_i}{\partial \eta}\left(z_i + \frac{\zeta}{2}\tilde{V}_{3zi}\right) \\ \frac{1}{2}\sum N_i \tilde{V}_{3xi} & \frac{1}{2}\sum N_i \tilde{V}_{3yi} & \frac{1}{2}\sum N_i \tilde{V}_{3zi} \end{bmatrix} \tag{6}$$

It is now desired to find out the normal vector at node *i*. Let the vector be defined as $\overline{V}_{3i}$. This vector is determined as the gradient of the surface from the equation of the surface. Then it is necessary to get two orthogonal vectors at the node *i*, such that all three vectors $\overline{V}_{3i}$, $\overline{V}_{1i}$ and

$\overline{V}_{2i}$ are mutually perpendicular to one another.As $\xi$ and $\eta$ may not be orthogonal and their directions may vary from point to point, the following scheme is adopted to get the pair of orthogonal tangent vectors $\overline{V}_{1i}$ and $\overline{V}_{2i}$ where $\overline{V}_{3i}$ will always lie in *x*-*z* plane.

$$\overline{V}_{1i} = j \times \overline{V}_{3i} \tag{7}$$

$$\overline{V}_{2i} = \overline{V}_{3i} \times \overline{V}_{1i} \tag{8}$$

where *j* is unit vector in the *y* direction

Now these vectors $\overline{V}_{1i}$, $\overline{V}_{2i}$ and $\overline{V}_{3i}$ may be normalized to get the corresponding unit vectors $\overline{v}_{1i}$, $\overline{v}_{2i}$ and $\overline{v}_{3i}$ as

$$\overline{v}_{1i} = \frac{\overline{V}_{1i}}{\left|\overline{V}_{1i}\right|} = \begin{Bmatrix} l_{1i} \\ m_{1i} \\ n_{1i} \end{Bmatrix} \tag{9}$$

$$\overline{v}_{2i} = \frac{\overline{V}_{2i}}{\left|\overline{V}_{2i}\right|} = \begin{Bmatrix} l_{2i} \\ m_{2i} \\ n_{2i} \end{Bmatrix} \tag{10}$$

$$\overline{v}_{3i} = \frac{\overline{V}_{3i}}{\left|\overline{V}_{3i}\right|} = \begin{Bmatrix} l_{3i} \\ m_{3i} \\ n_{3i} \end{Bmatrix} \tag{11}$$

Now eqn. (2) may be rewritten with the nodal unit normal vector $\overline{v}_{3i}$ and thickness $h_i$ as

$$\begin{Bmatrix} x \\ y \\ z \end{Bmatrix} = \sum N_i \begin{Bmatrix} x_i \\ y_i \\ z_i \end{Bmatrix} + \sum N_i \frac{\zeta h_i}{2} \begin{Bmatrix} l_{3i} \\ m_{3i} \\ n_{3i} \end{Bmatrix} \tag{12}$$

In a similar manner, eqn. (6) may also be rewritten as

$$[J] = \begin{bmatrix} \sum \frac{\partial N_i}{\partial \xi}\left(x_i + \frac{\zeta h_i}{2} l_{3i}\right) & \sum \frac{\partial N_i}{\partial \xi}\left(y_i + \frac{\zeta h_i}{2} m_{3i}\right) & \sum \frac{\partial N_i}{\partial \xi}\left(z_i + \frac{\zeta h_i}{2} n_{3i}\right) \\ \sum \frac{\partial N_i}{\partial \eta}\left(x_i + \frac{\zeta h_i}{2} l_{3i}\right) & \sum \frac{\partial N_i}{\partial \eta}\left(y_i + \frac{\zeta h_i}{2} m_{3i}\right) & \sum \frac{\partial N_i}{\partial \eta}\left(z_i + \frac{\zeta h_i}{2} n_{3i}\right) \\ \sum N_i \frac{h_i}{2} l_{3i} & \sum N_i \frac{h_i}{2} m_{3i} & \sum N_i \frac{h_i}{2} n_{3i} \end{bmatrix} \tag{13}$$

## Displacement field

The displacement field may be defined in terms of three displacements components ($u_i$, $v_i$ and $w_i$) and two rotational components ($\theta_{xi}$ and $\theta_{yi}$) at the mid-surface nodes (Fig. 3.1) as follows

$$\begin{Bmatrix} u \\ v \\ w \end{Bmatrix} = \sum_{i=1}^{8} N_i \begin{Bmatrix} u_i \\ v_i \\ w_i \end{Bmatrix} - \sum_{i=1}^{8} N_i \frac{\varsigma h_i}{2} \begin{bmatrix} l_{1i} & l_{2i} \\ m_{1i} & m_{2i} \\ n_{1i} & n_{2i} \end{bmatrix} \begin{Bmatrix} \theta_{xi} \\ \theta_{yi} \end{Bmatrix} = \left[N_D\right]\{\delta\} \tag{14}$$

where $h_i$ is the thickness of the shell at the nodal point $i$, the displacements components ($u_i$, $v_i$ and $w_i$) are taken along Cartesian coordinate system ($x$, $y$ and $z$) and the rotational components ($\theta_{xi}$ and $\theta_{yi}$) are taken about $\overline{v}_{2i}$ and $\overline{v}_{1i}$.

$$\{\delta\} = \begin{bmatrix} u_1 & v_1 & w_1 & \theta_{x1} & \theta_{y1} & u_2 & v_2 & \dots & \dots & \theta_{y8} \end{bmatrix}^T \tag{15}$$

## Strain-displacement relation

The components of strains and stresses at a surface having a specific value of $\zeta$ are taken along the local orthogonal axes system. The local axes system is defined as ($x'$, $y'$ and $z'$) which is similar to that at the mid-surface corresponding to $\overline{V}_{1i}$, $\overline{V}_{2i}$ and $\overline{V}_{3i}$. It is assumed that the normal stress and strain components in the thickness direction are sufficiently small and these taken to be zero. The displacement component along $x'$, $y'$ and $z'$ are $u'$, $v'$ and $w'$ respectively. So the strain components may be defined as

$$\{\varepsilon'\} = \begin{Bmatrix} \varepsilon_{x'} \\ \varepsilon_{y'} \\ \gamma_{x'y'} \\ \gamma_{y'z'} \\ \gamma_{x'z'} \end{Bmatrix} = \begin{Bmatrix} \dfrac{\partial u'}{\partial x'} \\ \dfrac{\partial v'}{\partial y'} \\ \dfrac{\partial u'}{\partial y'} + \dfrac{\partial v'}{\partial x'} \\ \dfrac{\partial v'}{\partial z'} + \dfrac{\partial w'}{\partial y'} \\ \dfrac{\partial u'}{\partial z'} + \dfrac{\partial w'}{\partial x'} \end{Bmatrix} = [H] \begin{Bmatrix} \dfrac{\partial u'}{\partial x'} \\ \dfrac{\partial u'}{\partial y'} \\ \dfrac{\partial u'}{\partial z'} \\ \dfrac{\partial v'}{\partial x'} \\ \dfrac{\partial v'}{\partial y'} \\ \dfrac{\partial v'}{\partial z'} \\ \dfrac{\partial w'}{\partial x'} \\ \dfrac{\partial w'}{\partial y'} \\ \dfrac{\partial w'}{\partial z'} \end{Bmatrix} \tag{16}$$

where,

$$[H] = \begin{bmatrix} 1 & 0 & 0 & 0 & 0 & 0 & 0 & 0 & 0 \\ 0 & 0 & 0 & 0 & 1 & 0 & 0 & 0 & 0 \\ 0 & 1 & 0 & 1 & 0 & 0 & 0 & 0 & 0 \\ 0 & 0 & 0 & 0 & 0 & 1 & 0 & 1 & 0 \\ 0 & 0 & 1 & 0 & 0 & 0 & 1 & 0 & 0 \end{bmatrix} \tag{17}$$

Then again three mutually perpendicular vectors at any point are necessary to be determined. These are required to transfer the local strain components in global coordinate. These three vectors can be established by shape function interpolation from nodal values as

$$\bar{V}_{1\varsigma} = \sum N_i \bar{V}_{1i}\ , \qquad \bar{V}_{2\varsigma} = \sum N_i \bar{V}_{2i} \qquad \text{and} \qquad \bar{V}_{3\varsigma} = \sum N_i \bar{V}_{3i} \tag{18}$$

in which proper $\xi$ , $\eta$ and $\zeta$ values of the point are to be supplied. These vectors $\bar{V}_{1\varsigma}$, $\bar{V}_{2\varsigma}$ and $\bar{V}_{3\varsigma}$ are normalized to get the corresponding unit vectors $\bar{v}_{1\varsigma}$, $\bar{v}_{2\varsigma}$ and $\bar{v}_{3\varsigma}$ as

$$\bar{v}_{1\zeta} = \frac{\bar{V}_{1\varsigma}}{\left|\bar{V}_{1\varsigma}\right|} = \begin{Bmatrix} l_{1\zeta} \\ m_{1\zeta} \\ n_{1\zeta} \end{Bmatrix} \tag{19}$$

$$\bar{v}_{2\zeta} = \frac{\bar{V}_{2\varsigma}}{\left|\bar{V}_{2\varsigma}\right|} = \begin{Bmatrix} l_{2\zeta} \\ m_{2\zeta} \\ n_{2\zeta} \end{Bmatrix} \tag{20}$$

$$\bar{v}_{3\zeta} = \frac{\bar{V}_{3\varsigma}}{\left|\bar{V}_{3\varsigma}\right|} = \begin{Bmatrix} l_{3\zeta} \\ m_{3\zeta} \\ n_{3\zeta} \end{Bmatrix} \tag{21}$$

Now the local strain components can be expressed in terms of those in global coordinate system as follows.

$$\begin{bmatrix} \frac{\partial u'}{\partial x'} & \frac{\partial v'}{\partial x'} & \frac{\partial w'}{\partial x'} \\ \frac{\partial u'}{\partial y'} & \frac{\partial v'}{\partial y'} & \frac{\partial w'}{\partial y'} \\ \frac{\partial u'}{\partial z'} & \frac{\partial v'}{\partial z'} & \frac{\partial w'}{\partial z'} \end{bmatrix} = [\alpha]^T \begin{bmatrix} \frac{\partial u}{\partial x} & \frac{\partial v}{\partial x} & \frac{\partial w}{\partial x} \\ \frac{\partial u}{\partial y} & \frac{\partial v}{\partial y} & \frac{\partial w}{\partial y} \\ \frac{\partial u}{\partial z} & \frac{\partial v}{\partial z} & \frac{\partial w}{\partial z} \end{bmatrix} [\alpha] \tag{22}$$

where the matrix $[\alpha]$ can be formed with the unit local vectors $\overline{v}_{1\zeta}$, $\overline{v}_{2\zeta}$ and $\overline{v}_{3\zeta}$ as defined in eqns. (19) - (21) and the matrix may be presented as

$$[\alpha] = \begin{bmatrix} \overline{v}_{1\zeta} & \overline{v}_{2\zeta} & \overline{v}_{3\zeta} \end{bmatrix} = \begin{bmatrix} l_{1\zeta} & l_{2\zeta} & l_{3\zeta} \\ m_{1\zeta} & m_{2\zeta} & m_{3\zeta} \\ n_{1\zeta} & n_{2\zeta} & n_{3\zeta} \end{bmatrix} \tag{23}$$

With the help of eqn. (22) and (23), the local strain vector as expressed eqn. (16) may be rewritten as

$$\{\varepsilon'\} = [H]\begin{Bmatrix} \dfrac{\partial u'}{\partial x'} \\ \dfrac{\partial u'}{\partial y'} \\ \dfrac{\partial u'}{\partial z'} \\ \dfrac{\partial v'}{\partial x'} \\ \dfrac{\partial v'}{\partial y'} \\ \dfrac{\partial v'}{\partial z'} \\ \dfrac{\partial w'}{\partial x'} \\ \dfrac{\partial w'}{\partial y'} \\ \dfrac{\partial w'}{\partial z'} \end{Bmatrix} = [H]\,[T]\begin{Bmatrix} \dfrac{\partial u}{\partial x} \\ \dfrac{\partial u}{\partial y} \\ \dfrac{\partial u}{\partial z} \\ \dfrac{\partial v}{\partial x} \\ \dfrac{\partial v}{\partial y} \\ \dfrac{\partial v}{\partial z} \\ \dfrac{\partial w}{\partial x} \\ \dfrac{\partial w}{\partial y} \\ \dfrac{\partial w}{\partial z} \end{Bmatrix} \tag{24}$$

$$\{\varepsilon'\} = [H]\,[T]\begin{Bmatrix} \frac{\partial u}{\partial x} \\ \frac{\partial u}{\partial y} \\ \frac{\partial u}{\partial z} \\ \frac{\partial v}{\partial x} \\ \frac{\partial v}{\partial y} \\ \frac{\partial v}{\partial z} \\ \frac{\partial w}{\partial x} \\ \frac{\partial w}{\partial y} \\ \frac{\partial w}{\partial z} \end{Bmatrix} = [H]\,[T]\,[\Gamma]\begin{Bmatrix} \frac{\partial u}{\partial \xi} \\ \frac{\partial u}{\partial \eta} \\ \frac{\partial u}{\partial \zeta} \\ \frac{\partial v}{\partial \xi} \\ \frac{\partial v}{\partial \eta} \\ \frac{\partial v}{\partial \zeta} \\ \frac{\partial w}{\partial \xi} \\ \frac{\partial w}{\partial \eta} \\ \frac{\partial w}{\partial \zeta} \end{Bmatrix} \tag{25}$$

where

$$[T] = \begin{bmatrix} l_{1\zeta}[\alpha]^T & m_{1\zeta}[\alpha]^T & n_{1\zeta}[\alpha]^T \\ l_{2\zeta}[\alpha]^T & m_{2\zeta}[\alpha]^T & n_{2\zeta}[\alpha]^T \\ l_{3\zeta}[\alpha]^T & m_{3\zeta}[\alpha]^T & n_{3\zeta}[\alpha]^T \end{bmatrix} \tag{26}$$

and the matrix $[\Gamma]$ can be formed with the Jacobian matrix [*J*] as expressed in eqn. (13) and the matrix $[\Gamma]$ may be presented as

$$[\Gamma] = \begin{bmatrix} [J]^{-1} & 0 & 0 \\ 0 & [J]^{-1} & 0 \\ 0 & 0 & [J]^{-1} \end{bmatrix} \tag{27}$$

and

$$\begin{Bmatrix} \dfrac{\partial u}{\partial \xi} \\ \dfrac{\partial u}{\partial \eta} \\ \dfrac{\partial u}{\partial \zeta} \\ \dfrac{\partial v}{\partial \xi} \\ \dfrac{\partial v}{\partial \eta} \\ \dfrac{\partial v}{\partial \zeta} \\ \dfrac{\partial w}{\partial \xi} \\ \dfrac{\partial w}{\partial \eta} \\ \dfrac{\partial w}{\partial \zeta} \end{Bmatrix} = [L] \begin{Bmatrix} u_1 \\ v_1 \\ w_1 \\ \theta_{x1} \\ \theta_{y1} \\ \cdots \\ \cdots \\ \theta_{y8} \end{Bmatrix} = [L]\,\{\delta\} \tag{28}$$

The matrix $[L]$ can be determined easily from eqn. (14) [119]. Finally the strain vector (25) can be expressed in terms of nodal displacement vector $\{\delta\}$ as

$$\{\varepsilon'\} = [H][T][\Gamma][L]\{\delta\} = [B]\{\delta\} \tag{29}$$

## Stress-strain relation

The fiber reinforced laminated composite shell skin consists of a number of orthotropic layers having different orientations. For such a layer, the stress-strain relationship in the material axis system may be given by

$$\begin{Bmatrix} \sigma_1 \\ \sigma_2 \\ \tau_{12} \\ \tau_{23} \\ \tau_{31} \end{Bmatrix} = \begin{bmatrix} Q_{11} & Q_{12} & 0 & 0 & 0 \\ Q_{12} & Q_{22} & 0 & 0 & 0 \\ 0 & 0 & G_{12} & 0 & 0 \\ 0 & 0 & 0 & \beta_s G_{23} & 0 \\ 0 & 0 & 0 & 0 & \beta_s G_{31} \end{bmatrix} \begin{Bmatrix} \varepsilon_1 \\ \varepsilon_2 \\ \gamma_{12} \\ \gamma_{23} \\ \gamma_{31} \end{Bmatrix} \text{ Or } \{\sigma\} = [Q]\{\varepsilon\} \tag{30}$$

where $Q_{11} = \dfrac{E_1}{1-\nu_{12}\nu_{21}}$, $Q_{22} = \dfrac{E_2}{1-\nu_{12}\nu_{21}}$, $Q_{12} = \dfrac{\nu_{21}E_1}{1-\nu_{12}\nu_{21}} = \dfrac{\nu_{12}E_2}{1-\nu_{12}\nu_{21}}$ and $\beta_s$ is the shear correction factor and it is taken as 5/6.

Though material axes 1-2 lie in $x'$ - $y'$ plane but it is oriented at an angle $\theta$ while axis 3 is directed along $z'$. With a simple coordinate transformation, the stress-strain relationship may be expressed in the local axis system ($x'$-$y'$-$z'$) as follows.

$$\{\sigma'\} = [D']\{\varepsilon'\} \tag{31}$$

where $[D'] = [T_e]^T [Q] \; [T_e]$ and the transformation matrix $[T_e]$ can be expressed as

$$[T_e] = \begin{bmatrix} \cos^2\theta & \sin^2\theta & \sin\theta\cos\theta & 0 & 0 \\ \sin^2\theta & \cos^2\theta & -\sin\theta\cos\theta & 0 & 0 \\ -2\sin\theta\cos\theta & 2\sin\theta\cos\theta & \sin^2\theta\cos^2\theta & 0 & 0 \\ 0 & 0 & 0 & \cos\theta & \sin\theta \\ 0 & 0 & 0 & -\sin\theta & \cos\theta \end{bmatrix} \tag{32}$$

### *3.3.2.1 Elastic stiffness matrix*

Once the matrices [$B$] and [$D$] are obtained, the elastic stiffness matrix of an element can be derived easily and it is expressed as

$$[k_e] = \int [B]^T [D'][B]\,dxdydz = \int [B]^T [D'][B]|J|\,d\xi d\eta d\varsigma \tag{33}$$

where $|J|$ is the determinant of the Jacobian matrix $[J]$, which can be obtained with the help of equation (12) taking derivatives of $x$, $y$ and $z$ with respect to $\xi$, $\eta$ and $\zeta$.

The integration in equation (33) is carried out numerically following Gauss quadrature integration technique where two-point integration scheme has been adopted. The scheme is applied to all the layers in an element and their contributions are added together as follows.

$$[k_e] = \sum_{l=1}^{nl}\sum_{i=1}^{2}\sum_{j=1}^{2}\sum_{k=1}^{2}\left[B(\xi_i,\eta_j,\varsigma_k)\right]^T [D'_l]\left[B(\xi_i,\eta_j,\varsigma_k)\right]\left|J(\xi_i,\eta_j,\varsigma_k)\right| w_i\, w_j\, w_k \tag{34}$$

where $nl$ is the number of layers in an element, $[D'_l]$ is the rigidity matrix $[D']$ as expressed in equation (31) of the $l$th layer, and $w_i$, $w_j$ and $w_k$ are the weight parameters. This technique is adopted in all the subsequent cases where integration is required to be carried out.

### *3.3.2.2 Mass matrix*

The consistent mass matrix has been adopted in the present study. Following the usual techniques, it can be derived with the help of equation (14) and is expressed as

$$[m_e] = \int \rho [N_D]^T [N_D] dxdydz = \int \rho [N_D]^T [N_D] |J| d\xi \, d\eta \, d\zeta \tag{35}$$

where $\rho$ is the material density.

### *3.3.2.3 Geometric stiffness matrix*

The geometric stiffness matrix may be obtained from the strain energy $U_\sigma$ due to initial stress and it is expressed in terms of initial stress vector $\{\sigma'\}$ and nonlinear strain vector $\{\varepsilon_n'\}$ in the local axis system ($x'$ - $y'$ - $z'$) as

$$U_\sigma = \frac{1}{2}\int \begin{bmatrix} \sigma_{x'} & \sigma_{y'} & \tau_{x'y'} & \tau_{y'z'} & \tau_{z'x'} \end{bmatrix} \begin{Bmatrix} \left(\frac{\partial u'}{\partial x'}\right)^2 + \left(\frac{\partial v'}{\partial x'}\right)^2 + \left(\frac{\partial w'}{\partial x'}\right)^2 \\ \left(\frac{\partial u'}{\partial y'}\right)^2 + \left(\frac{\partial v'}{\partial y'}\right)^2 + \left(\frac{\partial w'}{\partial y'}\right)^2 \\ \frac{\partial u'}{\partial x'}\frac{\partial u'}{\partial y'} + \frac{\partial v'}{\partial x'}\frac{\partial v'}{\partial y'} + \frac{\partial w'}{\partial x'}\frac{\partial w'}{\partial y'} \\ \frac{\partial u'}{\partial y'}\frac{\partial u'}{\partial z'} + \frac{\partial v'}{\partial y'}\frac{\partial v'}{\partial z'} + \frac{\partial w'}{\partial y'}\frac{\partial w'}{\partial z'} \\ \frac{\partial u'}{\partial z'}\frac{\partial u'}{\partial x'} + \frac{\partial v'}{\partial z'}\frac{\partial v'}{\partial x'} + \frac{\partial w'}{\partial z'}\frac{\partial w'}{\partial x'} \end{Bmatrix} dv$$

Or

$$U_\sigma = \int \{\sigma'\}^T \{\varepsilon_n'\} dv \tag{36}$$

The above equation may be rewritten as

$$U_\sigma = \frac{1}{2}\int \left\{\varepsilon_g\right\}^T [\tau]\left\{\varepsilon_g\right\} dv \tag{37}$$

where

$$\left\{\varepsilon_g\right\} = \left[\frac{\partial u'}{\partial x'} \quad \frac{\partial u'}{\partial y'} \quad \frac{\partial u'}{\partial z'} \quad \frac{\partial v'}{\partial x'} \quad \frac{\partial v'}{\partial y'} \quad \frac{\partial v'}{\partial z'} \quad \frac{\partial w'}{\partial x'} \quad \frac{\partial w'}{\partial y'} \quad \frac{\partial w'}{\partial z'}\right]^T \tag{38}$$

and

$$\left[\tau\right] = \begin{bmatrix} [\tau^1] & 0 & 0 \\ 0 & [\tau^1] & 0 \\ 0 & 0 & [\tau^1] \end{bmatrix} \tag{39}$$

The sub matrix $\left[\tau^1\right]$ within the initial stress matrix $\left[\tau\right]$ in the above equation is

$$[\tau^1] = \begin{bmatrix} \sigma'_x & \tau'_{xy} & \tau'_{xz} \\ \tau'_{xy} & \sigma'_y & \tau'_{yz} \\ \tau'_{xz} & \tau'_{yz} & 0 \end{bmatrix} \tag{40}$$

Now the strain vector $\left\{\varepsilon_g\right\}$ in equation (38) may be expressed in terms of nodal displacement vector with the help of equation (2) as

$$\left\{\varepsilon_g\right\} = \left[B_g\right]\{\delta\} \tag{41}$$

With the help of above equation, the strain energy $U_\sigma$ in equation (37) may be written as

$$U_\sigma = \frac{1}{2}\{\delta\}^T \left[k_g\right]\{\delta\} \tag{42}$$

where $[k_g]$ is the geometric stiffness matrix and it may be expressed as

$$\left[k_g\right] = \int [B_G]^T [\tau][B_G] \, dv = \int [B_G]^T [\tau][B_G] \, |J| \, d\xi d\eta d\zeta \tag{43}$$

### 3.3.3 Stiffener Element

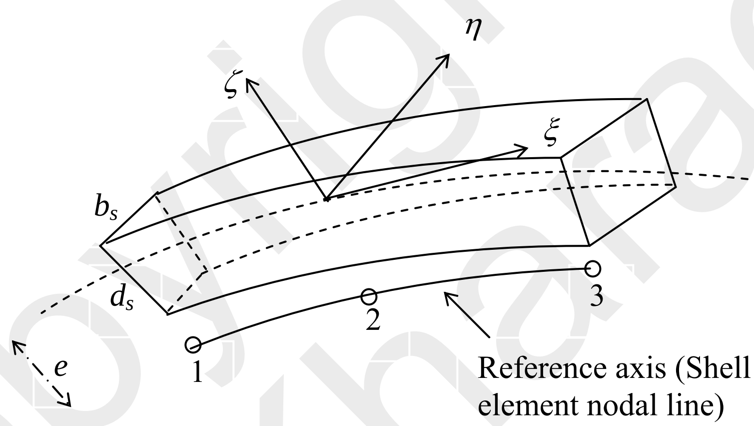


**Fig.3.2 Degenerated curved beam element**

The derivation of the stiffener element (Fig.3.2) is based on the basic concept used to derive the shell element. In this case the stiffener element modeled with three dimensional solid element is degenerated with the help of certain extractions obtained from the consideration that the dimension across stiffener depth as well as breadth is small compared to that along the length. The stiffener element follows an edge of a shell element where the parameters of three nodes lying on that shell element edge are used to express the geometry and deformation of the stiffener utilizing compatibility between shell and stiffeners. It helps to eliminate the involvement of additional degrees of freedom for the modeling of stiffeners. The stiffener element having any arbitrary curved geometry is mapped into a regular domain in $\xi$-$\eta$-$\zeta$ co-ordinate system where all these coordinates vary from –1 to +1. Again $\xi$ is taken along the stiffener axis while $\eta$ and $\zeta$ are taken along the width and depth directions respectively. It has been found that the vectors $\bar{v}_{1i}$, $\bar{v}_{2i}$ and $\bar{v}_{3i}$ are quite useful for the representation of geometry and deformation of the shell element. For the stiffener element a similar set of vectors $\bar{v}_{1i}^s$, $\bar{v}_{2i}^s$ and $\bar{v}_{3i}^s$ are used and these may be obtained from those of the shell element ($\bar{v}_{1i}$, $\bar{v}_{2i}$ and $\bar{v}_{3i}$) as

$$\bar{v}_1^s = \bar{v}_1 \cos\theta_s + \bar{v}_2 \sin\theta_s \;,\; \bar{v}_2^s = -\bar{v}_1 \sin\theta_s + \bar{v}_2 \cos\theta_s \text{ and } \bar{v}_3^s = \bar{v}_3 \tag{44}$$

where ($\bar{v}_{1i}^s$ - $\bar{v}_{2i}^s$) is oriented at an angle of $\theta_s$ with respect to ($\bar{v}_{1i}$ - $\bar{v}_{2i}$) and $\bar{v}_{1i}^s$ follows the stiffener axis.

With these vectors, the co-ordinate at any point within the stiffener may be expressed in terms of co-ordinates ($x_i$, $y_i$, $z_i$) of those three nodes of the corresponding shell element edge as

$$\begin{Bmatrix} x \\ y \\ z \end{Bmatrix} = \sum_{i=1}^{3} N_{si} \begin{Bmatrix} x_i \\ y_i \\ z_i \end{Bmatrix} + \sum_{i=1}^{3} N_{si} \left( \frac{\zeta d_s}{2} + e \right) \begin{Bmatrix} l_{3i}^s \\ m_{3i}^s \\ n_{3i}^s \end{Bmatrix} + \sum_{i=1}^{3} N_{si} \left( \frac{\eta b_s}{2} \right) \begin{Bmatrix} l_{2i}^s \\ m_{2i}^s \\ n_{2i}^s \end{Bmatrix} \tag{45}$$

where $b_s$ is stiffener width, $d_s$ is its depth and $e$ is the eccentricity (distance of the stiffener axis from the shell mid surface). The expressions of the quadratic shape functions $N_{si}$ along $\xi$ are as follows.

$N_{s1} = \xi(\xi - 1)/2,\ N_{s2} = 1 - \xi^2,\ N_{s3} = \xi(\xi + 1)/2$

Now considering the deformation of the stiffener element, the present formulation differs from the usual one [13,35,71] where six degrees of freedom are generally taken to represent the biaxial bending apart from torsion and axial deformation. In the present study the bending of the stiffener in the tangential plane of the shell is not considered. This has helped to eliminate the involvement the sixth degrees of freedom $\theta_z$ like that of shell element. Moreover the usual formulation [13,35,71] overestimates the torsional rigidity and it cannot be corrected simply with some correction factor since it got mixed with other terms. The present formulation facilitates to treat it nicely where a torsion correction factor is introduced for parallel as well as perpendicular stacking schemes. Actually this is the primary object for the reformulation of the stiffener element. Based on this the displacement components at any point within the stiffener may be expressed as

$$\begin{Bmatrix} u \\ v \\ w \end{Bmatrix} = \sum_{i=1}^{3} N_{si}\left[T_{vi}\right]\begin{Bmatrix} u_i \\ v_i \\ w_i \end{Bmatrix} - \sum_{i=1}^{3} N_{si}\left(\frac{\zeta d_s}{2} + e\right)\begin{bmatrix} l_{1i} & l_{2i} \\ m_{1i} & m_{2i} \\ n_{1i} & n_{2i} \end{bmatrix}\begin{Bmatrix} \theta_{xi} \\ \theta_{yi} \end{Bmatrix} = \left[N_{Ds}\right]\left\{\delta_s\right\} \qquad (46)$$

where $\left\{\delta_s\right\} = \left[u_1 \quad v_1 \quad w_1 \quad \theta_{x1} \quad \theta_{y1} \quad u_2 \quad v_2 \quad \ldots\ldots. \quad \ldots\ldots. \quad \theta_{y3}\right]^T$ and $l_1$, $m_1$ and $n_1$ are the direction cosine of the vectors $\bar{v}_{1i}^{s}$, $\bar{v}_{2i}^{s}$ and $\bar{v}_{3i}^{s}$ with respect to the global co-ordinates ($x$, $y$ and $z$), the matrix [$T_{vi}$] is used to make the component of translational displacement along $\bar{v}_{2i}^{s}$ at shell mid-plane zero since the bending of the stiffener in the tangential plane of the shell is not considered. Its effect should be insignificant since bending deformation in this mode will be very small due to high in-plane rigidity of the shell skin. Moreover the flexural rigidity of stiffener in this mode is usually found to be small.

The matrix [$T_{vi}$] used in the above equation may be expressed with the help of $\bar{v}_{1i}^{s}$, $\bar{v}_{2i}^{s}$ as

$$\left[T_{vi}\right]=\begin{bmatrix} l_{1i}^{s} & 0 & l_{3i}^{s} \\ m_{1i}^{s} & 0 & m_{3i}^{s} \\ n_{1i}^{s} & 0 & n_{3i}^{s} \end{bmatrix}\begin{bmatrix} l_{1i}^{s} & m_{1i}^{s} & n_{1i}^{s} \\ l_{2i}^{s} & m_{2i}^{s} & n_{2i}^{s} \\ l_{3i}^{s} & m_{3i}^{s} & n_{3i}^{s} \end{bmatrix} \tag{47}$$

Similar to shell element, the stress and strain components at any point within the stiffener element are taken in a local axis system ($x'$ - $y'$ - $z'$) corresponding to $\overline{v}_{1i}^{s}$, $\overline{v}_{2i}^{s}$ and $\overline{v}_{3i}^{s}$. The relationship between them may be expressed as

$$\begin{Bmatrix} \sigma_{x'} \\ \tau_{x'z'} \\ \tau_{x'y'} \end{Bmatrix}=\begin{bmatrix} \overline{Q}_{1m} & 0 & 0 \\ 0 & \beta_s\overline{Q}_{5m} & 0 \\ 0 & 0 & \beta_t\overline{Q}_{6m} \end{bmatrix}\begin{Bmatrix} \varepsilon_{x'} \\ \gamma_{x'z'} \\ \gamma_{x'y'} \end{Bmatrix} \text{ or } \{\sigma'\}=\left[D_s'\right]\{\varepsilon'\} \tag{48}$$

where $\beta_s$ is the shear correction factor, which is taken as 5/6. The torsion correction factor $\beta_t$ and other rigidity parameters in the rigidity matrix $\left[D_s'\right]$ are presented below for two different types of stacking arrangements of the stiffener as shown in Fig. 3.3. For both the arrangements, the stress-strain relationship of a lamina in its axis system ($x'$ - r - s) may be written as

$$\begin{Bmatrix} \sigma_{x'} \\ \sigma_{r} \\ \tau_{x'r} \\ \tau_{x's} \\ \tau_{rs} \end{Bmatrix}=\begin{bmatrix} \overline{Q}_{11} & \overline{Q}_{12} & \overline{Q}_{16} & 0 & 0 \\ \overline{Q}_{21} & \overline{Q}_{22} & \overline{Q}_{26} & 0 & 0 \\ \overline{Q}_{61} & \overline{Q}_{62} & \overline{Q}_{66} & 0 & 0 \\ 0 & 0 & 0 & \overline{Q}_{55} & \overline{Q}_{54} \\ 0 & 0 & 0 & \overline{Q}_{45} & \overline{Q}_{44} \end{bmatrix}\begin{Bmatrix} \varepsilon_{x'} \\ \varepsilon_{r} \\ \gamma_{x'r} \\ \gamma_{x's} \\ \gamma_{rs} \end{Bmatrix} \tag{49}$$

where the rigidity matrix in the above equation is identical to $[D']$ of the shell element obtained in equation (31) without the shear correction factor because the shear correction factor is included in eqn.(48).

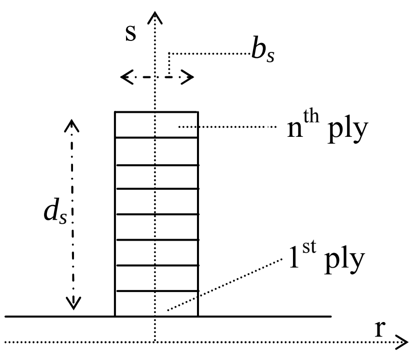


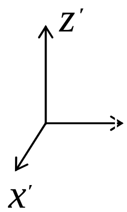


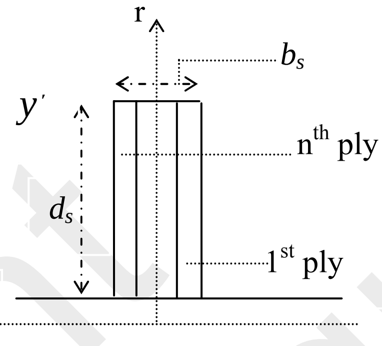


**Fig. 3.3a Ply arrangement I (parallel)** **Fig. 3.3b Ply arrangement II (perpendicular)**



The rigidity parameters $[D'_s]$ of equation (48) may be obtained from equation (49), utilizing the conditions ($\sigma_r = 0$) and ($\tau_{rs} = 0$). For ply arrangement I, the rigidity parameters will be

$$\bar{Q}_{1m} = \bar{Q}_{11} + \bar{Q}_{12}\frac{\bar{Q}_{61}\bar{Q}_{26} - \bar{Q}_{21}\bar{Q}_{66}}{\bar{Q}_{22}\bar{Q}_{66} - \bar{Q}_{62}\bar{Q}_{26}} + \bar{Q}_{16}\frac{\bar{Q}_{61}\bar{Q}_{22} - \bar{Q}_{21}\bar{Q}_{62}}{\bar{Q}_{26}\bar{Q}_{62} - \bar{Q}_{66}\bar{Q}_{22}}$$

$$\bar{Q}_{5m} = \bar{Q}_{55} - \bar{Q}_{54}\frac{\bar{Q}_{45}}{\bar{Q}_{44}} \text{ and } \bar{Q}_{6m} = \bar{Q}_{66}$$

For ply arrangement II, the rigidity parameters are as follows.

$$\bar{Q}_{1m} = \bar{Q}_{11} + \bar{Q}_{12}\frac{\bar{Q}_{61}\bar{Q}_{26} - \bar{Q}_{21}\bar{Q}_{66}}{\bar{Q}_{22}\bar{Q}_{66} - \bar{Q}_{62}\bar{Q}_{26}} + \bar{Q}_{16}\frac{\bar{Q}_{61}\bar{Q}_{22} - \bar{Q}_{21}\bar{Q}_{62}}{\bar{Q}_{26}\bar{Q}_{62} - \bar{Q}_{66}\bar{Q}_{22}}$$

$$\bar{Q}_{5m} = \bar{Q}_{66} \text{ and } \bar{Q}_{6m} = \bar{Q}_{55} - \bar{Q}_{54}\frac{\bar{Q}_{45}}{\bar{Q}_{44}}$$

The torsion correction factor $\beta_t$ for these two cases may be written as

Ply arrangement I:
$$\beta_t = \frac{3kb_s^2 \sum_{i=1}^{nls} \bar{Q}_{5m}^i \left(s_{i+1} - s_i\right)}{\sum_{i=1}^{nls} \bar{Q}_{6m}^i \left(s_{i+1}^3 - s_i^3\right)}$$

Ply arrangement II:
$$\beta_t = \frac{12kd_s \sum_{i=1}^{nls} \bar{Q}_{5m}^i \left(s_{i+1}^3 - s_i^3\right)}{\left[\left(d_s + h/2\right)^3 - \left(h/2\right)^3\right] \sum_{i=1}^{nls} \bar{Q}_{6m}^i \left(s_{i+1} - s_i\right)}$$

where *nls* is the number of layers of the stiffener rib and *k* is the factor to get torsion constant of an isotropic beam having rectangular section, which is a function of $b_s/d_s$ ratio of the rectangular section [153].

Now equations (44) – (48) may be used to derive the elastic stiffness matrix $\left[k_{es}\right]$, mass matrix $\left[m_{es}\right]$ and geometric stiffness matrix $\left[k_{gs}\right]$ of a stiffener element following the procedure used for shell element and these matrices may be expressed as follows.

$$\left[k_{es}\right] = \int \left[B_s\right]^T \left[D_s'\right]\left[B_s\right] dx\, dy\, dz = \int \left[B_s\right]^T \left[D_s'\right]\left[B_s\right] |J|\, d\xi\, d\eta\, d\zeta \tag{50}$$

$$\left[m_{es}\right] = \int \rho \left[N_{Ds}\right]^T \left[N_{Ds}\right] dxdydz = \int \rho \left[N_{Ds}\right]^T \left[N_{Ds}\right] |J|\, d\xi\, d\eta\, d\zeta \tag{51}$$

$$\left[k_{gs}\right] = \int \left[B_{Gs}\right]^T [\tau] \left[B_{Gs}\right] \, dxdydz = \int \left[B_{Gs}\right]^T [\tau] \left[B_{Gs}\right] |J| \, d\xi \, d\eta \, d\zeta \tag{52}$$

where $\left[B_s\right]$ and $\left[B_{Gs}\right]$ are analogous to $[B]$ and $\left[B_G\right]$ respectively. The initial stress matrix $[\tau]$ looks identical to that of shell (39) but its sub matrix $\left[\tau^1\right]$ for stiffener element is.

$$[\tau^1] = \begin{bmatrix} \sigma'_x & 0 & 0 \\ 0 & 0 & 0 \\ 0 & 0 & 0 \end{bmatrix} \tag{53}$$

The elastic stiffness matrix, mass matrix and geometric stiffness matrix are computed for all the shell elements and stiffener elements of the entire structure and these matrices are accordingly assembled together to form the corresponding global matrices $[K]$, $[M]$ and $\left[K_G\right]$ where the skyline storage algorithm is used to keep these big size matrices in single array.

## 3.4 Governing Equations

With the stiffness matrix $[K]$, mass matrix $[M]$ and geometric stiffness matrix $\left[K_G\right]$ of the structure obtained in the previous section, the equation of motion of the structure can be written as

$$[M]\left\{\ddot{q}\right\} + [[K] - P[K_G]]\{q\} = \{0\} \tag{54}$$

This is a general equation and it can be reduced as a special case to get the governing equations for buckling, vibration and dynamic stability problems as follows.

### 3.4.1 Buckling

$$[\ [K] - P_{cr}[K_G]\ ]\{q\} = \{0\} \tag{55}$$

where $P_{cr}$ is the critical load of buckling.

### 3.4.2 Vibration

$$[\ [K] - P\ [K_G]\ ]\{q\} - \omega^2[M]\{q\} = \{0\} \tag{56}$$

where ω is the vibration frequency of the structure subjected to in-plane load and it becomes the natural frequency of vibration if *P* is made zero.

### 3.4.3 Dynamic stability

Equation (54) can also be used to solve the dynamic stability problem. Let the in-plane load *P* be periodic and may be expressed as

$$P(t) = P_s + P_t \cos \Omega t \tag{57}$$

where $\Omega$ is the frequency of excitation $P_s$ is the static component of *P* and $P_t$ is the amplitude of its dynamic component, which may be expressed in terms of static buckling load $P_{cr}$ as follows.

$$P_s = \alpha P_{cr} \ , \ \ P_t = \beta P_{cr} \tag{58}$$

where $\alpha$ and $\beta$ may be defined as static and dynamic load factors respectively. Now equation (54) can be written as

$$[M]\{\ddot{q}\} + \Big[[K] - \alpha P_{cr}[K_G] - \beta P_{cr}[K_G]\cos \Omega t\Big]\{q\} = 0 \tag{59}$$

The above equation represents a system of second order differential equation with periodic coefficient, which is basically the Mathieu-Hill equation. The boundaries of dynamic instability regions can be found by the periodic solutions having period of $T$ and $2T$, where $T = 2\pi/\Omega$. The range of primary instability region with period of $2T$ is of practical importance [17] where the solution can be achieved by expressing $\{q\}$ in the form of the trigonometric series as

$$\{q\} = \sum_{k=1,3,5}^{\infty} \left[\{a_k\}\sin\frac{k\Omega t}{2} + \{b_k\}\cos\frac{k\Omega t}{2}\right] \tag{60}$$

After substitution of the above equation in equation (55) and taking the first term of the series, the quantities associated with sin $\Omega t/2$ and cos $\Omega t/2$ are separated out and processed accordingly to eliminate the time dependent component and it leads to

$$\left[[K] - \alpha P_{cr}[K_G] \pm \frac{1}{2}\beta P_{cr}[K_G] - \frac{\Omega^2}{4}[M]\right]\{q_{ab}\} = 0 \tag{61}$$

where $\{q_{ab}\}$ is either $\{a_k\}$ or $\{b_k\}$ depending on the use of plus or minus of the dynamic in-plane load component respectively. It is basically an eigenvalue problem and it can be solved for known value of $\alpha$, $\beta$ and $P_{cr}$. The two frequencies corresponding to plus and minus will indicate the boundaries of the dynamic instability region.

### 3.5 Method of Solution

In the present investigation the analysis for vibration, buckling (static stability) and dynamic stability of the isotropic and laminated composite stiffened shell panels with and/or without cutout are implemented by a computer program written in Fortran-90. An attempt has been made to make the program as general as possible to carryout any type of analysis within the scope of the present investigation. The details of the computer program and the method of solution are explained in the Appendix. The equations are solved using the technique proposed by Corr and Jennings [28] where the matrices [$K$], [$M$] and [$K_G$] are stored in single array according to skyline storage algorithm. In all the cases, the stiffness matrix [$K$] is factorized according to Cholesky's decomposition technique. With this, the solution for displacement is simply obtained by its forward elimination and backward substitution techniques. These displacements components are used to find out the stress field. These stresses are used to calculate the geometric stiffness matrices. The solution of eqns. (55), (56) and (61) go through a number of operations [28]. Moreover it requires a number of iterations to get the solution since these equations come under the category of eigenvalue problem. In such cases, the solution of eigen vector and eigen value is more than one where the different solutions correspond to different modes of vibration or different modes of buckling. The mode which gives lowest value of the eigen value is quite important and it is known as fundamental mode. In vibration analysis, it is required to get the solution for first few lower modes from practical purpose while the solution of fundamental mode is usually required in buckling and dynamic stability analysis.

# Chapter-4

# Problem Description

## 4.1 Introduction

**T**he descriptions of the problem considered in the present investigation as mentioned in the Chapter-2 are presented here. This chapter also includes the details about the geometry, loading type, material properties, boundary conditions and non-dimensionalisation of parameters.

## 4.2 Geometry of the stiffened panels

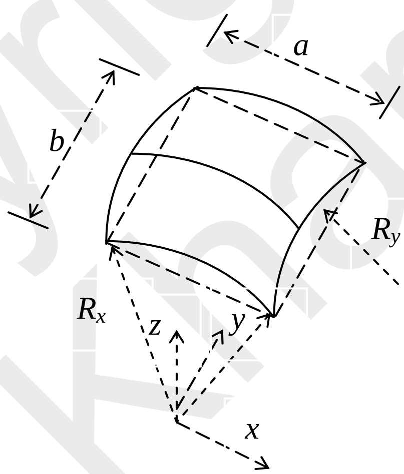


**Fig. 4.1 Geometry of a doubly curved stiffened shell panel**

It is a doubly curved laminated shell panel having laminated stiffeners with and without cutout. Figure 4.1 shows the panel with a central stiffener without cutout. The stiffeners can be provided in any positions along *x* and *y* direction. The radii of curvatures are taken in such a manner to get some specific geometry such as flat plate ($a/R_x$ = 0.0, $b/R_y$ = 0.0), cylindrical shell panel ($a/R_x$ = 0.0, $b/R_y$ = 0.5), spherical shell panel ($a/R_x$ = 0.5, $b/R_y$ = 0.5) and hyperbolic hyperboloid ($a/R_x$ = -0.5, $b/R_y$ = 0.5). All the panels are shown in Fig 4.2. The stiffeners are attached at different positions of the panels during the analysis. In most of the cases the aspect ratio (*a/b*) is taken as 1. To get different value of *a/b* the dimension *a* is changed keeping *b* as constant. The load is applied along *x*-direction throughout the analysis.

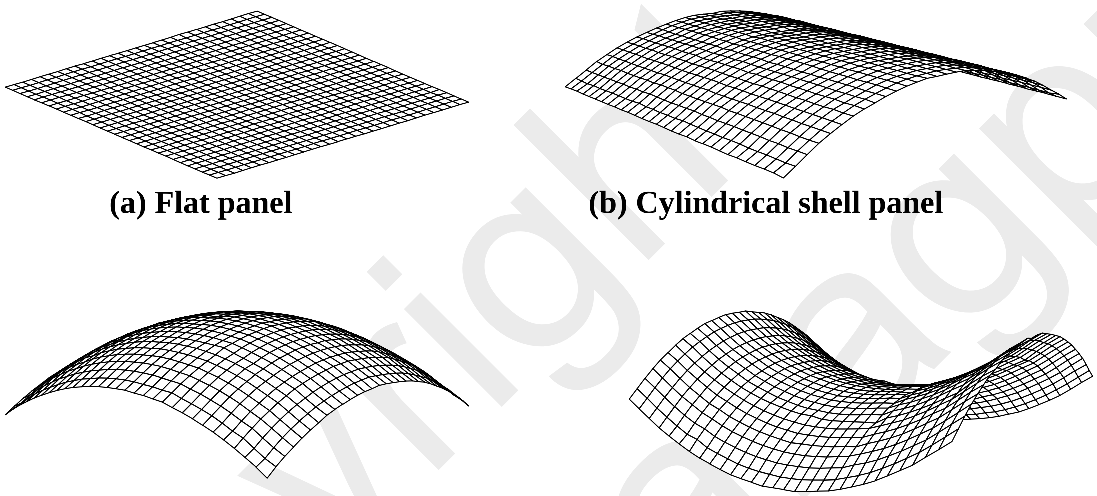

**(a) Flat panel** **(b) Cylindrical shell panel**

**(c) Spherical shell panel** **(d) Hyperbolic hyperboloid shell panel**

**Fig. 4.2 Geometry of different shell panels**

## 4.3 Non-uniform loading type

The different non-uniform loading types considered in the analysis are as shown in Fig 4.3. The panels become uniformly loaded when the non-uniform load bandwidth ratio (*c/b*) in Type-I and Type-II becomes 1.0 and in Type-III becomes 0.5.

Loading Type-I – Localized edge loading from one end of two opposite side.

Loading Type-II – Localized edge loading from the center of two opposite side.

Loading Type-III – Localized edge loading from both ends of two opposite side.

Loading Type-IV – Concentrated edge loading of two opposite side.

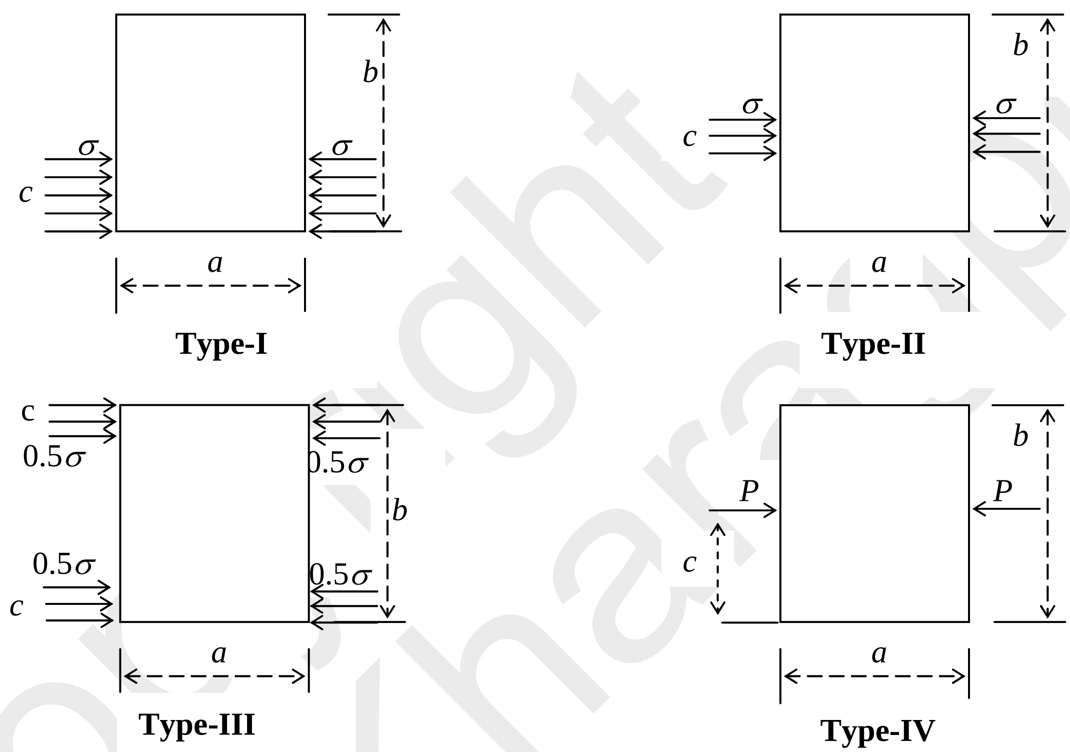


**Fig. 4.3 Different non-uniform loading type (plan view)**

### 4.4 Boundary conditions

The numerical results are presented for isotropic and laminated composite stiffened shell panels with different combination of boundary conditions with various geometry of the stiffened shell panels. In the discussions, letter S, C and F denotes a stiffened shell panels with the edge as simply supported, clamped and free edges respectively. Any notation like SCFS indicates that Side-1 is simply supported, Side-2 is clamped, Side-3 is free and Side-4 is simply supported (Fig 4.4). Side-1 and Side-2 are at $y = 0$ and $y = b$ respectively. Similarly Side-3 and Side-4 are at $x = - a/2$ and $x = a/2$ respectively.

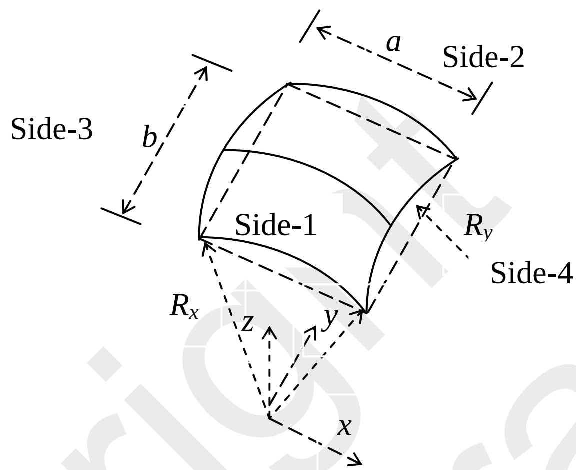


**Fig. 4.4 Detail of the edges of the shell panels**

The restraints imposed for different boundary conditions are,

S-Simply Supported - (For Side-1 and Side-2), $u = w = \theta_x = 1$ and $v = \theta_y = 0$

- (For Side-3 and Side-4), $v = w = \theta_y = 1$ and $u = \theta_x = 0$

C-Clamped- (For all sides) $u = v = w = \theta_x = \theta_y = 1$

F-Free - (For all sides) $u = v = w = \theta_x = \theta_y = 0$.

'1' means movement not allowed

'0' means movement allowed

For the comparison of results, the boundary conditions considered are as reported in the respective studies in the literature.

### 4.5 Material properties

In the present study both isotropic and composite materials are considered with the following properties, but all the results are presented in non-dimensional form. The composite material properties (M2) are the properties of a typical graphite/epoxy laminate [14]. The material properties of the panel skin and stiffeners are same. For the comparison of results, the material properties considered are as reported in the respective studies in the literature.

Isotropic ($M_1$) – $E_{11}/E_{22}$ =1.0, $E_{11}=E_{22}=E$, $G_{12} = G_{13} = G_{23} = G = E/2(1+\nu)$ and $\nu = 0.3$

Composite ($M_2$) - $E_{11}/E_{22}$=40.0, $G_{12} = G_{13} = 0.6E_{22}$, $G_{23} = 0.5E_{22}$ and $\nu_{12} = 0.25$

### 4.6 Non-dimensionalisation of parameters

Most of the model parameters and results are presented in non-dimensional form to make them independent of panel size, thickness, material properties etc for the convenience of the analysis. The non-dimensionalisation of different parameter like natural frequency of vibration, buckling load and excitation frequency of load in dynamic stability analysis is taken as shown in the Table 4.1 in line with references [68,125,141].

**Table 4.1 Non-dimensionalisation of parameters**

| Non-dimensional parameters | Non-dimensional values | |
|---|---|---|
| | Isotropic | Composite |
| Natural frequency of vibration ($\varpi$) | $\omega b^2\sqrt{\rho h/D}$ | $\omega b^2\sqrt{\rho/E_{22}h^2}$ |
| Buckling load ($\bar{P}_{cr}$) | $P_{cr}b/D$ | $P_{cr}b/E_{22}h^3$ |
| Excitation frequency ($\bar{\Omega}$) | $\Omega b^2\sqrt{\rho h/D}$ | $\Omega b^2\sqrt{\rho/E_{22}h^2}$ |

Where, $D = \dfrac{Eh^3}{12(1-\upsilon^2)}$

$h$ = Thickness of the panel

$\rho$ = Material density

## 4.7 Problems of stiffened shell panel identified for the present investigation

As discussed in Chapter-2 the different stiffened shell panel problems identified for present investigation as follow,

1. Stiffened shell panels without cutout under uniform loading
2. Laminated composite stiffened shell panels without cutout under non-uniform loading
3. Laminated composite stiffened shell panels with square cutout under uniform/non-uniform loading

### 1. Stiffened shell panels without cutout under uniform loading

In this problem both laminated composite and isotropic stiffened shell panels are considered with uniform edge loading. In both the stiffened panels the stress field is taken to be uniform, without solving the pre-bucking stress analysis. The detail description of both the panels is as follows.

**(Part-I) Laminated composite stiffened shell panels**

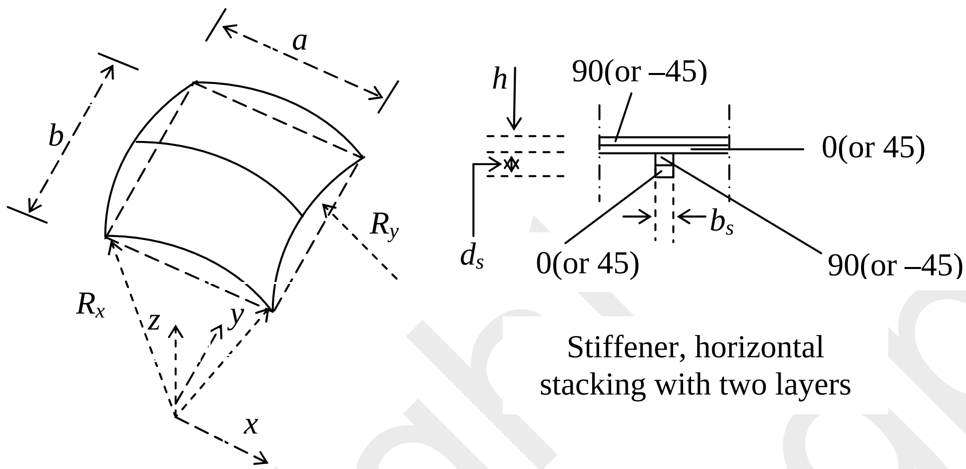


**Fig. 4.5 A doubly curved laminated shell panel with a central laminated stiffener (xst)$_b$**

The problem considered is a doubly curved laminated shell panel having laminated stiffeners subjected to uniform edge loading (*c/b*=1.0, loading Type-I) along *x*-direction. Figure 4.5 shows the panel with a central stiffener. All four types of stiffened panels such as flat plate, cylindrical shell panel, spherical shell panel and hyperbolic hyperboloid panel as mentioned in Section 4.1 are considered for the analysis. The lamination scheme for the shell and the stiffener adopted is (0/90/0/90/---) in one case and (45/-45/45/-45/---) in the other case. The number of layers in the skin of shell panel and stiffener are taken to be same in all the cases. However this is varied from two to eight layers. For the stiffener, parallel stacking scheme is adopted except the case in which the effect of stacking scheme is considered. In many cases the depth to width ratio ($d_s/b_s$) of the stiffener is varied where the stiffener width is always taken as the shell thickness ($h$). Moreover the thickness ratio ($a/h$) and aspect ratio ($a/b$)

taken are 100 and 1 respectively in all the cases. The stiffener is placed at the inner surface of the shell panel except the case in which the effect of eccentricity is considered. In all the cases the four sides of the shell panel are taken to be simply supported and the material properties used for shell panel as well as stiffener is M2 as described in Section 4.5.

**(Part-II)Isotropic stiffened shell panels**

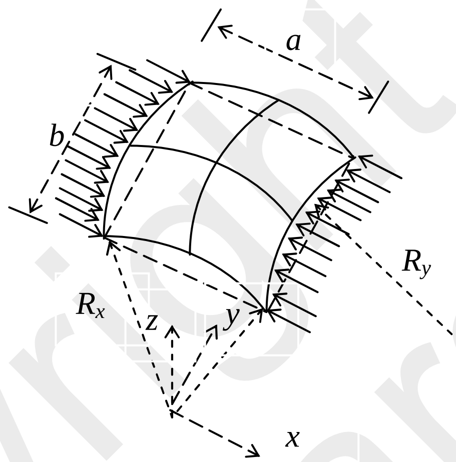


**Fig. 4.6 A doubly curved shell panel with two orthogonal stiffeners**

It is a doubly curved stiffened shell panel subjected to uniform edge loading along *x*-direction. Figure 4.6 shows the panel with two orthogonal stiffeners. The radii of curvatures are taken in a manner so as to get different geometry such as flat plate, cylindrical shell panel, spherical shell panel and hyperbolic hyperboloid as mentioned in section 4.2 In many cases the depth to width ratio ($d_s/b_s$) of the stiffener is varied where the stiffener width ($b_s$) is always taken as twice the shell thickness ($2h$). The thickness ratio ($a/h$) and aspect ratio ($a/b$) are taken as 100 and 1 respectively. The stiffeners are placed at the inner surface of the shell panel unless specified. Moreover three types of placement for the stiffeners are considered, those are *x*-orientation, *y*-orientation and orthogonal stiffeners. For all these three orientations the numbers of stiffeners taken are 1, 3, 5 and 7. The stiffener number one is placed along the center line and the other stiffeners are placed symmetrically on each nodal line from both side of the center line stiffener. This arrangement of placing the stiffeners is considered for all three orientations. The material properties of the shell skin and stiffeners are as M1 stated in section 4.5. The results obtained in the analyses are presented in non-dimensional form as section 4.6.

**2. Laminated composite stiffened shell panels without cutout under non-uniform loading**

In this problem the laminated composite shell panels are considered with non-uniform edge loading. The pre-bucking stress analysis is carried out and these stresses are used to determine the geometric stiffness matrix. The detail description of the panel is as given below,

The problem considered here is a doubly curved laminated shell panel having laminated stiffeners subjected to non-uniform edge loading (Fig.4.3) along *x*-direction. Figure 4.7 shows the panel with two orthogonal stiffeners with loading Type-I. The radii of curvatures are taken in a similar manner to get the specific geometry of flat plate, cylindrical shell panel, spherical shell panel and hyperbolic hyperboloid panel as mentioned in section 4.2. The lamination scheme for the shell and the stiffener adopted is (0/90/0/90/---) in one case and (45/-45/45/-45/---) in the other case. The number of layers in the skin of shell panel and stiffener are taken to be same in all the cases. However this is varied from two to eight layers. For the stiffener, parallel stacking scheme is adopted unless it is not mentioned specifically. The stiffener width ($b_s$) is always taken as twice the shell thickness ($2h$). Moreover the thickness ratio ($a/h$) and aspect ratio ($a/b$) taken are 100 and 1 respectively in all the cases if otherwise not stated. The stiffeners are placed at the inner surface of the shell panels unless specified. Two types of placement for the stiffeners are considered, those are *x*-direction and orthogonal (*x* and *y* direction) stiffeners. For these two orientations the numbers of stiffeners taken are 1, 3, 5 and 7. The stiffener number one is placed along the center line and the other stiffeners are placed symmetrically on each nodal line from both side of the center line stiffener. In all the cases the four sides of the shell panel are taken to be simply supported if otherwise not stated and the material properties used for shell panel as well as stiffener is M2 as described in section 4.5**.**

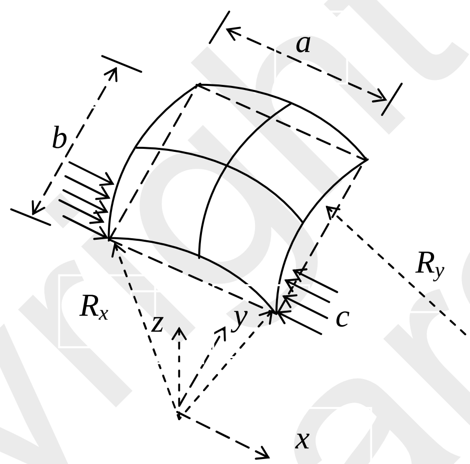


**Fig.4.7 A doubly curved shell panel with two orthogonal stiffeners with loading Type-I**

**3. Laminated composite stiffened shell panels with square cutout under uniform/non-uniform loading**

In this problem the laminated composite shell panels with square cutout are considered with both uniform and non-uniform edge loading. Similar to the previous problem, the pre-bucking stress analysis is carried out and these stresses are used to determine the geometric stiffness matrix. The detail description of the panel is as given below,

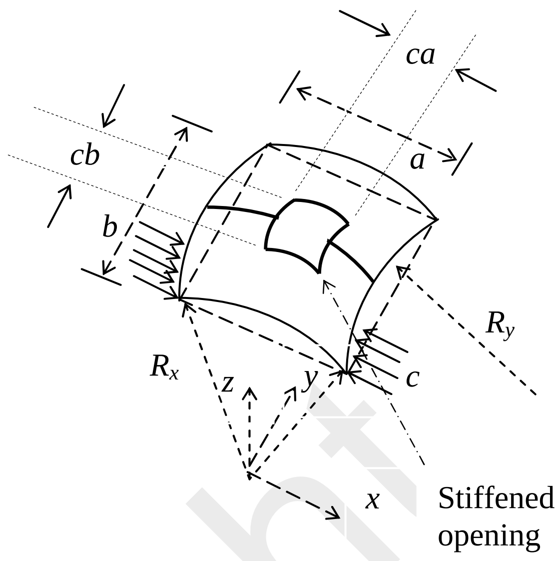


**Fig. 4.8 A doubly curved shell panel with stiffened square opening with a central *x*-stiffener subjected to loading Type-I**

The problem considered is a doubly curved laminated shell panel with square cutout located at the center of the panel having laminated stiffeners subjected to non-uniform edge loading (Fig.4.3) along *x*-direction. The panels are attached with one stiffener along *x*-direction and also four stiffeners are attached to the four sides of the opening; length of each stiffener is equal to the size of the cutout. The cutout is square ($ca/cb$ = 1) in all cases and located at the center of the panels. Figure 4.8 shows the panel with stiffened opening with a *x*-stiffener along the center line with loading Type-I. All four types of stiffened panels such as flat plate, cylindrical shell panel, spherical shell panel and hyperbolic hyperboloid panel as mentioned in Section 4.2 are considered for the analysis. The lamination scheme for the shell and the stiffener adopted is (45/-45/45/-45) if otherwise not stated. The number of layers in the skin of shell panel and stiffener are taken to be same in all the cases. For the stiffener, parallel stacking scheme is adopted unless it is not mentioned specifically. In all cases the depth to width ratio ($d_s/b_s$) of the stiffener is 4.0 and the stiffener width is always taken as twice the shell thickness (2$h$). Moreover the thickness ratio ($a/h$) and aspect ratio ($a/b$) taken are 100 and 1 respectively in all the cases. The stiffener is placed at the inner surface of the shell panel unless specified. In all the cases the four sides of the shell panel are taken to be simply supported (SSSS). The material properties used for shell panel as well as stiffener is M2 as described in section 4.5.

The results of the problems considered are elaborated in Chapter-5 for different parameters.

# Chapter-5
# Results and Discussions

## 5.1 Introduction

**I**n this chapter the results from the theoretical investigations dealing with static and dynamic stability of laminated composite and isotropic stiffened shell panels with and without cutout with various uniform and non-uniform in-plane edge loading are presented using finite element formulations given in Chapter-3. If the applied load is non-uniform at the edges or there are geometric discontinuities (cutout, cracks etc.) in the panel, the in plane stress distribution becomes non-uniform within the panel. The state of non-uniform stress distribution may have significant influence on the static and dynamic stability behaviour of the laminated stiffened shell panels.

## 5.2 Stiffened shell panels without cutout under uniform loading

The problem of laminated composite and isotropic stiffened shell panels without cutout with uniform loading ($c/b$ = 1.0, loading Type-I) is investigated for buckling (static stability), vibration and dynamic stability characteristics in this section, for establishment of convergence and validity of the present analysis.

### 5.2.1 Convergence and validation study

The convergence and accuracy of the proposed method are first established by comparing the results of various problems with those of earlier investigators' available in the literature.

***(a)Free vibration of a simply supported stiffened plate***

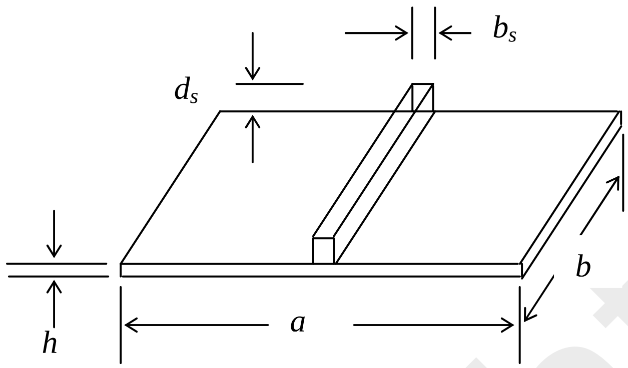


$a$ = 0.6096m
$b$ = 0.4046m
$h$ = 0.00635m
$b_s$ = 0.0127m
$E = 2.11\times10^{11}$ N/m$^2$
$\rho$ = 7842.72 Kg/m$^3$
$\nu$ = 0.3

**Fig.5.1 Simply supported rectangular stiffened plate**

**Table 5.1 Natural frequencies (Hz) of simply supported rectangular stiffened plate**

| Reference | Mode1 | | | Mode2 | | |
|---|---|---|---|---|---|---|
| | $d_s$ (m) | | | $d_s$ (m) | | |
| | 0.0 | 0.0254 | 0.0508 | 0.0 | 0.0254 | 0.0508 |
| Present (2×2) | 197.750 | 381.348 | 703.148 | 1419.06 | 1949.09 | 1572.55 |
| Present (4×4) | 137.525 | 270.400 | 305.941 | 279.151 | 293.429 | 348.586 |
| Present (6×6) | 136.901 | 263.784 | 291.624 | 264.098 | 279.250 | 325.867 |
| Present (8×8) | 136.846 | 262.932 | 290.413 | 263.255 | 278.285 | 323.185 |
| Present (10×10) | 136.857 | 262.765 | 290.181 | 263.109 | 278.102 | 322.692 |
| Present (12×12) | 136.855 | 262.718 | 290.110 | 263.053 | 278.046 | 322.552 |
| Present (14×14) | 136.854 | 262.702 | 290.082 | 263.047 | 278.023 | 322.500 |
| Thomas and Abbas [151] | 136.5 | 259.1 | 293.8 | 265.5 | 280.9 | 332.4 |
| Long [81] | | 267.1 | 273.8 | | 280.3 | 331.8 |

The problem of simply supported stiffened plate as shown in Fig.5.1 is used to carry out the convergence study. The whole structure is modeled with different mesh sizes for the free vibration analysis. The details of the stiffened plate are given in the Fig.5.1. The results for first two natural frequencies are shown in the Table 5.1. It shows a rapid convergence with mesh refinement. Again a mesh size of 8×8 is found to be sufficient to attain the convergence. For the purpose of validation, the frequencies are compared with those of Thomas and Abbas [151] and Long [81]. The results are in good agreement.

***(b)Free vibration of a spherical shell panel of square base having two stiffeners along its two centerlines***

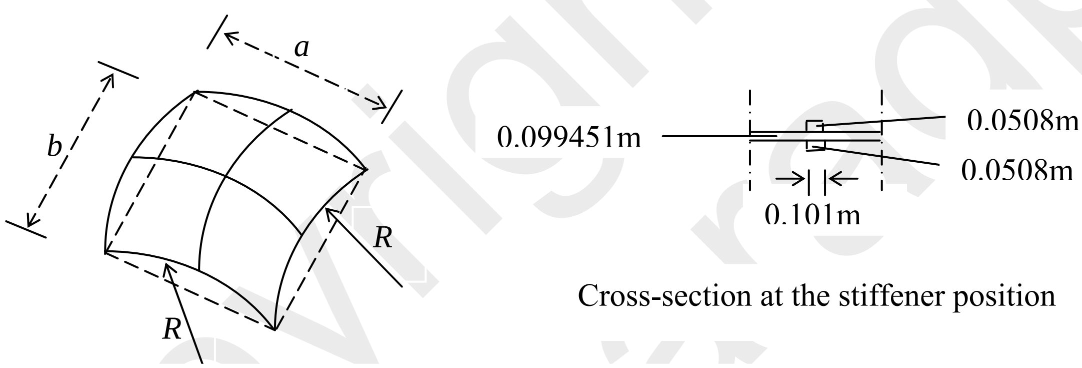


Cross-section at the stiffener position

$a = b = 1.5698$m, $R = 2.54$m, Thickness of the shell ($h$) = 0.099451m,
$\rho = 7732.24$ Kg/m$^3$, $E = 68.97\times10^6$N/m$^2$,

**Fig. 5.2 Stiffened spherical shell panel having square base**

The stiffened spherical shell panel as shown in Fig.5.2 is also used to carry out the convergence study taking its four sides as simply supported (SSSS) as well as clamped (CCCC) conditions. The details of the shell and stiffeners are given in Fig. 5.2 where the stiffeners are taken to be symmetric with respect to the shell mid surface. Similar to the previous problem the structure is modeled with a number of mesh sizes to carry out the analysis. The first two natural frequencies for both the boundary conditions are plotted in Fig. 5.3. It is observed that with mesh refinement the results are converging rapidly. Here also a mesh size of 8×8 is found to be sufficient to attain the convergence. To validate the results, the first five frequencies (mesh size 8×8) for the simply supported boundary condition are compared with the results of finite element solutions of Nayak and Bandopadhyay [100], Samanta and Mukhopadhyay [127] and Prusty [113] in Table 5.2. The results are found to be in good agreement.

**Table 5.2 Natural frequency (rad/sec) of simply supported spherical shell panel with two stiffeners along the two central lines**

| Mode Number | Present (8×8) | Nayak and Bandopadhyay [100] | | Samanta and Mukhopadhyay [127] (8×8) | Prusty [113] (16×16) |
|---|---|---|---|---|---|
| | | El-8[a] (8×8) | El-9[b] (8×8) | | |
| 1 | 40.2300 | 40.26 | 40.26 | 41.70 | 40.81 |
| 2 | 69.0282 | 70.98 | 70.97 | 74.11 | 72.13 |
| 3 | 69.1158 | 70.98 | 70.97 | 74.36 | 72.13 |
| 4 | 91.2984 | 96.06 | 96.06 | 99.18 | 92.92 |
| 5 | 105.6800 | | | 104.94 | 105.69 |

[a] Eight noded element, [b] Nine noded element

(The mesh size is considered taking the full structure in all cases)

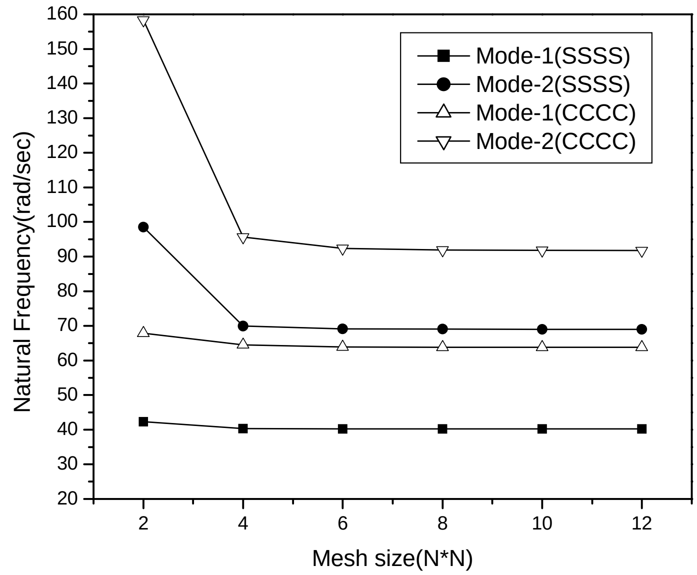


(The mesh size is considered taking the full structure)

**Fig. 5.3 Convergence for frequency of vibration with mesh size of a stiffened spherical shell panel having square base**

***(c)Free vibration of a rectangular composite stiffened plate***

The laminated (0/90/0) rectangular plate with three unidirectional laminated (0/90/0) stiffeners as shown in Fig. 5.4 is analyzed taking simply supported boundary condition at the four sides. The detail of geometry and material properties are given in Fig. 5.4. In the analysis the whole structure is divided in 8×8 mesh. The frequencies for first five modes obtained in the present analysis are presented in Table 5.3 with some other finite element results reported by Prusty [113], Chao and Lee [25] and Chattopadhyay *et al.* [27]. The table shows that the results agreed well.

**Table 5.3 Natural frequencies (Hz) of a simply supported stiffened composite plate**

| References | Mode 1 | Mode 2 | Mode 3 | Mode 4 | Mode 5 |
|---|---|---|---|---|---|
| Present (8×8) | 65.216 | 98.643 | 168.36 | 231.96 | 255.64 |
| Chao and Lee [25] | 65.000 | 101.00 | | 228.00 | 260.00 |
| Prusty [113] | 63.510 | 95.840 | 162.97 | 223.09 | 245.37 |
| Chattopadhyay *et al.* [27] | 63.000 | 95.000 | | 225.00 | 250.00 |

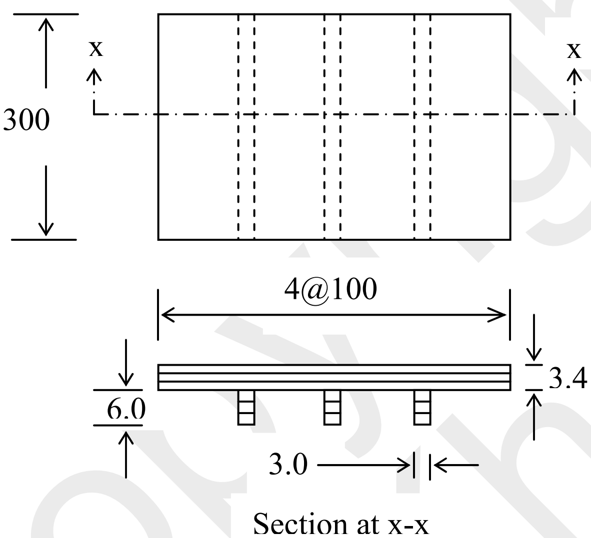


$E_{11}$=9.71*10$^9$ N/m$^2$
$E_{22}$=3.25*10$^9$ N/m$^2$
$G_{12}$=$G_{13}$=0.9025*10$^9$ N/m$^2$
$G_{23}$=0.23*10$^9$ N/m$^2$
$\nu_{12}$=0.29
$\rho$=1347.0 Kg/m$^3$

These properties are same for plate and stiffeners. All dimensions are in mm

**Fig. 5.4 Simply supported laminated plate with three unidirectional laminated stiffeners**

***(d) Free vibration of a composite stiffened spherical shell panel of square base***

The laminated spherical shell panel having two laminated central stiffeners (Fig. 5.5) placed inside the shell surface is analyzed taking stacking sequence for the shell and the stiffener as

0/90/0/90 in one case (I) and 45/-45/45/-45 in other case (II). The numbering of layers starts from bottom to top both in stiffener and panel skin. The analysis is carried out for three different values of curvature ratio ($R/a$) taking simply supported (SSSS) boundaries at the four edges. In the analysis the whole structure is divided in 8×8 mesh. The data used are $a$ = $b$ = 500mm, $E_{11} = 25* E_{22}$, $a/h = 50$, $E_{22} = 1.0*10^4$ N/mm$^2$, $G_{12} = G_{13} = 0.5*E_{22}$, $G_{23} = 0.2*E_{22}$, $\nu_{12} = 0.25$, $\rho = 1.0*10^{-4}$ Kg/mm$^3$. The fundamental frequencies obtained in the present analysis are presented with finite element solution of Prusty [113] in Table 5.4, which shows that the results are in good agreement.

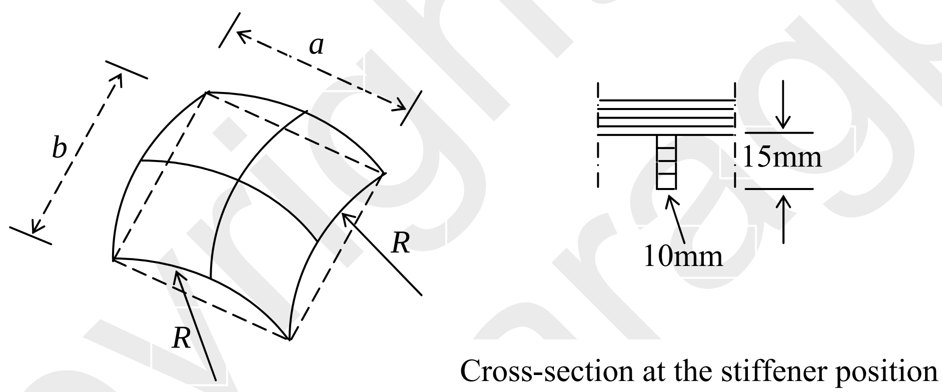


**Fig. 5.5 Laminated spherical shell panel with two central laminated stiffeners attached to the bottom surface**

**Table 5.4 Natural frequencies (Hz) of a laminated composite spherical shell panel with two central laminated stiffeners attached to the bottom surface**

| Lamination | References | $R/a$ = 5 | $R/a$ = 10 | $R/a$= 100 |
|---|---|---|---|---|
| Case – I | Present (8×8) | 1.415 | 1.239 | 1.183 |
| | Prusty [113] | 1.410 | 1.238 | 1.183 |
| Case – II | Present (8×8) | 2.426 | 1.596 | 1.207 |
| | Prusty [113] | 2.446 | 1.682 | 1.358 |

### *(e) Buckling of a rectangular plate with a central stiffener under uniaxial load*

The problem of the rectangular stiffened plate (Fig. 5.6) having simply supported boundary conditions at its four edges is investigated for different plate aspect ratio (*a*/*b*) and stiffener parameters ($\delta = A_s / bh$ , $\gamma = EI_s / bD$ where $A_s$- cross-sectional area of the stiffener, $I_s$-moment of inertia of the stiffener). The simply supported boundary condition is as SSSS in section 4.1.3. The plate thickness ratio (*a*/*h*) and isotropic plate and stiffener material (ν) are taken as 100 and 0.3 respectively. The dimension *a* is varied keeping *b* as constant to get different values of aspect ratio (*a*/*b*). In the analysis the whole structure is divided in 8×8 mesh. The non-dimensional critical buckling stress parameter $k = \sigma_{cr} / (\pi^2 D / b^2 h)$ obtained in the present analysis is presented in Table 5.5 with the analytical solution of Timoshenko and Gere [152] and finite element solution of Mukhopadhyay [93]. The table shows that the agreement between the results is very good. As Timoshenko and Gere [152] have not considered the effect of stiffener eccentricity and torsional rigidity, these parameters are taken as zero in the present problem.

**Table 5.5 Buckling load parameter (*k*) for a simply supported rectangular stiffened plate under uniaxial compression**

| *a*/*b* | $\gamma$ = 10, $\delta$ = 0.05 | | | $\gamma$ =5, $\delta$=0.2 | | |
|---|---|---|---|---|---|---|
| | Present (8×8) | Timoshenko and Gere [152] | Mukhopadhyay [93] | Present | Timoshenko and Gere [152] | Mukhopadhyay [93] |
| 0.6 | 16.403 | 16.5 | | 16.463 | 16.5 | |
| 0.8 | 16.686 | 16.8 | | 12.729 | 13.0 | |
| 1.0 | 15.908 | 16.0 | 15.91 | 9.612 | 9.72 | 9.65 |
| 2.0 | 10.110 | 10.2 | 10.16 | 6.244 | 6.24 | 6.24 |
| 3.0 | 11.867 | 12.0 | 11.94 | 6.512 | 6.53 | 6.48 |
| 4.0 | 10.135 | 10.2 | | 6.264 | 6.24 | |

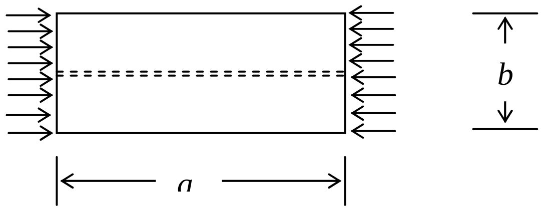


**Fig. 5.6 Simply supported stiffened rectangular plate under uniaxial compression**

***(f) Buckling of a laminated cylindrical shell panel under axial compression***

The laminated (0/90/0/90/0) cylindrical shell panel of square base ($a$×$a$) simply supported along all four edges is analyzed taking curvature ratio $R/a$ = 20 and thickness ratio $a/h$ = 10, 20, 30, 50 and 100. In the analysis the whole structure is divided in 8×8 mesh. The values of non-dimensional buckling load parameter $\overline{N}_{cr} = N_{cr}a^2 / E_{22}h^3$ obtained in the present analysis are presented with those of Sciuva and Crrera [128] Table 5.6, which shows that the results agreed well. The material properties used are: $E_{11} = 40E_{22}$, $G_{12} = G_{13} = 0.5E_{22}$, $G_{23} = 0.6E_{22}$ and $\nu_{12} = 0.25$.

**Table 5.6 Non-dimensional buckling load parameter of a simply supported cross-ply cylindrical shell panel under axial compression**

| References | $a/h$ | | | | |
|---|---|---|---|---|---|
| | 10 | 20 | 30 | 50 | 100 |
| Present (8×8) | 23.964 | 31.792 | 33.981 | 35.395 | 36.845 |
| Sciuva and Crrera [128] | 24.19 | 31.91 | 34.04 | 35.42 | 36.86 |

***(g) Dynamic instability of un-stiffened simply supported square plate***

The problem of un-stiffened simply supported square plate ($a \times a$) is also used to carry out the convergence study. The *a/h* ratio of the plate is 100. The plate is subjected to uniform loading in the two opposite edges. The whole structure is modeled with a number of mesh sizes to carry out the analysis. The non-dimensional ($\bar{\Omega} = \Omega a^2 \sqrt{\rho h / D}$) lower and upper bounding excitation frequencies of the dynamic instability zones are shown in Table 5.7 for two sets of $\alpha$ and $\beta$ values for all the mesh sizes. It shows a rapid convergence with mesh refinement. Again a mesh size of 8×8 is found to be sufficient to attain the convergence and this is used for all the subsequent analyses. For validation, the results are compared with those of Hutt and Salam [42] and Srivastava *et al.* [142]. The results obtained in these studies (Hutt and Salam [42] and Srivastava *et al.* [142]) are found to be in good agreement compared to present results.

**Table 5.7 Non-dimensional bounding frequency ($\bar{\Omega}$) for un-stiffened simply supported square plate**

| Non-dimensional bounding frequency ($\bar{\Omega}$) | | | | |
|---|---|---|---|---|
| Analysis | $\alpha = 0.0$ and $\beta = 0.8$ | | $\alpha = 0.6$ and $\beta = 0.32$ | |
| | L[a] | U[b] | L[a] | U[b] |
| Present (2×2) | 50.82 | 77.27 | 32.22 | 49.11 |
| Present (4×4) | 30.80 | 47.06 | 19.48 | 29.76 |
| Present (6×6) | 30.58 | 46.71 | 19.34 | 29.54 |
| Present (8×8) | 30.57 | 46.69 | 19.33 | 29.53 |
| Present (10×10) | 30.56 | 46.69 | 19.33 | 29.53 |
| Present (12×12) | 30.56 | 46.69 | 19.33 | 29.53 |
| Present (14×14) | 30.56 | 46.69 | 19.33 | 29.53 |
| Present (16×16) | 30.56 | 46.69 | 19.33 | 29.53 |
| Present (18×18) | 30.56 | 46.69 | 19.33 | 29.53 |
| Hutt and Salam [42] | 30.57 | 46.69 | 19.53 | 29.60 |
| Srivastava *et al.* [142] | 30.57 | 46.71 | 19.33 | 29.54 |

[a] Lower boundary of the instability zone

[b] Upper boundary of the instability zone

***(h) Dynamic instability of a laminated composite square plate simply supported at the four sides***

The simply supported laminated square plate ($a \times a$), (standard case, Moorthy *et al.* [91]) with four layer, symmetric cross-ply (0/90/90/0) laminates under in-plane pulsating load along the direction of 0 degree laminate is analyzed for different values of dynamic load factor $\beta$ taking static load factor $\alpha$ to be zero. The plate parameters are, $a$ = 0.254m, $a/h$=25, $\rho$ =2.7712×10$^4$ Kg/m$^3$, $E_{22}$ =6.8982×10$^{10}$ N/m$^2$, $E_{11}/E_{22}$ = 40.0, $G_{12}$ = $G_{13}$ =0.6$E_{22}$, $G_{23}$ = 0.5$E_{22}$ and $\nu_{12}$ =0.25. In the analysis the whole structure is divided in 8×8 mesh. The values of bounding frequencies obtained in the present analysis are plotted with those of Moorthy *et al.* [91] in Fig. 5.7, which shows that the agreement between the results is very good.

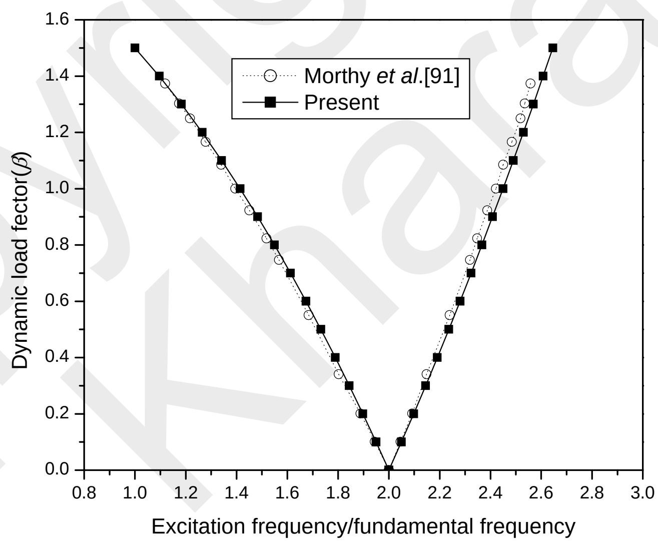


**Fig. 5.7 Comparison of upper and lower bounding frequencies for a simply supported laminated composite square plate**

***(i) Dynamic instability of stiffened square plate simply supported at all the four sides***

The square plate (0.6m×0.6m×0.00633m) is attached with a stiffener ($b_s$ = 0.0127m and $d_s$ = 0.0222m) on the bottom surface along its one center line. The load is acting at the edges uniformly in the direction of the stiffener. All the sides are simply supported. The non-dimensional excitation frequency ($\bar{\Omega} = \Omega a^2 \sqrt{\rho h / D}$) is obtained taking first mode buckling load of the stiffened plate. The static load factor ($\alpha$) is kept as 0.2. In the analysis the whole structure is divided in 8×8 mesh. The results of upper and lower bounding frequencies for the dynamic instability region are compared with the results given in Fig.10 of Srivastava *et al.* [141] in Table 5.8 and it shows that the results are in good agreement.

**Table 5.8 Non-dimensional excitation frequency of square simply supported stiffened plate uniaxial compression**

| $\beta$ | Present (8×8) | | Srivastava *et al.* [141] | |
|---|---|---|---|---|
| | $\bar{\Omega}^l$ | $\bar{\Omega}^u$ | $\bar{\Omega}^l$ | $\bar{\Omega}^u$ |
| 0 | 56.49 | 56.49 | 56.37 | 56.37 |
| 0.2 | 52.85 | 59.91 | 52.83 | 59.76 |
| 0.4 | 48.94 | 63.15 | 48.89 | 62.99 |
| 0.6 | 44.68 | 66.22 | 44.56 | 66.06 |
| 0.8 | 39.96 | 69.16 | 39.92 | 68.89 |
| 1 | 34.61 | 71.98 | | |
| 1.2 | 28.26 | 74.68 | | |

$^l$ Lower boundary of the instability zone, $^u$ Upper boundary of the instability zone

### 5.2.2 Problems under investigation

After obtaining the validity of the present analysis, the free vibration, buckling and dynamic instability analyses are carried out for laminated stiffened shell problem in Part-I and the buckling and dynamic instability analysis are carried out for an isotropic stiffened shell panel in Part-II. In both the cases different parameters are varied in a wide range to study the effect of these parameters on the behavior of the structure.

**(Part-I) Laminated composite stiffened shell panels**

The laminated composite stiffened shell panel problem without cutout is considered here. The numerical results are presented for the problem 1, part-I as described in 4.7, under varying parameters.

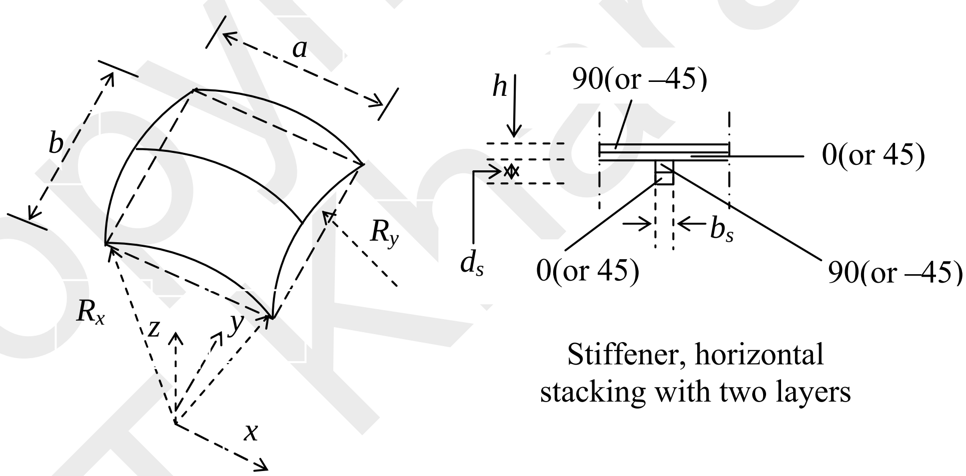


**Fig. 5.8 A doubly curved laminated shell panel with a central laminated stiffener $(xst)_b$**

**Numerical results**

The numerical results for the free vibration, buckling and dynamic instability analyses are presented for all four (flat plate, cylindrical shell panel, spherical shell panel and hyperbolic hyperboloid panel) laminated composite stiffened shell panels. The parameters like stiffener size, lamination scheme, stiffening scheme, stiffener eccentricity, stacking scheme in stiffener etc. are varied in a wide rage to study the effect of these parameters on the behavior of the structure. The detail is given below. In all the analysis the whole structure is divided in 8×8 mesh as this mesh size (8×8) is found sufficient to attain convergence and for validation of results (5.2.1).

**(a) Free vibration studies**

The free vibration analysis is carried out for 2, 4, 6 and 8 layer configurations taking ($d_s/b_s$) ratios of the stiffener as 2, 4, 6 and 8. The results obtained are presented in Table 5.9 and Table 5.10 for cross-ply and angle-ply stacking respectively.

**Table 5.9 Non-dimensional fundamental frequency of cross-ply laminated shell panel with cross-ply laminated stiffener**

| Shell panel/ stiffener lamination | $d_s/b_s$ | Flat plate | Cylindrical panel | Spherical panel | Hyperbolic hyperboloid panel |
|---|---|---|---|---|---|
| $(0/90)_1$ | 2 | 17.276 | 35.960 | 74.401 | 16.814 |
| | 4 | 28.686 | 35.928 | 77.189 | 28.690 |
| | 6 | 31.461 | 35.831 | 82.138 | 38.773 |
| | 8 | 31.358 | 35.464 | 86.019 | 44.199 |
| $(0/90)_2$ | 2 | 21.434 | 42.349 | 75.445 | 20.955 |
| | 4 | 32.096 | 47.857 | 77.837 | 31.249 |
| | 6 | 42.422 | 51.492 | 82.538 | 41.730 |
| | 8 | 48.882 | 51.208 | 87.871 | 50.341 |
| $(0/90)_3$ | 2 | 22.042 | 42.656 | 75.617 | 21.569 |

Continuing in the next page

| | | | | | |
|---|---|---|---|---|---|
| | 4 | 32.253 | 47.952 | 77.849 | 31.394 |
| | 6 | 42.605 | 53.887 | 82.397 | 41.759 |
| | 8 | 50.738 | 53.590 | 87.703 | 50.493 |
| $(0/90)_4$ | 2 | 22.231 | 42.754 | 75.671 | 21.762 |
| | 4 | 32.220 | 47.929 | 77.817 | 31.362 |
| | 6 | 42.537 | 54.705 | 82.277 | 41.648 |
| | 8 | 50.782 | 54.404 | 87.551 | 50.416 |

**Table 5.10 Non-dimensional fundamental frequency of angle-ply laminated shell panel with angle-ply laminated stiffener**

| Shell panel/ stiffener lamination | $d_s/b_s$ | Flat plate | Cylindrical panel | Spherical panel | Hyperbolic hyperboloid panel |
|---|---|---|---|---|---|
| $(45/-45)_1$ | 2 | 18.456 | 41.394 | 108.622 | 18.601 |
| | 4 | 19.973 | 41.351 | 106.707 | 19.864 |
| | 6 | 22.973 | 41.224 | 104.405 | 22.359 |
| | 8 | 26.972 | 40.992 | 102.137 | 25.697 |
| $(45/-45)_2$ | 2 | 24.221 | 57.729 | 123.078 | 23.788 |
| | 4 | 25.069 | 57.639 | 122.770 | 24.558 |
| | 6 | 27.303 | 57.442 | 122.130 | 26.544 |
| | 8 | 30.754 | 57.101 | 121.022 | 29.555 |
| $(45/-45)_3$ | 2 | 24.952 | 60.229 | 124.354 | 24.470 |
| | 4 | 25.743 | 60.132 | 124.017 | 25.188 |
| | 6 | 27.892 | 59.925 | 124.372 | 27.108 |
| | 8 | 31.265 | 59.569 | 122.274 | 30.065 |
| $(45/-45)_4$ | 2 | 25.196 | 61.080 | 124.795 | 24.698 |
| | 4 | 25.969 | 60.981 | 124.449 | 25.400 |
| | 6 | 28.091 | 60.771 | 124.801 | 27.298 |
| | 8 | 31.437 | 60.409 | 122.706 | 30.236 |

It is observed that the ply orientation has effect on vibration characteristics of the structure. The frequency of angle-ply orientation is found to be more compared to that of cross-ply scheme for cylindrical and spherical panels. But for flat and hyperbolic hyperboloid panels the frequency of angle-ply orientation is less compared to that of cross-ply scheme for $d_s/b_s$ equals to 4,6 and 8. Again the frequency of cylindrical and spherical panels is always more than that of flat plate and this is due to the fact that the curvature introduces additional stiffening effect. This situation in hyperbolic hyperboloid is different since the curvatures in the two principal directions are opposite in nature. In case of cross-ply lamination scheme, the frequency is found to be always increasing with the increase of stiffener depth except $(0/90)_1$in flat and cylindrical panel. In angle-ply stacking sequence the frequency is increasing with increase in stiffener depth for flat and hyperbolic hyperboloid panel, but in case of cylindrical and spherical panels the frequency is increasing with the increase in stiffener depth up to certain depth and after that the frequency is dropping down. With the increase in the number of layers the frequencies values are increasing in all the cases.

**(b)Buckling (Static stability)**

Similar to the vibration analysis presented above, the buckling analysis is carried out in this section and the results obtained in the form of non-dimensional buckling load parameters are presented in Table 5.11 and Table 5.12 for cross-ply and angle-ply stacking respectively. It is observed that the non-dimensional buckling loads of flat plate and hyperbolic hyperboloid panel for $(45/-45)_n$ and $d_s/b_s = 2$ is more compared to that of $(0/90)_n$ and $d_s/b_s = 2$. For cylindrical shell panel the buckling loads are more in case of angle-ply lamination compared to cross-ply lamination scheme. In spherical shell panel the non-dimensional buckling load for $(45/-45)_n$ is less compared to that of $(0/90)_n$ and $d_s/b_s = 2$, while it is more for other values of $d_s/b_s$ ratios. With the increase in stiffener depth the buckling load increases up to certain value and decreases thereafter in case of cross-ply arrangement while it increases and does not drop down in case of angle-ply arrangement.

**Table 5.11 Non-dimensional buckling load of cross-ply laminated shell panel with cross-ply laminated stiffener**

| Lamination (Shell panel/Stiffener) | ($d_s/b_s$) ratio | Flat plate | Cylindrical panel | Spherical panel | Hyperbolic hyperboloid panel |
|---|---|---|---|---|---|
| $(0/90)_1$ | 2 | 30.242 | 87.249 | 139.001 | 28.357 |
| | 4 | 51.961 | 87.354 | 139.015 | 50.603 |
| | 6 | 51.999 | 87.234 | 138.648 | 50.641 |
| | 8 | 51.829 | 86.768 | 112.516 | 50.491 |
| $(0/90)_2$ | 2 | 46.547 | 154.154 | 226.849 | 44.047 |
| | 4 | 104.371 | 154.138 | 226.698 | 97.899 |
| | 6 | 119.865 | 153.712 | 212.964 | 116.826 |
| | 8 | 113.870 | 113.886 | 112.928 | 116.144 |
| $(0/90)_3$ | 2 | 49.226 | 166.470 | 242.790 | 46.669 |
| | 4 | 105.400 | 166.430 | 242.610 | 98.808 |
| | 6 | 132.316 | 165.951 | 213.123 | 129.052 |
| | 8 | 113.948 | 113.964 | 112.996 | 116.250 |
| $(0/90)_4$ | 2 | 50.073 | 170.717 | 248.360 | 47.505 |
| | 4 | 105.179 | 170.751 | 248.170 | 98.606 |
| | 6 | 136.680 | 170.250 | 213.185 | 133.357 |
| | 8 | 113.980 | 113.996 | 113.023 | 116.283 |

**Table 5.12 Non-dimensional buckling load of angle-ply laminated shell panel with angle-ply laminated stiffener**

| Lamination (Shell panel/Stiffener) | $(d_s/b_s)$ ratio | Flat plate | Cylindrical panel | Spherical panel | Hyperbolic hyperboloid panel |
|---|---|---|---|---|---|
| $(45/\text{-}45)_1$ | 2 | 33.406 | 111.530 | 132.026 | 34.481 |
| | 4 | 39.887 | 126.283 | 175.215 | 39.385 |
| | 6 | 52.897 | 126.077 | 183.267 | 49.838 |
| | 8 | 72.565 | 125.328 | 182.087 | 65.668 |
| $(45/\text{-}45)_2$ | 2 | 59.383 | 196.003 | 212.475 | 56.766 |
| | 4 | 63.645 | 243.136 | 265.487 | 60.434 |
| | 6 | 75.501 | 296.434 | 327.062 | 70.494 |
| | 8 | 95.790 | 324.427 | 335.345 | 87.251 |
| $(45/\text{-}45)_3$ | 2 | 61.072 | 206.283 | 222.577 | 60.062 |
| | 4 | 65.414 | 254.039 | 275.656 | 63.568 |
| | 6 | 77.831 | 310.666 | 347.772 | 73.514 |
| | 8 | 99.466 | 348.480 | 360.197 | 90.273 |
| $(45/\text{-}45)_4$ | 2 | 63.190 | 209.863 | 226.097 | 61.183 |
| | 4 | 67.453 | 257.775 | 279.178 | 64.637 |
| | 6 | 79.813 | 315.470 | 354.877 | 74.543 |
| | 8 | 101.443 | 354.823 | 368.940 | 91.298 |

**(c) Dynamic stability**

After obtaining the free vibration and static buckling characteristics it is now pertinent to study the dynamic instability of stiffened shell panels. In all the dynamic stability analysis, the non-dimensional buckling load of the four layered cross-ply $(0/90)_2$ stiffened flat plate with $(0/90)_2$ stiffener ($d_s/b_s$= 4) is taken as the reference load, so as to plot the instability zones. The effect of parameters like lamination scheme, eccentricity of stiffener and the stacking sequence are presented taking the case of spherical shell panel with a single stiffener $(xst)_b$ attached to the bottom edge. The stiffener depth to breadth ratio ($d_s/b_s$) is kept as 4 and the static load factor ($\alpha$) is 0.2 in all cases. The dynamic load factor $\beta$ varies from 0.0 to 1.5.

### *i. Effect of lamination scheme*

The effect of lamination scheme on the excitation frequencies of stiffened spherical shell panel is presented in this section. The lamination schemes are $(0/90)_2$ and $(45/-45)_2$. The plots of the dynamic instability region (DIR) are shown in the Fig.5.9.

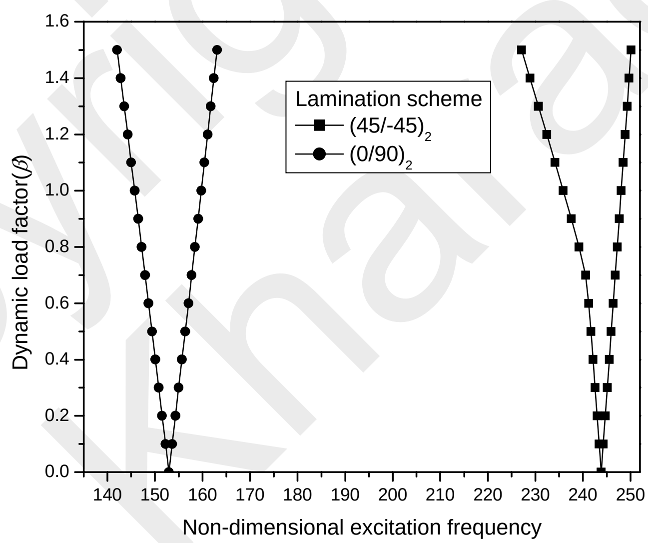


**Fig. 5.9 Effect of lamination scheme on dynamic instability region on spherical shell**

It is observed that for $(45/-45)_2$ lamination scheme the instability region shifts to the higher frequency zone in comparison to $(0/90)_2$ lay up. The plot shows that the onset of instability appears early for cross-ply scheme for stiffened spherical shell panel, indicating that the angle-ply lay up is more dynamically stable than the cross-ply scheme for the given stiffener configuration of the shell panel.

### *ii. Effect of geometry of the shells*

The comparison of the dynamic instability regions for $(45/-45)_2$ stiffened plate, cylindrical shell, spherical shell and hyperbolic hyperboloid shell are presented in this section. The plots are shown in the Fig. 5.10.

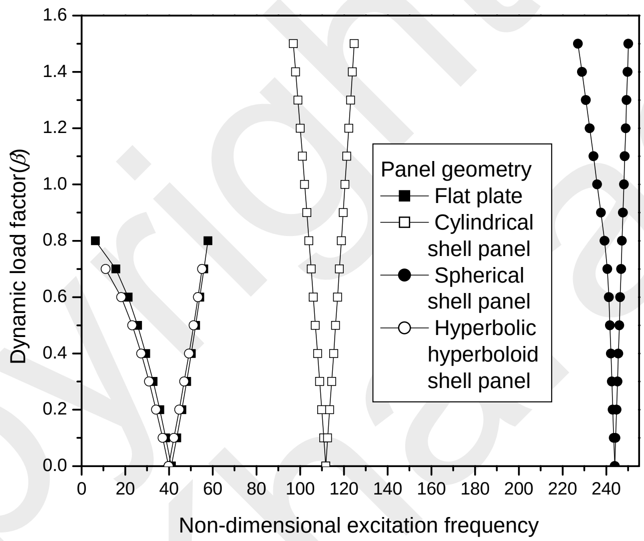


**Fig. 5.10 Effect of geometry on dynamic instability regions**

It is observed that the DIR for the spherical shell is at the highest frequency zone and the width of the instability region is smaller in this case as compared to the other cases. The DIR gradually shifts to the lower frequency zone side for cylindrical shell, hyperbolic hyperboloid shell and plate respectively.

This behaviour indicates that for a given ply lay up and stiffener configuration, the spherical stiffened shell panel is dynamically more stable in comparison to the other panel geometries.

***iii. Effect of eccentricity of the stiffener***

The eccentricity of the stiffener has its effect on the dynamic instability region of the stiffened shell. To illustrate this a $(45/-45)_2$ stiffened spherical shell panel with stiffener with bottom and top eccentricity is analyzed. From the plot (Fig. 5.11), it is observed that the width of the instability region is higher for the eccentric top stiffener.

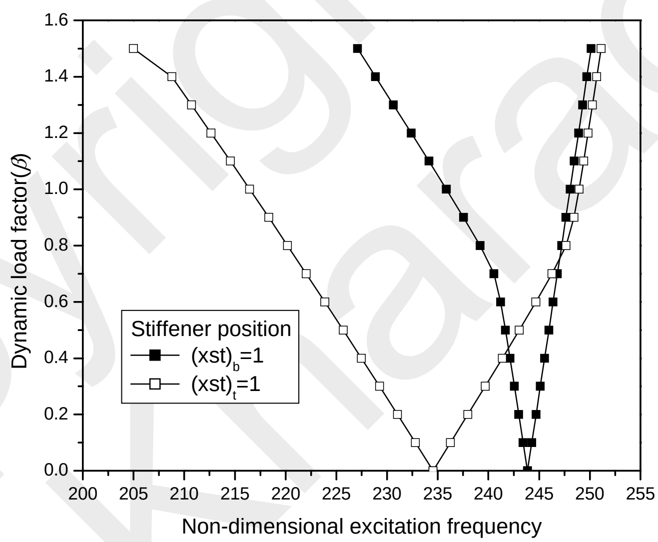


**Fig. 5.11 Effect of eccentricity of the stiffener on dynamic instability region of spherical shell**

### *iv. Effect of stacking in stiffener*

The effect of the stacking of layers in the stiffener on dynamic instability region of the spherical stiffened shell panel is presented in this section (Fig.5.12). The stiffener is eccentric to bottom surface.

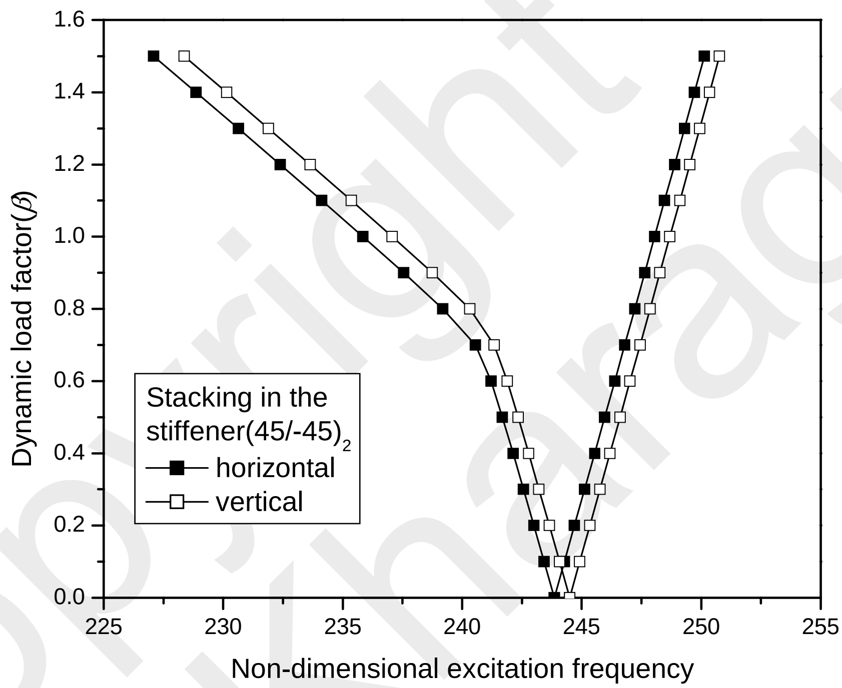


**Fig. 5.12a Effect of stacking in stiffener on dynamic in stability region of the spherical shell panel for $(45/-45)_2$ lamination scheme in the stiffener**

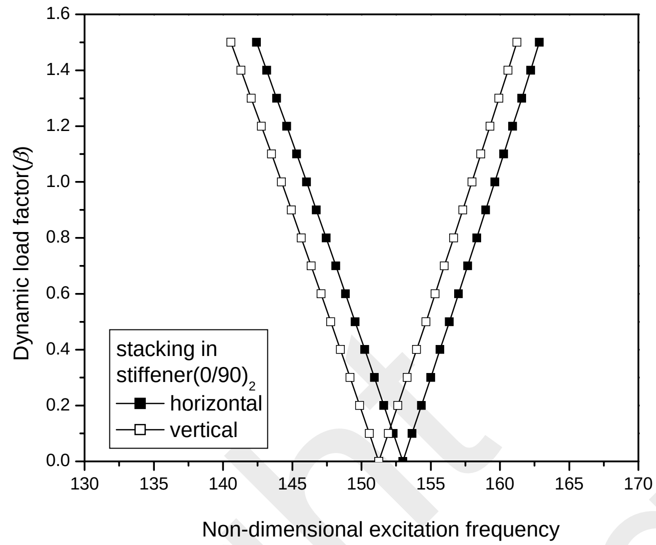


**Fig.5.12b Same as Fig. 5.12a but for $(0/90)_2$ lamination scheme in the stiffener**

In the vertical stacking the dynamic instability region shifts a little to the higher frequency zone side and the width of the instability regions are similar in the case of (45/-45) lamination scheme. But in the case of (0/90) lamination scheme the dynamic instability region shifts a little to the higher frequency zone side for horizontal stacking in the stiffener and here also the instability regions are almost same. This indicates that the stacking scheme of the stiffener has very little effect on the dynamic instability behaviour for the particular geometry and stiffener scheme of the spherical shell panel.

***v. Effect of stiffener scheme***

To find out the effect of number of stiffeners on dynamic instability region a spherical shell with $(45/-45)_2$ panel skin and stiffeners are taken. Four sets of stiffener are placed in both the directions. Set one is of one stiffener in both direction at position of $y$-stiffener at $x = 0$ and $x$-stiffener at $y = 0.5b$.

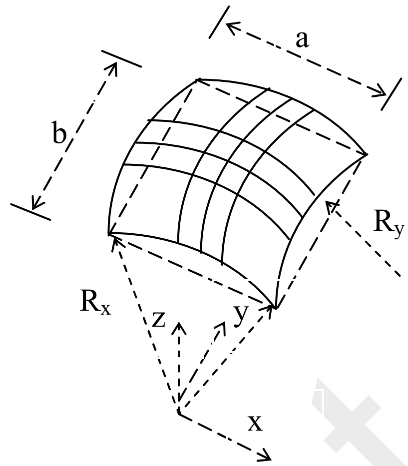


**Fig. 5.13 Stiffened spherical shell panel with three $(xst)_b$ and three $(yst)_b$ stiffeners**

Set two (Fig.5.13) is of three stiffeners in both direction at position of *y*-stiffeners at $x$ = -0.125*a*, 0 and 0.125*a* and *x*-stiffeners at $y$ = 0.375*b*, 0.5*b* and 0.625*b*. Set three is of five stiffeners in both direction at position of *y*-stiffeners at $x$ = -0.25*a*, -0.125*a*, 0, 0.125a and 0.25*a* and *x*-stiffeners at $y$ = 0.25*b*, 0.375*b*, 0.5*b*, 0.625*b* and 0.75*b*. Set four is of seven stiffeners in both direction at position of *y*-stiffeners at $x$ = -0.375*a*, -0.25*a*, -0.125*a*, 0, 0.125*a*, 0.25*a* and 0.375*a* and *x*-stiffeners at $y$ = 0.125*b*, 0.25*b*, 0.375*b*, 0.5*b*, 0.625*b*, 0.75*b* and 0.875*b*. The dynamic instability regions are plotted in the Fig. 5.14.

It is observed from Fig 5.14 that the dynamic instability zone for the stiffener arrangement of set two ($(xst)_b$=3 and $(yst)_b$=3) is at the higher frequency zone side. It indicates that this arrangement is dynamically more stable in comparison to the other stiffener schemes.

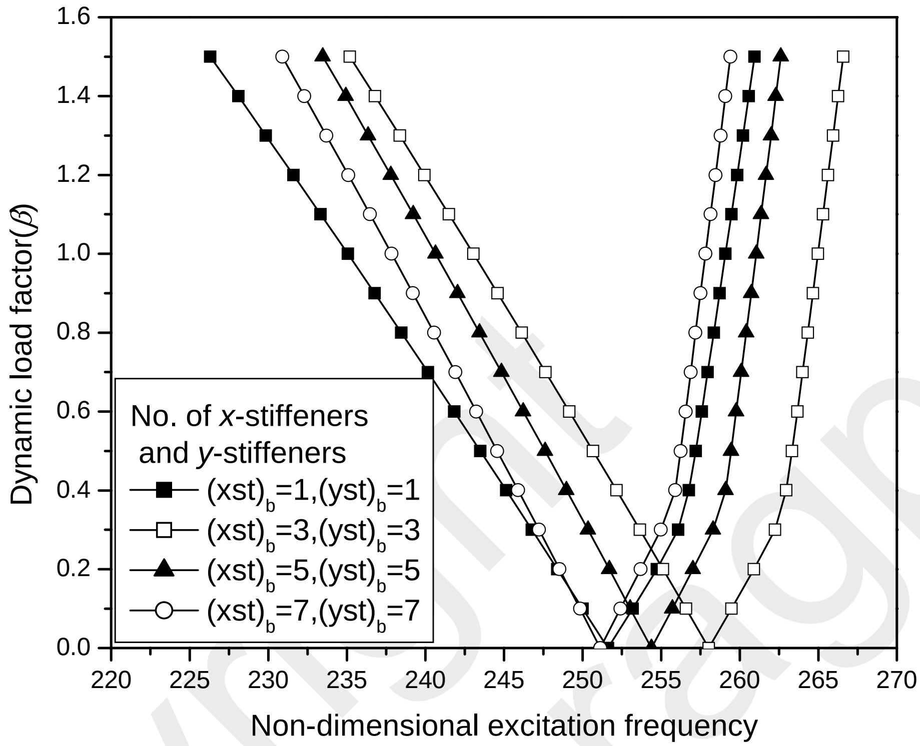


**Fig.5.14 Effect of stiffener scheme on dynamic in stability region of the spherical shell panel**



**(Part-II) Isotropic stiffened shell panels**

The isotropic stiffened shell panel problem without cutout is considered here. The numerical results are presented for the problem 1, part-II as described in 4.7, under varying parameters.

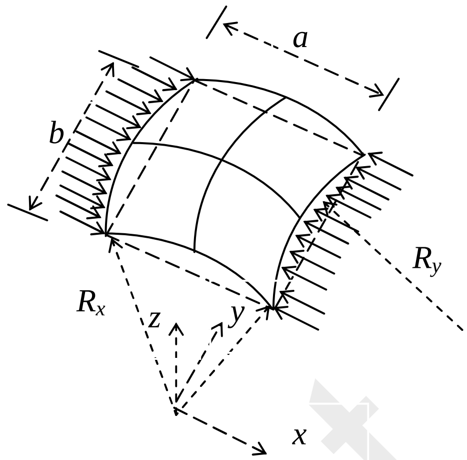


**Fig. 5.15 A doubly curved shell panel with two orthogonal stiffeners**

**Numerical results**

In this study the buckling and dynamic instability analyses are carried out for a stiffened shell problem where its different parameters are varied in a wide rage to study the effect of these parameters on the behavior of the structure. The detail is given below. In all the analysis the whole structure is divided in 8×8 mesh.

**(a) Buckling (Static stability)**

The buckling analysis of the shell panels is carried out in this section. The non-dimensional buckling load parameters are presented for stiffeners in *x*-orientation, *y*-orientation and orthogonal stiffeners in Table 5.13, Table 5.14 and Table 5.15 respectively considering $d_s/b_s$ to be 2, 4, 6 and 8. In all the cases the number of stiffeners varied is 1, 3, 5 and 7.

**Table 5.13 Non-dimensional buckling load of shell panel with x-orientation stiffeners**

| Number of stiffeners | $(d_s/b_s)$ ratio | Flat plate | Cylindrical panel | Spherical panel | Hyperbolic hyperboloid panel |
|---|---|---|---|---|---|
| 1 | 2 | 119.168 | 347.952 | 435.232 | 103.468 |
| | 4 | 189.012 | 355.486 | 442.226 | 185.162 |
| | 6 | 195.585 | 357.387 | 443.259 | 191.386 |
| | 8 | 197.158 | 355.148 | 437.476 | 193.389 |
| 3 | 2 | 198.872 | 397.412 | 585.987 | 176.364 |
| | 4 | 381.840 | 494.936 | 604.195 | 408.698 |
| | 6 | 388.482 | 497.371 | 603.536 | 416.009 |
| | 8 | 385.208 | 486.731 | 566.344 | 412.121 |
| 5 | 2 | 238.069 | 395.207 | 1108.485 | 218.262 |
| | 4 | 835.983 | 901.951 | 1197.502 | 716.747 |
| | 6 | 956.216 | 956.254 | 955.062 | 958.448 |
| | 8 | 565.632 | 565.702 | 564.971 | 566.807 |
| 7 | 2 | 252.220 | 404.863 | 1163.032 | 233.211 |
| | 4 | 870.918 | 979.529 | 1648.037 | 807.646 |
| | 6 | 954.445 | 954.699 | 953.595 | 956.642 |
| | 8 | 564.936 | 565.059 | 564.381 | 566.154 |

It is observed from the table that in case of spherical panel the buckling load is highest compared to other panels. When the ratio $d_s/b_s$ is increasing from 2 to 4 in spherical panel with single stiffener the buckling load is increasing, the rate of increase is around 1.5 percent, but with seven stiffeners the rate of increase is around 40.0 percent. Further increase in $d_s/b_s$ ratio the buckling load is decreasing. Similar nature is observed in case of cylindrical panel. For flat plate and hyperbolic hyperboloid panel when the ratio $d_s/b_s$ is increasing from 2 to 4 with single stiffener the rate of increase in buckling load is around 60 percent and with seven stiffeners the rate of increase is around 250 percent. When the number of stiffener is increasing from 1 to 3 with $d_s/b_s$ = 4 the rate of increase in buckling load for spherical and cylindrical panel is around 37 percent, but for flat plate and hyperbolic hyperboloid panel the increase in buckling load is around 200 percent. It can be concluded from the analysis that it is better to increase the number of stiffener instead of increasing the size of stiffeners for resisting the buckling load. The non-dimensional buckling load parameters of the shell panels for y-orientation stiffeners are presented in Table 5.14.

**Table 5.14 Non-dimensional buckling load of shell panel with y-orientation stiffeners**

| Number of stiffeners | ($d_s/b_s$) ratio | Flat plate | Cylindrical Panel | Spherical panel | Hyperbolic hyperboloid panel |
|---|---|---|---|---|---|
| 1 | 2 | 67.036 | 335.981 | 351.404 | 145.187 |
| | 4 | 73.053 | 339.095 | 357.001 | 182.412 |
| | 6 | 77.535 | 340.404 | 361.155 | 188.150 |
| | 8 | 80.935 | 341.423 | 364.290 | 191.521 |
| 3 | 2 | 95.191 | 344.839 | 361.672 | 267.030 |
| | 4 | 130.465 | 355.017 | 372.459 | 276.256 |
| | 6 | 140.736 | 368.332 | 393.586 | 279.521 |
| | 8 | 146.315 | 371.333 | 407.647 | 281.772 |
| 5 | 2 | 143.779 | 356.441 | 373.294 | 322.779 |
| | 4 | 232.242 | 382.432 | 397.899 | 352.874 |
| | 6 | 270.647 | 411.652 | 424.865 | 381.951 |
| | 8 | 288.830 | 427.353 | 438.976 | 398.483 |
| 7 | 2 | 177.561 | 368.708 | 387.251 | 333.180 |
| | 4 | 400.627 | 416.329 | 432.242 | 394.700 |
| | 6 | 677.818 | 552.996 | 557.022 | 545.555 |
| | 8 | 935.664 | 768.074 | 772.204 | 764.994 |

It is observed that in all the cases that the non-dimensional buckling load parameters are less compared to the non-dimensional buckling load parameters with *x*-orientation stiffener except for the case of seven stiffeners with $d_s/b_s = 8$. The results obtained in the form of non-dimensional buckling load parameters are presented in Table 5.15 for the stiffened shell panels with orthogonal stiffeners.

**Table 5.15 Non-dimensional buckling load of shell panel with orthogonal stiffeners**

| Number of stiffeners in both directions | $(d_s/b_s)$ ratio | Flat plate | Cylindrical Panel | Spherical panel | Hyperbolic hyperboloid panel |
|---|---|---|---|---|---|
| 1 | 2 | 191.247 | 352.793 | 450.624 | 188.175 |
| | 4 | 212.044 | 364.242 | 467.509 | 212.113 |
| | 6 | 220.679 | 367.993 | 472.806 | 223.083 |
| | 8 | 223.516 | 365.332 | 467.146 | 227.105 |
| 3 | 2 | 383.995 | 523.113 | 671.022 | 402.247 |
| | 4 | 458.760 | 559.915 | 702.158 | 499.304 |
| | 6 | 469.355 | 564.470 | 702.563 | 511.229 |
| | 8 | 462.215 | 547.192 | 622.373 | 501.878 |
| 5 | 2 | 516.371 | 735.254 | 1258.192 | 497.756 |
| | 4 | 1253.092 | 1281.195 | 1392.868 | 1257.805 |
| | 6 | 1135.778 | 1150.735 | 1188.344 | 1143.978 |
| | 8 | 685.021 | 685.870 | 681.277 | 697.019 |
| 7 | 2 | 547.602 | 745.516 | 1297.399 | 529.386 |
| | 4 | 2060.793 | 1874.418 | 2375.505 | 1971.070 |
| | 6 | 1985.650 | 2003.551 | 1960.270 | 2063.188 |
| | 8 | 1053.639 | 1062.681 | 1034.510 | 1098.874 |

It is observed that in all the cases that the non-dimensional buckling load parameters are more compared to the non-dimensional buckling load parameters with x-orientation stiffener and y-orientation stiffener. The rate of increases of buckling load with seven stiffeners in both directions for spherical shell panel is about 45.0 percent compared to the buckling load with seven x-orientation stiffeners.

**(b) Dynamic stability**

The dynamic instability study of stiffened shell panels are presented in this section. In all the dynamic stability analysis, the non-dimensional buckling load of the spherical shell panel with single x-stiffener ($d_s/b_s$=2) is taken as the reference load, so as to plot the instability zones. The effect of parameters stiffener size, eccentricity of stiffener, stiffening scheme and number of stiffeners are presented for the stiffened shell panel The stiffener depth to breadth ratio ($d_s/b_s$) is kept as 4 and the static load factor ($\alpha$) is 0.4 in all cases. The dynamic load factor $\beta$ varies from 0.0 to 1.5.

***i. Effect of orientation of the stiffener***

The effect of orientation of stiffeners (panel with *x*-stiffener, *y*-stiffener or cross-stiffener) is studied taking all the panels with five stiffeners ($d_s/b_s$ = 4). The stiffeners are attached to the bottom surface of the panel. The variations of non-dimensional excitation frequencies with dynamic load factor ($\beta$) for stiffened spherical, cylindrical, hyperbolic hyperboloid and flat panel are shown in Fig 5.16a-d respectively.

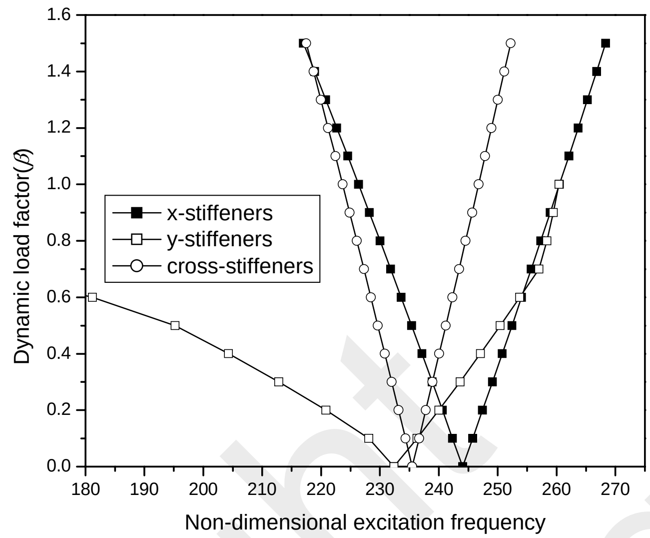


**Fig.5.16a Effect of stiffener orientation on dynamic instability region of spherical shell panel**

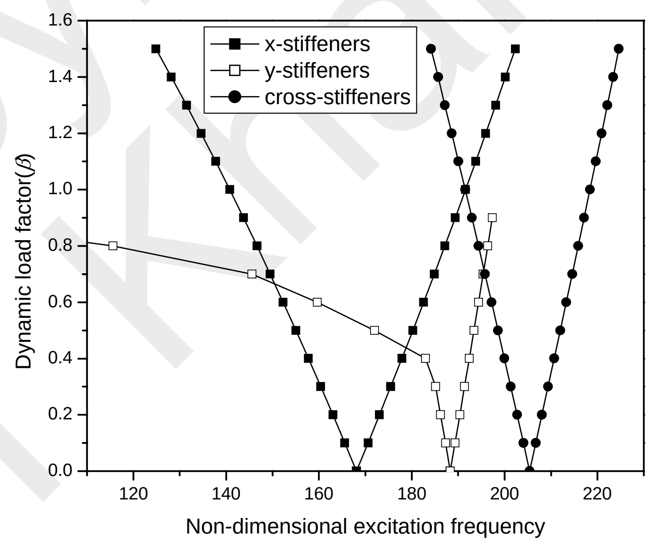


**Fig.5.16b As Fig 5.16a, but for cylindrical shell panel**

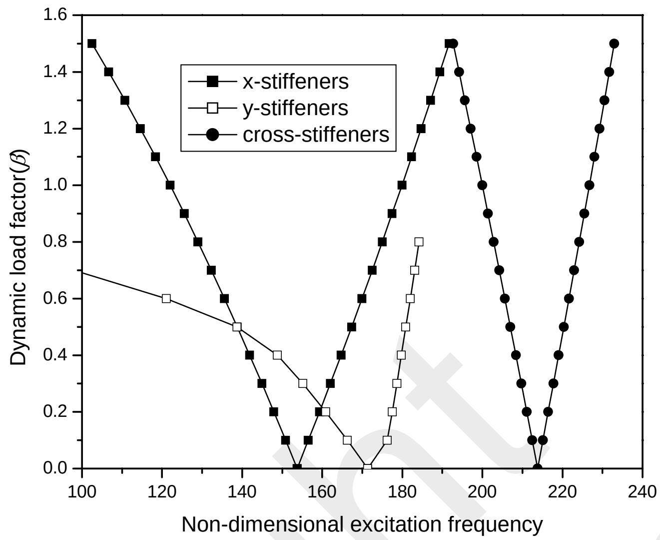


**Fig. 5.16c As Fig 5.16a, but for hyperbolic hyperboloid shell panel**

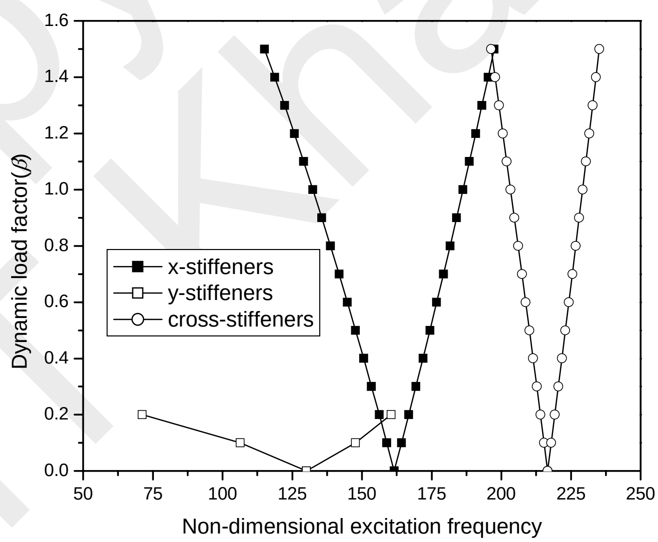


**Fig. 5.16d As Fig 5.16a, but for flat panel**

It is observed in the case of stiffened spherical panel that the panel is dynamically more stable with *x*-stiffeners only. The dynamic instability region (DIR) with *x*-stiffeners is at higher frequency zone with smaller width. In the other panels the DIR with cross-stiffeners is at higher frequency zone with smaller width. All panels are dynamically less stable with *y*-stiffeners.

### *ii. Effect of eccentricity of the stiffener*

The effect of eccentricity of stiffeners is studied taking stiffened spherical, cylindrical and hyperbolic hyperboloid panel with five *x*-stiffeners ($d_s/b_s$ = 4). The variations of non-dimensional excitation frequencies with dynamic load factor ($\beta$) for stiffened spherical, cylindrical and hyperbolic hyperboloid shell panels are shown in Fig 5.17a-c, respectively. It is observed that the dynamic instability region is at higher frequency zone for eccentric top stiffener in all the three cases.

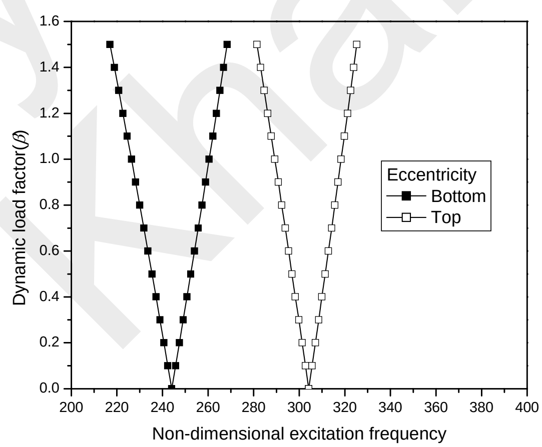


**Fig. 5.17a Effect of stiffener eccentricity on dynamic instability region of spherical shell panel**

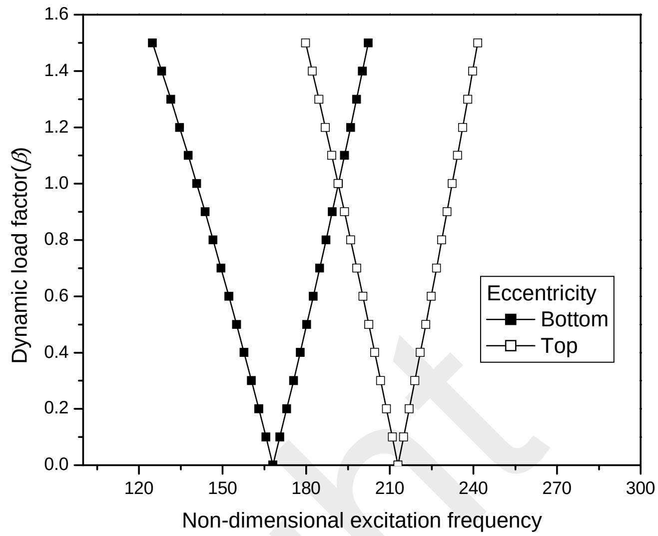


**Fig. 5.17b As Fig. 5.17a, but for cylindrical shell panel**

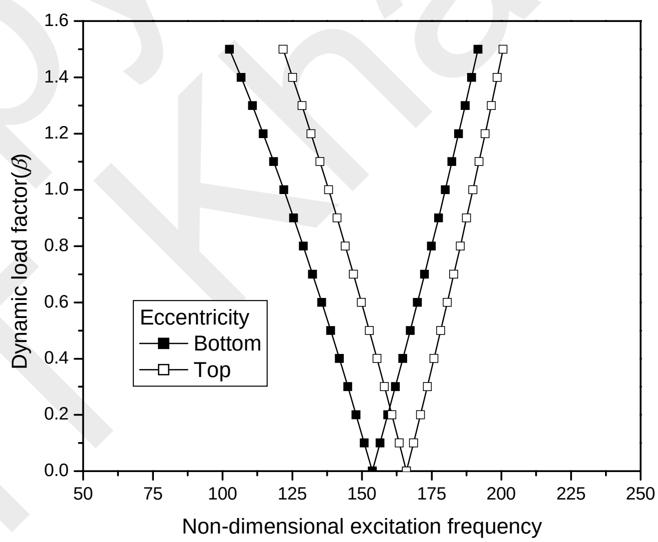


**Fig. 5.17c As Fig 5.17a, but for hyperbolic hyperboloid shell panel**

***iii. Effect of size of the stiffener***

The effect of size of stiffeners on dynamic instability region is presented in this section. The stiffened spherical panel with five x-stiffeners is used to carryout the analysis. The stiffener depth to breadth ratio ($d_s/b_s$) is taken as 2, 4, 6 and 8. The stiffeners are fixed to the bottom surface of the panel. It is observed from Fig 5.18 that the dynamic instability region is at higher frequency zone for $d_s/b_s = 6$.

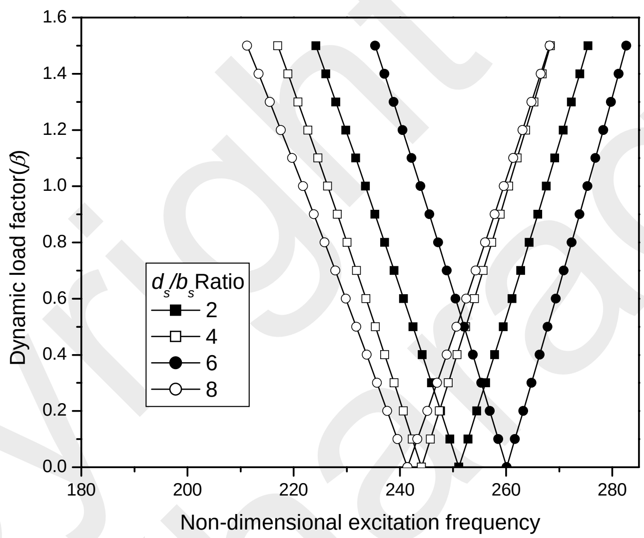


**Fig. 5.18 Effect of stiffener size on dynamic instability region of spherical shell panel**

***iv. Effect of number of stiffeners***

The number of the stiffeners has effect on the dynamic instability region of the stiffened shell panel. To illustrate this a stiffened spherical shell panel with *x*-stiffener and cross-stiffener arrangements are used in the analysis. The stiffeners depth to breadth ratio ($d_s/b_s$) is kept as 4 and is attached to the bottom surface of the panels.

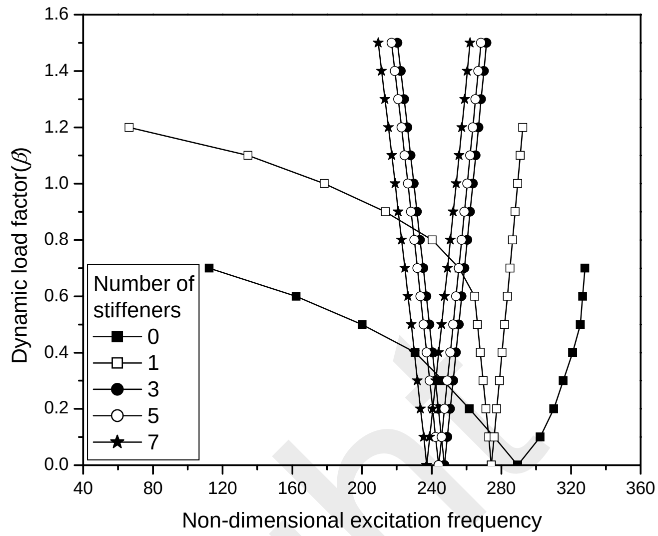


**Fig. 5.19a Effect of stiffener scheme on dynamic in stability region of the spherical shell panel (*x*-stiffeners)**

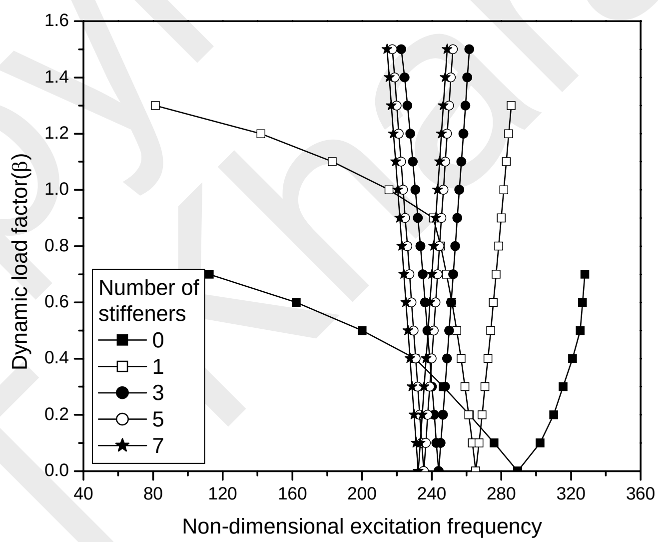


**Fig. 5.19b Effect of stiffener scheme on dynamic in stability region of the spherical shell panel (cross-stiffeners)**

It is observed from the Fig 5.19a that the stiffened spherical shell panel with 3,5 and 7 x-stiffeners the dynamic instability zones is almost same. However the panel with single stiffener the instability zone shifts a little to the higher frequency zone but when dynamic load factor $\beta$ is more than 0.9 the instability zone widens moving towards the lower frequency side. The dynamic instability zone for the panel without stiffener is at higher frequency zone compared to the stiffened panel but when $\beta$ increases beyond 0.4, the instability zone starts widening entering to the lower frequency side. Similar behaviour is observed for the stiffened spherical panel with cross-stiffener arrangements Fig 5.19b.

## 5.3 Laminated composite stiffened shell panels without cutout under non-uniform loading

The problem of laminated composite stiffened shell panels without cutout with four types of non-uniform loading (Type-I, Type-II, Type-III and Type-IV as Fig.4.3) is investigated for buckling (static stability), vibration and dynamic stability characteristics in this section. The convergence and accuracy of the proposed model is established again for non-uniform loading cases.

### 5.3.1 Convergence and validation study

The convergence and accuracy of the proposed method are established again by comparing the results of various problems with those of earlier investigators' available in the literature.

### *(a)Buckling of isotropic plate with concentrated edge load*

The problem of un-stiffened simply supported plate ($a \times b$) is also used to carry out the convergence study. The *a/h* ratio of the plate is 100. The plate is subjected to concentrated loading (Type-IV) in the two opposite edges with *c/b*=0.5. The whole structure is modeled with a number of mesh sizes to carry out the analysis. The first mode non-dimensional buckling loads ($\overline{P}_{cr} = P_{cr} * b / D$) are shown in Table 5.16 for three aspect ratios for all the mesh sizes. It shows a rapid convergence with mesh refinement. Again a mesh size of 10×10 is found to be sufficient to attain the convergence. For validation, the results are compared with those of Leissa and Ayoub [63] and Brown [18]. The results obtained in these studies (Leissa and Ayoub [63] and Brown [18]) are found to be in good agreement compared to present results.

**Table 5.16 The non-dimensional buckling load for a plate centrally loaded by concentrated force (*c/b*=0.5), all sides simply supported with *a/b*=0.5, *a/b*=1.0 and *a/b*=2.0.**

| Mesh size | *c/b*=0.5 | | |
|---|---|---|---|
| | *a/b*=0.5 | *a/b*=1.0 | *a/b*=2.0 |
| 2×2 | 53.541 | 73.397 | 161.648 |
| 4×4 | 29.993 | 25.898 | 42.036 |
| 6×6 | 29.561 | 25.645 | 29.790 |
| 8×8 | 29.586 | 25.644 | 28.791 |
| 10×10 | 29.603 | 25.647 | 28.656 |
| 12×12 | 29.611 | 25.649 | 28.625 |
| 14×14 | 29.614 | 25.649 | 28.616 |
| 16×16 | 29.616 | 25.650 | 28.613 |
| Leissa and Ayoub [63] | 30.090 | 25.814 | 28.482 |
| Brown [18] | 29.530 | 25.446 | 28.274 |

***(b) Buckling of a unstiffened rectangular plate with partial load starting from one end***

The problem of the square plate (*a/b* = 1) as Fig 5.20 having simply supported boundary conditions at its four edges with partial load starting from one end (Type-I) to its full length is investigated. The full plate is modeled with 8×8 mesh for the analysis. The results are plotted along with the results of Deolasi *et al.* [31] in the Fig 5.21. It shows the results are in good agreement.

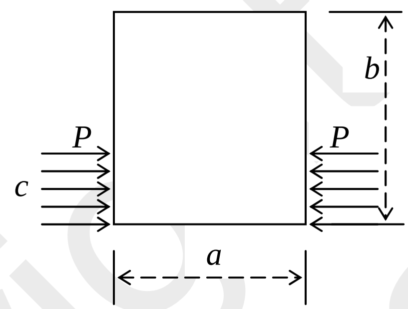


**Fig. 5.20 Simply supported square plate with partial load starting from one end**

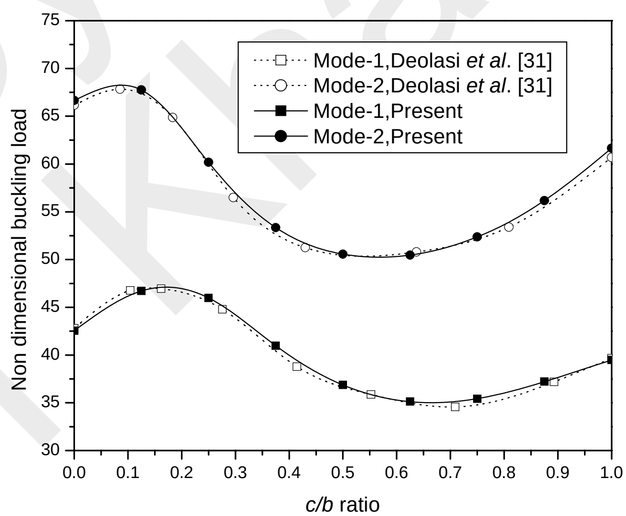


**Fig 5.21 Comparisons of non-dimensional buckling load.** $\overline{P}_{cr} = P_{cr} b / D$

***(c) Dynamic instability of eccentrically stiffened square plate simply supported at all the four sides***

The square plate (0.6m×0.6m×0.00633m) is attached with a stiffener ($b_s$ = 0.0127m and $d_s$ = 0.0222m) on the bottom surface along its one center line. The non-uniform loading Type-I is acting in the direction of the stiffener. All the sides are simply supported. The loading width considered are *c/b*=0.2 and *c/b*=0.6. The non-dimensional excitation frequency ($\bar{\Omega} = \Omega a^2 \sqrt{\rho h / D}$) is obtained taking first mode buckling load of the stiffened plate. The static load factor is kept as 0.2. The whole plate is divided with 10×10 mesh. The results of upper and lower bounding frequencies for the dynamic instability region are compared with the results given in Fig. 10 of Srivastava *et al.* [141] in Fig 5.22 and it shows that the results are in good agreement.

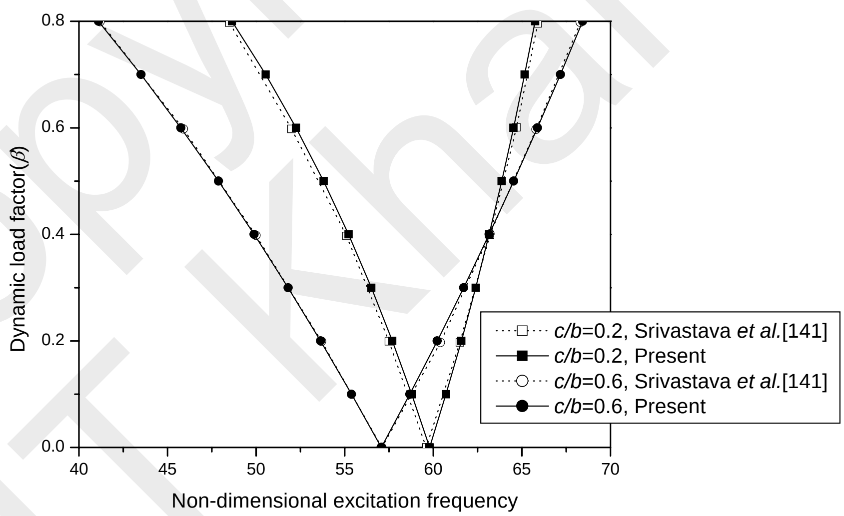


**Fig. 5.22 Dynamic instability region for eccentrically stiffened square plate.**

### 5.3.2 Problems under investigation

After obtaining the validity of the present analysis for non-uniform loading cases, the buckling, vibration with the applied and dynamic instability analyses are carried out for a laminated composite stiffened shell problem (Problem 2, described in 4.7) (Fig 5.23) for all the four types of non-uniform loading cases (Fig.4.3). In all cases the different parameters are varied in a wide range to study the effects of these parameters on the behavior of the shell panels.

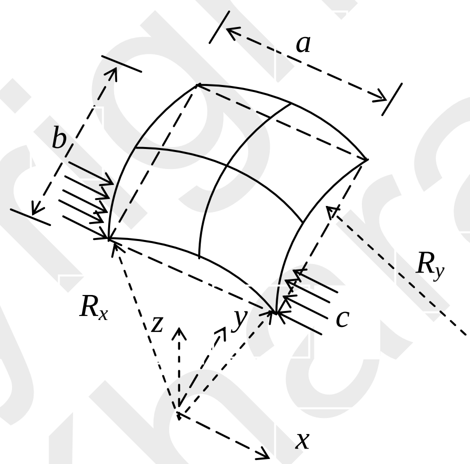


**Fig.5.23 A doubly curved shell panel with two orthogonal stiffeners with loading Type-I**

### Numerical results

The numerical results for the buckling, vibration with applied load and dynamic instability analyses are presented for all four (flat plate, cylindrical shell panel, spherical shell panel and hyperbolic hyperboloid panel) laminated composite stiffened shell panels with the four types of non-uniform loading cases (Fig. 4.3). The parameters like loading type, stiffener size, lamination scheme, stiffening scheme, stiffener eccentricity, stacking scheme in stiffener etc. are varied in a wide rage to study the effect of these parameters on the behavior of the structure. The detail is given below. In all the analysis the whole structure is divided in 10×10 mesh as this mesh size (10×10) is found sufficient to attain convergence and for validation of results (5.3.1).

**Loading Type-I**

The vibration, buckling and dynamic stability characteristics of the laminated composite stiffened shell problem (Fig.5.23) for the partial loading Type-I (Localized edge loading from one end of two opposite side) are presented in this section. The different parameters are varied in a wide rage to study the effect of these parameters on the behavior of the shell panels. The details are described below.

### (a) Buckling

The effects of bandwidth ratio(*c/b*) of the patch loading for all the four types of stiffened shell panels are discussed here. The load width ratios *c/b* are taken as 0.1, 0.2, 0.3,…, 1.0 for the buckling analysis. The panels are attached with a single stiffener $(xst)_b$ along the center line in all the cases. The stiffener depth to breadth ratio ($d_s/b_s$) is kept as 2.0. The lamination in the panel skin and stiffeners is taken as $(0/90)_1$. The stacking scheme in the stiffener is horizontal. The laminated composite stiffened shell panels are simply supported (SSSS) along all the four sides. The plots in the Fig.5.24 show the variation of non-dimensional buckling load for the laminated stiffened flat, cylindrical, spherical, and hyperbolic hyperboloid panels.

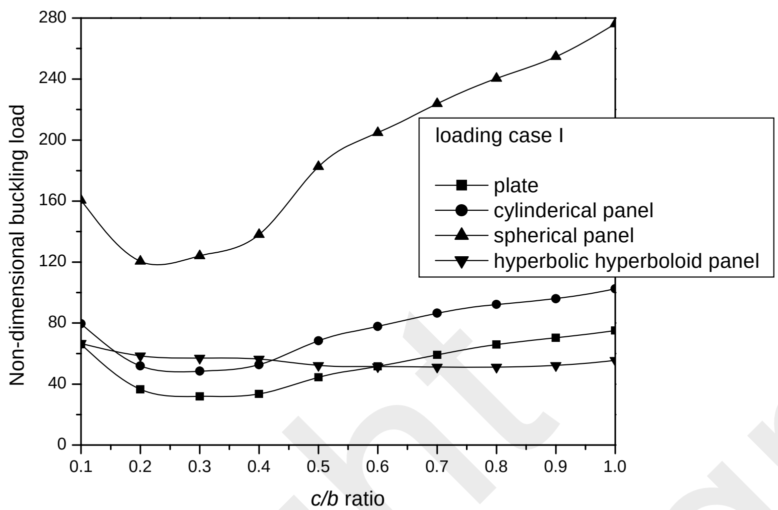


**Fig. 5.24 Variation of non-dimensional buckling load with *c/b* ratios**

It is observed from Fig. 5.24 that when the *c/b* ratio is 0.1, it takes higher load for the buckling of the hyperbolic hyperboloid panel. When *c/b* is increasing the buckling load is decreasing gradually up to *c/b* = 0.8 and then again it is increasing a little up to *c/b* =1.0. However the variation is not very significant. In flat plate, cylindrical and spherical panel when c/b ratio is increased from 0.1 to 0.2 there is a significant reduction (about 45 percent in plate and 35 percent in cylindrical and 25 percent in spherical panel) in the buckling load. After that the reduction in buckling load is not prominent, and then an increase in buckling load is observed from *c/b*, 0.3 in plate and cylindrical panel, and from *c/b* = 0.2 in spherical panel to *c/b* = 1.0. The rate of increase in spherical panel is higher compared to plate and cylindrical panel. This may be due to the fact that for loading near the edges, the edge restraint increases the capacity to withstand higher loads and as *c/b* increases the effect of edge restraint decreases but after that again the load carrying capacity increase due to the stiffener present along the center line of the panels.

**(b) Vibration**

The above mentioned stiffened shell panels are studied for the variation of frequency with the loading. The effects of all *c/b* ratios (0.1, 0.3, 0.5, 0.8 and 1.0) are considered for all the four types of panels. Figures 5.25-5.28 show the plot of the variation of first mode frequencies with the loading for plate, cylindrical, spherical, and hyperbolic hyperboloid panels respectively. It is observed from the plots (Fig.5.25-5.28) that when the load is zero the frequencies correspond to natural frequency of vibration. As the load increases the frequency of vibration gradually decreases and becomes zero when the load reaches the critical value.

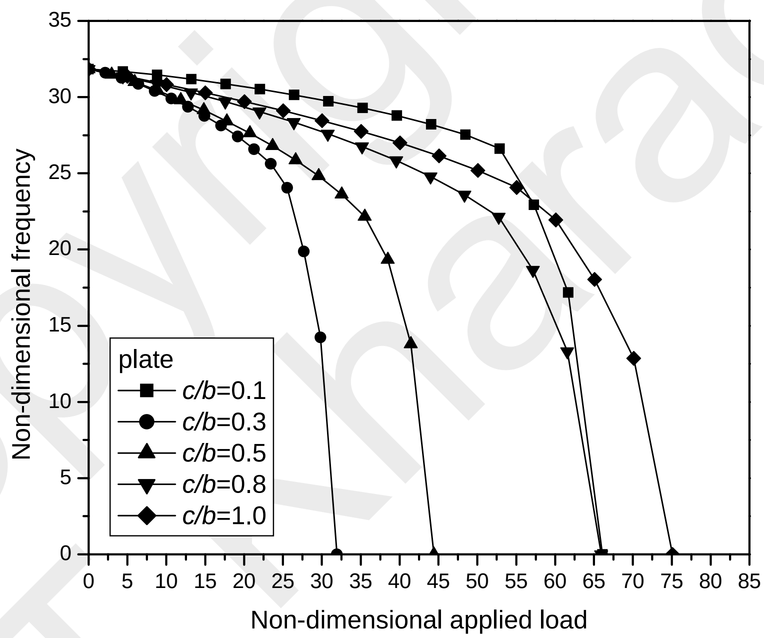


**Fig. 5.25 Variation of frequency with load, plate**

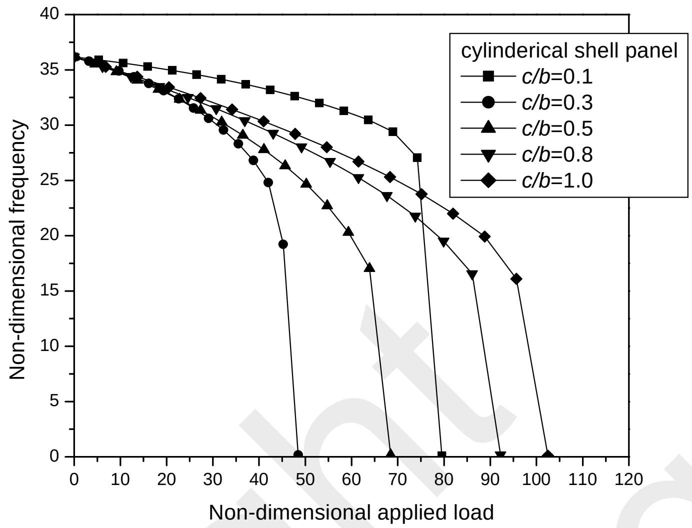


**Fig. 5.26 Same as Fig. 5.25 but for, cylindrical panel**

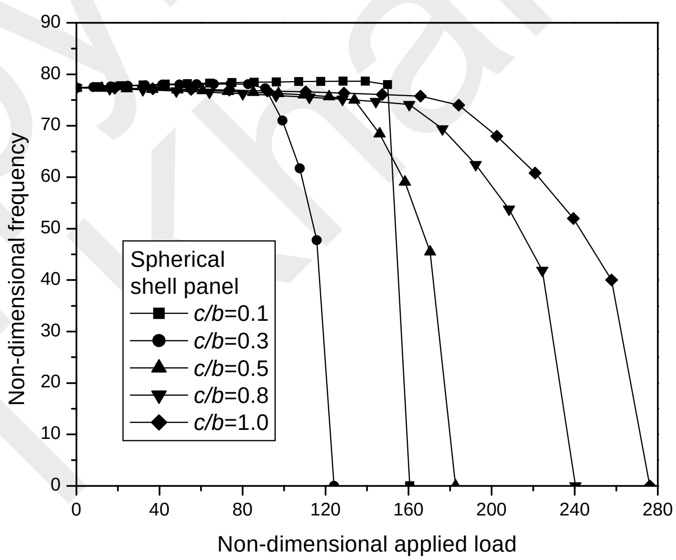


**Fig. 5.27 same as Fig. 5.25 but for, spherical panel**

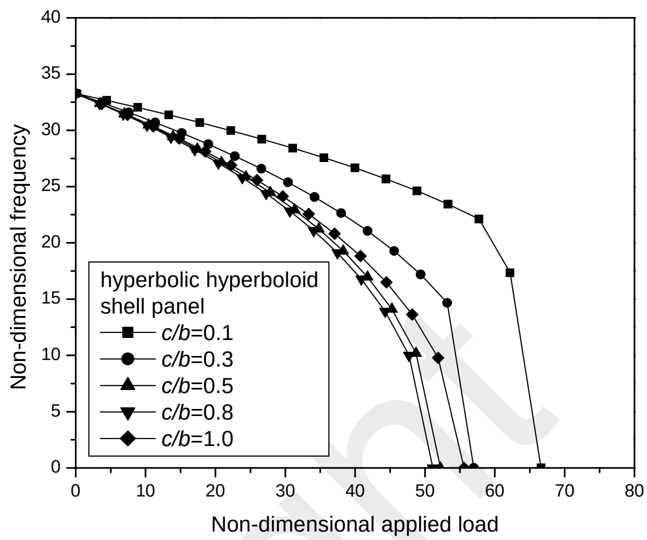


**Fig. 5.28 same as Fig. 5.25 but for, hyperbolic hyperboloid shell panel**

## (c) Dynamic stability

After obtaining the free vibration and static buckling characteristics it is now pertinent to study the dynamic instability of stiffened shell panels. In all the dynamic stability analysis, the non-dimensional buckling stress, with uniformly loaded ($c/b$ = 1.0, in Type-I loading), two layered simply supported (SSSS) cross-ply $(0/90)_2$ stiffened flat plate with a single $(xst)_b$ stiffener ($d_s/b_s$= 2) along the center line with $(0/90)_2$ lamination scheme and horizontal stacking, is taken as the reference load, so as to plot the instability zones. The effect of parameters like number of stiffeners, stiffening scheme ($x$-direction and orthogonal stiffeners), number of layers, lamination scheme, eccentricity of stiffener, stacking sequence, stiffener size, boundary condition etc. on dynamic instability regions are presented. The static load factor ($\alpha$) is 0.2 in all cases. The dynamic load factor ($\beta$) varies from 0.0 to 1.5.

***i. Effect of load bandwidth ratio (c/b)***

The effect of load bandwidth ratio(*c/b*) on dynamic instability regions (DIR) for laminated composite stiffened flat, cylindrical, spherical, and hyperbolic hyperboloid panels is analyzed here. The panels are attached with a single $(xst)_b$ stiffener along the center line in all the cases. The stiffener depth to breadth ratio ($d_s/b_s$) is kept as 2.0. The lamination scheme in the panel skin and stiffeners is taken as $(0/90)_1$. The stacking scheme in the stiffener is horizontal. The laminated composite stiffened shell panels are simply supported (SSSS) along all the four sides. The load width ratios *c/b* are taken as 0.1, 0.2, 0.3,…, 1.0 for the dynamic stability analysis. Figures 5.29-5.32 show the plots of the dynamic instability regions for plate, cylindrical, spherical, and hyperbolic hyperboloid panels respectively.

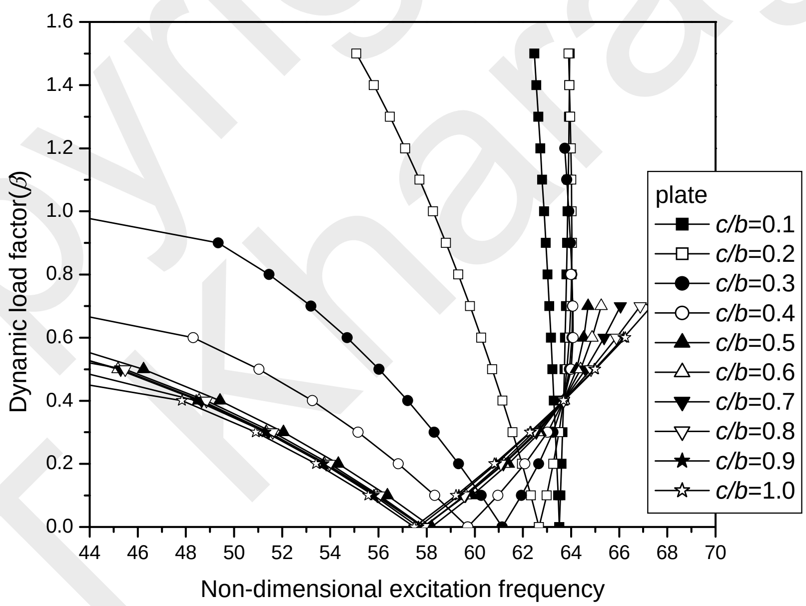


**Fig. 5.29 Dynamic instability region for different *c/b* ratio, plate**

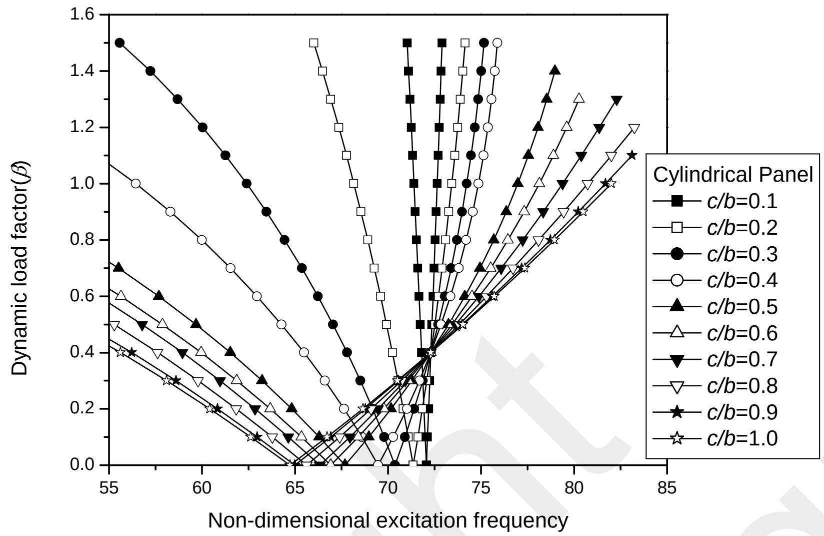


**Fig. 5.30 Same as Fig. 5.29 but for, cylindrical panel**

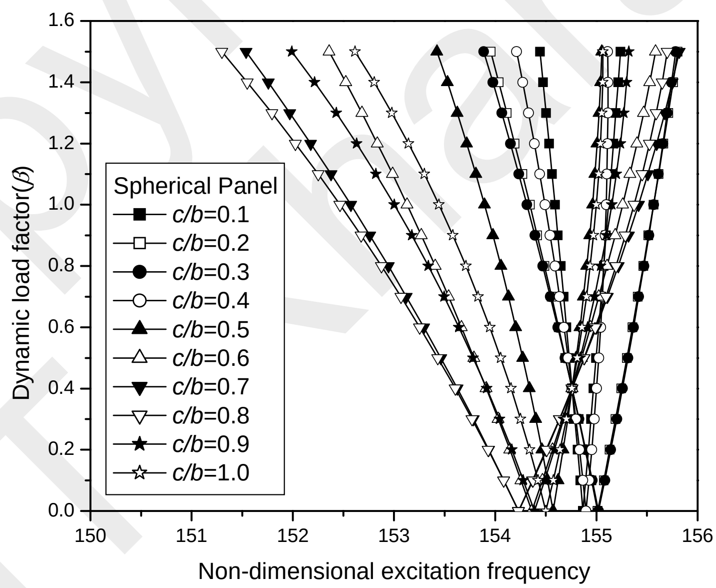


**Fig. 5.31 Same as Fig. 5.29 but for, spherical panel**

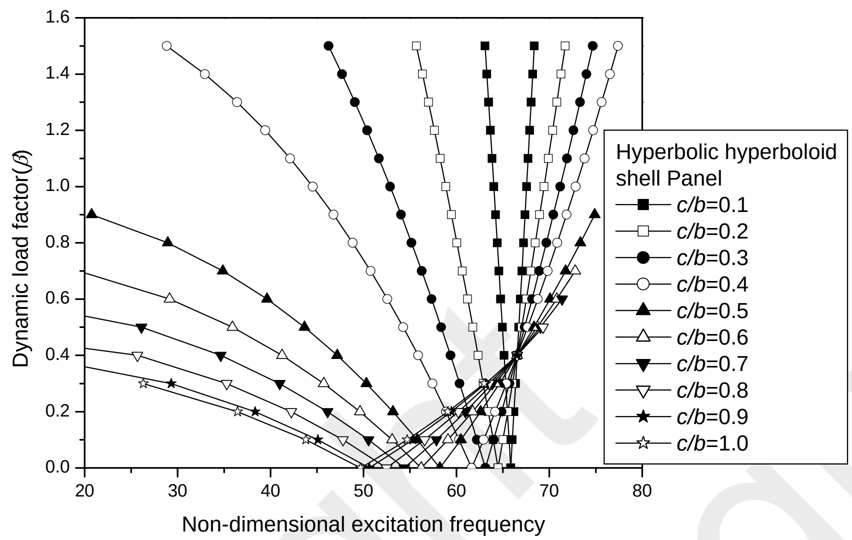


**Fig. 5.32 Same as Fig. 5.29 but for, hyperbolic hyperboloid shell panel**

In the stiffened plate (Fig.5.29), cylindrical (Fig.5.30) and hyperbolic hyperboloid panel (Fig.5.32) with increase in *c/b* ratio; the dynamic stability region is shifting to the lower frequency zone side with wider width. This indicates, these three panels are dynamically more unstable with higher load bandwidth. In the stiffened spherical panel (Fig.5.31) with increase in *c/b* ratio, the dynamic stability region is shifting to the higher frequency zone side with wider width up to *c/b*=0.3 and after that it is shifting to the lower frequency zone side. In all the cases of *c/b* the laminated stiffened spherical shell panel is dynamically more stable compared to the other three panels.

***ii. Effect of number of layers***

The effect of number of layers on dynamic instability regions (DIR) for laminated composite stiffened cylindrical and spherical shell panel is analyzed here. The stiffened cylindrical and spherical shell panels are considered. The panels are attached with a single $(xst)_b$ stiffener along the center line in all the cases. The stiffener depth to breadth ratio ($d_s/b_s$) is kept as 2.0. The lamination scheme in the panel skin and stiffeners is taken as $(0/90)_1$, $(0/90)_2$, $(0/90)_3$ and $(0/90)_4$ in four different cases. The stacking scheme in the stiffener is horizontal. The laminated composite stiffened shell panels are simply supported (SSSS) along all the four sides with $c/b$ = 0.5. Figures 5.33-5.34 show the plots of the dynamic instability regions for cylindrical and spherical panels respectively.

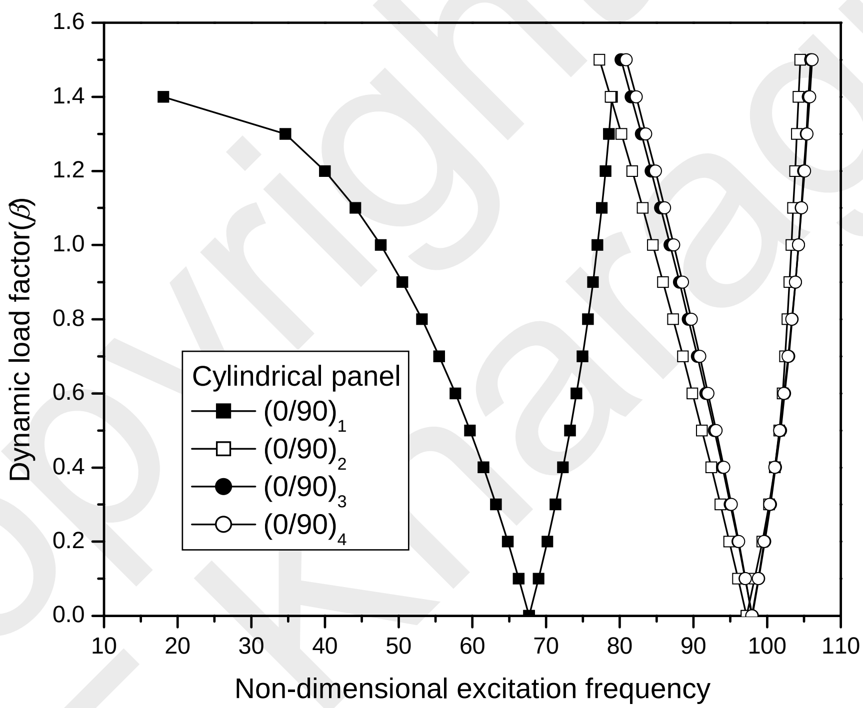


**Fig. 5.33 Dynamic instability region for different number of layers, cylindrical panel**

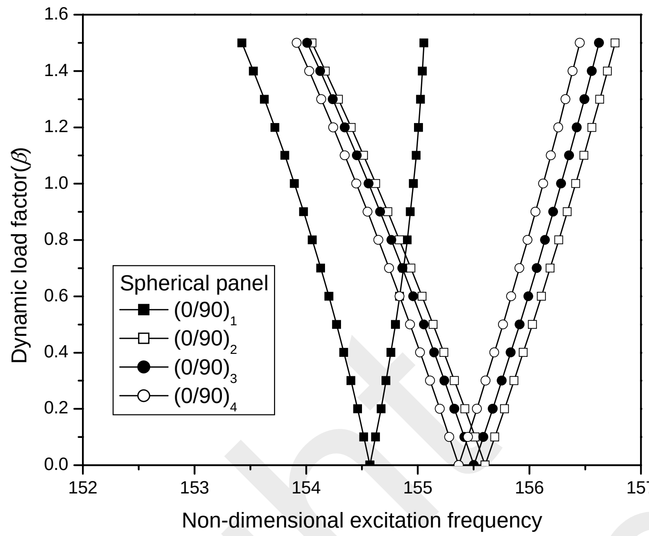


**Fig. 5.34 Same as Fig. 5.33 but for spherical shell panel**

In both the panels when the number of layer in panel skin and stiffeners are increasing, the dynamic instability regions (DIR) are shifting to higher frequency zone side. This indicates that with the increase in number of layers the panels become dynamically more stable. The instability regions are almost same for 4, 6 and 8 layered cases.

***iii. Effect of size of stiffeners***

The effect of size of stiffeners on dynamic instability regions (DIR) for all four types of panels is analyzed. The panels are attached with a single $(xst)_b$ stiffener along the center line in all the cases. The lamination scheme in the panel skin and stiffeners is taken as $(0/90)_2$. The stacking scheme in the stiffener is horizontal. The laminated composite stiffened shell panels are simply supported (SSSS) along all the four sides with $c/b$ = 0.5. Four different sizes of stiffeners with $d_s/b_s$ equals to 2, 4, 6 and 8 are taken. The size of stiffeners is changed by increasing the depth ($d_s$) of the stiffener keeping width ($b_s$) as constant. The dynamic instability regions for cylindrical and spherical panels are plotted in Fig. 5.35-5.36 respectively.

It is observed with the increase in stiffener depth the dynamic instability regions shift to higher frequency zone with wider width and then shifts to lower frequency zone with narrower width. The instability region initiates at higher frequency value at $d_s/b_s$=4.0 in cylindrical panel and at $d_s/b_s$=6.0 in spherical panel compared to other $d_s/b_s$ values. This indicates that the contribution of the stiffener to make the structure dynamically more stable is maximum at a particular depth of the stiffeners.

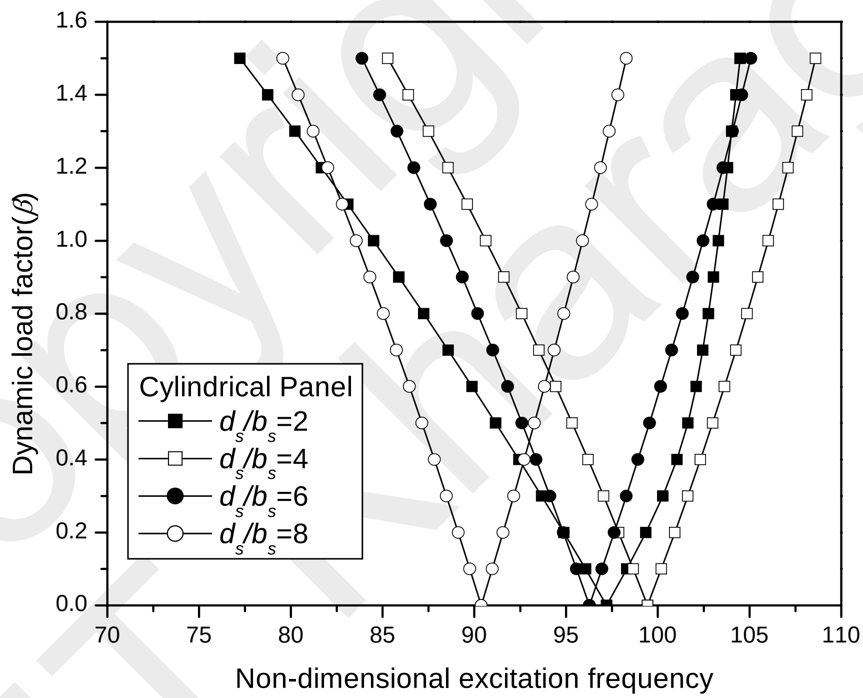


**Fig. 5.35 Dynamic instability region for different size of stiffeners, cylindrical panel**

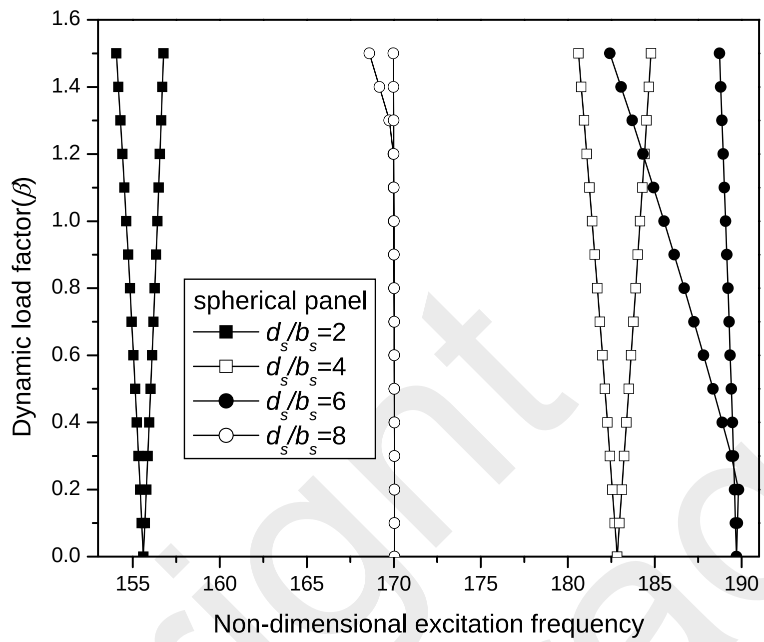


**Fig. 5.36 Same as Fig. 5.35 but for spherical shell panel**

***iv. Effect of stiffening scheme***

The problems of laminated composite stiffened cylindrical and spherical shell panels are analyzed for different stiffening scheme. The panels with simply supported (SSSS) boundary condition with load bandwidth ratio, $c/b$ = 0.5 is considered. The analysis is carried out for the two types of stiffener orientations, $x$-direction stiffener $(xst)_b$ in one case and orthogonal stiffeners $(xst)_b$ and $(yst)_b$ in the other case. In both the cases the number of stiffeners taken are 1,3,5 and 7. The lamination scheme in the panel skin and stiffeners is taken as $(0/90)_2$. The stacking scheme in the stiffener is horizontal. The stiffener depth to breadth ratio ($d_s/b_s$) is kept as 4.0. Figures 5.37-5.38 show the variation of dynamic instability regions for different number of $x$-stiffeners ($(xst)_b$) for cylindrical and spherical shell panels respectively.

Similarly, Figure 5.39-5.40 show the variation of dynamic instability regions for different number of orthogonal (*x* and *y*) stiffeners ($(xst)_b$ and $(yst)_b$) for cylindrical and spherical shell panels respectively. In both types of stiffeners for both cylindrical and spherical shell panels the dynamic instability regions (DIR) shift to the higher frequency zone with narrower width with the increase in the number of stiffeners.

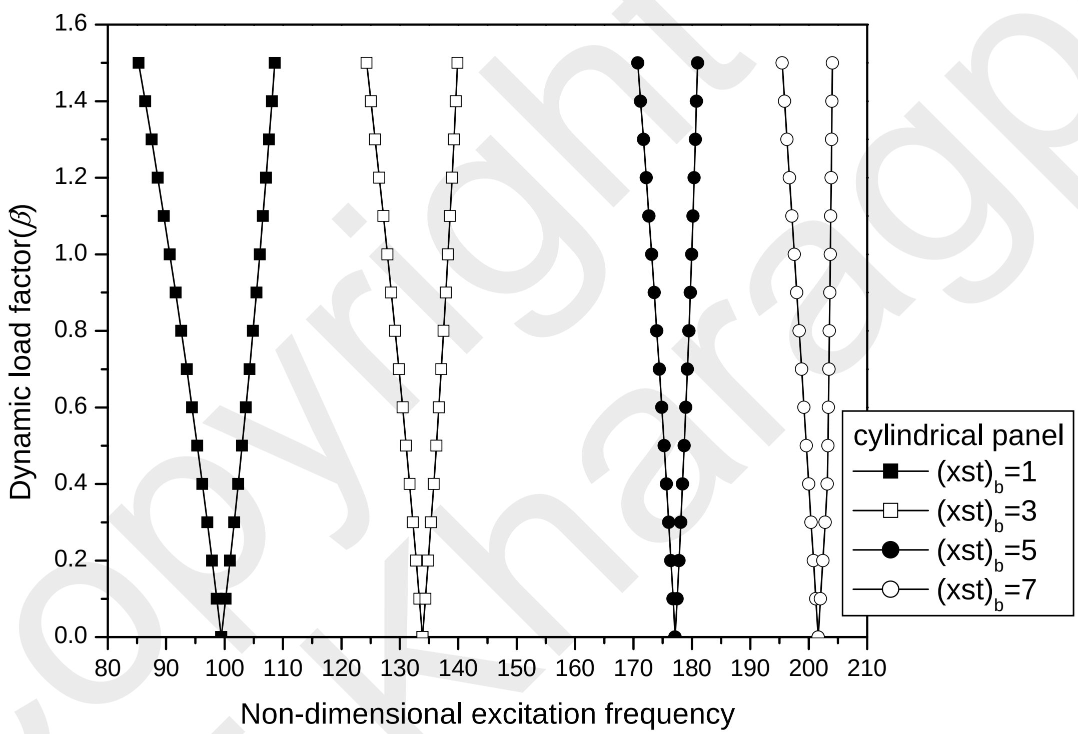


**Fig. 5.37 Dynamic instability region for different number of x-stiffeners $(xst)_b$, cylindrical panel**

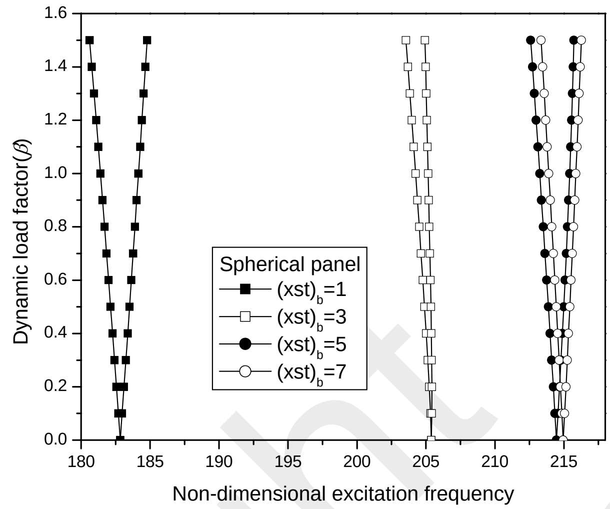


**Fig. 5.38 Same as Fig. 5.37, but for spherical panel**

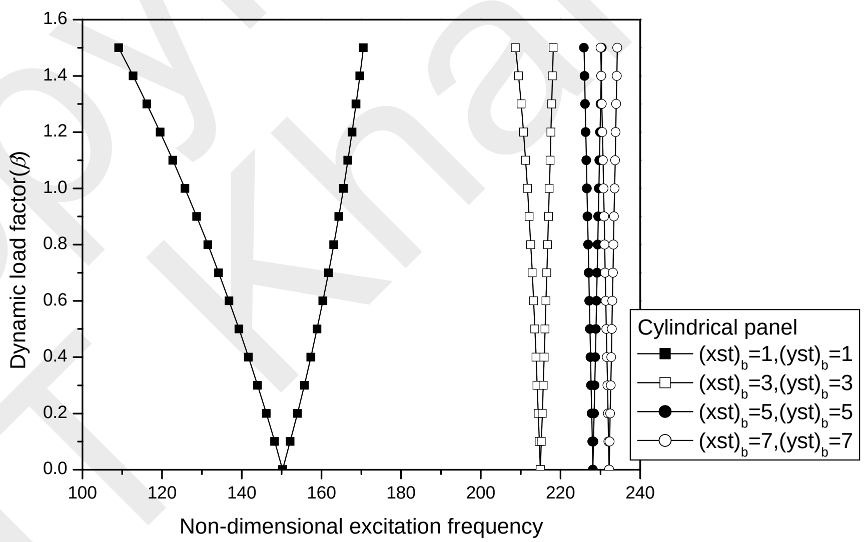


**Fig. 5.39 Dynamic instability region for different number of orthogonal stiffeners $(xst)_b$ and $(yst)_b$, cylindrical panel**

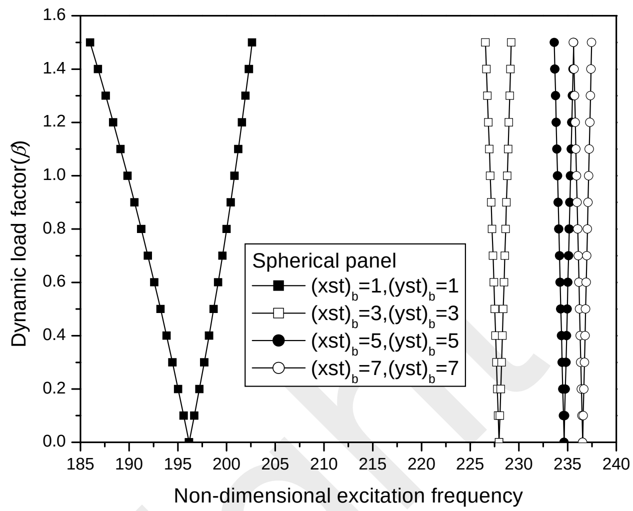


**Fig. 5.40 Same as Fig. 5.39, but for spherical panel**

***v. Effect of lamination scheme***

The effects of lamination schemes ($(0/90)_2$ and $(45/-45)_2$) in panel skin and stiffener on dynamic instability regions (DIR) for stiffened cylindrical and spherical shell panels are presented in this section. The panels taken are simply supported (SSSS) along all the four boundaries with load bandwidth ratio, $c/b$ = 0.5. The stiffening scheme for the panels taken is $(xst)_b$=5 and $(yst)_b$=5. The stacking scheme in the stiffeners is horizontal. The stiffener depth to breadth ratio ($d_s/b_s$) is kept as 4.0. The variations of non-dimensional excitation frequencies ($\bar{\Omega}$) with dynamic load factor ($\beta$) for cross-ply $(0/90)_2$ and angle-ply $(45/-45)_2$ lamination scheme in panel skin and stiffeners is shown in Fig. 5.41-5.42 for stiffened cylindrical and spherical shell panels respectively. In case of cylindrical panel the dynamic instability region shifts to the higher frequency zone side with lower width in cross-ply lamination pattern. On the other hand the dynamic instability region shifts to the higher frequency zone side with lower width in angle-ply lamination scheme.

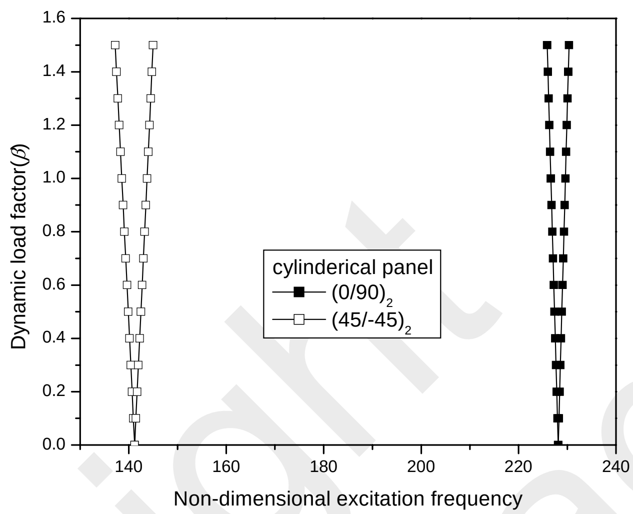


**Fig. 5.41 Dynamic instability region for different lamination scheme, cylindrical panel**

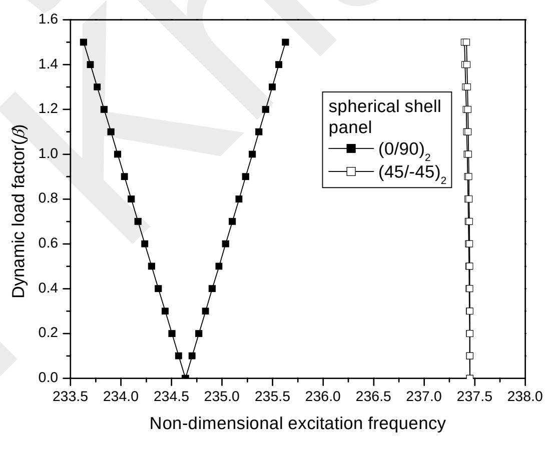


**Fig. 5.42 Same as Fig. 5.41, but for spherical panel**

### *vi. Effect of eccentricity of stiffener*

The effect of eccentricity (whether attached to bottom or top surface of the panels) of the stiffeners on dynamic instability region for cylindrical and spherical shell panels is considered here. Both cross-ply (($(0/90)_2$) and angle-ply (($(45/45)_2$) lamination scheme for panel and stiffener are taken. The panels taken are simply supported (SSSS) along all the four boundaries with load bandwidth ratio, $c/b$ = 0.5. The number of stiffeners in both $x$ and $y$ directions is taken as 5. The stiffener depth to breadth ratio ($d_s/b_s$) is kept as 4.0. The stacking scheme in the stiffeners is horizontal. The dynamic instability region (DIR) with eccentric top and bottom stiffener with $(0/90)_2$ for laminated composite stiffened cylindrical and spherical shell panels are shown in Fig. 5.43-5.44 respectively. Figures 5.45-5.46 show the instability regions for $(45/-45)_2$. In case of cross-ply lamination scheme for both the panels the instability region is at higher frequency zone with the stiffeners attached in top surface. But in case of angle-ply lamination scheme for both the panels the instability region is at higher frequency zone with the stiffeners attached in bottom surface.

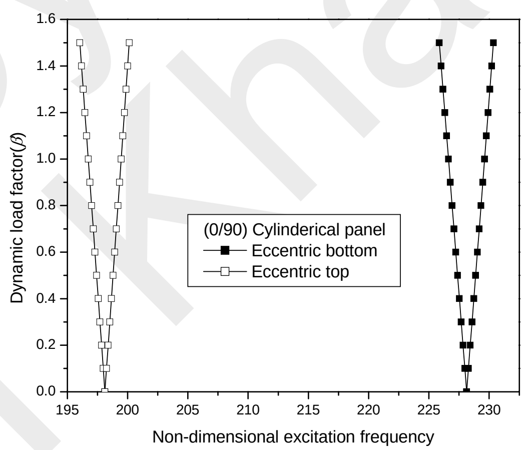


**Fig. 5.43 Dynamic instability region with top and bottom stiffener with $(0/90)_2$, cylindrical panel**

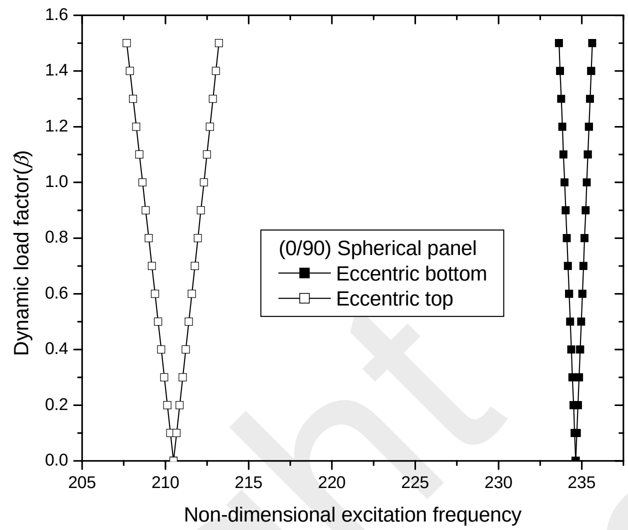


**Fig. 5.44 Same as Fig. 5.43, but for spherical panel**

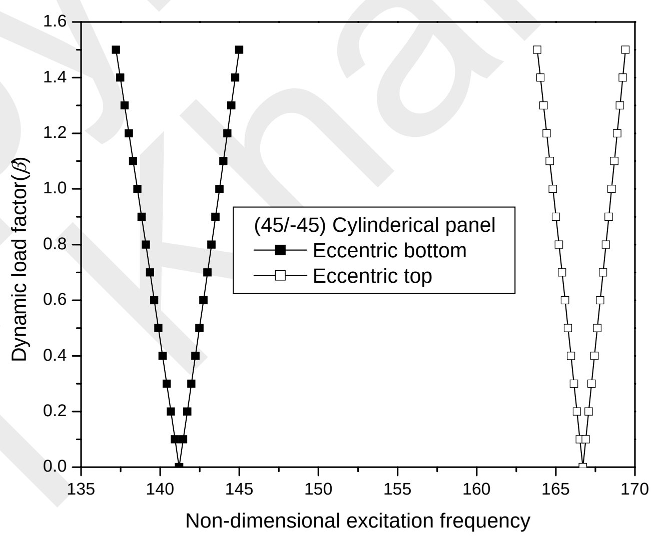


**Fig. 5.45 Dynamic instability region with top and bottom stiffener with $(45/-45)_2$, cylindrical panel**

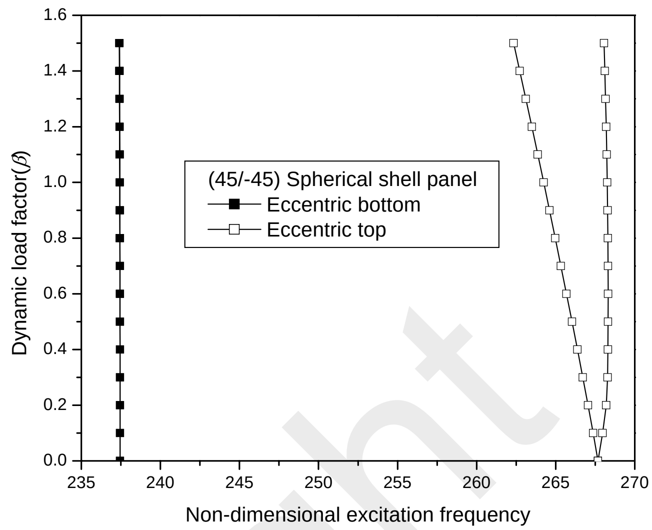


**Fig. 5.46 Same as Fig. 5.45, but for spherical panel**

***vii. Effect of stacking scheme of lamina in the stiffener***

The effect of stacking scheme of the lamina whether parallel or perpendicular to the lamina of the panel skin, on the instability region is discussed in this section. The problem of stiffened spherical shell panel with stiffener attached in both top and bottom surface also with both $(0/90)_2$ and $(45/-45)_2$ lamination schemes is taken for the analysis. The number of stiffeners is 5 each both in $x$ and $y$ directions. The panel is simply supported (SSSS) along all the four boundaries with load bandwidth ratio, $c/b$ = 0.5. The stiffener depth to breadth ratio ($d_s/b_s$) is kept as 4.0. In case of 0/90 lamination with stiffeners attached to bottom surface of the spherical panel, the DIR (Fig. 5.47) is at higher frequency zone with parallel stacking scheme. On the other hand when the stiffeners are attached to top surface, the DIR (Fig. 5.48) is at higher frequency zone with perpendicular stacking scheme. But in the case of 45/-45 lamination scheme with stiffeners attached to both bottom and top surfaces the instability region is at higher frequency zone with perpendicular stacking scheme as shown in Fig. 5.49-5.50 respectively.

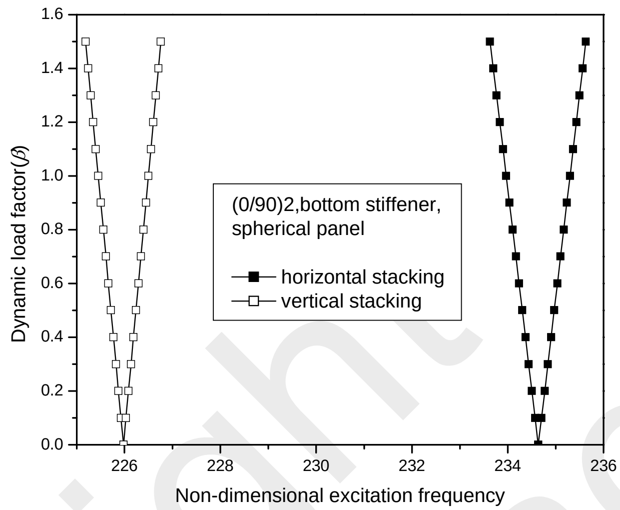


**Fig. 5.47 Dynamic instability region with parallel and perpendicular stacking with $(0/90)_2$, bottom stiffener**

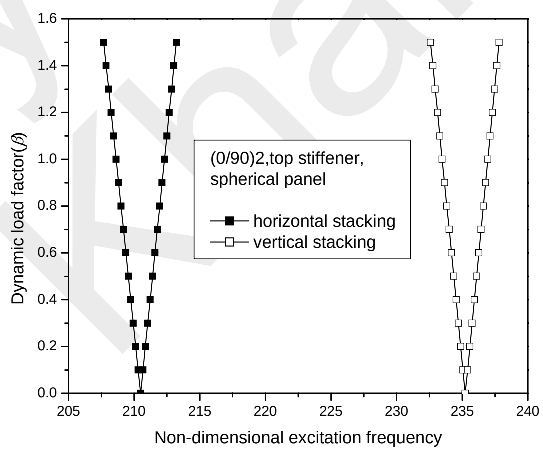


**Fig. 5.48 Same as Fig. 5.47, but for top stiffener**

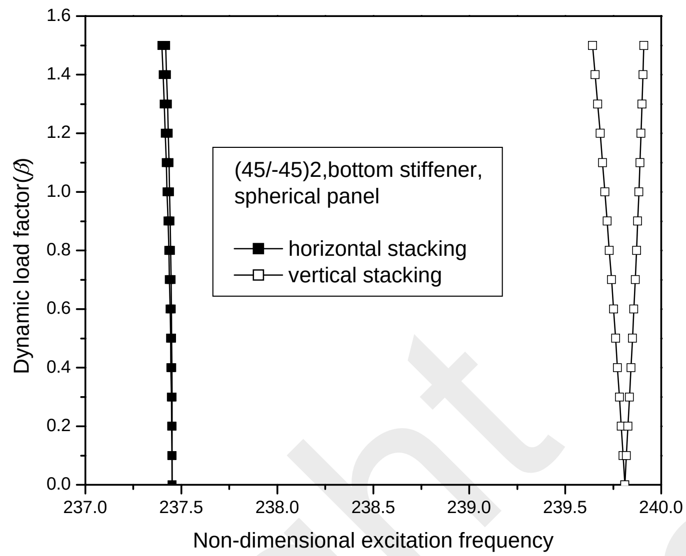


**Fig. 5.49 Dynamic instability region with parallel and perpendicular stacking with (45/-45)$_2$, bottom stiffener**

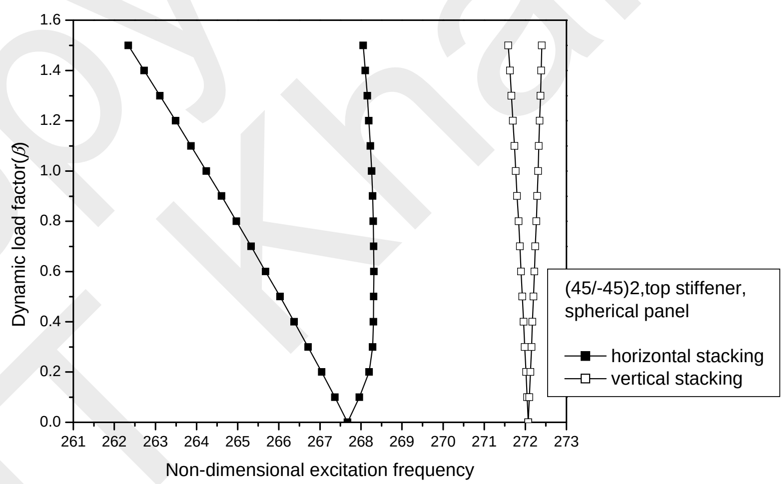


**Fig. 5.50 Same as Fig. 5.49, but for top stiffener**

***viii. Effect of boundary condition***

The effect of boundary condition on instability region of the spherical shell panel with orthogonal stiffeners ($(xst)_t$=5 and $(yst)_t$=5) attached to top surface with perpendicular stacking scheme is discussed in this section. The load bandwidth ratio *c/b* is 0.5. The stiffener depth to breadth ratio ($d_s/b_s$) is kept as 4.0. The lamination scheme in panel skin and stiffener is $(0/90)_2$. The boundary conditions considered here are SSSS, CCSS, CCFF, CFCF, and CCCf. From Fig. 5.51 it is seen that out all these boundary conditions the instability region with CCSS is at highest frequency zone with narrower width.

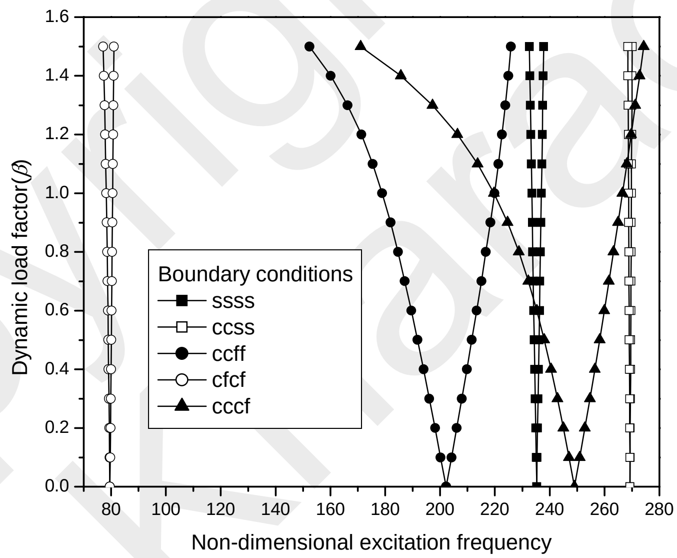


**Fig. 5.51 Dynamic instability region with different boundary conditions**

## Loading Type-II

The vibration, buckling and dynamic stability characteristics of the laminated composite stiffened shell problem (Fig 5.23) for the partial loading Type-II (Localized edge loading from center of two opposite side) are presented in this section. The different parameters are varied in a wide rage to study the effect of these parameters on the behavior of the shell panels. The details are described below.

**(a) Buckling**

The effects of load bandwidth ratio(*c/b*) of the patch loading for all the four types of stiffened shell panels are discussed here. The ratios *c/b* are taken as 0.2, 0.4, 0.6, 0.8 and 1.0 for the buckling analysis. The panels are attached with a single $(xst)_b$ stiffener along the center line in all the cases. The stiffener depth to breadth ratio ($d_s/b_s$) is kept as 4.0. The lamination in the panel skin and stiffeners is taken as $(0/90)_2$. The stacking scheme in the stiffener is horizontal. The laminated composite stiffened shell panels are simply supported (SSSS) along all the four sides. The plots in the Fig. 5.52 show the variation of non-dimensional buckling load for the laminated stiffened flat, cylindrical, spherical, and hyperbolic hyperboloid panels.

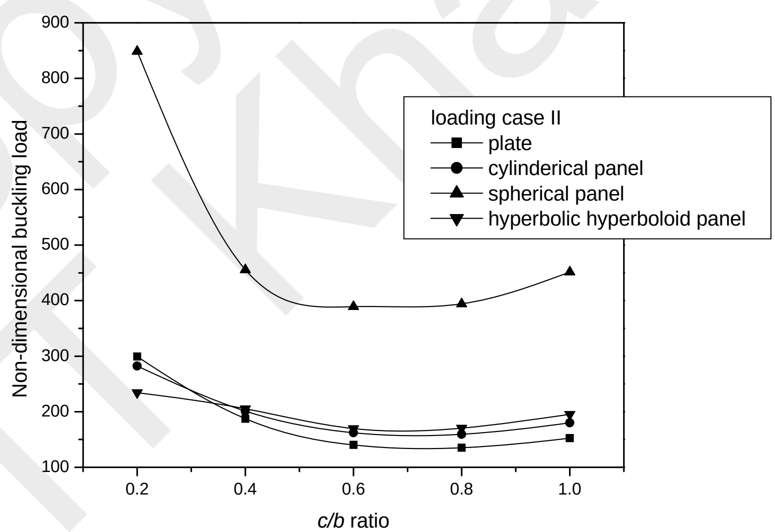


**Fig. 5.52 Variation of non-dimensional buckling load with *c/b* ratio**

When the load bandwidth ration *c/b*=0.2 the buckling load is highest for all the panels. As the load width increases from center towards the edge the buckling load decreases and again it increases after some bandwidth of load.

### (b) Vibration

The above mentioned stiffened shell panels are studied for the variation of frequency with the applied loading. The effects of *c/b* ratios (0.2, 0.4, 0.6, 0.8 and 1.0) are considered for all the four types of panels. Figures 5.53a-d show the plot of the variation of first mode frequencies with the loading for plate, cylindrical, spherical, and hyperbolic hyperboloid panels respectively. It is observed from the plots (Fig. 5.53a-d) that when the load is zero the frequencies are natural frequency of vibration. As the load increases the frequency of vibration gradually decreases and becomes zero when the load reaches the critical value.

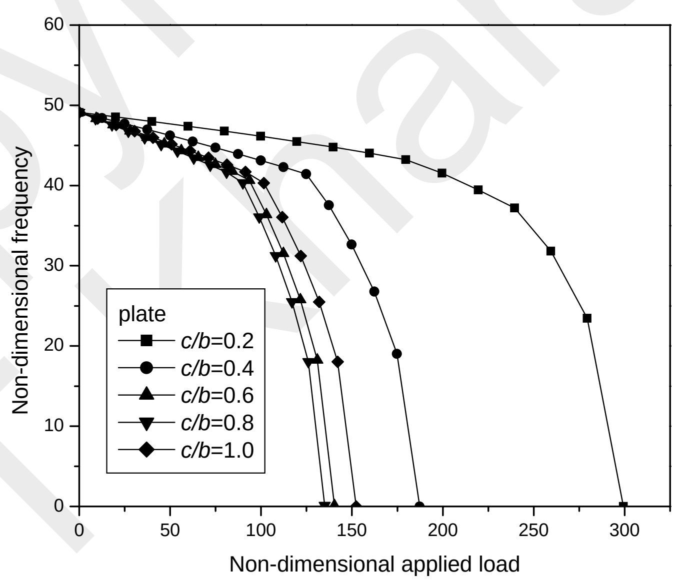


**Fig. 5.53a Variation of frequency with load, plate**

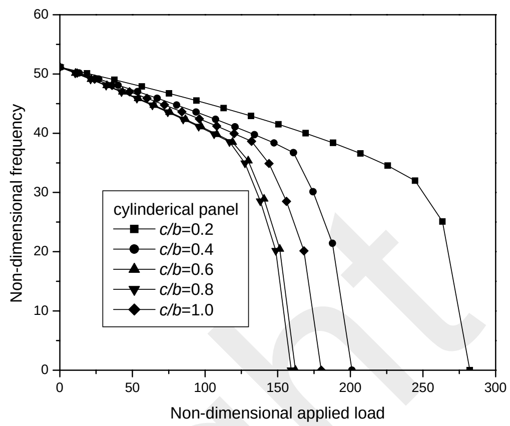


**Fig. 5.53b Same as Fig. 5.53a but for, cylindrical panel**

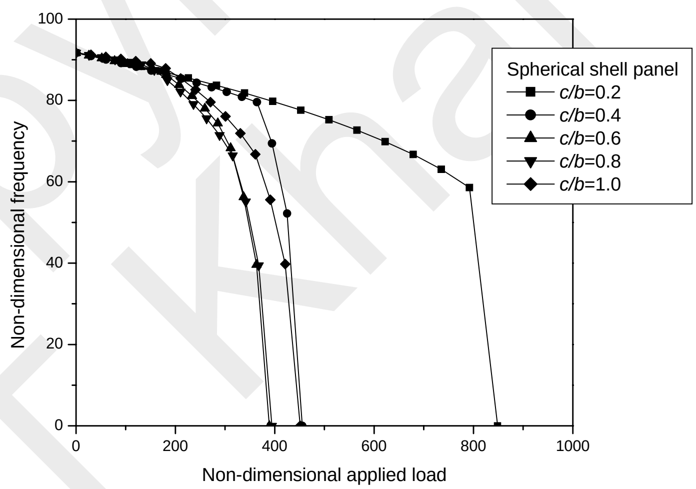


**Fig. 5.53c same as Fig. 5.53a but for, spherical panel**

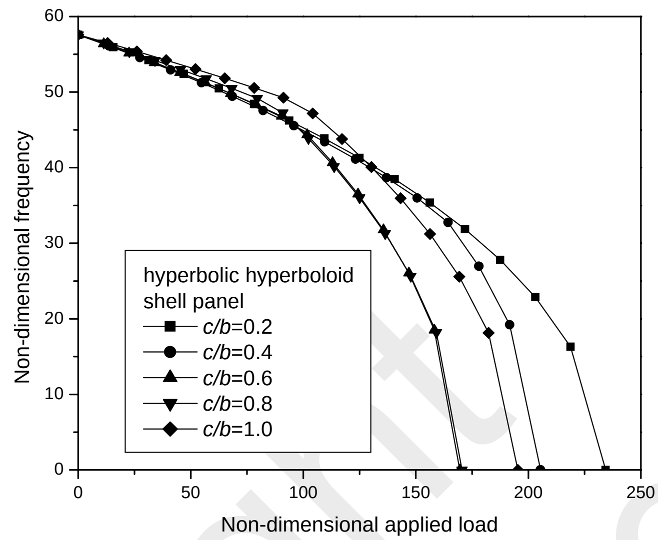


**Fig. 5.53d Same as Fig. 5.53a but for, hyperbolic hyperboloid shell panel**

**(c) Dynamic stability**

The dynamic instability analysis for all the four types of panels with different *c/b* ratios is carried out in this section. In the analysis, the non-dimensional buckling load (buckling stress factor = 131.727) uniformly loaded (*c/b* = 1.0, in Type-II loading) of the four layered simply supported (SSSS) cross-ply $(0/90)_2$ stiffened flat plate with a single $(xst)_b$ stiffener ($d_s/b_s$= 4) along the center line with $(0/90)_2$ lamination scheme and horizontal stacking, is taken as the reference load, so as to plot the instability zones. The static load factor ($\alpha$) is 0.2 in all cases. The dynamic load factor ($\beta$) varies from 0.0 to 1.5. Figures 5.54-5.57 show the plots of the dynamic instability regions for plate, cylindrical, spherical, and hyperbolic hyperboloid panels respectively.

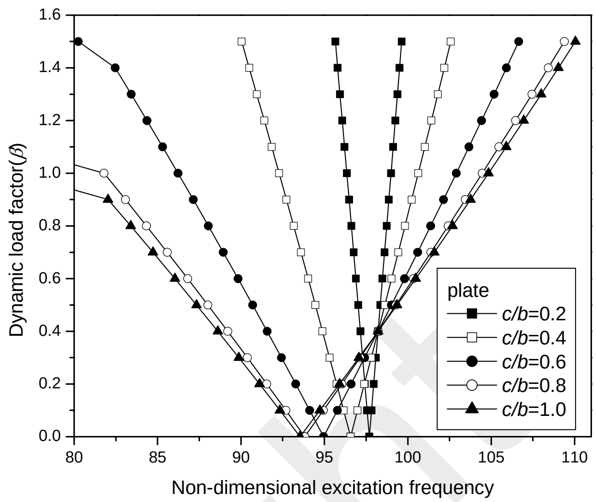


**Fig. 5.54 Dynamic instability region for different *c/b* ratio, plate**

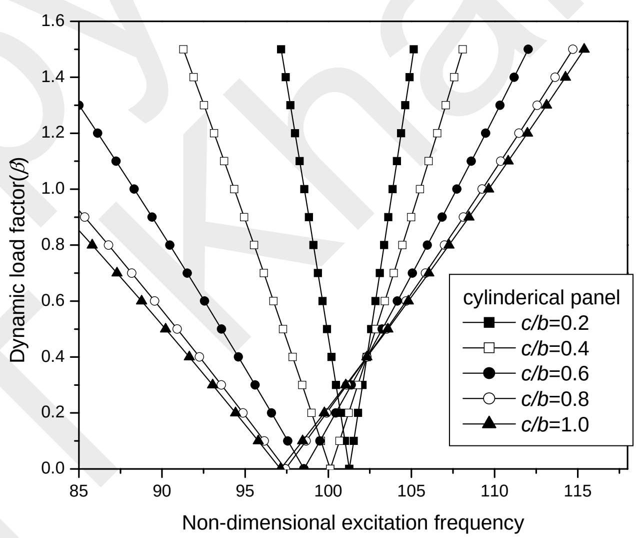


**Fig. 5.55 Same as Fig. 5.54 but for, cylindrical panel**

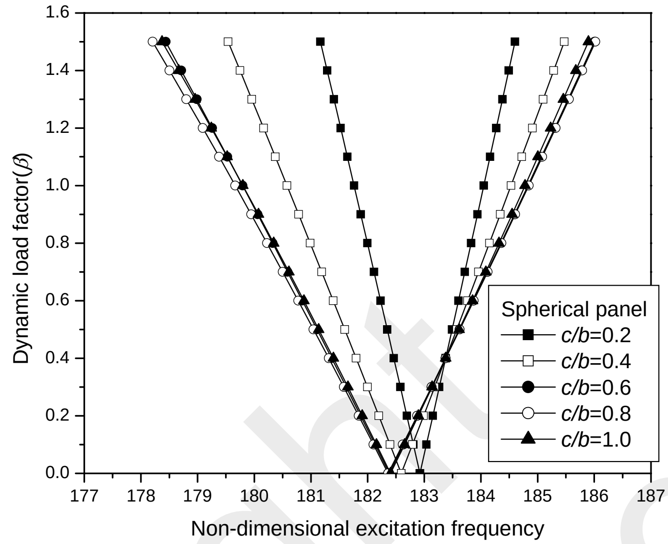


**Fig. 5.56 Same as Fig. 5.54 but for, spherical panel**

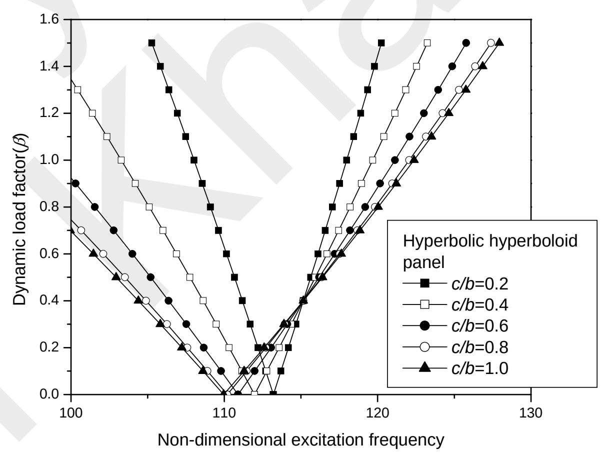


**Fig. 5.57 Same as Fig. 5.54 but for, hyperbolic hyperboloid shell panel**

In all cases it observed that with the increase in load width the instability regions shift to lower frequency zone with wider width for all types of panel.

## Loading Type-III

The vibration, buckling and dynamic stability characteristics of the laminated composite stiffened shell problem (Fig.5.23) for the partial loading Type-III (Localized edge loading from both ends of two opposite side) are presented in this section. The different parameters are varied in a wide rage to study the effect of these parameters on the behavior of the shell panels. The details are described below.

### (a) Buckling

The effects of bandwidth ratio($c/b$) of the patch loading for all the four types of stiffened shell panels are discussed here. The load width ratios $c/b$ are taken as 0.1, 0.2, 0.3, 0.4 and 0.5 for the buckling analysis. The panels are attached with a single $(xst)_b$ stiffener along the center line in all the cases. The stiffener depth to breadth ratio ($d_s/b_s$) is kept as 4.0. The lamination in the panel skin and stiffeners is taken as $(0/90)_2$. The stacking scheme in the stiffener is horizontal. The laminated composite stiffened shell panels are simply supported (SSSS) along all the four sides. The plots in the Fig. 5.58 show the variation of non-dimensional buckling load for the laminated stiffened flat, cylindrical, spherical, and hyperbolic hyperboloid panels.

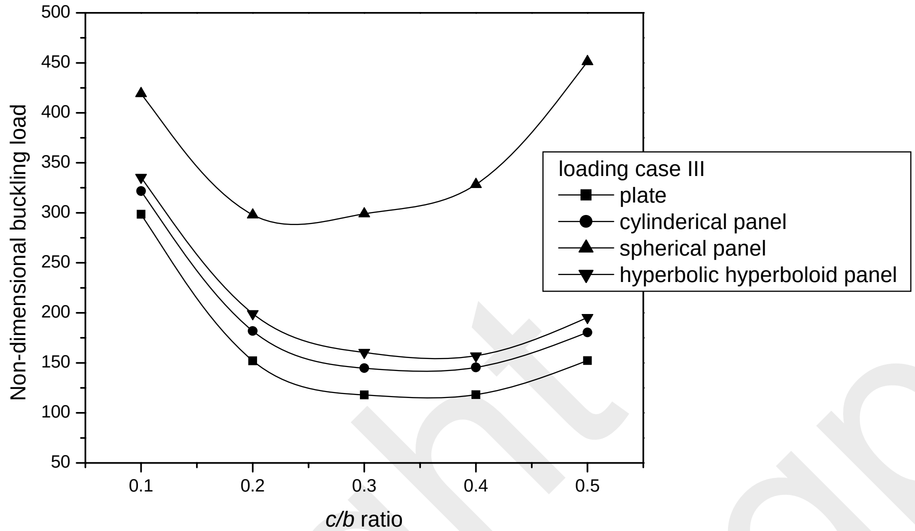


**Fig. 5.58 Variation of non-dimensional buckling load with *c/b* ratio**

It is seen that when the patch load is near to the support the buckling load is highest in all the types of panels except the spherical shell panel. In spherical panel the buckling load is highest when it is loaded uniformly. As the both the loading patches increase towards the center, there is a decrease in buckling load upto certain length of the patch and after that again there is an increase in the load.

**(b) Vibration**

The above mentioned stiffened shell panels are studied for the variation of frequency with the loading. The effects of all *c/b* ratios (0.1, 0.2, 0.3, 0.4 and 0.5) are considered for all the four types of panels. Figures 5.59a-d show the plot of the variation of first mode frequencies with the applied loading for plate, cylindrical, spherical, and hyperbolic hyperboloid panels respectively. It is observed from the plots (Fig. 5.59a-d) that when the load is zero the frequencies are natural frequency of vibration. As the load increases the frequency of vibration gradually decreases and becomes zero when the load reaches the critical value.

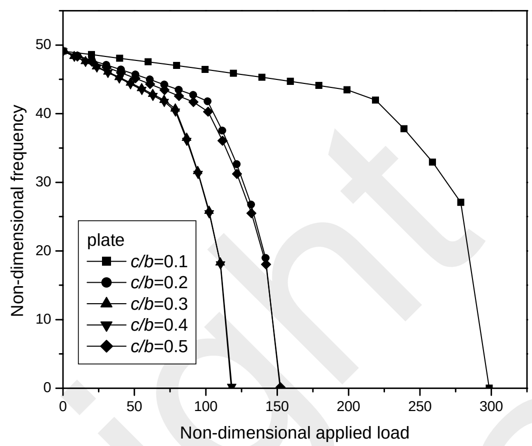


**Fig. 5.59a Variation of frequency with load, plate**

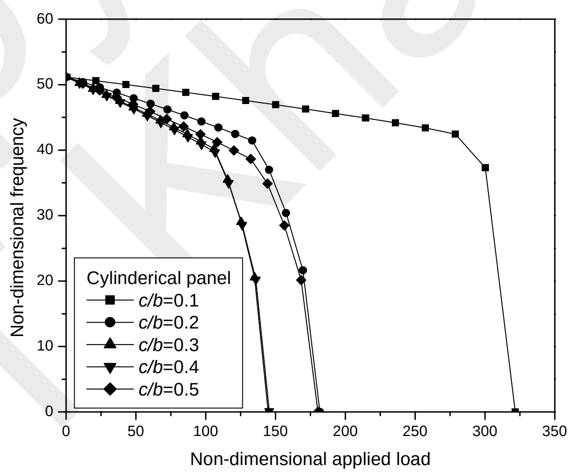


**Fig. 5.59b Same as Fig. 5.59a but for, cylindrical panel**

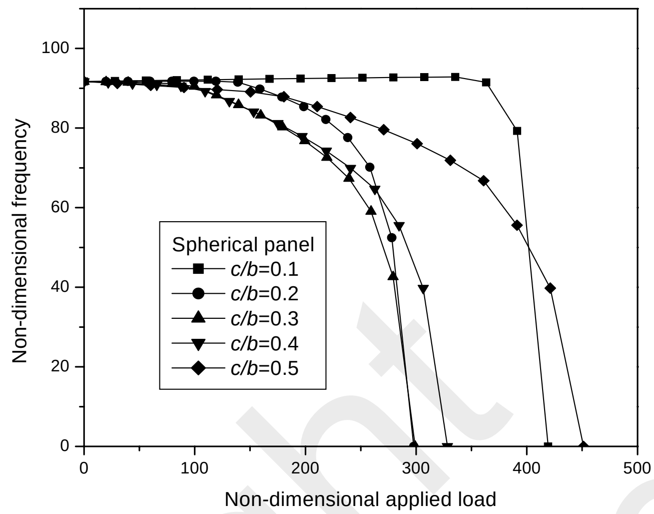


**Fig. 5.59c Same as Fig. 5.59a but for, spherical panel**

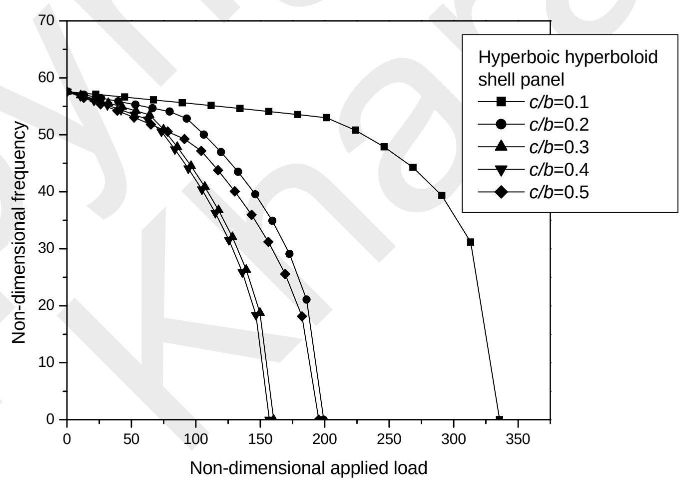


**Fig. 5.59d Same as Fig. 5.59a but for, hyperbolic hyperboloid shell panel**

### (c) Dynamic stability

The dynamic instability analysis for all the four types of panels with different *c/b* ratios is carried out in this section. In the analysis, the non-dimensional buckling stress, of uniformly loaded (*c/b* = 0.5, in Type-III loading) four layered simply supported (SSSS) cross-ply $(0/90)_2$ stiffened flat plate with a single $(xst)_b$ stiffener ($d_s/b_s$= 4) along the center line with $(0/90)_2$ lamination scheme and horizontal stacking, is taken as the reference load, so as to plot the instability zones. The static load factor ($\alpha$) is 0.2 in all cases. The dynamic load factor ($\beta$) varies from 0.0 to 1.5. Figures 5.60-5.63 show the plots of the dynamic instability regions for plate, cylindrical, spherical, and hyperbolic hyperboloid panels respectively.

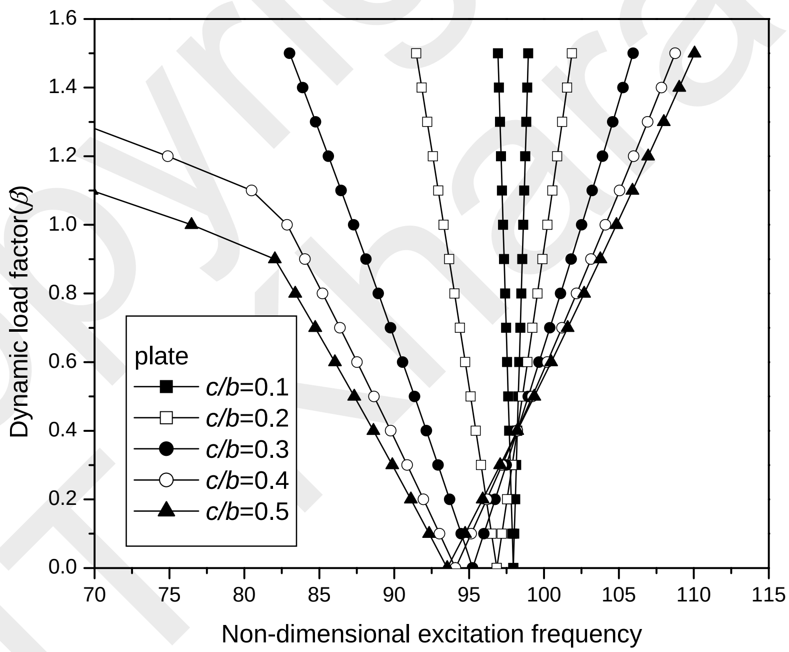


**Fig. 5.60 Dynamic instability region for different *c/b* ratio, plate**

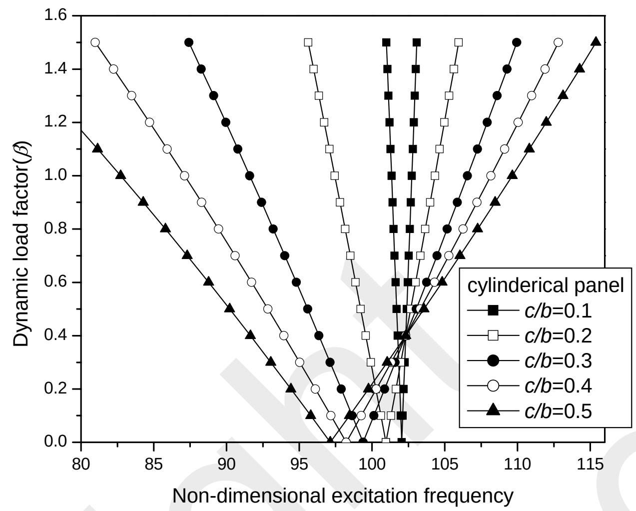


**Fig. 5.61 Same as Fig. 5.60 but for, cylindrical panel**

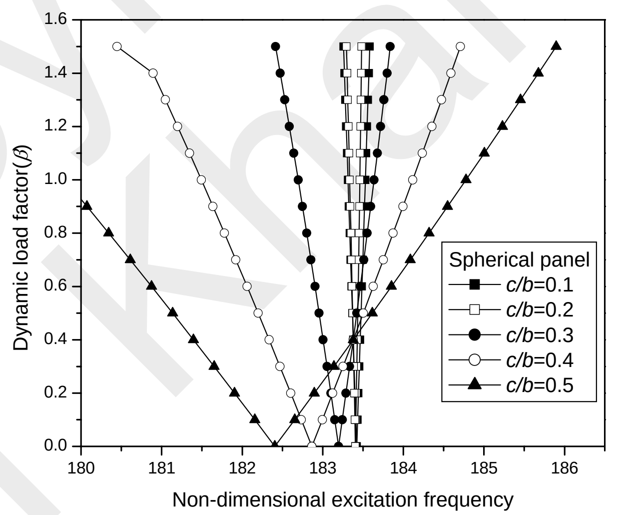


**Fig. 5.62 Same as Fig. 5.60 but for, spherical panel**

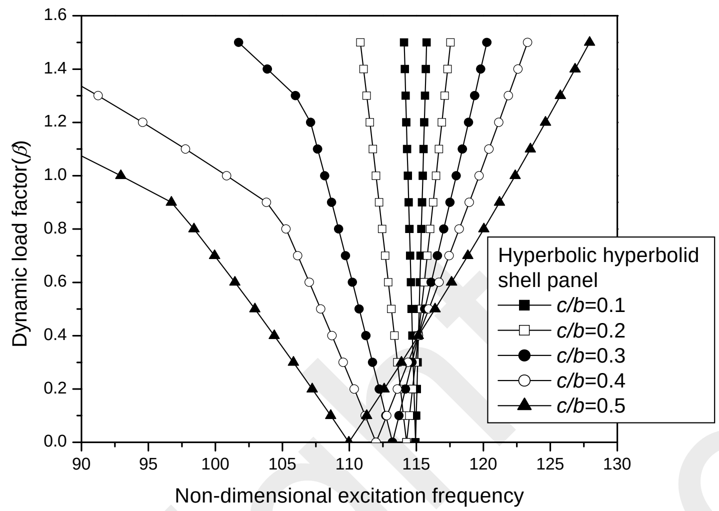


**Fig. 5.63 Same as Fig. 5.60 but for, hyperbolic hyperboloid shell panel**

In all cases it observed that with the increase in load width the instability region shifts to lower frequency zone with wider width for all types of panel except the spherical shell panel. The spherical panel is dynamically more stable with $c/b$ = 0.2.

## Loading Type-IV

The vibration, buckling and dynamic stability characteristics of the laminated composite stiffened shell problem (Fig. 5.23) for the partial loading Type-IV (Concentrated edge loading of two opposite side) are presented in this section. The different parameters are varied in a wide rage to study the effect of these parameters on the behavior of the shell panels. The details are described below.

**(a) Buckling**

The effects of position (*c/b*) of the concentrated loading for all the four types of stiffened shell panels are discussed here. The ratios *c/b* are taken as 0.1, 0.2, 0.3, 0.4, 0.5, 0.6, 0.7, 0.8 and 0.9 for the buckling analysis. The panels are attached with a single $(xst)_b$ stiffener along the center line in all the cases. The stiffener depth to breadth ratio ($d_s/b_s$) is kept as 4.0. The lamination in the panel skin and stiffeners is taken as $(0/90)_2$. The stacking scheme in the stiffener is horizontal. The laminated composite stiffened shell panels are simply supported (SSSS) along all the four sides. The plots in the Fig. 5.64 show the variation of non-dimensional buckling load for the laminated stiffened flat, cylindrical, spherical, and hyperbolic hyperboloid panels.

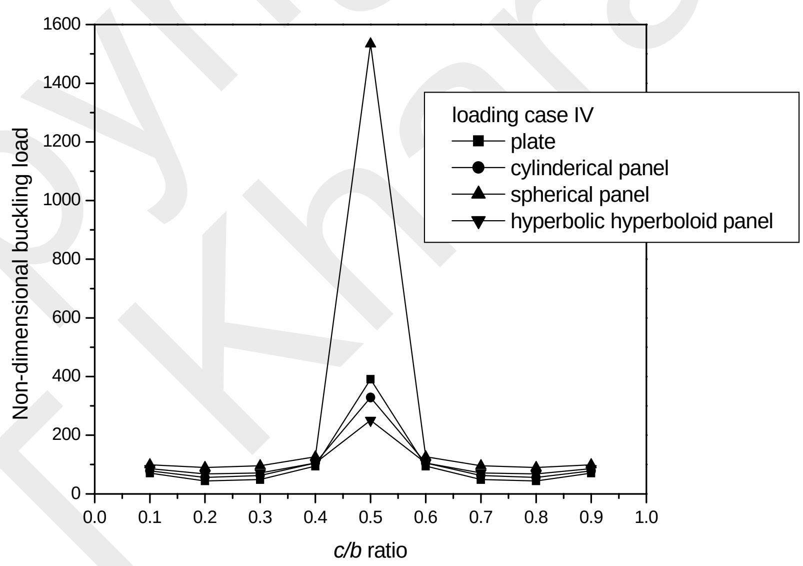


**Fig. 5.64 Variation of non-dimensional buckling load with different position of the concentrated load, loading Type-IV**

It is observed that when the concentrated load is at the stiffener position (*c/b* = 0.5) the panels buckle at higher load. When the load move from *c/b* = 0.1 to *c/b* = 0.2, there is a decrease in buckling load and again when is moves from *c/b* = 0.2 to *c/b* = 0.3 and beyond upto *c/b* = 0.5 an increase in buckling load is observed in all the panels. The stiffened spherical shell panel carries very high load at the load position of c/*b* = 0.5 in comparison to other panels. It indicates that for the given configuration the spherical panel is statically more stable.

**(b) Vibration**

The above mentioned stiffened shell panels are studied for the variation of frequency with the applied loading. The effects of *c/b* ratios (0.1, 0.2, 0.3, 0.4 and 0.5) are considered for all the four types of panels. Figures 5.65a-d show the plot of the variation of first mode frequencies with the applied loading for plate, cylindrical, spherical, and hyperbolic hyperboloid panels respectively. It is observed from the plots (Fig. 4.69a-d) that when the load is zero the frequencies are natural frequency of vibration. As the load increases the frequency of vibration gradually decreases and becomes zero when the load reaches the critical value.

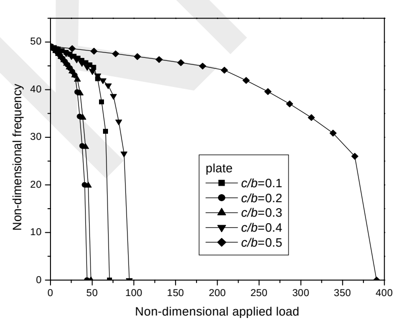


**Fig. 5.65a Variation of frequency with load, plate**

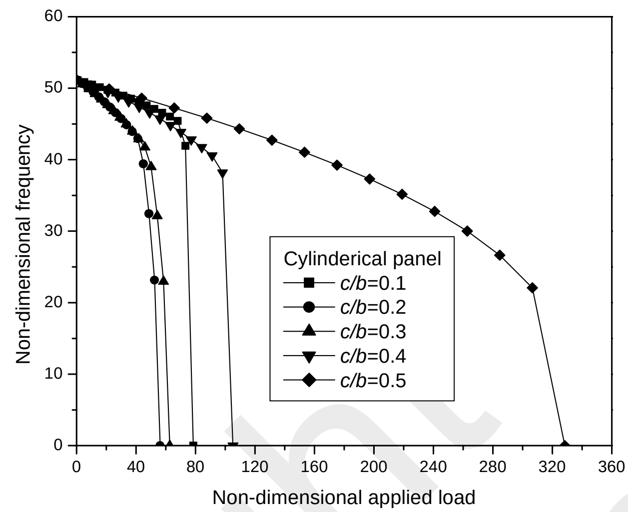


**Fig. 5.65b Same as Fig. 5.65a but for, cylindrical panel**

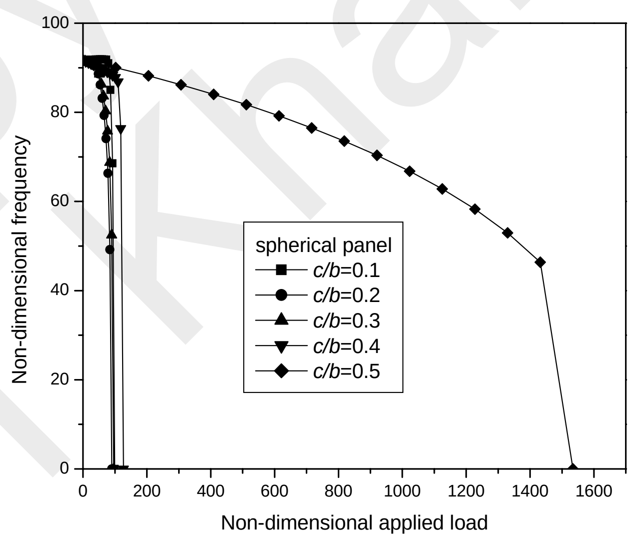


**Fig. 5.65c Same as Fig. 5.65a, but for spherical panel**

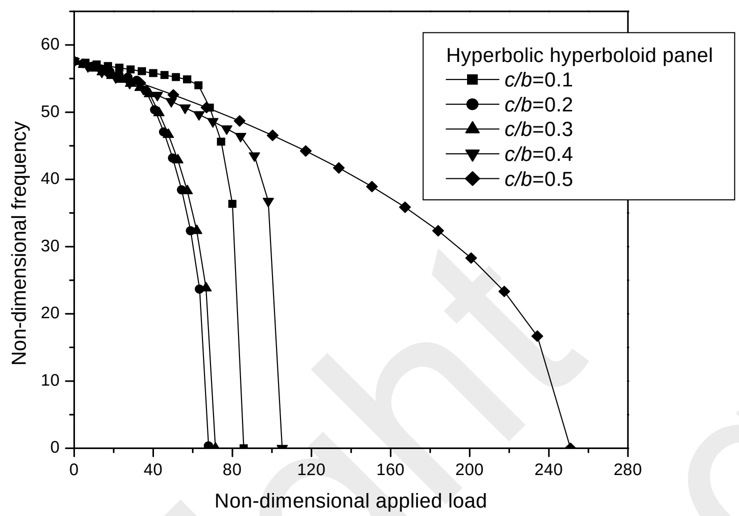


**Fig. 5.65d Same as Fig. 5.65a, but for hyperbolic hyperboloid shell panel**

**(c) Dynamic stability**

The dynamic instability analysis for all the four types of panels with different *c/b* ratios is carried out in this section. In the analysis, the non-dimensional buckling load, with load position at *c/b* = 0.1 in Type-IV loading, of the four layered simply supported (SSSS) cross-ply $(0/90)_2$ stiffened flat plate with a single $(xst)_b$ stiffener ($d_s/b_s$= 4) along the center line with $(0/90)_2$ lamination scheme and horizontal stacking, is taken as the reference load, so as to plot the instability zones. The static load factor ($\alpha$) is 0.2 in all cases. The dynamic load factor ($\beta$) varies from 0.0 to 1.5. Figures 5.66-5.69 show the plots of the dynamic instability regions for plate, cylindrical, spherical, and hyperbolic hyperboloid panels respectively.

It is observed that the flat plate (Fig. 5.66) and cylindrical shell panel (Fig. 5.67) are dynamically more stable when the load is at the center(*c/b* = 0.5), for all other positions of the load the instability zones shift to lower frequency zone with wider width. But the spherical (Fig. 5.68) and hyperbolic hyperboloid (Fig. 5.69) shell panels are dynamically more stable when the load is near the edge (*c/b* = 0.1). For all other position of the load the instability zone shifts to lower frequency zone with wider width. Though all the panels are statically more stable at loading position *c/b* = 0.5, the spherical and hyperbolic hyperboloid shell panels are dynamically less stable for this loading position. So if a structure is statically more stable for a particular loading position, it may or may not be dynamically more stable for that loading position.

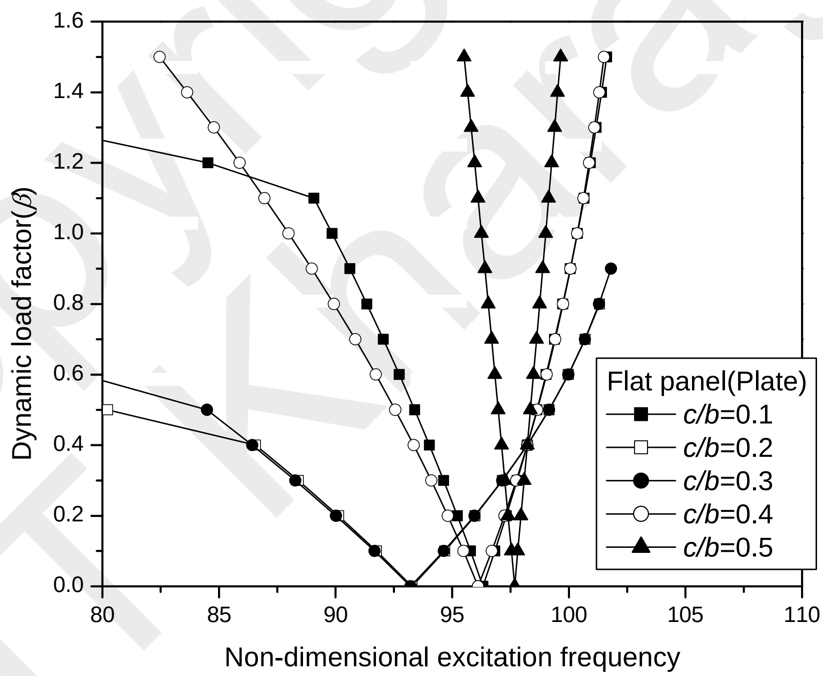


**Fig. 5.66 Dynamic instability region for different *c/b* ratio, plate**

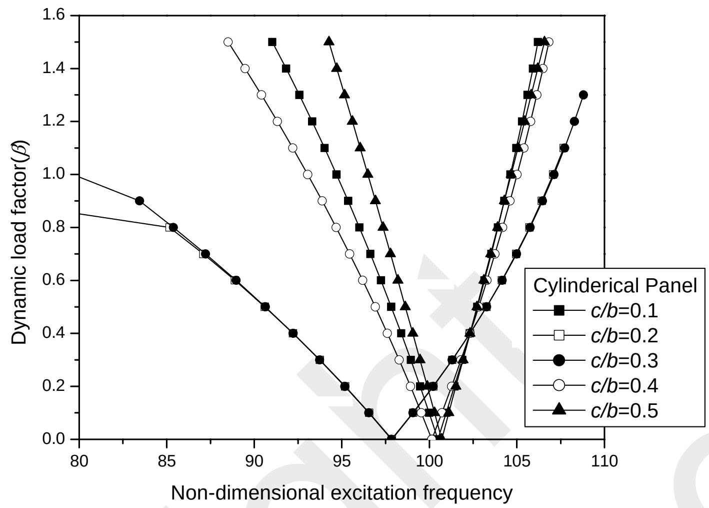


**Fig. 5.67 Same as Fig. 5.66 but for, cylindrical panel**

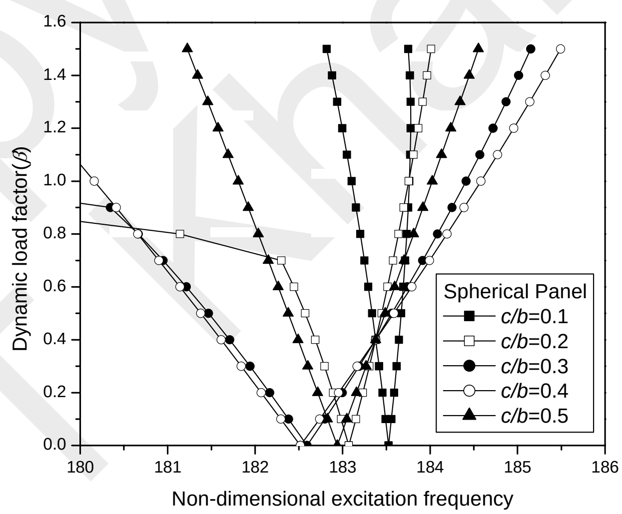


**Fig. 5.68 Same as Fig. 5.66 but for, spherical panel**

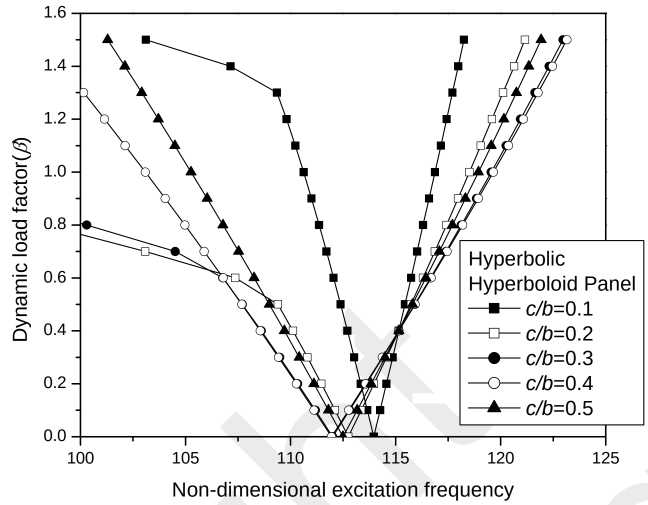


**Fig. 5.69 Same as Fig. 5.66 but for, hyperbolic hyperboloid shell panel**

## 5.4 Laminated composite stiffened shell panels with cutout under non-uniform loading

The problem of laminated composite stiffened shell panels with square cutout, located at the center of the panels with four types of non-uniform loading (Type-I, Type-II, Type-III and Type-IV as Fig.4.3) is investigated for buckling (static stability), vibration and dynamic stability characteristics in this section. The four sides of the opening are attached with four stiffeners; length of each stiffener is equal to the size of the cutout. The convergence and accuracy of the proposed model is established further for non-uniform loading cases with cutout taking various problems of the earlier investigators' available in the literature.

### 5.4.1 Convergence and validation study

The convergence and accuracy of the proposed method are established again by comparing the results of various problems available in the literature.

***(a) Dynamic instability of un-stiffened simply supported laminated composite plate with cutout***

This problem of uniformly loaded laminated composite plate with square cutout is taken to carry out the convergence study. The dimensions of plate are $a$ = $b$ = 500mm, $h$ = 2mm and lamination properties is $[45/-45/-45/45]_2$. The properties of the material taken are $E_{11}$ = 191.13Gpa, $E_{22}$ = 124.73Gpa, $G_{12} = G_{13} = G_{23}$ = 56.19Gpa and $\nu_{12}$ = 0.3. The static load factor $\alpha$ is taken as 0.0. The reference load is the first mode critical buckling load of the plate without cutout. The cutouts are square in size and located at the center of the plate. The whole structure is modeled with different mesh sizes for the dynamic instability analysis. The non-dimensional lower and upper excitation frequencies ($\bar{\Omega} = \Omega a^2 \sqrt{\rho / E_{22} h^2}$) of the instability zones for three (0.0, 0.2 and 0.6) values of dynamic load factor ($\beta$) are shown in Table 1 taking the cutout size *ca/a* = 0.5 for all mesh sizes. It shows a rapid convergence with mesh refinement. Again a mesh size of 8×8 is found to be sufficient to attain the convergence. For validation the results obtained in the present analysis are compared with those of Sahu and Datta [125] in Table 5.17. To validate the formulation further the instability zones for two cutout sizes *ca/a* = 0.4 and *ca/a* = 0.8 are plotted in Fig. 5.70 along with the given results [125] taking 10×10 mesh of the full structure. The present results are well in agreement with the available result [125].

**Table 5.17 Non-dimensional bounding frequency ($\bar{\Omega}$) for un-stiffened simply supported square laminated composite plate with cutout (*ca/a*=0.5)**

| Non-dimensional bounding frequency ($\bar{\Omega}$) | | | | | | |
|---|---|---|---|---|---|---|
| Analysis | $\beta = 0.0$ | | $\beta = 0.2$ | | $\beta = 0.6$ | |
| | $L^a$ | $U^b$ | $L^a$ | $U^b$ | $L^a$ | $U^b$ |
| Present (4×4) | 16.468 | 16.468 | 15.493 | 17.370 | 13.254 | 18.992 |
| Present (8×8) | 16.302 | 16.302 | 15.314 | 17.211 | 13.027 | 18.832 |
| Present (12×12) | 16.212 | 16.212 | 15.221 | 17.123 | 12.920 | 18.744 |
| Present (16×16) | 16.178 | 16.178 | 15.186 | 17.092 | 12.884 | 18.708 |
| Sahu and Datta [125] | 16.343 | 16.343 | 15.372 | 17.314 | 13.170 | 18.770 |

[a] Lower boundary of the instability zone

[b] Upper boundary of the instability zone

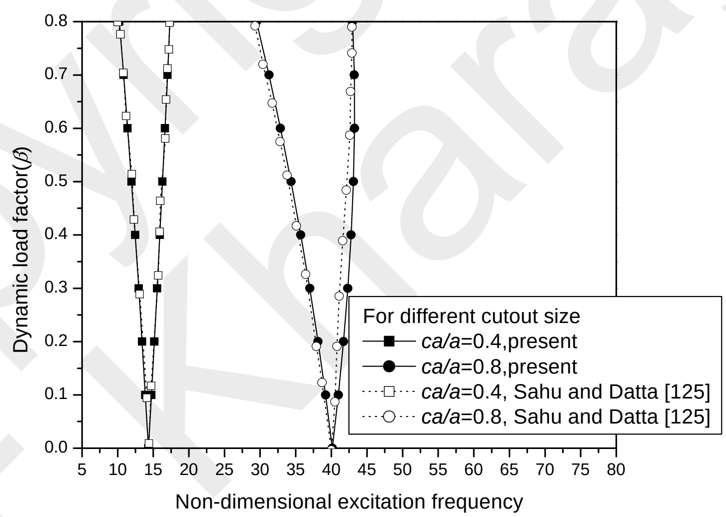


**Fig. 5.70 Effect of cutout size on dynamic instability region of simply supported laminated plate**

***(b) Vibration of stiffened plate with cutout***

The problem of simply supported square stiffened plate with square cutout is used to carry out the vibration analysis. The plate is attached with an eccentric stiffener along the center line in. The cutouts are square in size and located at the center of the plate. The data of the stiffened plate is $a = b = 0.6$m, $h = 0.001$m, $b_s = 0.00331$m, $d_s = 0.02025$m, $E = 68.7\times10^9$ N/m$^2$, $\nu = 0.34$, $\rho = 2780$ Kg/m$^3$. Four different sizes of cutouts with *ca/a* equal to 0.2, 0.4, 0.6 and 0.8 are taken. The whole plate is divided in 10×10 mesh. The first mode non-dimensional ($\varpi = \omega b^2\sqrt{\rho h / D}$) natural frequency obtained in the present analysis are plotted in Fig. 5.71 along with the finite element results given by Srivastava [140]. The present results are well in agreement with the available results [140].

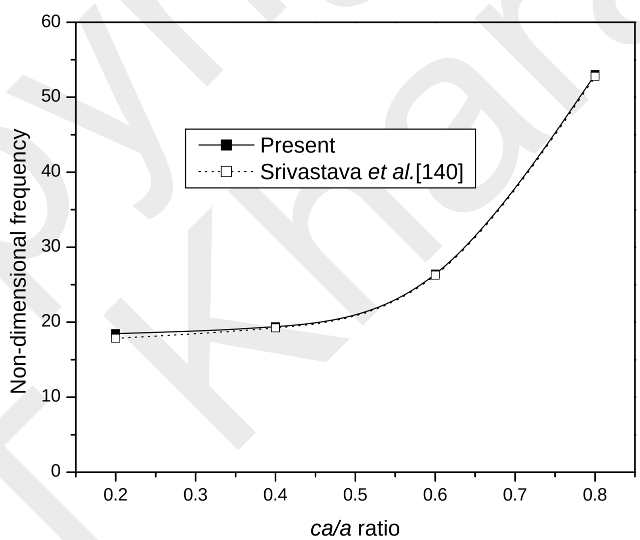


**Fig. 5.71 Variation of frequency with cutout size**

***(c) Dynamic stability of simply supported stiffened plate with square cutout***

The problem of simply supported square stiffened plate with square cutout at the center is used to investigate the dynamic instability characteristics. The plate is attached with an eccentric stiffener along the center line. The cutouts are square in size and located at the center of the plate. The data of the stiffened plate is $a$ = $b$ = 0.6m, $h$ = 0.001m, $b_s$ = 0.00331m, $d_s$ = 0.02025m, $E$ = 68.7×10$^9$ N/m$^2$, $\nu$ = 0.34, $\rho$ = 2780 Kg/m$^3$. Two different sizes of cutout with *ca/a* equals to 0.4 and 0.8 are considered. The load acting on the plate is non-uniform loading Type-I with *c/b* ratio as 0.4 along the stiffener direction. The static load factor $\alpha$ is taken as 0.2. The whole plate is divided in 10×10 mesh. The non-dimensional ($\bar{\Omega} = \Omega b^2 \sqrt{\rho h / D}$) excitation frequencies are plotted in Fig.5.72 for the two cutouts along with the results reported by Srivastava [140]. The present results are in good agreement with the results given by [140].

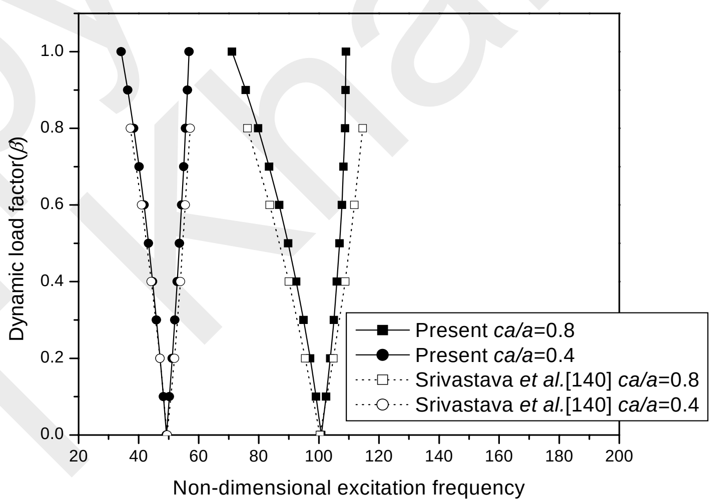


**Fig. 5.72 Dynamic stability region of the stiffened late with different cutout size, loading Type-I, *c/b*=0.4**

### 5.4.2 Problems under investigation

After obtaining the validity of the present analysis, the buckling, vibration and dynamic instability analyses are carried out for a laminated composite stiffened shell panel(Problem 3, described in 4.7) with square cutout located at the center (Fig 5.73) for all the four types of non-uniform loading cases (Fig.4.3). In all cases the different parameters are varied in a wide range to study the effect of these parameters on the behavior of the shell panels. The numerical results are presented along with the problem definition taking various parameters into consideration.

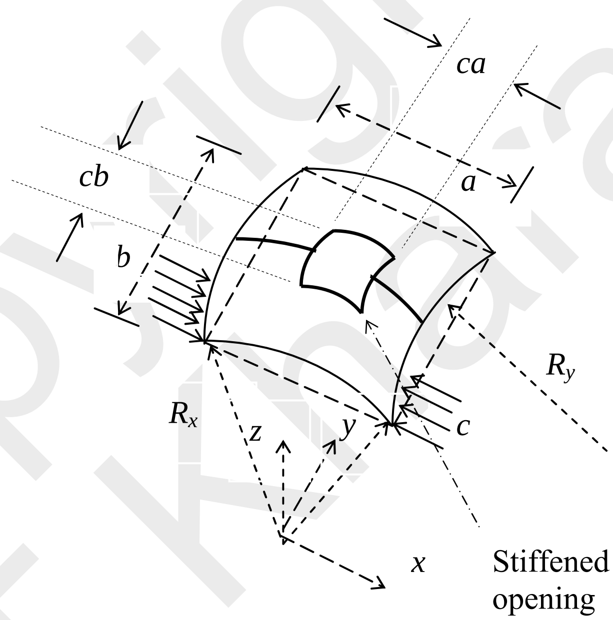


**Fig. 5.73 A doubly curved shell panel with stiffened square opening with a central *x*-stiffener subjected to loading Type-I**

**Numerical results**

The numerical results for the buckling, vibration and dynamic instability analyses are presented for all four (flat plate, cylindrical shell panel, spherical shell panel and hyperbolic hyperboloid panel) laminated composite stiffened shell panels with cutout for the four types of non-uniform loading cases (Fig. 4.2). The parameters like loading type, cutout size, lamination scheme, stiffener eccentricity, stacking scheme in stiffener etc. are varied in a wide range to study the effects of these parameters on the behavior of the structure. The detail is given below. In all the analysis the whole panel is divided in to 10×10 mesh as this mesh size (10×10) is found sufficient to attain convergence and for validation of results (5.4.1).

## Loading Type-I

The vibration, buckling and dynamic stability characteristics of the laminated composite stiffened shell panels with cutout (Fig. 5.73) for the partial loading Type-I (Localized edge loading from one end of two opposite side) are presented in this section. The effect of cutout size and the loading width are considered to study the behavior of the shell panels.

### (a) Buckling

The effects of load bandwidth ratio ($c/b$) of the patch loading (Type-I) and cutout ratio ($ca/a$) on buckling for all the four types of stiffened shell panels are discussed here. The analysis to study the effect of cutout size is carried out with uniformly distributed loading ($c/b$=1.0) on the panel edges. The cutout ratios ($ca/a$) taken are 0.2, 0.4 and 0.6. The panels are attached with single $(xst)_b$ stiffener along the center line and the four sides of the opening are stiffened with four stiffeners; length of each stiffener is equal to the size of the opening. These four stiffeners are also attached to the bottom surface. The stiffener depth to breadth ratio ($d_s/b_s$)

for all stiffeners is kept as 4.0. The lamination in the panel skin and stiffeners is taken as $(45/-45)_2$. The stacking scheme in the stiffeners is parallel to the stacking in the panel skin. The study for the effect of load bandwidth ratio(*c/b*) is carried out with the cutout size *ca/a* = 0.4. The ratios *c/b* are taken as 0.1, 0.2, 0.3,…, 1.0 for the buckling analysis. Figure 5.74 shows the effect of cutout size (*ca/a*) for all four panels and Fig. 5.75 shows the effect of load bandwidth ratio(*c/b*) for flat plate and spherical shell panel, on buckling load.

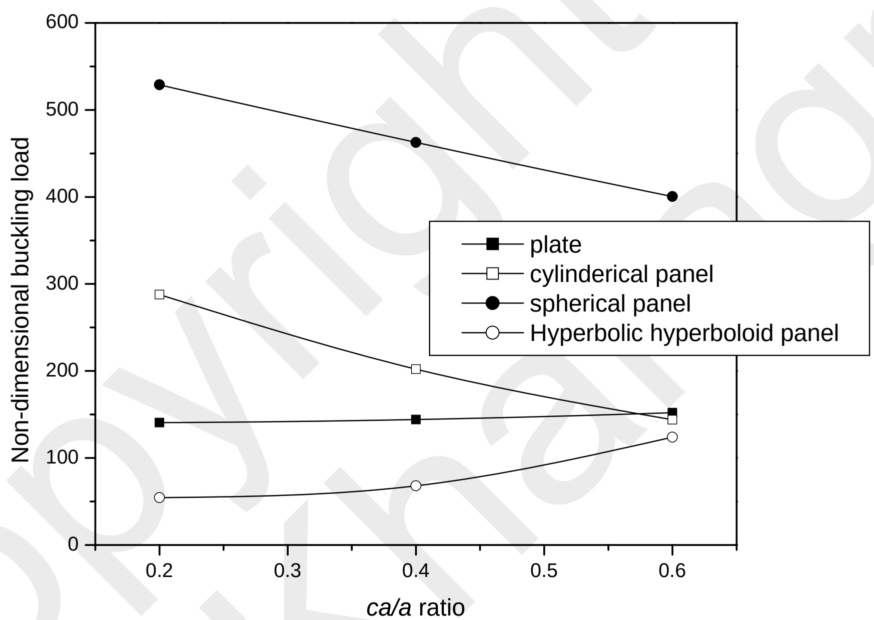


**Fig. 5.74 Variation of non-dimensional buckling load with *ca/a* ratio, (*c/b*=1.0)**

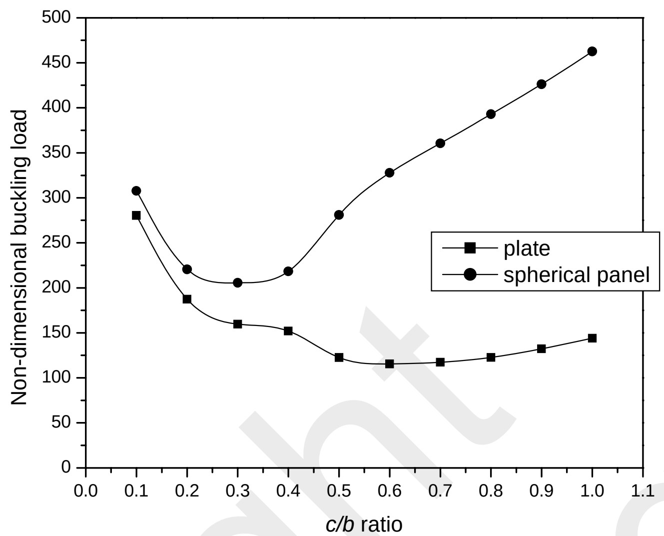


**Fig. 5.75 Variation of non-dimensional buckling load with *c/b* ratios, (*ca/a*=0.4)**

It is observed from Fig. 5.74 that with the increase in cutout size the buckling load is slightly increasing in plate and hyperbolic hyperboloid shell panel while it is decreasing significantly for the cylindrical and spherical panels. This may be due to the reason that the stiffness is reduced due to cutout in the spherical and cylindrical panel. Fig. 5.75 shows that the buckling load is decreasing with the increase in load width upto $c/b$ = 0.3 in spherical panel and then it is increasing gradually, but in plate the buckling load is decreasing upto $c/b$ = 0.6 and then it is increasing slowly compared to stiffened spherical panel.

## (b) Vibration

The first mode natural frequency of the above four panels with the same configuration are plotted in Fig. 5.76 with three cutout sizes. The behaviour is observed to be similar to that of the buckling load with cutout as mentioned in the above section.

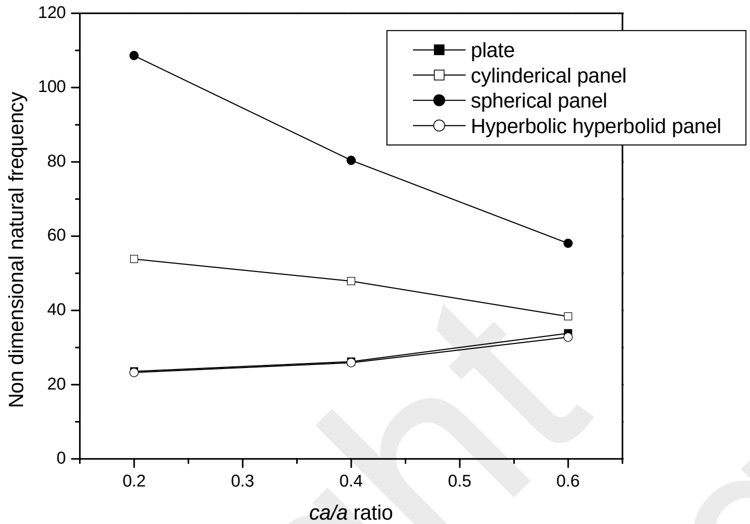


**Fig. 5.76 Variation of non-dimensional frequency with *ca/a* ratio, (*c/b*=1.0)**

### (c) Dynamic stability

The dynamic instability analysis of the panels is carried out in this section. In all the dynamic stability analysis, the non-dimensional buckling stress, with uniformly loaded ($c/b$ = 1.0, in Type-I loading), four layered simply supported (SSSS) angle-ply $(45/-45)_2$ stiffened flat plate without cutout with a four layered single $(\text{xst})_b$ stiffener ($d_s/b_s$= 4) along the center line with $(45/-45)_2$ lamination scheme and horizontal stacking, is taken as the reference load, so as to plot the instability zones. The panels are attached with single $(\text{xst})_b$ stiffener along the center line and the four sides of the opening are stiffened with four stiffeners, length of the stiffeners is equal to the length of the opening. These four stiffeners are also attached to the bottom surface. The stiffener depth to breadth ratio ($d_s/b_s$) for all the stiffeners is kept as 4.0. The lamination in the panel skin and stiffeners is taken as $(45/-45)_2$. The stacking scheme in the stiffeners is parallel to the stacking in the panel skin. The static load factor ($\alpha$) is 0.2 in all cases. The dynamic load factor ($\beta$) varies from 0.0 to 1.0.

### *i. Effect of cutout sizes*

The effect of cutout sizes on dynamic instability regions (DIR) for laminated composite stiffened flat, cylindrical, spherical, and hyperbolic hyperboloid panels is analyzed here. Three different sizes of cutout with *ca/a* equal to 0.2, 0.4 and 0.6 are taken for the analysis. The panels are loaded with uniformly load (*c/b*=1.0). Figures 5.77-5.80 show dynamic instability regions for different cutout sizes for plate, cylindrical, spherical, and hyperbolic hyperboloid panels respectively. It is observed for the stiffened plate with cutout (Fig. 5.77) and stiffened hyperbolic hyperboloid panel with cutout (Fig. 5.80) that the instability regions are shifting to higher frequency zones with the increase in cutout size while the behaviour is reversed for stiffened cylindrical (Fig. 5.78) and spherical (Fig.5.79) shell panels with cutout. The presence of cutout is adding extra stiffening effect in plate and hyperbolic hyperboloid panel while in cylindrical and spherical shell panels the presence of cutout is reducing the stiffness.

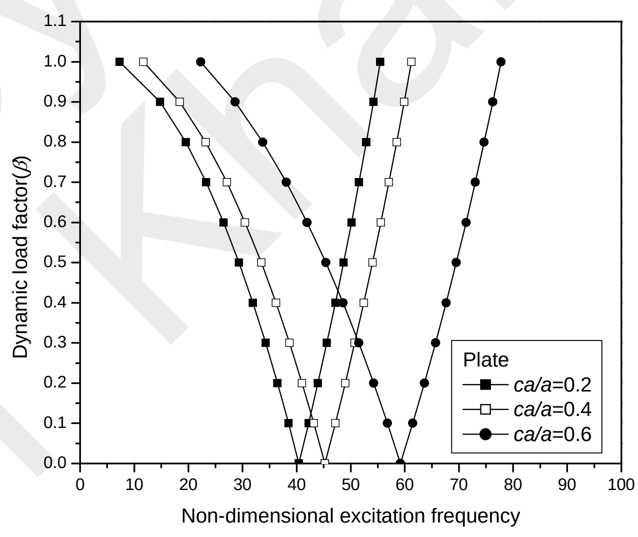


**Fig. 5.77 Dynamic instability region for different cutout sizes, with *c/b*=1.0, plate**

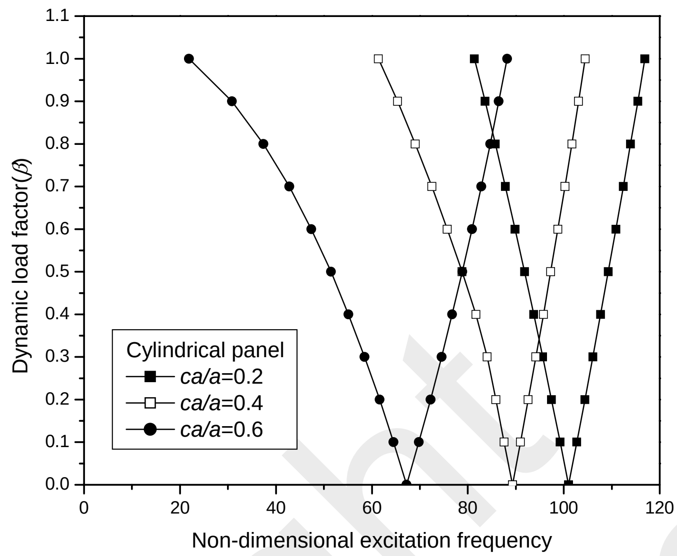


**Fig. 5.78 Same as Fig. 5.77 but for, cylindrical panel**

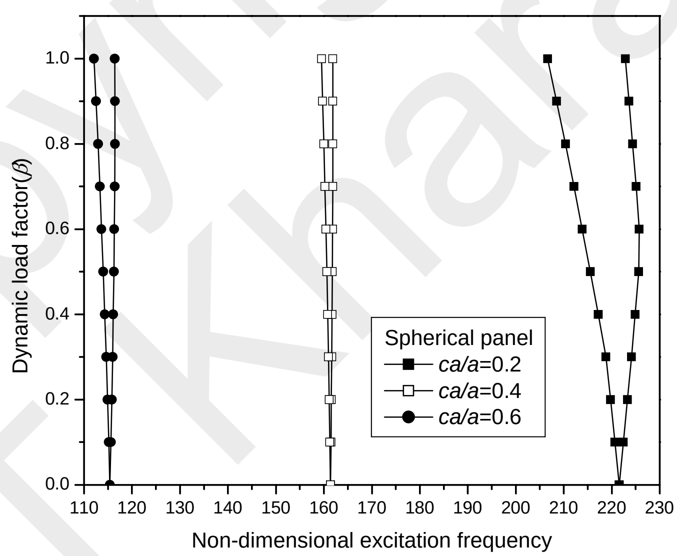


**Fig. 5.79 Same as Fig. 5.77 but for, Spherical shell panel**

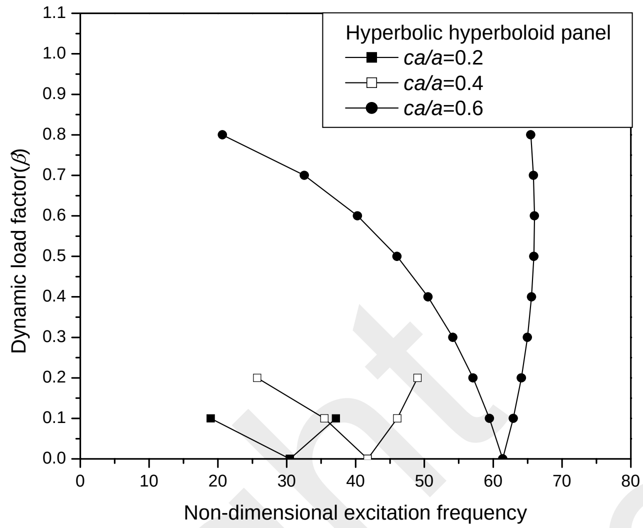


**Fig. 5.80 Same as Fig. 5.77 but for, hyperbolic hyperboloid shell panel**

### *ii. Effect of load bandwidth ratio (c/b)*

The effect of load bandwidth ratio(*c/b*) on dynamic instability regions (DIR) for laminated composite stiffened flat and spherical panel with cutout is considered here. The cutout size is *ca/a* = 0.4 in all cases. The ratios *c/b* are taken as 0.1, 0.2, 0.3,…, 1.0 for the buckling analysis. Figures 5.81-5.82 show the dynamic instability regions for different loading patch for flat plate and spherical panel respectively. It is observed from Fig. 5.81 that in case of plate the dynamic instability regions are shifting gradually to lower frequency zone side with increased width with the increase in *c/b* ratio. But in case of spherical panel (Fig. 5.82) the dynamic instability regions are shifting gradually to higher frequency zone side with increased width with the increase in *c/b* ratio.

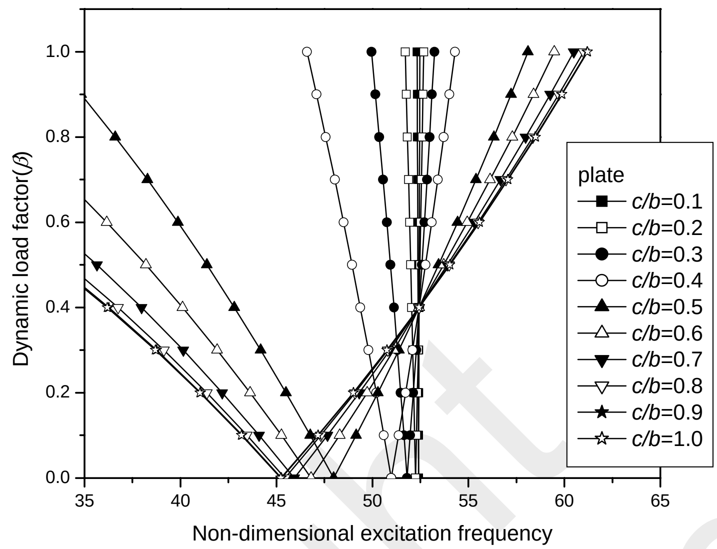


**Fig. 5.81 Dynamic instability region for different *c/b* ratio, with *ca/a*=0.4, plate**

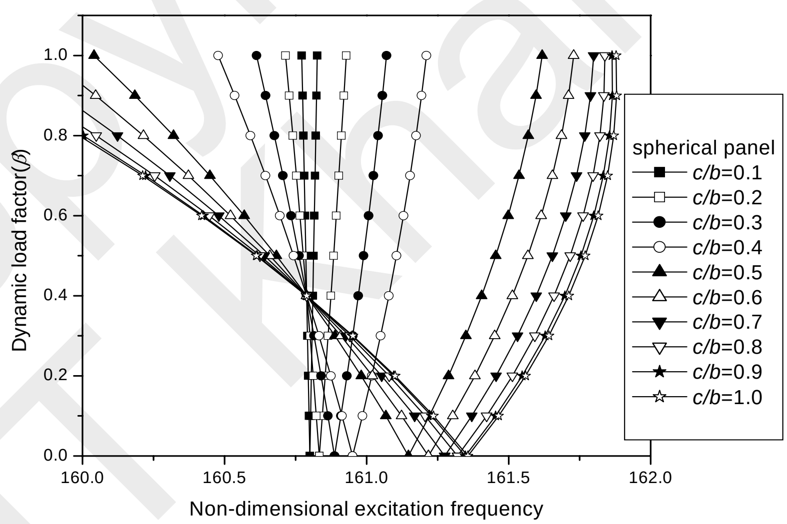


**Fig. 5.82 Same as Fig. 5.81 but for, Spherical shell panel**

## Loading Type-II

The vibration, buckling and dynamic stability characteristics of laminated composite stiffened shell problem (Fig. 5.73) for the partial loading Type-II (Localized edge loading from the center of two opposite side) are presented in this section. The effects of cutout size and the loading width are considered to study the behavior of the shell panels. The details are described below.

### (a) Buckling

The effects of load bandwidth ratio (*c/b*) of the patch loading (Type-II) and cutout ratio (*ca/a*) on buckling of the laminated composite stiffened plate and spherical shell panels with cutout are discussed here. The panels are attached with single $(xst)_b$ stiffener along the center line and the four sides of the opening are stiffened with four stiffeners; length of each stiffener is equal to the size of the cutout. These four stiffeners are also attached to the bottom surface. The stiffener depth to breadth ratio ($d_s/b_s$) for all stiffeners is kept as 4.0. The lamination in the panel skin and stiffeners is taken as $(45/\text{-}45)_2$. The stacking scheme in the stiffeners is parallel to the stacking in the panel skin.

The cutout ratios (*ca/a*) taken are 0.2, 0.4, 0.6 and 0.8. In the analysis of the effect of cutout size on buckling load the load bandwidth ratio (*c/b*) is kept as 0.4. Figure 5.83 shows the variation of non-dimensional buckling load with *ca/a* ratio of the plate and spherical panel. The cutout size with ratio *ca/a* is kept as 0.4 in the analysis of buckling load for different *c/b* ratios. Five loading patches are considered with *c/b* equals to 0.2, 0.4, 0.6, 0.8 and 1.0. The variation of non-dimensional buckling load with *c/b* is shown in Fig. 5.84.

With the given loading width (*c/b*=0.4) the load carrying capacity in the spherical panel decreases gradually with the increase in cutout size. In plate when *ca/a* increases from 0.2 to 0.4 the buckling load decreases and again it increases with low rate with the increase in cutout size beyond 0.4 (Fig. 5.83). With the cutout size of *ca/a*=0.4 the load carrying capacity of both plate and spherical panel increases with the increase of the loading patch from center to both edges *i.e.* when *c/b* is increasing the buckling load is increasing (Fig. 5.84).

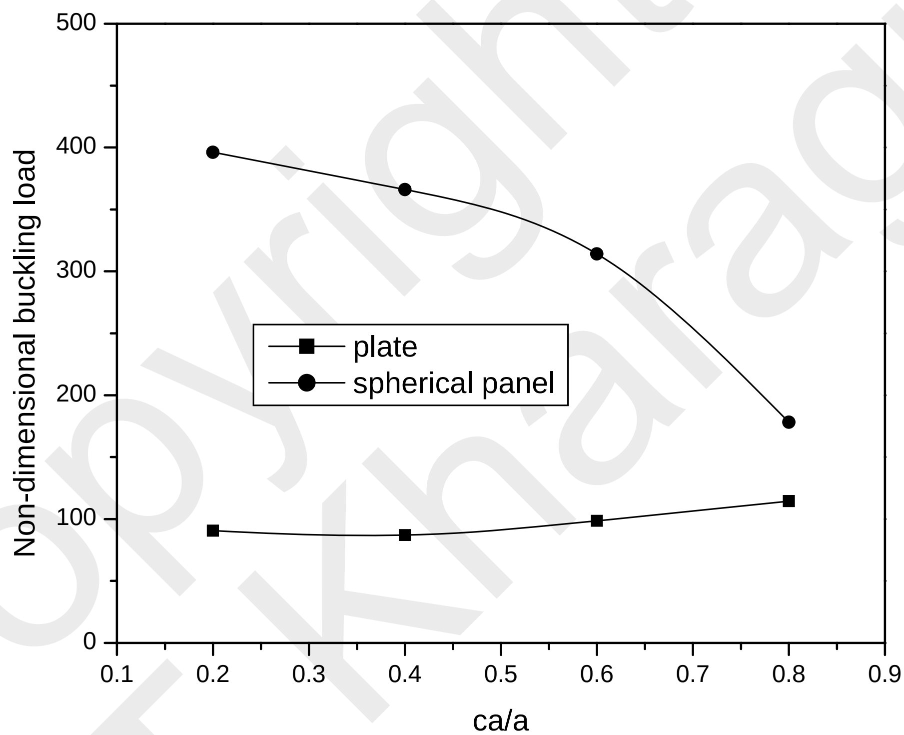


**Fig. 5.83 Variation of non-dimensional buckling load with *ca/a* ratio, (*c/b*=0.4)**

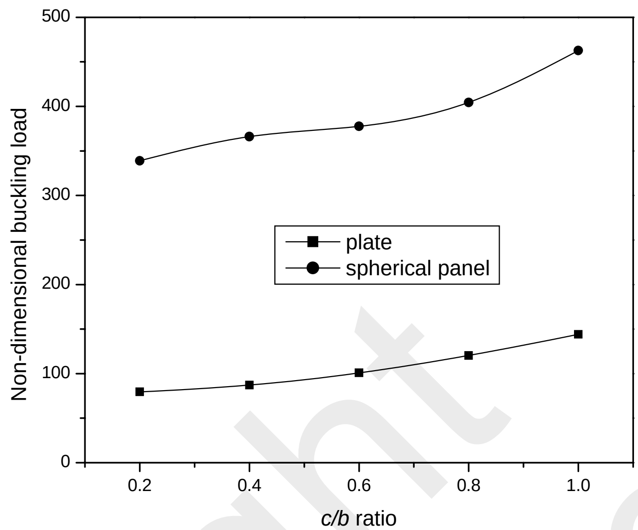


**Fig. 5.84 Variation of non-dimensional buckling load with *c/b* ratios, (*ca/a*=0.4)**

## (b) Vibration

The analysis of variation of frequencies with the applied load for the stiffened plate and spherical panel with above configuration is carried out with loading patch *c/b* = 0.4. The cutout ratios (*ca/a*) taken are 0.2, 0.4, 0.6 and 0.8. Figures 5.85-5.86 show the plot of the variation of first mode frequencies with the loading for plate and spherical panel respectively. In plate (Fig. 5.85) the natural frequency is increasing with the increase in cutout size. But the buckling load is decreased when the cutout size (*ca/a*) is increased from 0.2 to 0.4 and again the load carrying capacity is increasing beyond *ca/a* = 0.4. When the applied loads are increasing the frequency of vibrations are decreasing and finally attains zero value at the corresponding critical loads. In spherical shell panel (Fig. 5.86) the natural frequency and buckling load are decreasing with the increase in cutout size.

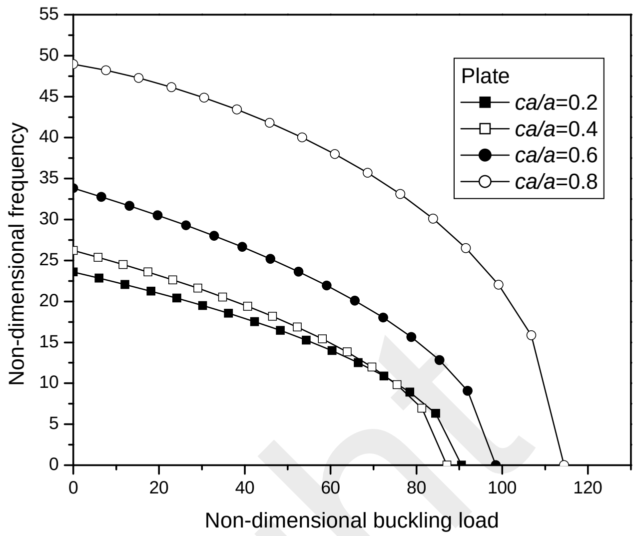


**Fig. 5.85 Variation of frequency with load for different cutout sizes, *c/b*=0.4,plate**

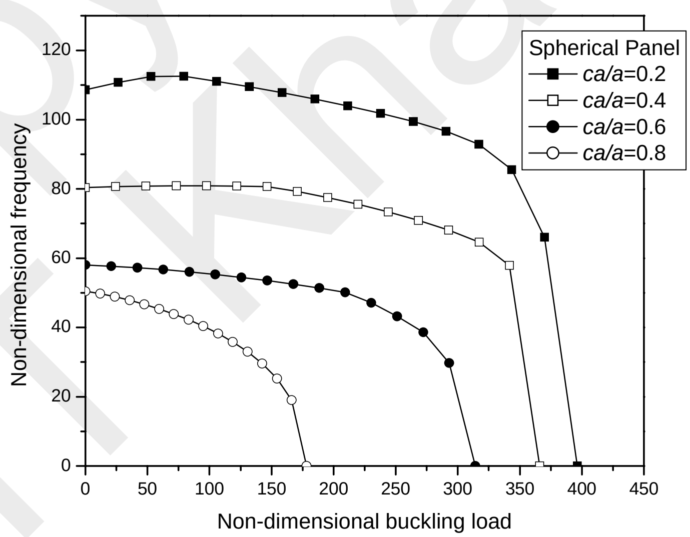


**Fig. 5.86 Same as Fig. 5.85, but for spherical panel**

**(c) Dynamic stability**

The dynamic instability analysis of the laminated composite stiffened plate and spherical panel with cutout is carried out in this section. The panels are attached with single $(xst)_b$ stiffener along the center line and the four sides of the opening are stiffened with four stiffeners, length of the stiffeners is equal to the length of the opening. These four stiffeners are also attached to the bottom surface. The stiffener depth to breadth ratio ($d_s/b_s$) for all stiffeners is kept as 4.0. The lamination in the panel skin and stiffeners is taken as $(45/-45)_2$. The stacking scheme in the stiffeners is parallel to the stacking in the panel skin.

The non-dimensional buckling stress, of a uniformly loaded ($c/b$ = 1.0, in Type-II loading), four layered simply supported (SSSS) angle-ply $(45/-45)_2$ stiffened flat plate without cutout with a four layered single $(xst)_b$ stiffener ($d_s/b_s$= 4) along the center line with $(45/-45)_2$ lamination scheme and horizontal stacking, is taken as the reference load, so as to plot the instability zones.

The static load factor ($\alpha$) is 0.2 in all cases. The dynamic load factor ($\beta$) varies from 0.0 to 1.0.

***i. Effect of cutout sizes***

The effect of cutout sizes on dynamic instability regions (DIR) for laminated composite stiffened flat and spherical panel is analyzed here. Four different sizes of cutout with *ca/a* equal to 0.2, 0.4, 0.6 and 0.8 are taken for the analysis. The panels are loaded with patch load ($c/b$=0.4). Figures 5.87-5.88 show dynamic instability regions for different cutout sizes for plate and spherical panel respectively. In stiffened plate with cutout (Fig. 5.87) the instability regions are shifting to higher frequency zones with the increase in cutout size while the behaviour is reversed for stiffened spherical (Fig. 5.88) shell panels with cutout. It indicates that with the given configuration the spherical shell panel becomes dynamically more unstable with the increase in cutout size.

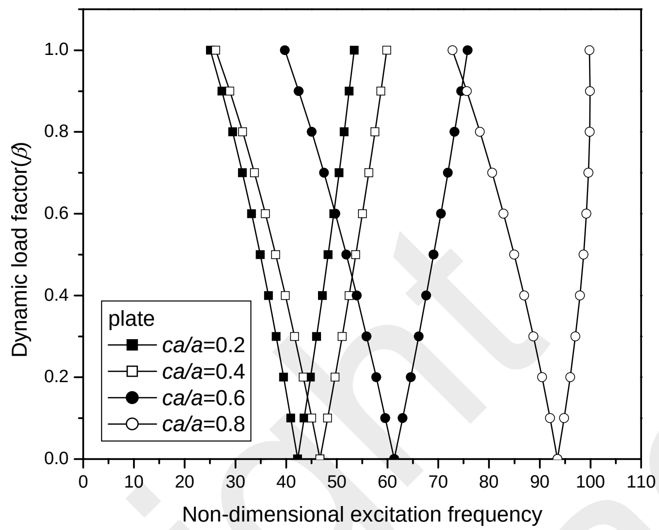


**Fig. 5.87 Dynamic instability region for different cutout sizes, with *c/b*=0.4, Plate**

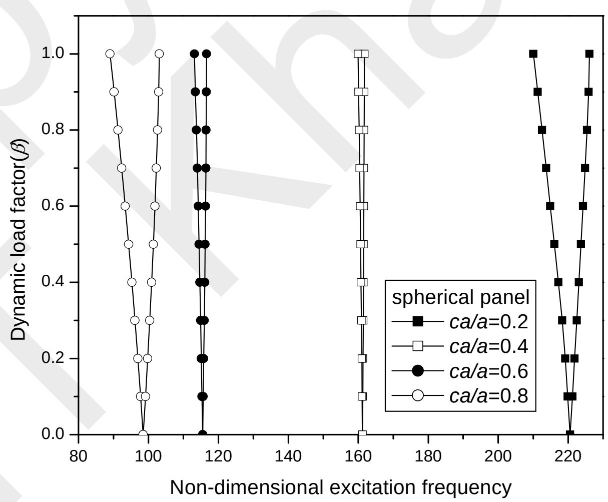


**Fig. 5.88 Same as Fig. 5.87, but for spherical panel**

***ii. Effect of load bandwidth ratio (c/b)***

The effect of load bandwidth ratio (*c/b*) on dynamic instability regions (DIR) for laminated composite stiffened flat and spherical panel with cutout is considered here. The cutout size is *ca/a* = 0.4 in all cases. The ratios *c/b* are taken as 0.2, 0.4, 0.6, 0.8 and 1.0 for the dynamic stability analysis. Figures 5.89-5.90 show the dynamic instability regions for all five loading patches for flat plate and spherical panel respectively. In case of plate (Fig. 5.89) the dynamic instability regions are shifting gradually to lower frequency zone side with increased width with the increase in *c/b* ratio. But in case of spherical panel (Fig. 5.90) the dynamic instability regions are shifting gradually to higher frequency zone side with increased width with the increase in *c/b* ratio.

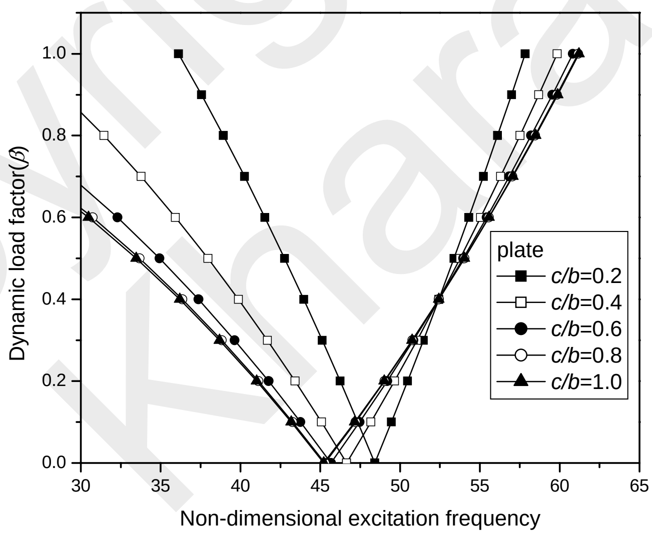


**Fig. 5.89 Dynamic instability region for different *c/b* ratio, with *ca/a*=0.4, loading Type-II, $\alpha$ = 0.2, plate**

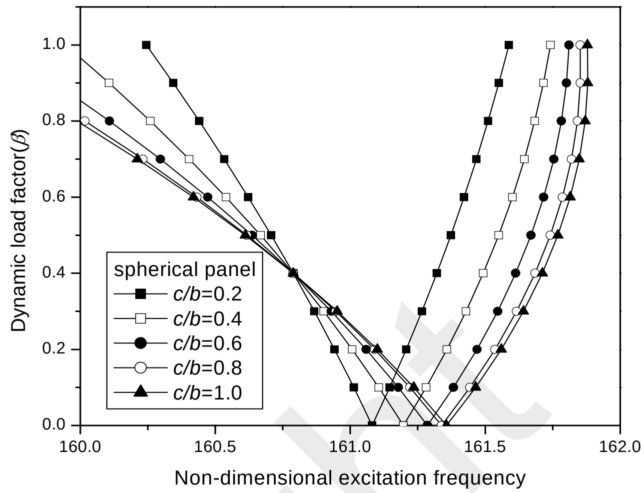


**Fig. 5.90 Same as Fig. 5.89, but for spherical panel**

## Loading Type-III

The vibration, buckling and dynamic stability characteristics of the laminated composite stiffened shell problem (Fig. 5.73) for the partial loading Type-III (Localized edge loading from both ends of two opposite side) are presented in this section. The effect of cutout size and the loading width are considered to study the behavior of the shell panels. The details are described below.

### (a) Buckling

The effects of load bandwidth ratio (*c/b*) of the patch loading (Type-III) and cutout ratio (*ca/a*) on buckling of the laminated composite stiffened plate and spherical shell panels with cutout are discussed here. The panels are attached with single $(xst)_b$ stiffener along the center line and the four sides of the opening are stiffened with four stiffeners, length of the stiffeners is equal to the length of the opening. These four stiffeners are also attached to the bottom surface. The stiffener depth to breadth ratio ($d_s/b_s$) for all stiffeners is kept as 4.0. The lamination in the panel skin and stiffeners is taken as $(45/-45)_2$. The stacking scheme in the stiffeners is parallel to the stacking in the panel skin.

The cutout ratios (*ca/a*) taken are 0.2, 0.4, 0.6 and 0.8. In the analysis of the effect of cutout size on buckling load the load bandwidth ratio(*c/b*) is kept as 0.2. Figure 5.91 shows the variation of non-dimensional buckling load with *ca/a* ratio of the plate and spherical panel. The cutout size with ratio *ca/a* is kept as 0.4 in the analysis of buckling load for different *c/b* ratios. Five loading patches are considered with load bandwidth ratio *c/b* equal to 0.1, 0.2, 0.3, 0.4 and 0.5. The variation of non-dimensional buckling load with *c/b* is shown in Fig. 5.92.

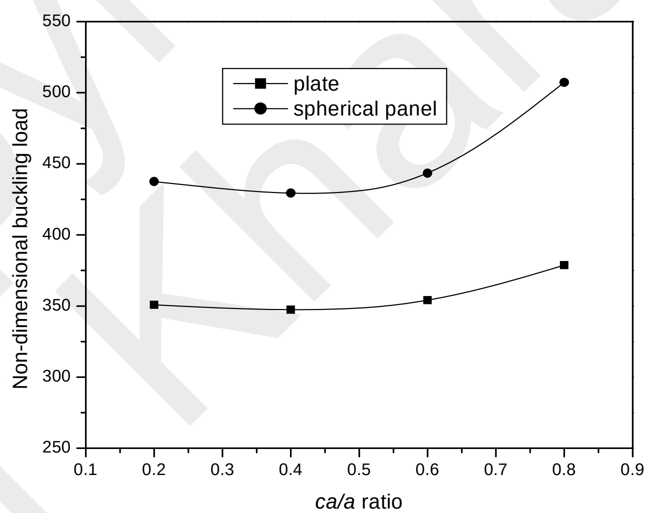


**Fig. 5.91 Variation of non-dimensional buckling load with *ca/a* ratio, (*c/b*=0.2), loading Type-III.**

Figure 5.91 shows that the buckling load of both panels decreases when the cutout ratio is increased from 0.2 to 0.4 and after *ca/a*=0.4 the buckling load is gradually increasing.

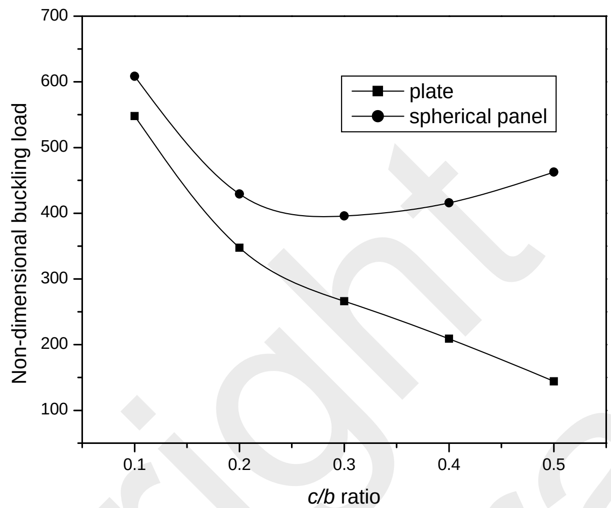


**Fig. 5.92 Variation of non-dimensional buckling load with *c/b* ratios, (*ca/a*=0.4)**

When the *c/b* ratio is increasing the load carrying capacity of the spherical shell panel decreasing upto *c/b*=0.3 and beyond that it is increasing upto *c/b*=0.5. But in case of plate the buckling load is gradually decreasing with the increase in the loading width (Fig. 5.92).

**(b) Vibration**

The analysis of variation of frequencies with the applied load for the stiffened plate and spherical panel with above configuration is carried out with loading patch *c/b*=0.2. The cutout ratios (*ca/a*) taken are 0.2, 0.4, 0.6 and 0.8. Figures 5.93-5.94 show the plot of the variation of first mode frequencies with the loading for plate and spherical panel respectively for all four *ca/a* ratios. In plate (Fig. 5.93) the natural frequency is increasing with the increase in cutout size and with the increase of the applied loads the frequency of vibrations are decreasing gradually and finally attains zero value at the corresponding critical loads. In spherical shell panel (Fig. 5.94) the natural frequency is decreasing with the increase in cutout size and with the increase in the applied load the frequency of vibration is almost remaining constant and just near to the critical value the frequency of vibration becomes zero.

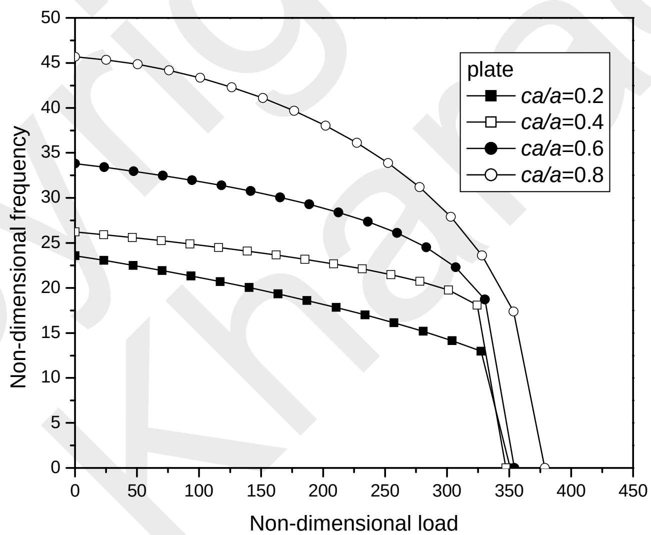


**Fig. 5.93 Variation of frequency with load for different cutout sizes, *c/b*=0.2, plate**

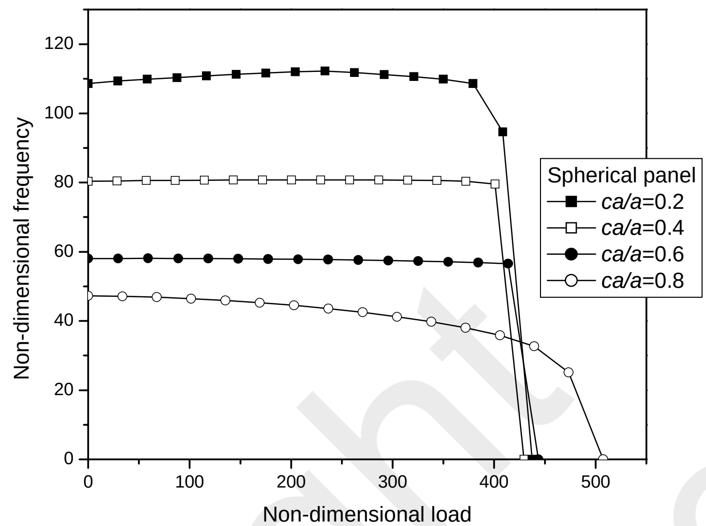


**Fig. 5.94 Same as Fig. 5.93, but for spherical panel**

**(c) Dynamic stability**

The dynamic instability analysis of the laminated composite stiffened plate and spherical panel with cutout is carried out in this section. The panels are attached with single $(xst)_b$ stiffener along the center line and the four sides of the opening are stiffened with four stiffeners, length of the stiffeners is equal to the length of the opening. These four stiffeners are also attached to the bottom surface. The stiffener depth to breadth ratio ($d_s/b_s$) for all stiffeners is kept as 4.0. The lamination in the panel skin and stiffeners is taken as $(45/-45)_2$. The stacking scheme in the stiffeners is parallel to the stacking in the panel skin.

The non-dimensional buckling stress, with uniformly loaded ($c/b$ = 0.5, in Type-III loading), four layered simply supported (SSSS) angle-ply $(45/-45)_2$ stiffened flat plate without cutout with a four layered single $(xst)_b$ stiffener ($d_s/b_s$= 4) along the center line with $(45/-45)_2$

lamination scheme and horizontal stacking, is taken as the reference load, so as to plot the instability zones. The static load factor ($\alpha$) is 0.2 in all cases. The dynamic load factor ($\beta$) varies from 0.0 to 1.0.

***i. Effect of cutout sizes***

The effect of cutout sizes on dynamic instability regions (DIR) for laminated composite stiffened flat and spherical panel is analyzed here. Four different sizes of cutout with *ca/a* equal to 0.2, 0.4, 0.6 and 0.8 are taken for the analysis. The panels are loaded with patch load (*c/b* = 0.2). Figures 5.95-5.96 show dynamic instability regions for different cutout sizes for plate and spherical panel respectively. In stiffened plate with cutout (Fig. 5.95) the instability regions are shifting to higher frequency zones with the increase in cutout size while the behaviour is reversed for stiffened spherical (Fig. 5.96) shell panels with cutout. The spherical panel becomes dynamically unstable at constant frequencies of the applied load with *ca/a* equals to 0.4, 0.6 and 0.8 and the instability effect increase with the increase in cutout size. It indicates that with the given configuration the spherical shell panel becomes dynamically more unstable with the increase in cutout size.

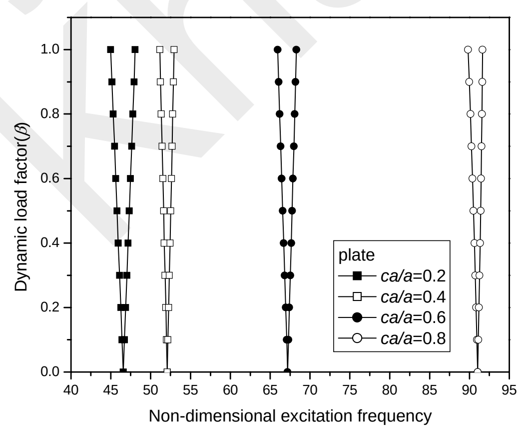


**Fig. 5.95 Dynamic instability region for different cutout sizes, with *c/b*=0.2, Plate**

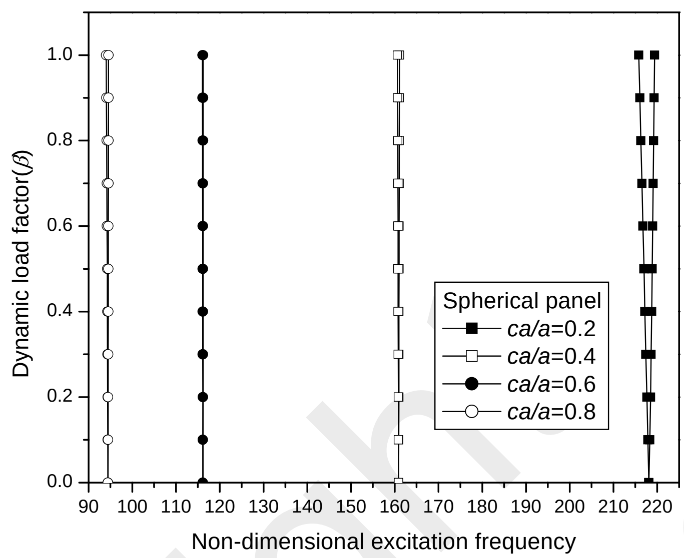


**Fig. 5.96 Same as Fig. 5.95, but for spherical panel**

### *ii. Effect of load bandwidth ratio (c/b)*

The effect of load bandwidth ratio(*c/b*) on dynamic instability regions (DIR) for laminated composite stiffened flat and spherical panel with cutout is considered here. The cutout size is *ca/a* = 0.4 in all cases. The ratios *c/b* are taken as 0.1, 0.2, 0.3, 0.4 and 0.5 for the dynamic stability analysis. Figures 5.97-5.98 show the dynamic instability regions for all five loading patches for flat plate and spherical panel respectively. In case of plate (Fig. 5.97) the dynamic instability regions are shifting gradually to lower frequency zone side with increased width with the increase in *c/b* ratio. But in case of spherical panel (Fig. 5.98) the dynamic instability regions are shifting gradually to higher frequency zone side with increased width with the increase in *c/b* ratio.

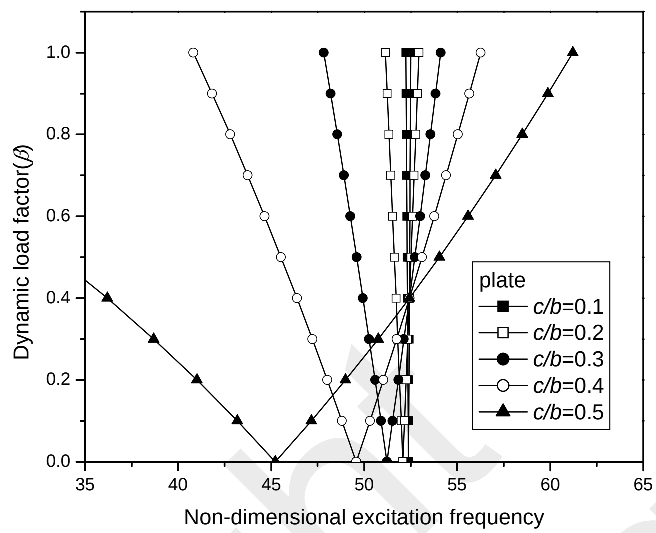


**Fig. 5.97 Dynamic instability region for different *c/b* ratio, with *ca/a* = 0.4, loading Type-III, $\alpha$ = 0.2, plate**

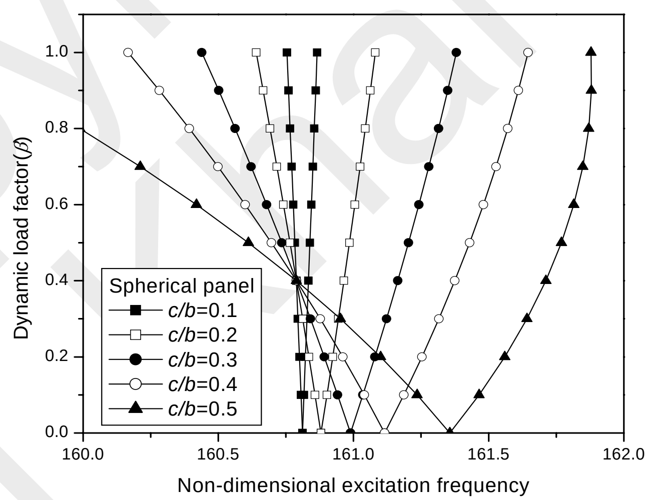


**Fig. 5.98 Same as Fig. 5.97, but for spherical panel**

### Loading Type-IV

The vibration, buckling and dynamic stability characteristics of the laminated composite stiffened shell problem (Fig. 5.73) for the partial loading Type-IV (Concentrated edge loading of two opposite side) are presented in this section. Various parameters are considered to study the behavior of the shell panels. The details are described below.

### (a) Buckling

The effects of load position (*c/b*) of the concentrated loading (Type-IV) and cutout ratio (*ca/a*) on buckling of the laminated composite stiffened plate and spherical shell panels with cutout are discussed here.

In the analysis of the effect of cutout size on buckling load the load position (*c/b*) is kept as 0.5. The cutout ratios (*ca/a*) taken are 0.2, 0.4, 0.6 and 0.8. The panels are attached with single $(xst)_t$ stiffener along the center line and the four sides of the opening are stiffened with four stiffeners, length of the stiffeners is equal to the length of the opening. These four stiffeners are also attached to the top surface. The stiffener depth to breadth ratio ($d_s/b_s$) for all stiffeners is kept as 4.0. The lamination in the panel skin and stiffeners is taken as $(45/-45)_4$. The stacking scheme in the stiffeners is perpendicular to the stacking in the panel skin. Figure 5.99 shows the variation of non-dimensional buckling load with *ca/a* ratio of the plate and spherical panel. It is observed from Fig. 5.99 that the buckling load of the plate is decreased when *ca/a* is increased from 0.2 to 0.4 and beyond that upto 0.8 the buckling load is gradually increasing. But in spherical shell panel the buckling load is gradually increasing with the increase in cutout size upto 0.6 and then it starts decreasing from *ca/a* = 0.6 to *ca/a* = 0.8.

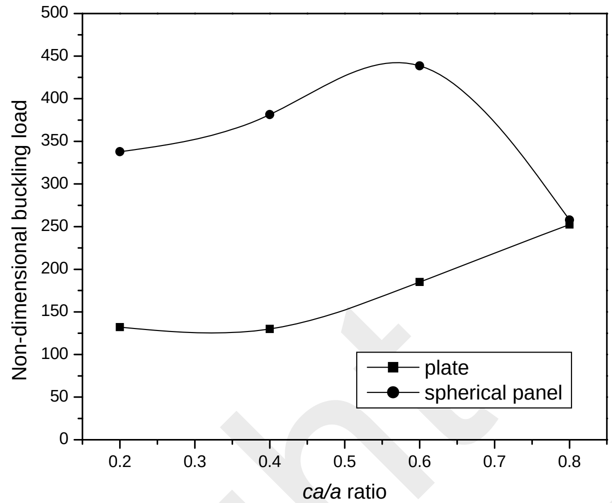


**Fig. 5.99 Variation of non-dimensional buckling load with *ca/a* ratio, (*c/b*=0.5), loading Type-IV.**

In the analysis of the effect of load position (*c/b*) on buckling load the cutout size is kept as *ca/a* = 0.4. Five loading positions are considered with *c/b* equal to 0.1, 0.2, 0.3, 0.4 and 0.5. The panels are attached with single $(xst)_b$ along the center line and the four sides of the opening are stiffened with four stiffeners, length of the stiffeners is equal to the length of the opening. These four stiffeners are also attached to the bottom surface. The stiffener depth to breadth ratio ($d_s/b_s$) for all stiffeners is kept as 4.0. The lamination in the panel skin and stiffeners is taken as $(45/\text{-}45)_2$. The stacking scheme in the stiffeners is parallel to the stacking in the panel skin. The variation of non-dimensional buckling load with *c/b* is shown in Fig. 5.100. When the concentrated load moves from the edge with *c/b*=0.1 to the center *c/b*=0.5, the buckling load in plate decreases gradually but the buckling load in spherical panel decreases upto *c/b*=0.2 and then starts increasing upto *c/b*=0.5.

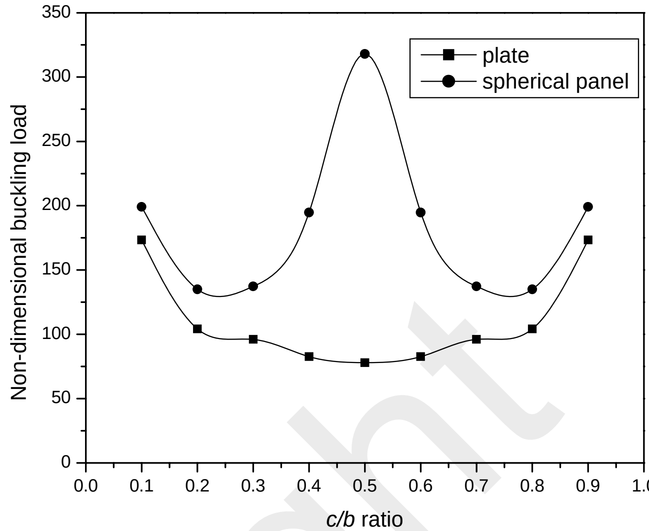


**Fig. 5.100 Variation of non-dimensional buckling load with *c/b* ratios, (*ca/a*=0.4)**

### (b) Vibration

The analysis of variation of frequencies with the applied load for the stiffened plate and spherical panel is carried out with loading position *c/b*=0.5. The panels are attached with single $(xst)_t$ stiffener along the center line and the four sides of the opening are stiffened with four stiffeners, length of the stiffeners is equal to the length of the opening. These four stiffeners are also attached to the top surface. The stiffener depth to breadth ratio ($d_s/b_s$) for all stiffeners is kept as 4.0. The lamination in the panel skin and stiffeners is taken as $(45/-45)_4$. The stacking scheme in the stiffeners is perpendicular to the stacking in the panel skin. The cutout ratios (*ca/a*) taken are 0.2, 0.4, 0.6 and 0.8. Figures 5.101-5.102 show the plot of the variation of first mode frequencies with the loading for plate and spherical panel respectively for all four *ca/a* ratios.

In plate (Fig. 5.101) the natural frequency is increasing with the increase in cutout size and in spherical shell panel (Fig. 5.102) the natural frequency is decreasing with the increase in cutout size. With the increase in the applied load the frequencies of vibration are decreasing gradually and finally attain zero value at the corresponding critical loads in both cases.

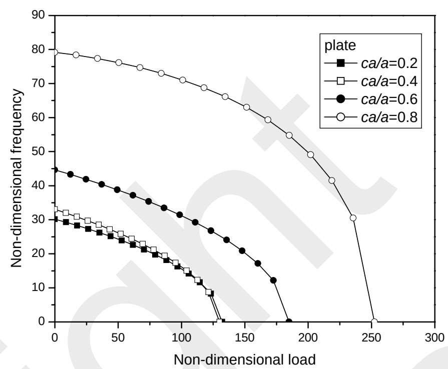


**Fig. 5.101 Variation of frequency with load for different cutout sizes, *c/b*=0.5, plate**

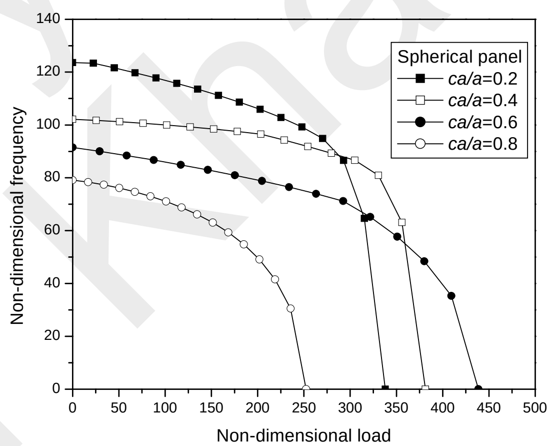


**Fig. 5.102 Same as Fig. 5.101, but for spherical panel**

## (c) Dynamic Stability

The dynamic instability analysis of the laminated composite stiffened plate and spherical panel with cutout is carried out in this section. The non-dimensional buckling load, of four layered simply supported (SSSS) angle-ply $(45/-45)_2$ stiffened flat plate with cutout size *ca/a*=0.4, with a four layered single $(xst)_b$ stiffener ($d_s/b_s$= 4) along the center line with $(45/-45)_2$ lamination scheme is taken as the reference load, so as to plot the instability zones. The four sides of the opening are stiffened with four stiffeners ($d_s/b_s$= 4); length of each stiffener is equal to the size of the opening. These stiffeners are also attached to the bottom surface. To calculate the buckling load the load is kept at position *c/b* = 0.1, in Type-IV loading. The stacking in all stiffeners is parallel to the stacking in the plate. The static load factor ($\alpha$) is 0.2 in all cases. The dynamic load factor ($\beta$) varies from 0.0 to 1.0.

### *i. Effect of cutout sizes*

The effect of cutout sizes on dynamic instability regions (DIR) for laminated composite stiffened flat and spherical panel is analyzed here. Four different sizes of cutout with *ca/a* equal to 0.2,0.4, 0.6 and 0.8 are taken for the analysis. The panels are loaded with concentrated load position at *c/b*=0.5. The panels are attached with single $(xst)_t$ stiffener along the center line and the four sides of the opening are stiffened with four stiffeners, length of each stiffener is equal to the size of the opening. These four stiffeners are also attached to the top surface. The stiffener depth to breadth ratio ($d_s/b_s$) for all stiffeners is kept as 4.0. The lamination in the panel skin and stiffeners is taken as $(45/-45)_4$. The stacking scheme in the stiffeners is perpendicular to the stacking in the panel skin.

Figures 5.103-5.104 show dynamic instability regions for different cutout sizes for plate and spherical panel respectively. In stiffened plate with cutout (Fig. 5.103) the instability regions are shifting to higher frequency zones with the increase in cutout size while the behaviour is reversed for stiffened spherical (Fig. 5.104) shell panels with cutout.

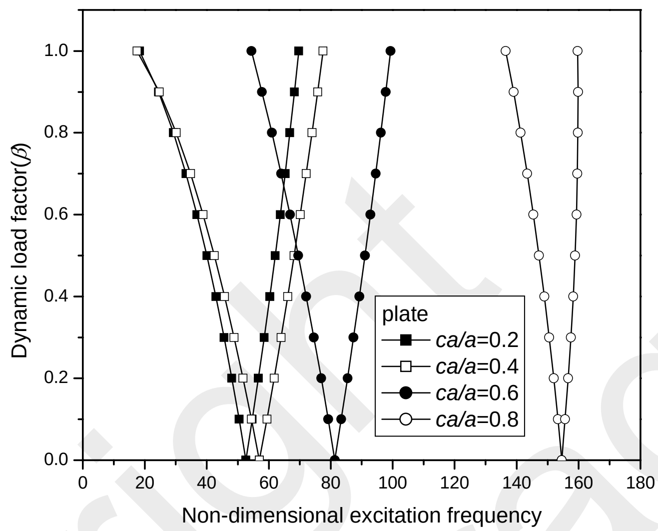


**Fig. 5.103 Dynamic instability region for different cutout sizes, with *c/b*=0.5, loading Type-IV, Plate**

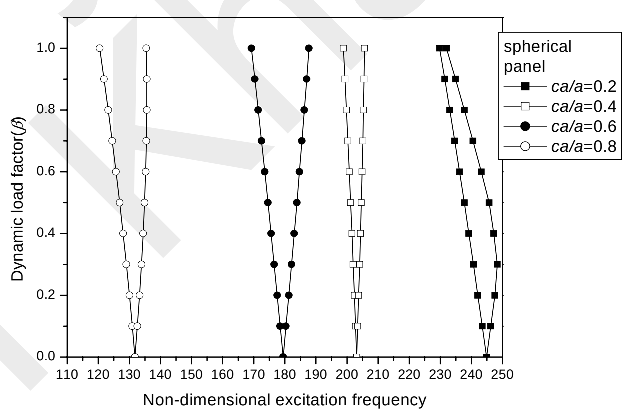


**Fig. 5.104 Same as Fig. 5.103, but for spherical panel**

***ii. Effect of load position(c/b)***

The effect of position of the concentrated load on dynamic instability regions (DIR) for laminated composite stiffened flat and spherical panel with cutout is analyzed. The cutout size is kept as *ca/a*=0.4 for the analysis. Five loading positions are considered with *c/b* equal to 0.1, 0.2, 0.3, 0.4 and 0.5. The panels are attached with single $(xst)_b$ stiffener along the center line and the four sides of the opening are stiffened with four stiffeners, length of the stiffeners is equal to the length of the opening. These four stiffeners are also attached to the bottom surface. The stiffener depth to breadth ratio ($d_s/b_s$) for all stiffeners is kept as 4.0. The lamination in the panel skin and stiffeners is taken as $(45/-45)_2$. The stacking scheme in the stiffeners is parallel to the stacking in the panel skin.

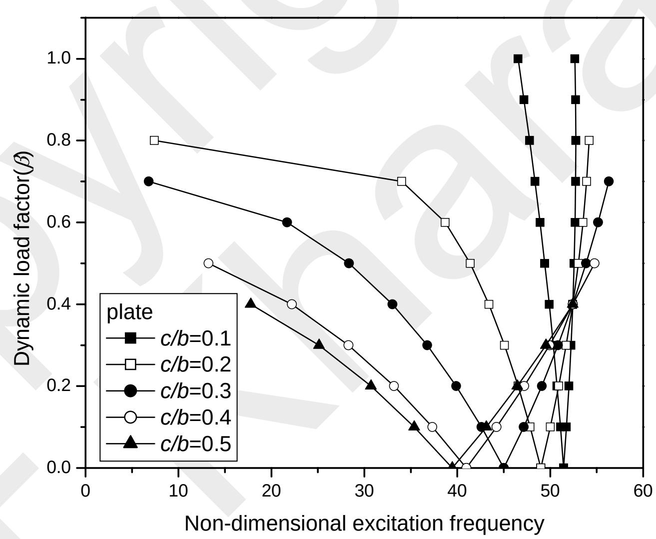


**Fig. 5.105 Dynamic instability region for different *c/b* ratio, with *ca/a*=0.4, loading Type-IV, $\alpha = 0.2$, plate**

Figures 5.105-5.106 show the dynamic instability regions for all five loading position for flat plate and spherical panel respectively. In case of plate (Fig. 5.105) the dynamic instability regions are shifting gradually to lower frequency zone side with increased width with the increase in *c/b* ratio. But in case of spherical panel (Fig. 5.106) the dynamic instability regions are shifting gradually to higher frequency zone side with increased width with the increase in *c/b* ratio. Both the panels are dynamically more stable at load position near the edge at *c/b*=0.1.

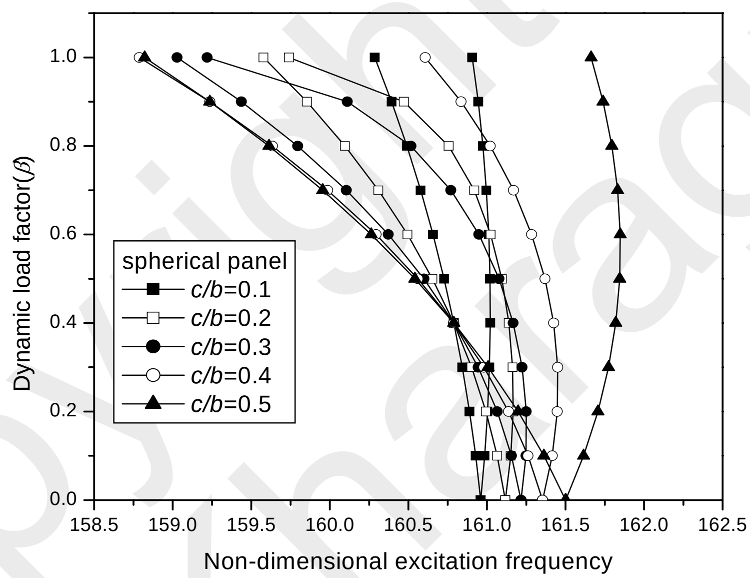


**Fig. 5.106 Same as Fig. 5.105, but for spherical panel**

***iii. Effect of number of layers***

The effect of number of layers on dynamic instability behaviour of the stiffened spherical shell panel with cutout size *ca/a*=0.4 and loading position at *c/b*=0.5 is analyzed. The spherical panel is attached with single $(xst)_b$ stiffener along the center line and the four sides of the opening are stiffened with four stiffeners, length of each stiffener is equal to the size of the opening. These four stiffeners are also attached to the bottom surface. The stiffener depth to breadth ratio ($d_s/b_s$) for all stiffeners is kept as 4.0. The stacking scheme in the stiffeners is parallel to the stacking in the panel skin. The numbers of layers are taken as 4 in one case and 8 in other case. In both cases the cross ply (0/90) and angle ply (45/-45) lamination scheme is taken. Fig. 5.107 shows the dynamic instability regions (DIR) of the stiffened spherical panel for both number of layers and lamination scheme. In both lamination schemes the instability regions with 8 numbers of layers is at higher frequency zone in comparison to that of with 4 numbers of layers. Again for both numbers of layers the angle-ply lamination scheme shows the instability zone at higher frequency zone with lower width. This indicates the spherical panel is dynamically more stable with angle-ply lamination pattern.

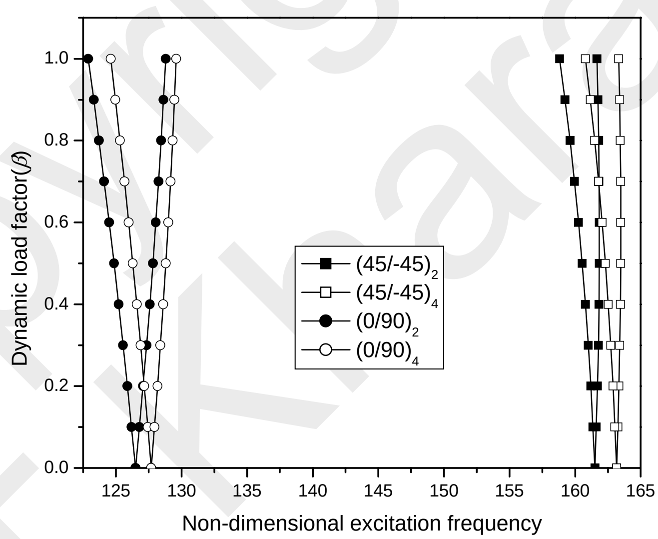


**Fig. 5.107 Dynamic instability region for different number of layers with both lamination scheme, *c/b*=0.5, loading type-IV, Spherical panel**

***iv. Effect of stacking scheme in the stiffeners***

The effect of stacking scheme (whether parallel or perpendicular) on dynamic stability characteristics of the stiffeners is analyzed taking the problem of spherical shell panel with cutout (*ca/a*=0.4) and load position at *c/b*=0.5. The spherical panel is attached with single $(xst)_b$ stiffener along the center line and the four sides of the opening are stiffened with four stiffeners, length of each stiffener is equal to the size of the opening. These four stiffeners are also attached to the bottom surface. The stiffener depth to breadth ratio ($d_s/b_s$) for all stiffeners is kept as 4.0. The angle-ply lamination scheme with $(45/\text{-}45)_4$ is taken for both panel skin and stiffeners. The instability regions for both parallel and perpendicular stacking in the stiffeners are plotted in Fig. 5.108. With the given configuration the stiffened spherical shell panel with cutout is dynamically more stable with perpendicular stacking scheme in the stiffeners.

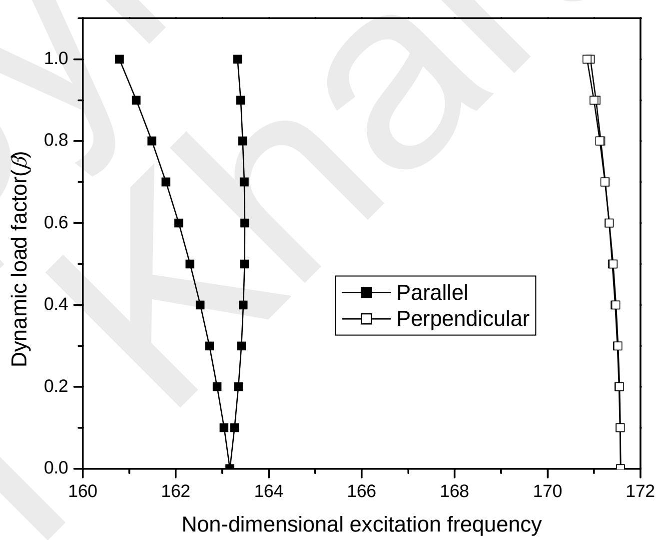


**Fig. 5.108 Dynamic instability region for both types of stacking, *c/b*=0.5, loading type-IV, Spherical panel**

### *v. Effect of eccentricity of the stiffeners*

The effect of stiffeners positions (attached to bottom or top surface) on dynamic stability characteristics of the spherical shell panel is analyzed with cutout (*ca/a*=0.4) and load position at *c/b*=0.5. The spherical panel is attached with single stiffener along the center line and the four sides of the opening are stiffened with four stiffeners, length of each stiffener is equal to the size of the opening. The stiffener depth to breadth ratio ($d_s/b_s$) for all stiffeners is kept as 4.0. The stacking in the stiffeners is perpendicular in all stiffeners. The angle-ply lamination scheme with $(45/-45)_4$ is taken for both panel skin and stiffeners. All the stiffeners are attached to bottom surface in one case and to the top surface in other case. Figure 5.109 shows the dynamic instability regions of the stiffened spherical shell panel with cutout for both stiffener positions. The spherical shell panel is dynamically more stable when the stiffeners are attached to the top surface of the panel.

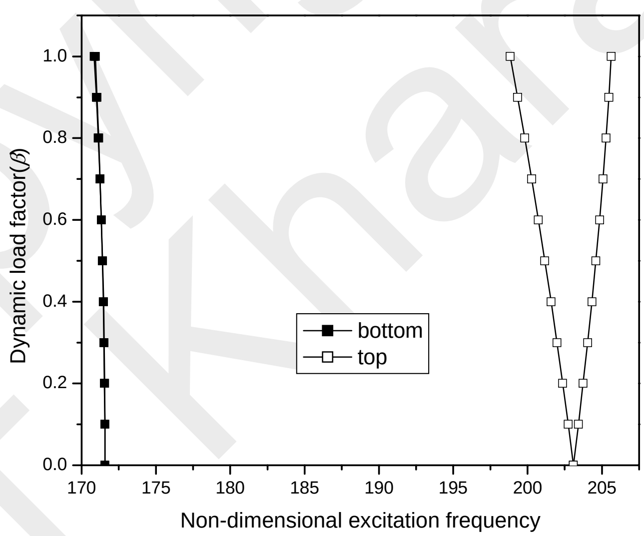


**Fig. 5.109 Dynamic instability region for both stiffener eccentricity, *c/b*=0.5, loading type-IV, Spherical panel**

# Chapter-6
# Conclusions

**T**he theoretical investigations of the vibration, buckling and dynamic stability behaviour of isotropic and laminated composite stiffened shell panels with/without cutout, subjected to uniform and various non-uniform in-pane edge loadings have been carried out using the finite element method. The proposed finite element model consists of an eight-noded isoparametric degenerated shell element and a compatible three-noded curved beam element for the representation of shell skin and stiffeners respectively. It has exhibited very good performance in terms of accuracy and convergence without involving any numerical disturbance. The numerical results are presented and discussed in Chapter 5. The presentation of conclusions is divided in two parts. The major findings are listed first and the conclusions based on specific problems are presented subsequently.

**Major Findings:**

1. An efficient stiffener element is proposed, which is compatible to degenerated shell element. Its combination with the shell element has given a unique tool for analyzing composite stiffened shell having a wide variety. The analysis tool is equipped in such a way that it can be used to solve vibration, buckling and dynamic instability problems having a wide range of parameters.
2. When the stiffener depth is more than certain value in case of all four types of laminated stiffened shell panels with (0/90/0/90---) lamination scheme with stiffener in the loading direction, the global buckling load gets reduced. This may be due to the local buckling effects of the stiffener. This behaviour is not observed in the panels with (45/-45/45/-45---) lamination scheme.
3. In the isotropic stiffened shell panels, the local buckling behaviour is observed for the four types of panels considered with stiffeners are placed along $x$-direction (load direction) and $x$-$y$-directions (orthogonal direction). This behaviour is not observed in the panels with stiffeners placed perpendicular to the load direction.

4. In case of isotropic stiffened spherical shell panel subjected to uniform loading, when the stiffeners are placed in the top surface of the panels the dynamic stability performance is better. On the other hand for the laminate composite stiffened spherical shell panel with ((45/-45/45/-45---) lamination scheme, the dynamic stability performance is better when the stiffeners are placed in the bottom surface.
5. The dynamic stability region shifts to the higher frequency zone with the increase of orthogonal stiffeners in the case of a laminated stiffened spherical shell panel with (45/-45/45/-45) lamination scheme in uniform loading case. It is optimum for certain number of stiffeners. If the number of stiffeners is more than that value the shell panels becomes dynamically less stable. But for non-uniform loading case (load width from edge to centre of the panel) with (0/90/0/90) lamination scheme, the dynamic instability region gradually shifts to the higher frequency zone with the increase in number of stiffeners, converging to a particular region, in both spherical and cylindrical stiffened shell panels with stiffeners placed along the load direction and along orthogonal directions.
6. In the isotropic stiffened spherical shell panel with stiffeners placed along load direction and along orthogonal directions, the instability region without any stiffener is at higher frequency zone. But with increase in dynamic load factor keeping static load factor constant, the lower boundary of the instability zone widen significantly to the lower frequency side. However, the instability region shifts to the lower frequency side with smaller width with the increase in number of stiffeners converging to a particular region.
7. Keeping the width of the stiffener constant, the spherical and cylindrical stiffened shell panels give an optimum instability region with certain value of stiffener depth. If the depth of the stiffener is more than that value, the shell panel becomes dynamically less stable.
8. The arrangement of layers (stacking scheme) has also significant effect on the dynamic stability behaviour of laminated composite stiffened spherical shell panel. For non-uniform loading case (load width from edge to centre of the panel)

with $(0/90)_2$ lamination scheme, the dynamic instability region is at higher frequency zone with horizontal stacking in the stiffeners for stiffeners located in the top side. But the dynamic instability region shifts to higher frequency zone with vertical stacking for stiffeners located on the bottom side. The dynamic instability shifts to higher frequency zone with vertical stacking for the stiffeners located on bottom and top surface with $(45/-45)_2$ lamination scheme.

9. In most of the case the dynamic instability region shifts to lower frequency zone with increase in loading width. This is because the stiffness of the panels reduces with the increase in loading width.
10. Almost in all stiffened shell panels with all loading types the frequency of vibration with in-plane load gradually decreases with increase in the load magnitude and attains zero value when the load becomes critical. In some loading cases of spherical panel the frequency almost remains constant and suddenly becomes zero when the load becomes critical. This may be due to the reason that the reduction in stiffness is not significant when the load is below critical.
11. The loading width has significant effect on the buckling load of the panels. The effect is different for laminated stiffened shell panels with cutout and without cutout.
12. The natural frequency of vibration of the spherical and cylindrical shell panels with cutout decreases with the increase in the cutout size, but the behaviour is opposite for stiffened flat plate and hyperbolic hyperboloid panel with cutout. This effect may be due to the variation of the stiffness of the panels having different parameters. The natural frequency of a structure increases either due to the reduction of mass or increase in the stiffness. But with the presence of cutout the stiffness of the structure reduces. So the combined effect of reduction of stiffness and mass is such that the natural frequency in plate and hyperbolic hyperboloid panel is increasing. On the other hand the natural frequency is decreasing in spherical and cylindrical shell panels with the presence of cutout. In the curved panels with cutout the rate of reduction of stiffness is more compared to flat plate. However, the hyperbolic hyperboloid panel is behaving like a plate because of

positive and negative curvature in both directions. Similar behaviour is also observed for isotropic un-stiffened curved panels [124].

13. The stiffened flat plate with cutout becomes dynamically more stable with the increase in the cutout size, but the stiffened spherical shell panel with cutout becomes dynamically more unstable with the increase in the cutout size for all loading cases.
14. For the given configurations, in all four loading types, the laminated stiffened spherical shell panel without cutout is dynamically more stable compared to the other three panels.

**Other findings:**

Based on the observations in regard with the particular problem the findings of the present study are summarized below.

**Stiffened shell panels without cutout under uniform loading:**

**(Part-I) Laminated composite stiffened shell panels**

1. In most of the cases the non-dimensional buckling loads and frequencies are higher for angle-ply (45/-45/45/-45/---) stiffened shell panels in comparison to the cross-ply (0/90/0/90/---) lamination scheme.
2. The stiffened panel with angle-ply lay up is dynamically more stable than the cross-ply scheme for the given geometry and stiffener configuration of the shell panel.
3. For a given ply lay up and stiffener configuration, the spherical stiffened shell panel is dynamically more stable in comparison to the other panel geometries.

4. With regard to dynamic instability, for the given stiffener and lamination scheme it is better to place the stiffener in the bottom surface of the spherical shell panel.
5. In case of vertical stacking scheme the onset of dynamic instability region shifts towards the higher frequency zone side for $(45/-45)_2$ lamination scheme and towards lower frequency zone side for $(0/90)_2$ lamination scheme for the spherical stiffened shell.
6. For the stiffened spherical shell panel with three stiffeners in each direction, the onset of dynamic instability zone is at higher frequency zone in comparison to other stiffener arrangement.

**(Part-II) Isotropic stiffened shell panels**

1. In all the stiffened panels the non-dimensional buckling load parameters with cross-stiffener arrangement are more compared to the non-dimensional buckling load parameters with x-orientation stiffener and y-orientation stiffener.
2. In all the stiffened panels the non-dimensional buckling load parameters with *y*-orientation stiffener are less compared to the non-dimensional buckling load parameters with other two stiffener arrangements.
3. For the stiffened spherical panel, it is dynamically more stable with *x*-stiffeners only. But for other panels, those are dynamically more stable with cross-stiffeners arrangements.
4. The onset of dynamic instability is at higher frequency zone for the stiffeners placed on the top surface of the panels (spherical, cylindrical and hyperbolic hyperboloid).
5. For the stiffened spherical panel the dynamic instability region is at higher frequency zone for $d_s/b_s = 6$ for the given number of stiffeners.

6. The dynamic instability zones are almost same for the stiffened spherical shell panel with 3, 5 and 7 *x*-stiffeners. Similar behaviour is observed for cross-stiffener arrangements.

**Laminated composite stiffened shell panels without cutout under non-uniform loading:**

1. The width of the loading patches (type-I, type-II and type-III) and the position of the concentrated load (type-IV) has shown considerable effect on the buckling (static stability) and dynamic stability behaviour of all four types of panels.
2. With the given configurations, the spherical shell panels buckles at higher load in all cases in comparison to cylindrical, flat and hyperbolic hyperboloid panels.
3. In case of loading type-I, the buckling load reduces with the increase in loading width, but after some width it again starts increasing till the load patch covers the whole edge in spherical, cylindrical and flat stiffened panels. All these three panels take the highest load when they are loaded with full length of the edge load. The hyperbolic hyperboloid panel takes almost same load for all loading width.
4. In type-II loading, the buckling behaviour of all four stiffened panels is same. They buckle at highest load when the loading patch is smaller. The buckling load decreases significantly with the increase in the loading width upto some length, and then the buckling load does not change much with further increase of the loading width.
5. In case of loading type-III, the buckling load decreases with the increase in the loading width upto some distance and then it again increases. The increase is very significant in spherical panel. The spherical panel buckles at highest load when loaded with full edge load, but the other three panels buckle at highest load when they are loaded with small patches of load from both ends.

6. In the concentrated loading case (type-IV), the panels buckle at the highest load when the load acts at the stiffener position.
7. In regard to the vibration with the applied load, the panels vibrate with their natural frequency when the applied load is zero and the frequency of vibration becomes zero when the applied load becomes critical.
8. In case of loading type-I, the onset of dynamic stability for stiffened flat, cylindrical and hyperbolic hyperboloid panel starts when the load covers the whole width ($c/b$ = 1.0) of the edges. When the loading width decreases ($c/b$ < 1.0) the DIR starts shifting to higher frequency zone side with smaller width. These three stiffened panels are dynamically more unstable with higher load bandwidth. In the stiffened spherical panel with increase in $c/b$ ratio from 0.1, the dynamic stability region is shifting to the higher frequency zone side with wider width up to $c/b$ = 0.3 and after that it starts shifting to the lower frequency zone side and the onset of dynamic instability takes place at the load width of $c/b$ = 0.8.
9. For a given ply lay up and stiffener configuration, for loading type-I, the dynamic instability regions of the cylindrical and spherical shell panels shift to higher frequency zone with the increase in the number of layers and then after some number of layers the change in DIR is insignificant.
10. The increase in stiffener size (increase in depth '$d_s$' keeping width '$b_s$' constant) enhances the dynamic instability characteristics of the cylindrical and spherical shell panels, but after some depth of the stiffeners the panels becomes more unstable.
11. The dynamic stability capacity increases with the increase in the number of stiffeners. Again after some number of stiffeners the DIR does not change much.
12. For the given configurations, the panels become dynamically more stable when the stiffener are provided in both $x$ and $y$ directions in comparison to the stiffeners in $x$ direction only.

13. In loading type-I, with same stiffeners configuration, the stiffened cylindrical panel is dynamically more stable with cross-ply (0/90) lamination scheme in comparison to angle-ply (45/-45) lamination scheme, but for spherical shell panel the behaviour is opposite.
14. The eccentricity of stiffeners has great impact on the dynamic instability behaviour of the stiffened panels. In general, panels with stiffeners placed at the bottom are dynamically more stable.
15. In case of loading type-II, all the four types of panels have similar behaviour, when the loading width is small the panels are dynamically more stable. With the increase in the loading width the DIR shifts to lower frequency zone with wider width. Similar behaviour is observed for loading type-III for all panels.
16. In loading type-IV, The panels are dynamically more stable when the concentrated load coincides with the location of the stiffener.
17. The effect of stacking scheme in the stiffeners has significant effect on the dynamic instability behaviour of the stiffened shell panels.
18. For the given configurations, in all four loading types, the laminated stiffened spherical shell panel is dynamically more stable compared to the other three panels.
19. The boundary conditions play important role in the behaviour of the stiffened shell panels.

**Laminated composite stiffened shell panels with square cutout under non-uniform loading:**

1. The (presence of) cutout in the panel and having different types of edge load show considerable effect on the vibration, buckling (static stability) and dynamic stability behaviour for all types of panels.
2. In loading type-I, the buckling load of the stiffened plate and spherical shell panel with cutout decreases with the increase in load width upto some loading width and then it starts increasing gradually, the rate of increase is significant

in stiffened spherical panel with cutout in comparison to that of the stiffened plate with cutout. The stiffened plate with cutout takes highest load when the loading width is small but the stiffened spherical panel takes highest load when it is loaded with full edge load.

3. When the panels are loaded with full edge load the buckling load of the spherical and cylindrical shell panels with cutout is decreasing with the increase in the cutout size, but the behaviour is opposite for stiffened flat plate and hyperbolic hyperboloid panel.
4. In case of loading type-II, the buckling load of the stiffened flat plate and spherical shell panel with cutout is increasing with the increase of the loading width. With the load width ratio *c/b* = 0.4, the buckling load of the spherical panel with cutout is decreasing with the increase in the cutout size, but the buckling load of the stiffened plate with cutout is increasing slowly with the increase in the cutout size.
5. In case of loading type-III, the load carrying capacity of the spherical shell panel with cutout is decreasing upto *c/b* = 0.3 and beyond that it is increasing upto *c/b* = 0.5. But in case of stiffened plate with cutout the buckling load is gradually decreasing with the increase in the loading width. With the load width ratio *c/b* = 0.2, the buckling load of both panels decreases when the cutout size (*ca/a*) is increased from 0.2 to 0.4 and after *ca/a* = 0.4 the buckling load is gradually increasing.
6. In loading type-IV, the buckling load of the stiffened spherical shell panel with cutout is maximum when the load is at the center (*c/b* = 0.5), but this is just opposite in stiffened plate with cutout. With the load position at the center, the buckling load of the plate is decreased when *ca/a* is increased from 0.2 to 0.4 and beyond that upto 0.8 the buckling load is gradually increasing. But in spherical shell panel the buckling load is gradually increasing with the increase in cutout size upto 0.6 and then it starts decreasing from *ca/a*=0.6 to *ca/a*=0.8.

7. The natural frequency of vibration of the spherical and cylindrical shell panels with cutout decreases with the increase in the cutout size, but the behaviour is opposite for stiffened flat plate and hyperbolic hyperboloid panel with cutout.
8. The panels vibrate with their natural frequency when the applied load is zero and the frequency of vibration becomes zero when the applied load becomes critical.
9. The stiffened flat plate with cutout becomes dynamically more stable with the increase in the cutout size, but the stiffened spherical shell panel with cutout becomes dynamically more unstable with the increase in the cutout size for all loading cases.
10. In case of loading type-I, the stiffened flat plate with cutout the dynamic instability region is at higher frequency zone with minimum width. With the increase in the loading width the instability zone shifts to the lower frequency zone with wider width. In stiffened spherical shell panel with cutout the instability zone shifts to higher frequency zone with wider width. Similar behaviour is observed for loading type-II and type-III.
11. In case of loading type-IV, when the load moves from a position nearer to edge to the centre in the stiffened flat plate with cutout the dynamic instability region gradually shifts from higher frequency zone to lower frequency zone with wider width. This behaviour is opposite in stiffened spherical shell panel with cutout.

## Future Scope of Research

There is a vast scope to carryout the present research work further considering different aspects. The possible extensions to the present study can be presented below,

- The present study deals with conservative compressive forces. This may be extended to non-conservative and tensile loading cases.

- The effect of material and geometric non-linearity can be taken into account for further extension of the dynamic stability analysis of stiffened shell panels.

- The different size of cutout (circular, elliptical etc.) and stiffeners (hat etc.) may be taken into account as future work.

- The effect of combination resonance can be investigated for these classes of problems.

- The varying thickness of the panel skin can be included as further study.

- The effecting of damping can be considered for future research.

- There is a large scope of experimental investigation on dynamic stability of laminated composite stiffened shell panels.

# References


1. **Ahmad, S.** (1970), Analysis of thick and thin shell structures by curved finite elements, *International Journal for Numerical Methods in Engineering*, **2**, 419-451.
2. **Aksu, G.** (1982), Free vibration of stiffened plates including the effect of in plane inertia, *Journal of Applied Mechanics, Trans of ASME*, **49**, 206-212.
3. **Aksu, G.** and **Ali, R.** (1976), Determination of dynamic characteristics of rectangular plates with cutouts using a finite difference formulation. *Journal of Sound and Vibration*, **44**(1), 147-158.
4. **Alagusundaramoorthy, P., Sundaravadivelu, R.** and **Ganapathy, C.** (1999), Experimental study on collapse load of stiffened panels with cutouts, *Journal of Constructional Steel Research*, **52**, 235-251.
5. **Ali, R.** and **Atwal, S.J.** (1980), Prediction of natural frequencies of vibration of rectangular plate with rectangular cutouts, *Computers and Structures*, **12**, 819-823.
6. **Anderson, R.G., Irons, B.M.** and **Zienkiewicz, O.C.** (1968). Vibration and stability of plates using finite element, *International Journal of Solids and Structures*, **55**(4), 1031-1055.
7. **Argento, A.** and **Scott, R.A.** (1993), Dynamic instability of layered anisotropic circular cylindrical shell, Part-I: Theoretical development, *Journal of Sound and Vibration*, **162**(2), 311-322.
8. **Argento, A.** and **Scott, R.A.** (1993), Dynamic instability of layered anisotropic circular cylindrical shell, Part-II: Numerical results *Journal of Sound and Vibration*, **162**(2), 323-332.
9. **Armenakas, A.E.** (1964), Influence of initial stress on the vibrations of simply supported circular cylindrical shell. *AIAA Journal*, **2**(9), 1607-1612.
10. **Avalosa, D.R.** and **Laurab P.A.A.** (2003), Transverse vibrations of simply supported rectangular plates with two rectangular cutouts, *Journal of Sound and Vibration*, **267**, 967–977.

11. **Bailey, R.** and **Wood, J.** (1996), Stability characteristics of composite panels with various cutout geometries. *Composite Structures*, **35**, 21-31.
12. **Basdekas, N.L.** and **Chi, M.** (1979), Dynamic response of plates with cutouts. *Shock and Vibration Bulletin*, **41**, 29-35.
13. **Bathe, K.J.** (1996), *Finite Element Procedure*, Prentice-Hall of India Private Limited, New Delhi.
14. **Bert, C.W.** and **Chen, T.L.C.** (1978) Effect of shear deformation on vibration of anti-symmetric angle-ply laminated rectangular plates. *International Journal of Solids and Structures*, **14**,465-473.
15. **Bhat, R.B., Chakraverty, S.** and **Sitharu, I.** (1999), Recent research on vibration of structures using boundary characteristics orthogonal polynomial in the Rayleigh-Ritz method, *Shock and vibration digest*, **31**(3), 187-194.
16. **Bhimaraddi, A., Carr, A.J.** and **Moss, P.J.** (1989), Finite element analysis of laminated shells of revolution with laminated stiffeners, *Computers and Structures*, **33**(1), 295-305.
17. **Bolotin, V.V.** (1964), *The dynamic stability of elastic systems*, Holden-day, Inc.
18. **Brown, C.J.** (1989), Elastic stability of plates subjected to concentrated loads, *Journal of Computers and Structures*, **33**(5), 1325-1327.
19. **Bruhn, E.F.** (1965) *Analysis and design of flight vehicle structures*, Tri-state offset company, Cincinnati, USA.
20. **Carrera, E.** (1991), The effect of shear deformation and curvature on buckling and vibrations cross-ply laminated composite shell. *Journal of Sound and Vibration*, **150**(3), 405-433.
21. **Chakravorty, D., Bandyopadhyay, J.N.** and **Sinha, P.K.** (1995), Finite element free vibration analysis of conoidal shells, *Computers and Structures*, **56**(6), 975-978.

22. **Chakravorty, D., Bandyopadhyay, J.N.** and **Sinha, P.K.** (1996), Finite element free vibration of doubly curved laminated composite shells, *Journal of Sound and Vibration*, **191**(4), 491-504.
23. **Chakravorty, D., Sinha, P.K.** and **Bandyopadhyay, J.N.** (1998), Application of FEM on free and forced vibration of laminated shells, *Journal of Engineering Mechanics, ASCE*. **124**(1), 1-8.
24. **Chandrashekhara, K.** (1989), Free vibration of anisotropic laminated doubly curved shells, *Journal of Computers and Structures,* **33**(2), 435-440.
25. **Chao, C.C.** and **Lee J.C.** (1980), Vibration of eccentrically stiffened laminates, *Journal of Composite Materials*, **14**,233-244.
26. **Chattopadhyay, A.** and **Radu, A.G.** (2000), Dynamic instability of composite laminates using a higher order theory, *Computers and Structures* ,**77**, 453-460.
27. **Chattopadhyay, B., Sinha, P.K.** and **Muhkopadhyay M.** (1992), Finite element free vibration analysis of eccentrically stiffened composite plates, *Journal of Reinforced Plastics and Composites,* **11**(10), 1003-1034.
28. **Corr, R.B.** and **Jennings, A.** (1976), A simultaneous iteration algorithm for symmetric eigenvalue problems, *International Journal for Numerical Methods in Engineering*, **10**, 647-663.
29. **Crawly, E.F.** (1979), The natural modes of graphite/epoxy cantilever plates and shells, *Journal of Composite Materials,* **13**, 195-205.
30. **Datta, P.K.** (1976), An experimental study of the static and dynamic behaviour of a tensioned sheet with rectangular opening. *Aeronautical Quarterly*, **27**, 257-261.
31. **Deolasi, P.J.** and **Datta, P.K.**(1995), Parametric instability characteristics of rectangular plates subjected to localized edge loading(compression or tension), *Computers and Structures* ,**54**(1),73-82.
32. **Deolasi, P.J., Datta, P.K.** and **Prabhakara, D.L.**(1995), Buckling and vibration of rectangular plates subjected to partial edge loading(compression or tension), *Journal of Structural Engineering*,**22**(3),135-144.

33. **Duffield, R.C.** and **Willems, N.** (1972) Parametric resonance of stiffened rectangular plates, *Journal of Applied Mechanics,* **39**,217-226.

34. **Evan-Iwanowsky, R.M.**(1965), On the parametric response of structures, *Applied Mechanics Review*, **18**(9),699-702.

35. **Ferguson, G.H.** and **Clark, R.D.** (1979), A variable thickness curved beam and shell stiffener with sheat deformation, *International Journal for Numerical Methods in Engineering*, **14**, 581-592.

36. **Ganapathi, M.** and **Balamurugan, V.** (1998), Dynamic instability of laminated composite circular cylindrical shell, *Computers and Structures*, **69**(1), 181-189.

37. **Gorman, D.J.** and **Ding, W.**(2003), Accurate free vibration analysis of completely free symmetric cross-ply rectangular laminated plates, *Composite Structures*, **60**,359-365.

38. **Guo, M., Harik, I.E.** and **Ren, W.** (2002), Buckling behavior of stiffened laminated plates, *International Journal of Solids and Structures*, **39**,3039-3055.

39. **Harik, I.E.** and **Guo, M.** (1993), Finite element analysis of eccentrically stiffened plates in free vibration, *Computers and Structures*, **49**(6), 1007-1015.

40. **Hilburger, M.W., Britt, V.O.** and **Nemeth, M.P.** (2001), Buckling behavior of compression-loaded quasi-isotropic curved panels with a circular cutout, *International Journal of Solids and Structures*, **38**, 1495-1522.

41. **Huang, M.** and **Sakiyama, T.** (1999), Free vibration analysis of rectangular plates with variously shaped holes. *Journal of Sound and vibration*, **226**(4), 769-786.

42. **Hutt, J.M.** and **Salam, A.E.** (1971), Dynamic stability of plates by finite element method, *Journal of Engineering Mechanics, ASCE*, **97**, 897-899.

43. **Ibrahim, R.A.**(1978), Parametric vibration, Part-III, Current problems(1), *Shock and Vibration Digest*, **10**(3),41-57.

44. **Kabir, H.R.H.** (1999), On the frequency response of moderately thick simply supported rectangular plates with arbitrary lamination. *International Journal of Solids and Structures*, **36**, 2285-2301.

45. **Kassenge, S.K.** and **Reddy, J.N.**(1998). Local behaviour of discretely Stiffened composite plates and cylindrical shells. *Composite Structures*, **41**,13-26.
46. **Kaushal, A.** and **Bhat, R.B.** (1993), A comparative study of vibration with cutouts using finite element and Raleigh-Ritz Methods. *Proceedings of Canadian Congress of Applied Mechanics*, CANCAM 93, Ontario.
47. **Khan, M.Z.** and **Walker, A.C.** (1972), Buckling of plates subjected to localized edge loading, *The structural Engineers*, **50**,225-232.
48. **Khdeir, A.A.** and **Reddy, J.N.**(1990), Influence of edge conditions on modal characteristics of cross-ply laminated shells, *Computers and Structures*, **34**(6), 817-826.
49. **Khdeir, A.A.** and **Reddy, J.N.**(1999), Free vibration of laminated composite plates using second order shear deformation theory, *Computers and Structures*, **71**,617-626.
50. **Khdeir, A.A., Reddy, J.N.** and **Frederick, D.**(1989), A study of bending, vibration and buckling of cross-ply circular cylindrical shells with various shell theories, *International Journal of Engineering Science*, **27**, 1337-1351.
51. **Kim, K.D.**(1996), Buckling behaviour of composite panels using the finite element method, *Composite Structures*, **36**,33-43.
52. **Kumai, T.** (1957) The flexural vibrations of a square plate with a central circular hole. *Proc. 2nd Japan National Cong. For Applied Mechanics*, 339-342.
53. **Kumar, L.R., Datta, P.K.** and **Prabhakara, D.L.** (2003), Tension buckling and dynamic stability behaviour of laminated composite doubly curved panels subjected to partial edge loading, *Journal of Composite Structures*, **60**, 171-181.
54. **Kumar, Y.V.S.** and **Mukhopadhyay, M.** (1999), A new finite element for buckling analysis of laminated stiffened plates, *Composite Structures*, **46**, 321-331.
55. **Lam, K.Y.** and **Hung, K.C.** (1990) Vibration study on plates with stiffened openings using orthogonal polynomial and partitioning method. *Computers and Structures*, **33**(3), 295-301.

56. **Lam, K.Y.** and **Ng, T.Y.** (1998), Dynamic stability of laminated composite cylindrical shells subjected to conservative periodic axial loads, *Composites Part B*, **29B**, 769-785.

57. **Lee, H.P., Lim, S.P.** and **Chow, S.T.** (1987), Free vibration of composite rectangular plates with rectangular cutout, *Computers and Structures*, **8**,63-81.

58. **Lee, H.P.** and **Lim, S.P.** (1992), Free vibration of isotropic and orthotropic square plates with square cutouts subjected to in-plane forces. *Computers and Structures*, **43**(3), 431-437.

59. **Lee, H.P., Lim, S.P.** and **Chow, S.T.** (1992), Effect of transverse shear deformation and rotary inertia on the natural frequencies of rectangular plates with cutouts. *International Journal of Solids and Structures*, **29**(11), 1351-1359.

60. **Lee, H.P., Lim, S.P.** and **Chow, S.T.**( 1990), Prediction of natural frequencies of rectangular plates with rectangular cutouts. *Computers and Structures*, **36**(5), 861-869.

61. **Lee, J.K, Leissa, A.W.** and **Wang, A.J.** (1983), Vibration of cantilevered circular shells, *International Journal of Mechanical Sciences*, **49**(3), 517-521.

62. **Lee, Y.J., Lin, H.J.** and **Lin, C.C.** (1989), A Study of Buckling Behaviour of an Orthotropic Square plate with Central Circular Hole, *Composite Structures*, **13**, 173-188.

63. **Leissa, A.W.** and **Ayoub, E.F.** (1988), Vibration and buckling of simply supported rectangular plate subjected to a pair of in-plane concentrated forces, *Journal of sound and vibration*, **127**, 155-171.

64. **Leissa, A.W.** and **Ayoub, E.F.** (1989), Tension buckling of rectangular sheets due to concentrated forces, *Journal of Engineering Mechanics*, **115**(12), 2749-2762.

65. **Leissa, A.W.** and **Kadi, A.S.** (1971), Curvature effects on shallow shells vibration, *Journal of Sound and Vibration*, **16**(2), 173-187.

66. **Leissa, A.W., Lee, J.K.** and **Wang, A.J.** (1981), Vibration of cantilevered shallow shells of rectangular planform, *Journal of Sound and Vibration*, **78**(3), 311-328.

67. **Leissa, A.W., Lee, J.K.** and **Wang, A.J.** (1983), Vibration of cantilevered doubly curves shells, *International Journal of Solids and Structures*,**19**(5), 411-424.

68. **Leissa, AW.** (1973), Free vibration of rectangular plates, *Journal of sound and vibration*, **31**, 257-293.

69. **Leissa, A.W.**(1987), Recent studies in plate vibration:1981-1985,Part-I,Classical theory, *Shock and vibration digest*,**19**(2),11-18.

70. **Leissa, A.W.**(1987), Recent studies in plate vibration:1981-1985,Part-II, Complicating effects, *Shock and vibration digest*,**19**(3),10-24.

71. **Liao, C.L.** and **Reddy, J.N.** (1990), Analysis of anisotropic, stiffened composite laminates using a continuum-based shell element, *Computers and Structures*, **34**(6), 805-815.

72. **Liao, C.L.** and **Cheng, C.R.** (1994), Dynamic stability of stiffened laminated composite plates and shells subjected to in-plane pulsating forces, *International Journal for Numerical Methods in Engineering*, **37**, 4167-4183.

73. **Liao, C.L.** and **Cheng, C.R.**.(1994), Dynamic stability of stiffened laminated composite plates and shells subjected to in-plane pulsating forces, *Journal of Sound and Vibration*,**174**(3),335-351.

74. **Librescu, L., Khdeir, A.A.** and **Frederick, D.**(1989), A shear deformable theory of laminated composite shallow shell type panels and their response analysis I: Free vibration and buckling, *Acta Mechanica*,**76**, 1-33.

75. **Liew, K.M., Xiang, Y.** and **Kittipornichai, S.** (1993), Transverse vibration of thick rectangular plates-I. Comprehensive sets of boundary conditions, *Computers and Structures*, **49**(10), 1-29.

76. **Liew, K.M., Xiang, Y.** and **Kittipornichai. S.** (1993), Transverse vibration of thick rectangular plates-IV. Influence of isotropic in-plane pressure. *Computers and Structures*, **49**(1), 69-78.

77. **Liew, K.M., Lim, C.W.** and **Kitipornchai, S.** (1997), Vibration of shallow shells: A review with bibliography, *Applied Mechanics Review, ASME*, **50**(8), 431-444.

78. **Liew, K.M., Xiang, Y.** and **Kitipornchai, S.** (1995), Research in thick plate vibration, A Literature Survey, *Journal of Sound and Vibration*, **180**(1), 163-176.
79. **Lim, C.W.** and **Liew, K.M.** (1995), A higher order theory for vibration of shear deformable cylindrical shells, *International Journal of Mechanical Sciences*, **37**(3), 277-295.
80. **Lin, C.C.** and **Kuo, C.S.** (1989), Buckling of laminated plates with holes. *Journal of composite materials*, **23**, 536-553.
81. **Long, B.R.** (1968), Vibration of eccentrically stiffened plates, *Shock and Vibration Bulletin*, **38**, 45-53.
82. **Matsunaga, H.** (1999), Buckling of homogeneous isotropic cylindrical shells under axial stresses, *Journal of Engineering Mechanics, ASCE*, **125**(6), 613-621.
83. **Matsunaga, H.** (2000), Vibration and stability of cross-ply laminated composite plates according to a global higher-order plate theory, *Journal of Composite and Structures*, **48**, 231-244.
84. **Matsunaga, H.** (2001), Vibration and stability of angle-ply laminated composite plates subjected to in-plane stresses, *International Journal of Mechanical Sciences*, **43**,1925-1944.
85. **Mead, D.J.** and **Bardell, N.S.** (1985), Free vibration of thin cylindrical shell with discrete axial stiffeners, *Journal of Sound and Vibration*, **111**(2), 229-250.
86. **Mead, D.J.** and **Bardell, N.S.** (1987), Free vibration of thin cylindrical shell with periodic circumferential stiffeners, *Journal of Sound and Vibration*, **115**(3), 499-520.
87. **Mermertas, M.** and **Belek, H.T.** (1991), Dynamic stability of radially stiffened annular plates. *Computers and Structures*, **40**(3), 651-657.
88. **Merrit, R.G.** and **Willems, N.**(1973), Parametric resonance of skew stiffened plates, *Journal of Applied Mechanics*, **40**,439-444.

89. **Moita, J.S., Soares, C.M.M.** and **Soares, C.A.M.** (1999), Buckling and dynamic behaviour of laminated composite structures using a discrete higher-order displacement model, *Journal of Computers and Structures*,**73**, 407-423.

90. **Monahan, I.J., Nemergut, P.J.** and **Maddux, G.E.** (1970), Natural frequencies and mode shapes of plates with interior cutouts, *The Shock and Vibration Bulletin*, **41**,37-49.

91. **Moorthy, J., Reddy, J.N.** and **Pault, R.H.** (1990), Parametric instability of laminated composite plates with transverse shear deformation, *International Journal of Solids and Structure*, **26**(7), 801-811.

92. **Mukherjee, A.** and **Mukhopadhyay, M.**(1987), Finite element free vibration of Eccentrically stiffened plates, *Computers and Structures*, **30**(6),1303-1317.

93. **Mukhopadhyay, M.** (1989), Vibration and stability analysis of stiffened plates by semi-analytic finite difference method, Part-I: Consideration of bending displacement only, *Journal of Sound and Vibration*, **130**(1), 27-39.

94. **Mundkur, G., Bhat, R.B.** and **Neria, S.** (1994), Vibration of plates with cutouts using boundary characteristic orthogonal polynomial functions in the Raleigh-Ritz method. *Journal of Sound and Vibration*, **176**(1), 136-144.

95. **Mustafa, B.A.J.** and **Ali, R.**(1987), Free vibration of analysis of multi-symmetric stiffened shells, *Computers and Structures*, **27**(6),803-810.

96. **Mustafa, B.A.J.** and **Ali, R.**(1987), Prediction of natural frequency of vibration of stiffened cylindrical shells and orthogonally stiffened curved panels, *Journal of Sound and Vibration*, **157**(1),317-327.

97. **Nair, S.L., Singh, G.** and **Rao, G.V.** (1996), Stability of laminated composite plates subjected to various types of in plane loadings, *International Journal of Mechanical Sciences*, **38**(2), 191-202.

98. **Narita, Y.** and **Leissa, A.W.** (1990), Buckling studies of simply supported symmetrically laminated rectangular plates, *International Journal of Mechanical Sciences*, **32**(11), 909-924.

99. **Nayak, A.N.** and **Bandyopadhyay, J.N.** (2002), Free vibration analysis and design aids of stiffened conoidal shells, *Journal of Engineering Mechanics, ASCE*, **128**(4), 419-427.

100. **Nayak, A.N.** and **Bandyopadhyay, J.N.** (2002), On free vibration of stiffened shallow shells, *Journal of Sound and Vibration*, **255**(2), 357-382.

101. **Nayak, A.N.** and **Bandyopadhyay, J.N.** (2003), Free vibration analysis of laminated stiffened shells, *Journal of Engineering Mechanics, ASCE*, **129**(11), 1245-1253.

102. **Nemeth, M.P.** (1996), Buckling and post buckling behaviour of laminated composite plates with cutout. *NASA Technical Paper*, 3587, 1-23.

103. **Nemeth, M.P.** (1988), Buckling behaviour of compression loaded symmetrically laminated angle-ply plates with holes. *AIAA Journal*, **26**, 330-336.

104. **Nosier, A.** and **Reddy, J.N.**(1992), Vibration and stability analysis of cross-ply laminated circular cylindrical shells. *Journal of Sound and Vibration*,**157**(1),139-159.

105. **Olson, M.D.** and **Hazell, C.R.** (1977),Vibration studies of some integral rib-stiffened plates. *Journal of Sound and Vibration*, **50**,43-61.

106. **Panda, S.C.** and **Natarajan, R.** (1979), Finite element analysis of laminated composite plates, *International Journal for Numerical Methods in Engineering*, **14**, 69-79.

107. **Paramasivam, P.** (1973), Free vibration of square plates with square openings. *Journal of sound and vibration*, **30**, 173-178.

108. **Paramshivam, P.** and **Sridhar Rao J.K.** (1973), Free vibration of square plate with stiffened square openings, *International Journal of Mechanical Science*, **15**,117-122.

109. **Patnaik, S.** and **Sankaran, G.V.**(1973), Vibration of initially stressed stiffened circular cylinders and panels, *Journal of Sound and Vibration*, **31**(1),369-382.

110. **Pellett, D.A., Costello, R.G.** and **Brock, J.E.** (1968), Buckling of a tension panel containing circular hole. *AIAA Journal*, 6, 2012.
111. **Petyt, M.** and **Fleischer, C.C.**(1981), Finite strip analysis of singly curved skin-stringer structures, *Journal of Sound and Vibration*, **77**(4),561-571.
112. **Prabhakara, D.L.** and **Datta, P.K.** (1997), Vibration, buckling and parametric instability behaviour of rectangular plates with centrally located cutouts subjected to in-plane edge load. *Thin walled Structures*, **27**(4), 287-310.
113. **Prusty, B.G.** (2001), Static, dynamic, buckling and failure analysis of composite stiffened shell structures, A finite element approach, PhD thesis, Indian Institute of Technology, Kharagpur.
114. **Prusty, B.G.** and **Satsangi, S.K.** (2001), Finite element transient dynamic analysis of laminated stiffened shells, *Journal of Sound and Vibration*, **248**(2), 215-233.
115. **Qatu, M.S.** and **Leissa, A.W.** (1991), Natural frequency for cantilevered doubly curved laminated composite shallow shells. *Journal of Composite Structures*, **17**, 227-255.
116. **Qatu, M.S.**(1992), Review of shallow shell vibration research, *Shock and vibration digest*,**24**(9),3-15.
117. **Rajamani, A.** and **Prabhakaran, R.** (1977), Dynamic response of composite plates with cutouts, Part I: Simply supported plates. *Journal of Sound and Vibration*, **54**(4), 549-564.
118. **Rajamani, A.** and **Prabhakaran. R.** (1977), Dynamic response of composite plates with cutouts, Part II: Clamped clamped plates. *Journal of Sound and Vibration*, **54**(4), 565-576.
119. **Rao, J.S.** (1999), *Dynamics of Plates*, Narosa Publishing House, New Delhi.
120. **Reddy, J.N.** (1984), Exact solution of moderately thick laminated shells, *Journal of Engineering Mechanics*, **110**(5), 974-809.

121. **Rikards, R., Chate, A,** and **Ozolinsh, O.** (2001), Analysis for buckling and vibration of composite stiffened shells and plates, *Composite Structures*, **51**,361-370.

122. **Ritchie, D.** and **Rhodes, J.** (1975), Buckling and post-buckling behaviour of plates with holes, *Aeronautical Quarterly*, **24**,181-296.

123. **Rossi, R.E.** (1999), Transverse vibrations of thin, orthotropic rectangular plates with rectangular cutouts with fixed boundaries, *Journal of Sound and Vibration*, **221**(4), 733-736.

124. **Sahu, S.K.** and **Datta, P.K.** (2002), Dynamic stability of curved panels with cutouts. *Journal of Sound and Vibration*, **251**(4), 683-696.

125. **Sahu, S.K.** and **Datta, P.K.** (2003), Dynamic stability of laminated composite curved panels with cutouts. *Journal of Engineering Mechanics, ASCE*, **129**(11), 1245-1253.

126. **Sahu, S.K.** and **Datta, P.K.**(2001), Parametric instability of doubly curved panels subjected to non-uniform harmonic loading, *Journal of Sound and Vibration*, **240**(1),117-129.

127. **Samanta, A.** and **Mukhopadhyay, M.** (2004), Free vibration of stiffened shells by the finite element technique, *European Journal of Mechanics A/Solids*, **23**,159-179.

128. **Sciuva, M.D.** and **Crrera, E.** (1990), Static buckling of moderately thick, anisotropic, laminated and sandwitch cylindrical shell panels, *Journal of American Institute of Aeronautics and Astronautics*, **28**,1782-1793.

129. **Shastry, B.P.** and **Rao, G.V.**(1977). Vibration of thin rectangular plates with arbitrary oriented stiffeners, *Computers and Structures*, **7**, 627-635.

130. **Sheikh, A.H.** and **Mukhopadhyay, M.** (1993), Free vibration analysis of stiffened plates with arbitrary planform the general spline finite strip method, *Journal of Sound and Vibration*, **162**(1), 147-164.

131. **Sheinman, I.** and **Reichman, Y.** (1992), A study of buckling and vibration of laminated shallow curved panels. *International Journal of Solids and Structures*, **29**(11), 1329-1338.
132. **Sheinman, I.** and **Simitses, G.J.** (1983), Buckling and post-buckling of imperfect cylindrical shells under axial compression. *Computers and Structures*, **17**(2), 277-285.
133. **Shigeru, S., Shunya, Y.** and **Noriyasu, E.** (1991), Buckling of plates with a hole under tension. *Thin Walled Structures*, **12**, 35-49.
134. **Simitses, G.J.** (1987). Instability of dynamically loaded structures, *Applied Mechanics Review*, **40**(10), 1403-1408.
135. **Sinha, G**. and **Mukhopadhyay, M.** (1995), Static, Free and forced vibration analysis of arbitrary non-uniform shells with tapered stiffeners, *Computers and Structures*, **62**(5), 919-933.
136. **Sivakumar, K., Iyengar, N.G.R.,** and **Deb, K.**( 1999), Free vibration of laminated composite plate with cutout. *Journal of Sound and Vibration*, **221**(3), 443-470.
137. **Sivasubramonian, B., Rao, G.V.** and **Krishnan, A.**(1999),Free vibration longitudinally stiffened curved panels with cutouts, *Journal of Sound and Vibration*, **226**,41-55.
138. **Sivasubramonian, B., Kulkarni, A.M., Rao, G.V.** and **Krishnan, A.** (1997) Free vibration of curved panels with cutout. *Journal of Sound and Vibration*, **200**(2), 227-234.
139. **Srivasta, K.S.** and **Murthy, A.V.K.** (1992), Stability of laminated composite plate with cutouts. *Computers and Structures*, **43**(2), 273-279.
140. **Srivastava, A.K.L.** (2002), Dynamic stability of stiffened plates with cutouts subjected to non-uniform harmonic in-plane loading, PhD thesis, Indian Institute of Technology, Kharagpur.

141. **Srivastava, A.K.L., Datta, P.K.** and **Sheikh, A.H.** (2003), Dynamic instability of stiffened plates subjected to non-uniform in-plane edge loading, *Journal of Sound and Vibration*, **262**,1171-1189.

142. **Srivastava, A.K.L., Datta, P.K.** and **Sheikh, A.H.** (2002), Vibration and dynamic stability of stiffened plates subjected to in-plane harmonic edge loading, *International Journal of Structural Stability and Dynamics*, **2**(2), 185-206.

143. **Srivastava, A.K.L., Datta, P.K.** and **Sheikh, A.H.** (2003), Buckling and vibration of stiffened plates subjected to partial edge loading, *International Journal of Mechanical Sciences*, **45**, 73-93.

144. **Srivastava, A.K.L., Datta P.K.** and **Sheikh, A.H.** (2003), Buckling and vibration analysis of stiffened plate subjected to in-plane concentrated load, *Structural Engineering and Mechanics*, **15**(6), 2003, 685-704

145. **Srivastava, A.K.L, Datta P.K.** and **Sheikh, A.H.** (2003), Dynamic instability of stiffened plates with cutout subjected to in-plane uniform edge loadings, *International Journal of Structural Stability and Dynamics*, **3**(3), 391-403.

146. **Srivastava, A.K.L., Datta P.K.** and **Sheikh, A.H.** (2004), Transverse vibration of stiffened plates with cutouts subjected to in-plane uniform edge loading at the plate boundary, *Shock and Vibration*, **11**, 9-19.

147. **Srivastava, A.K.L, Datta P.K.** and **Sheikh, A.H.** (2005), Dynamic stability of stiffened plates with cutout subjected to harmonic in-plane partial edge loading, *International Journal of crashworthiness*, **10**(4), 403-417.

148. **Stanley, A.J.** and **Ganesan, N.** (1995), Free vibration characteristics of stiffened cylindrical shells. *Computers and Structures*, **65**(1), 33-45.

149. **Sundaresan, P., Singh G.** and **Rao, G.V.** (1998), Buckling of Moderately thick rectangular composite plates subjected to partial edge compression, *International Journal of Mechanical Sciences*, **40**(11), 1105-1117.

150. **Tessler, A., Seather, E.** and **Tusi, T.** (1995), Vibration of thick laminated composite plates, *Journal of Sound and Vibration*, **179**(3), 475-498.

151. **Thomas, J.** and **Abbas, B.H.A.**(1983), Vibration characteristics and dynamic stability of stiffened plates. *AIAA Journal*, 277-285.

152. **Timoshenko, S.P.** and **Gere, J.M.** (1961), *Theory of elastic stability*, Tokyo, McGraw-hill, Kogakusha.

153. **Timoshenko, S.P.** and **Goodier, J.M.** (1951), *Theory of elasticity*, Tokyo, McGraw-hill, Kogakusha.

154. **Toda, S.**( 1997), Vibrations of circular cylindrical shells with cutouts. *Journal of Sound and Vibration,* **52**(4), 497-510.

155. **Tripathy, B.** and **Rao, K.P.** (1990), Stiffened composite cylindrical panels-optimum lay up for buckling by ranking, *Computers and Structures*, **42**(4),481-488.

156. **Troitsky, M.S.** (1976), *Stiffened Plates: Bending, stability and vibrations*, Elsevier scientific publishing company, Oxford, New York.

157. **Webster, J.J.**(1968),Free vibration of rectangular curved panels. *International Journal of Mechanical Sciences*, **22**(11), 571-578.

158. **Yang, T.Y.** and **Kim, H.W.** (1973), Vibration and buckling of shells under initial stress, *AIAA Journal,* **11**(11), 1525-1531.

159. **Yeh, Meng-Kao, Lin, Ming-Chyuan and Wu, Wen-Tsang** (1999) Bending buckling of an elastoplastic cylindrical shell with a cutout, *Engineering Structures*, **21**, 996–1005.

160. **Zienkiewicz, O.C.** (1977), *The Finite Element Method*, Tata Mc-Graw Hill Publishing Company Limited, New Delhi.

# Appendix

## Computer Program

**A** general finite element code in Fortran-90 has been developed by the author from scratch to carryout all the analysis in the present investigations. The program contains a main routine and a number of subroutines which perform different activities. These subroutines are either called by the main routine or by some other subroutines. The subroutines of eigenvalue solver and assembling the elemental matrices used in the present analysis are taken from the previous investigators. As the stress field is non-uniform, due to arbitrary nature of applied in-plane load, boundary conditions, stiffeners, and cutout in the structure the pre-buckling stress analysis is carried out first to determine the stresses. The static equation $[K]\{\Delta\}=\{F\}$ is solved to get the displacement field of the whole structure, where $\{\Delta\}$ is the global displacement vector of the structure. Then the nodal displacement vectors $\{\delta\}$ of all the elements are found out by taking the displacement values associated with the elements from the global displacement vector $\{\Delta\}$. With the help of these nodal displacement vectors $\{\delta\}$ the strain fields in the elements are calculated and the stresses are obtained in the Gauss points. Same operations are performed for both the shell element and stiffener element. These stresses at the Gauss points are used to formulate the geometric stiffness matrix. The elastic stiffness, mass and geometric stiffness matrices are computed for all the shell elements and stiffener elements of the entire structure. The elemental matrices are assembled together to form the corresponding global matrices and stored in a single array where skyline storage algorithm is used. The global stiffness matrix is modified with respect to the boundary conditions. The solution for eigen values and eigen vectors is performed by the simultaneous iteration technique proposed by Corr and Jennings [28].

## Method of Solution

The solution procedure for the static, free vibration, vibration with in-plane load and dynamic instability analysis are presented in this section.

### *Method of solution for linear static analysis*

The stiffness matrix is stored as a one-dimensional array through skyline storage scheme. The static equation of equilibrium can be written as the form $[A]\{X\}=\{B\}$, where $[A]$ is global stiffness matrix, $\{X\}$ is global nodal unknowns to be solved and $\{B\}$ is the global load vector. The Cholesky factorization is used for this purpose. The program performs the decomposition, forward elimination and backward substitution by the subroutines decom, for and back. The Cholesky decomposition constructs a lower triangular matrix $[L]$ in a way that its transpose $[L]^T$ serves as the upper triangular part. The matrix $[A]$ can be written as, $[L]\,[L]^T=[A]$. This is the advantage of the Cholesky decomposition that one need not have to find out two separate lower and upper triangular matrices of the global stiffness matrix $[A]$. Then the solution of the nodal unknowns $\{X\}$ is done in two steps.

(i) $[L]\{Y\}=\{B\}$ (a)

(ii) $[L]^T\{X\}=\{Y\}$ (b)

### *Method of solution for free vibration, vibration with in-plane load, buckling and dynamic stability*

The similar eigen value problem is solved for the free vibration, vibration with in-plane load, buckling and dynamic instability problems. The equation of motion is first transformed into a standard form. The characteristics equation for a discretised elastic structural system under going small displacement having material properties within the elastic range for free vibration analysis can be expressed as

$$[K]\{q\}-\omega^2[M]\{q\}=\{0\} \qquad \text{Or} \qquad \omega^2[M]\{q\}=[K]\{q\} \tag{c}$$

This equation can be written as

$$[K]^{-1}[M]\{q\}=\frac{1}{\omega^2}[I]\{q\} \text{ , where } [I] \text{ is the identity matrix.} \tag{d}$$

$$\text{Or}\left[[D]-\frac{1}{\omega^2}[I]\right]\{q\}=\{0\} \text{ , where } [D]=[K]^{-1}[M] \tag{e}$$

Equation (e) is a standard eigen value problem. This equation can be used to find out the eigen values and the corresponding eigen vectors. The equation (e) can be rewritten as

$$\left[[D]-\frac{1}{\omega_i^2}[I]\right]\{q_i\}=\{0\} \qquad \text{Or} \qquad \left[[D]-\lambda_i[I]\right]\{q_i\}=\{0\} \tag{f}$$

Where, $\lambda_i$ is the eigen value of equation (f). The corresponding eigen vector of $\lambda_i$ is $\{q_i\}$. The eigen value $\lambda_i=1/\omega_i^2$ is obtained and $\omega_i=\sqrt{1/\lambda_i}$ is calculated. Putting any $\omega_i$ in the equation (f) the eigen vector (displacement $\{q_i\}$) associated with that eigen value can be determined. Here $[M]$ and $[K]$ are the global mass and stiffness matrix of the structure, $\{q\}$ is the relative displacement in the vibration mode corresponding to the natural frequency $\omega$. The equation (f) can be solved in various methods. The technique used to solve equation (f) in the present investigation is developed by Corr and Jennings [28]. For this the stiffness matrix $[K]$ being positive definite can be decomposed by Cholesky factorization as

$$[L]\,[L]^T=[K] \tag{g}$$

Where, $[L]$ is a lower triangular matrix. Using equation (g), equation (c) can be written as

$$\left[L^{-1}\right][M]\left[L^{-T}\right]\left[L^T\right]\{q\}=\frac{1}{\omega^2}[I]\left[L^T\right]\{q\} \tag{h}$$

$$\text{Or}\left[\left[L^{-1}\right][M]\left[L^{-T}\right]-\frac{1}{\omega^2}[I]\right]\left\{\left[L^T\right]\{q\}\right\}=\{0\} \tag{i}$$

Or $\left[[A]-\lambda_i[I]\right]\{p_i\}=\{0\}$ (j)

The equation (j) is similar as equation (f). This shows that the symmetric matrix $[A]=\left[L^{-1}\right][M]\left[L^{-T}\right]$ has eigen values $\lambda_i=1/\omega_i^2$ and eigen vector $\{p_i\}$ is such that $\{p_i\}=\left[L^T\right]\{q_i\}$. So the eigen $\{q_i\}$ can be obtained as $\left[L^{-T}\right]\{p_i\}=\{q_i\}$. In this method one can find out the dominating required number of eigen values and corresponding eigen vectors. It gives the eigen values in the ascending order. Let the matrix [*A*] is of the order *n*×*n* and first *m* eigen values and corresponding eigen vectors are needed. Then the procedure of can be demonstrated very briefly as follows,

1. Set a trial vector (modal vector) $[U]_{n\times m}$ and orthonormalize it. The trial vector is generated randomly. All the values are between -0.5 to 0.5.
2. Back substitute $[L]_{n\times n}[X]_{n\times m}=[U]_{n\times m}$, $[X]_{n\times m}$ is determined.
3. Multiply $[Y]_{n\times m}=[M]_{n\times n}[X]_{n\times m}$, $[Y]_{n\times m}$ is determined.
4. Forward substitute $[L]^T_{n\times n}[V]_{n\times m}=[Y]_{n\times m}$, $[Y]_{n\times m}$ is determined.
5. Form $[B]_{m\times m}=[U]^T_{m\times n}[V]_{n\times m}$, the diagonal elements of the matrix $[B]_{m\times m}$ are the eigen values.
6. Construct $[T]_{m\times m}$ so that $t_{ij}=1$ if $i=j$

   $$\text{and } t_{ij}=\frac{-2b_{ij}}{\left(b_{ii}-b_{jj}\right)+s\sqrt{\left(b_{ii}-b_{jj}\right)^2+16b_{ij}^{\ 2}}} \text{ if } i\neq j$$

   where, $s$ is the sign of $(b_{ii}-b_{jj})$.
7. Multiply $[W]_{n\times m}=[V]_{n\times m}[T]_{m\times m}$, $[W]_{n\times m}$ is obtained.
8. Perform Schmidt orthonormalization to derive $\left[\bar{U}\right]_{n\times m}$ from $[W]_{n\times m}$.
9. Check the vector tolerance $[U]_{n\times m}-\left[\bar{U}\right]_{n\times m}$, the tolerance value kept here is $10^{-6}$.
10. If tolerance is not satisfactory go to step 2 with the modified $[U]_{n\times m}$ *i.e.* $\left[\bar{U}\right]_{n\times m}$.

This procedure is followed to solve the problem of vibration with in-plane load, buckling and dynamic instability of the isotropic and laminated composite stiffened shell panels with/without cutout subjected to in-plane uniform/non-uniform static and harmonic loads. In case of the buckling problem the geometric stiffness matrix $\left[K_G\right]$ is put in the place of mass matrix $\left[M\right]$. Any in-plane load or in-plane stress can be applied in the panels to generate $\left[K_G\right]$ matrix. The load or stress is applied in the structure as the equivalent joint load at the nodes in the corresponding degree of freedom. If stress is applied then the load due to the stress is found out and it is divided to the nodes coming under the stress patch. Then the result (eigen value) obtained from the eigen value problem is squared to get the buckling factor. Then this buckling factor is multiplied with the applied load or stress to get the buckling load or buckling stress of the stiffened panels. If the applied load or stress is of unit value then the square of the obtained result is directly the buckling load or stress. In the problem of vibration with in-plane load $\left[K\right]$ is modified as $\left[\left[K\right]-P\left[K_G\right]\right]$ in relation to equation (56). The load $P$ is in general sense, *i.e.* if $\left[K_G\right]$ is generated for applied load, $P$ is load and if $\left[K_G\right]$ is generated for applied stress, $P$ is stress. The value of $P$ should not be more than the obtained factor because in that case the stiffness of the structure becomes negative. If $P$ is zero the natural frequency of vibration is obtained and if $P$ is critical the frequency of vibration becomes zero in the first mode. Again for dynamic instability problem the matrix $\left[K\right]$ is modified as $\left[\left[K\right]-\alpha P\left[K_G\right]\pm\frac{1}{2}\beta P\left[K_G\right]\right]$ in line with equation (61). The sign plus and minus are used to get the upper and lower frequencies of the excited load respectively. The eigen value obtained is multiplied by 2.0 to get the frequency of the excited load. In all cases the obtained eigen vector associated with the eigen value can be used to examine the mode shapes. This technique of solving the eigen value problem works very well during the execution of the program. In certain cases when the input matrices supplied wrongly, the method does not converge. This happens because when the global matrices come out of this solver the originality of the matrices used is loosed. So when the matrices are used again for another eigen value extraction, this method does not converge. To avoid this it necessary to supply the original matrices in all different analysis.

## Description of the Computer Program

In the present investigation for vibration, buckling and dynamic in stability analysis of isotropic and laminated composite stiffened shell panels with/without cutout subjected to in-plane uniform/non-uniform static and harmonic edge loads is implement by a finite element computer program written if Fortran-90. The program involves three basic steps in terms of computational procedure as follows,

- ✓ **Preprocessor**
- ✓ **Processor**
- ✓ **Postprocessor**

### Preprocessor

The preprocessor reads the property of the structure and the type of the analysis. Theses are the inputs in the program. It reads the all the details of the structures such as geometry, material properties, boundary condition, loading configuration and magnitudes, stiffeners location, stiffener properties, cutout parameter, mesh parameters etc. Most of the data are supplied in the input file some are supplied in the executable screen during the execution (run) of the program. The subroutine **geo** generates the required data from the input, which are required for processing process.

#### *Inputs in the program*

**xl, yl…**Length of the panel in $x$ and $y$ direction,
**rx,ry…**Radius of curvature in $x$-$z$ and $y$-$z$ plane,
**nstr …**Structure code, plate-1,cylindrical -2,spherical -3,hyperbolic hyperboloid -4,

**nlayer…**Number of layers in the panel skin,

**thk,e1,e2,g12,g13,g23,pr12…**Properties of each layer: thickness of the layer, $E$ in the material axis-1, $E$ in the material axis-2, $G$ value in material axis-1-2, $G$ value in material axis-1-3, $G$ value in material axis-2-3, Poisson's ration in axis-1-2. These properties of all layers are same,

**ori (i), i = 1,nlayer…**Fiber orientation in all layers,

**nxd, nyd…**Number of mesh divisions in $x$ and $y$ directions,

**nbc(i), i =1,4…**Boundary condition codes for four sides: Side-1 code, Side-2 code Side-3 code and Side-4 code, simply supported - 1, fixed - 2, free -3, symmetry – 4,

**rho…**Density of the shell panel,

**nrqd…**Required number of frequencies,

**alfa…**Static load factor,

**no_x_st, no_y_st…N**umber of $x$ and $y$ directional stiffener,

if (no_x_st > 0), then

**nl_xst(i), no_ly_xst(i) ,ly_arr_xst(i), i=no_x_st…**Nodal line number of the $x$-stiffener, Number of line in the $x$-stiffener, Layer(ply) arrangements code in the $x$-stiffener, for all $x$-stiffeners,

Ply arrangement number: 1 - horizontal stacking,

Ply arrangement number: 2 - vertical stacking,

**b_xst(i),d_xst(i),e_xst(i),tc_xst(i), i=no_x_st…**Breadth of the $x$-stiffener, depth of the $x$-stiffener, eccentricity of the $x$-stiffener, torsional constant of the $x$-stiffener, for all $x$-stiffeners,

Eccentricity negative: Stiffeners on bottom surface,

Eccentricity positive: Stiffeners on top surface,

**ori_xst(i,j),j=1,no_ly_xst(i), i=no_x_st…**Fiber orientation in all layers of all $x$-stiffeners,

**e1_xst,e2_xst,g12_xst,g13_xst,g23_xst,pr12_xst…**Material properties of each layer of $x$-stiffeners. These properties of all layers of all $x$-stiffeners are same,

**rho_xst…**Density of $x$-stiffener, same for all $x$-stiffeners,

if(no_y_st > 0) then, Similar data as of $x$-stiffeners are taken.

**nci…**Number of cutout index.

nic = 0, Cutout present

nic = 1, Without cutout

**xlc,ylc…**Dimensions of cutout in *x* and *y* directions.

***Subroutine geo***

This subroutine generates the *x*, *y* and *z* coordinates of all nodes with reference to a global Cartesian coordinate *x-y-z* system for all types of shell panels. This also generates all the nodal vector parameter of all the nodes which are used for the element stiffness matrix formulation.

**Processor**

Based on the finite element formulation the processor unit of the computer code performs the following tasks,

- Generates elastic stiffness and mass matrix of the stiffened panel skin and stiffener elements.
- Assembles of the elemental stiffness and mass matrix of the panel skin and stiffeners to form the corresponding global matrices.
- Boundary conditions are imposed.
- Solution for nodal displacements and computation of the stress field is done.
- Free vibration analysis can be carried out if required.
- Generates geometric stiffness matrix of the stiffened panel skin and stiffener elements.
- Assembles of the elemental geometric stiffness matrix of the panel skin and stiffeners to form the global geometric stiffness matrix.
- Buckling analysis is carried out.
- Vibration analysis with in plane load can be performed.
- Dynamic instability analysis is carried out.

The various subroutines performing various operations which are used in the processor unit of the computer code are presented briefly.

***Subroutine, stif_mass_mat***

This subroutine generates the stiffness and mass matrix of the elements of the panel skin and also assembles these to form the corresponding global matrices. The also need the help of other subroutine such as *cutout, rigidmatrix, bmatrix* and *assem*. The global load vector is also specified here with the help of subroutine *global_load_vector*.

***Subroutine, cutout***

This subroutine computes total number of elements present in the cutout and finds their global number.

***Subroutine, rigidmatrix***

This subroutine finds the constitutive matrix (stress-strain relationship matrix-D-matrx) of the panel skin element.

***Subroutine, bmatrix***

This subroutine finds the strain-displacement relationship matrix (B-matrx) of the panel skin element. It takes the help of subroutine *shape_s*. The jacobian matrix is developed here.

***Subroutine, shape_s***

This subroutine finds the shape functions and their derivatives with respect to $\xi$ and $\eta$ of the shell element. This also develops the shape functions to find out B-matrx and mass matrix of the shell element.

***Subroutine, assem***

This subroutine assembles the elemental matrices to form the corresponding global matrices of the shell panel and stores the data in skyline storage scheme.

***Subroutine, global_load_vector***

This subroutine generates the global load vector for all four types of loading.

***Subroutine, stif_mass_mat_st_x***

This subroutine generates the global stiffness and mass matrix of the whole structure taking the developed global stiffness and mass matrix of the panel and adding the contribution of the *x*-stiffeners to it.

***Subroutine, stif_mass_mat_st_y***

This subroutine generates the global stiffness and mass matrix of the whole structure taking the developed global stiffness and mass matrix of the panel and *x*-stiffeners and adding the contribution of the *y*-stiffeners to it.

***Subroutine, geo_stif_mat***

This subroutine generates the global geometric stiffness matrix of the panel skin assembling the geometric stiffness matrix of all elements of the panel skin. It takes the stresses of all elements calculated in another subroutine called subroutine *stress*. This subroutine *stress* calculates the stress in each element and their effect is taken into account in generating the elemental geometric stiffness matrix of the shell element.

***Subroutine, geo_stif_mat_st_x***

This subroutine generates the global geometric stiffness structure taking the developed global geometric stiffness matrix of the panel and adding the contribution of the *x*-stiffeners to it. It takes the stresses of all stiffener elements calculated in another subroutine called subroutine *stress_st*. This subroutine *stress_st* calculates the stress in each stiffener element and their effect is taken into account in generating the elemental geometric stiffness matrix of the stiffener element.

***Subroutine, geo_stif_mat_st_y***

This subroutine generates the global geometric stiffness structure taking the developed global geometric stiffness matrix of the panel and *x*-stiffeners adding the contribution of the *y*-stiffeners to it.

***Subroutine, save***

This subroutine transfers the modified global stiffness, mass and geometric stiffness matrices into original one. This is necessary because when these matrices come out from the eigen value solver and Cholesky decomposition subroutine the originality is lost during the mathematical processes.

***Subroutine, bdry***

This subroutine imposes the necessary boundary condition.

***Subroutine, r8usiv***

This subroutine finds the required number of eigen values and corresponding eigen vector for free vibration, vibration with load, buckling and dynamic instability analysis.

The other subroutines like *matmult*, *matinv*, *search*, *crunch, rigid_matrix, rgd_st, decom, for, back, shape_st* and *bmatrix_st* are used in the processing unit of the program.

**Postprocessing**

In this part of the program the input data is echoed to check whether the specified information is correct or not. The output data in terms of displacement, stress, eigen values, eigen vector etc depending upon the analysis are stored in different output files. These data are used to plot curves or to prepare tables as necessary. The graphic software Origin (Version 6.0) is used to plot curves.

**Strength and limitations of the program**

***Strength***

1. The finite element model gives reasonably accurate results.
2. In relation to other numerical models (Spline finite strip method, Finite difference method, Boundary element method and Mesh free method), this finite element method is relatively easy (in complex geometry- shallow shell, deep shell and presence of cutout; boundary condition and variable material properties) to tackle the problem of vibration, buckling and dynamic stability of laminated composite stiffened shell panels with cutout.
3. It can analyze shells of any shape, boundary and loading condition.
4. The stiffeners may have horizontal as well as vertical stacking.

***Limitations***

1. Prediction of the local buckling load has not been considered.
2. Effect of nonlinearity (Geometric and Material) is not included.
3. The stiffener should have rectangular shape. The effect of Z-type and closed box type (Hat) stiffeners is not considered, however this can be incorporated.
4. Effect of other type of cutouts (Circular, Elliptical etc.) is not considered, however the other types of cutout can be incorporated.
5. Any imperfection in the structure is not considered.

**Impact of the present investigation**

In the present finite element model an efficient stiffener element is proposed, which is compatible to degenerated shell element. Its combination with the shell element has given a unique tool for analyzing composite stiffened shells having a wide variety. The analysis tool is equipped in such a way that it can be used to solve vibration, buckling and dynamic instability for a wide range of problems. The problem of laminated composite stiffened shell panels with uniform in-plane loading is analyzed. Four types of panel geometry are considered. The problem of isotropic stiffened panels is also taken in the present investigation. All the above mentioned analysis for laminated composite stiffened shell panels with non-uniform in-plane loading is done. Four types of different loading configurations are taken. Also the vibration, buckling and dynamic instability behaviour of the laminated composite stiffened shell panels with square cutout in the centre for in-plane uniform and non-uniform loading are investigated in the present study. This will help to enhance the understanding regarding the behavior of the structure and it will definitely help a designer. A number of new results are presented taking different parameters into aspect, which will help the future researchers in this field fur further investigation.

**Additional references relevance to the investigation**


- **Kumar, L.R., Datta, P.K.** and **Prabhakara, D.L.** (2002), Tension buckling and vibration behaviour of curved panels subjected to non-uniform in-plane edge loading, *International Journal of Structural Stability and Dynamics*, **2**(3), 409-424.
- **Kumar, L.R., Datta, P.K.** and **Prabhakara, D.L.** (2005), Vibration and stability behaviour of laminated composite curved panels with cutouts under partial in-plane loads, *International Journal of Structural Stability and Dynamics*, **5**(1), 1-18.
- **Lee, S.G., Kim, S.C.** and **Song, J.G.** (2001), Critical loads of square plates under different load configurations on opposite edges, *Journal of Structural Stability and Dynamics*, **1**(2), 283-291.
- **Sapountsakis, E.J.** and **Katsikadelis, J.T.** (2002), Influence of the inplane boundary condition on the vibration frequencies and buckling load of ribbed plates, *International Journal of Structural Stability and Dynamics*, **2**(1), 25-44.